

THE SYNTHETIC AND BIOINORGANIC CHEMISTRY OF CARBORANES

By

Paul Schaffer, B.Sc.

A Thesis

Submitted to the School of Graduate Studies

In Partial Fulfillment of the Requirements

For the Degree

Doctor of Philosophy

McMaster University

© Copyright by Paul Schaffer, March 2003.

THE SYNTHETIC AND BIOINORGANIC CHEMISTRY OF CARBORANES

DOCTOR OF PHILOSOPHY (2003)
(Chemistry)

McMASTER UNIVERSITY
Hamilton, Ontario

TITLE: The Synthetic and Bioinorganic Chemistry of Carboranes

Author: Paul Schaffer, B.Sc. (University of British Columbia)

Supervisor: Professor John Fitzmaurice Valliant

Number of Pages: xx, 229, CXXIII

Abstract

Dicarpa-*closo*-dodecaboranes, otherwise known as carboranes, are attractive synthons for the development of inorganic pharmaceuticals and biological probes because of their unique chemical and physical properties. This thesis describes the synthesis and characterization of carborane derivatives as novel pharmaceuticals, radiopharmaceuticals and boron neutron capture therapy (BNCT) agents. Two general strategies were undertaken to prepare such compounds.

The first strategy, discussed in chapter 2, involved incorporating a carborane within the backbone of a known anti-cancer agent. To this end, a stereoselective synthetic methodology for incorporating a carborane into the structure of tamoxifen was developed. The reported synthetic approach yielded the desired carborane derivative possessing a *nido*-carborane in place of one of the aromatic rings of tamoxifen. The *nido*-carborane **2.28** showed modest affinity to the estrogen receptor (ER) which suggests that the inclusion of a carborane into the basic core of tamoxifen is a viable strategy for developing new antiestrogens and BNCT agents.

Having established the synthetic methodology for the *nido*-carborane analogue of tamoxifen **2.28**, subsequent research efforts focused on attaching a metal center to the open face of the carborane cage. The $[\text{Re}(\text{CO})_3]^+$ core was attached to the open face of **2.28** as a test toward the feasibility of this approach. While the reaction did yield some of the target complex **2.31**, the yield was low and accompanied by the formation of a significant quantity of $\text{Re}(\text{CO})_3$ clusters, leaving mostly unreacted starting material as the

major reaction component. The detection of **2.31** demonstrates that the ^{99m}Tc analogue can be prepared and potentially used as a novel imaging agent.

In parallel to the work involving tamoxifen, chapters 4 and 5 discuss novel synthetic methodologies developed to facilitate the synthesis of metal-based BNCT agents. Two homoleptic Re(I) $[\text{Re}(\text{L}_6)]^+$ ($\text{L} = \textit{ortho}$ or *para*-carborane isonitrile) complexes of *ortho* and *para*-carborane isocyanide ligands were prepared. These compounds are designed to serve as a new class of BNCT agent whose distribution can be evaluated using standard radioimaging techniques. These complexes are attractive agents for neutron capture therapy because of their exceptionally high boron content, the ease with which they can be targeted to specific receptors, and the fact that the biodistribution can be determined non-invasively using radioimaging techniques.

The synthesis and coordination chemistry of both the *ortho*- and *para*-carborane isocyanide complexes were examined through the reaction of $[\text{Re}_2(\text{O}_2\text{CPh})_4\text{Cl}_2]$ and $[\text{Re}_2(\text{OAc})_4\text{Cl}_2]$ with 3-isocyano-1,2-dicarba-*closo*-dodecaborane and a unique *para*-carborane azetidine derivative respectively. This research revealed some unexpected differences between the chemistry of *ortho*- and *para*-carboranes.

Acknowledgements

First and foremost I would like to thank my supervisor Dr. John Valliant, who, with his continuous input and guidance, brought the work in this thesis to fruition. The past five years have been an all around amazing experience, mainly due to the research and the lab group I have been a part of.

My committee members, Drs. William "Willie" Leigh and Michael McGlinchey, have been a tremendous help with their continuous interest and input to the work presented in this document. They have challenged me in all areas of chemistry, both practical and theoretical; and with their combined experiences, have enriched my knowledge greatly.

To all members of the Valliant group, past and present, who have contributed to this work in some form, I thank you. I would like to thank my friends in the lab, Bola, Peter, Tina, Amanda, Matt and Bill. All of you have enriched my time here and I wish you all the most success and happiness in the future. Friends in the department are numerous, but I would like to particularly thank Paul and Tom, who, over many cups of coffee have deliberated many topics, from the world of chemistry to the world itself.

Much of this work would not have been possible without the help of various facilities staff in the department: Jim Britten, Don Hughes, Brian Sayer, Tadek Olech, George Timmins and Leah Allan have all been generous with their time and knowledge. I would like to add a special note for Jim who, as my X-ray mentor, has taught me everything I know about X-ray crystallography. One trip to Jim's office always serves to remind me how much more there is to know about X-ray.

From an administrative standpoint, the office staff: Carol Dada, Josie Petrie, Barbra DeJean and Tammy Feher have been a continuous help. All of you have been ardent problem solvers from day one making my (and many other's) time here a lot easier.

I would also like to thank my family for their continued support throughout my years as a student. Finally to the one special person who has been my motivation during the past five years, my wife and best friend Karen I would like to extend much thanks and appreciation. Over the last nine years you have shown me nothing but love and friendship, and with the completion of this part of our lives I eagerly await to see what the future holds for us.

Table of Contents

	Page
Chapter 1: Introduction	
1.1 Introduction to Polyhedral Boranes	1
1.2 Dicarba- <i>closo</i> -dodecaboranes	5
1.3 Synthesis of Carboranes	6
1.4 Isomerization of Dicarba- <i>closo</i> -dodecaboranes	8
1.5 Nomenclature of Carboranes	10
1.6 Derivatization of Icosahedral Carboranes	11
1.7 Degradation of Carboranes in Basic Solution	12
1.8 The Dicarbollide Dianion	15
1.9 The Medicinal Chemistry of Carboranes	16
1.10 Boron Neutron Capture Therapy (BNCT)	17
1.11 Carboranes in Drug Development	23
1.12 Metallocarboranes and Medical Imaging	25
1.13 Scope and Summary of Research	27
1.14 References	29
Chapter 2: Carborane Analogues of Tamoxifen	
2.1 Overview	35
2.2 Introduction to Antiestrogens	35

2.3 Analogues of Tamoxifen	38
2.4 Carboranes as Pharmacophores	39
2.5 Carborane-Derived Antiestrogens	42
2.6 Target Molecule and Retrosynthetic Analysis	42
2.7 The Total Synthesis of a <i>nido</i> -Carborane Analogue of Tamoxifen 2.28	43
2.8 X-ray Structural Characterization of Compound 2.25	53
2.9 Synthesis of the <i>nido</i> -Carborane Analogue of Tamoxifen	56
2.10 Relative Binding Affinity Study	61
2.11 Synthesis of a Rhenium Complex of Tamoxifen-Carborane	62
2.12 Attempted Synthesis of a para-Carborane Analogue of Tamoxifen	66
2.13 Rationale	67
2.14 Attempted Synthesis of 2.32 by C-C Single Bond Formation	68
2.15 Attempted Synthesis of 2.32 by C=C Double Bond Formation	70
2.16 Summary and Future Work	71
2.17 Experimental	74
2.18 References	83

Chapter 3: Organometallic Analogues of Tamoxifen

3.1 Introduction to Dicobalthexacarbonyl Analogues of Tamoxifen	86
3.2 Probing the Reactivity of the Alkyne 2.24 .	87
3.3 Dicobalthexacarbonyl Analogues of Tamoxifen	87
3.4 Single Crystal X-ray Analysis of Compound 3.4	91

3.5 Summary and Conclusions	93
3.6 Experimental	94
3.7 References	99
Chapter 4: The Synthesis, Characterization and Coordination Chemistry of <i>ortho</i>-Carborane Isonitriles	
4.1 Introduction	100
4.2 Synthesis of <i>ortho</i> -Carborane Isonitriles	102
4.3 X-ray Crystal Structure of 3-Formyl- <i>ortho</i> -carborane	107
4.4 Dehydration of 3-Formyl- <i>ortho</i> -carborane	109
4.5 X-ray Crystal Structure of 3-isonitrile- <i>ortho</i> -carborane	112
4.6 Formation of an Isocyanate from Burgess Reagent Dehydration	114
4.7 Dehydration of 4.2 with BOP-Cl	115
4.8 Tethered C-Substituted <i>ortho</i> -Carborane Isonitriles	116
4.9 Synthesis of Isonitrile Carboranes Containing Longer Alkyl Tethers	121
4.10 Mechanistic Consideration for the Formation of 4.19 and 4.20	132
4.11 Alternative Methods for the Synthesis of 4.14	133
4.12 Attempted Dehydration of the Tethered Formamide 4.18	136
4.13 Summary	139
4.14 3-isonitrile- <i>ortho</i> -carborane Complexes of Rhenium(I)	140
4.14.1 Disubstituted Rhenium(I) Complex	140
4.14.2 Trisubstituted Rhenium(I) Complex	144
4.14.3 Tetrasubstituted Rhenium(I) Complex	149

4.14.4 <i>ortho</i> -Carborane Homoleptic-Isonitrile Complexes of Re(I)	150
4.15 Summary and Future Work	156
4.16 Experimental	159
4.17 References	179
Chapter 5: The Synthesis and Coordination Chemistry of <i>para</i>-Carborane Isonitriles	
5.1 Overview	182
5.2 Synthetic Strategy	182
5.3 Synthesis and Characterization of 3-Formyl- <i>ortho</i> -carborane	183
5.4 Attempted Dehydration of 1-Formyl-1,12-dicarba-closo-dodecaborane	186
5.5 The Unexpected Formation of a Bis(imino)carboranyl Azetidine	191
5.6 Proposed Mechanism for the Formation of 5.7	199
5.7 Homoleptic <i>para</i> -Carborane Isonitrile Complex of Rhenium(I)	202
5.8 <i>Ortho</i> - versus <i>para</i> -Carborane Formamides	210
5.9 VTNMR Analysis of the Formyl-Carborane Isomers	211
5.10 Summary and Future Work	216
5.11 Experimental	217
5.12 References	225
Chapter 6: Conclusions	228
Appendix I: General Procedures	I
Appendix II: X-ray Data Tables	X

List of Figures and Schemes

List of Figures	PAGE
Chapter 1 – Introduction	
Figure 1.1 – Three-centered B-H-B and B-B-B bonds.	1
Figure 1.2 – Structure of $[\text{B}_{12}\text{H}_{12}]^{2-}$ (1.1) and $[\text{B}_{10}\text{H}_{10}]^{2-}$ (1.2) polyhedra.	2
Figure 1.3 – Representations of dodecahedral-based <i>closo</i> , <i>nido</i> and <i>arachno</i> polyhedra. Charges and hydrogen atoms removed for clarity.	3
Figure 1.4 – Representations of $[\text{B}_{12}\text{H}_{12}]^{2-}$ (1.1) and $\text{B}_{10}\text{H}_{14}$ (1.3).	3
Figure 1.5 – Icosahedral structures of $[\text{B}_{12}\text{H}_{12}]^{2-}$ (1.1), $[\text{CB}_9\text{H}_{12}]^{1-}$ (1.4) and $\text{C}_2\text{B}_{10}\text{H}_{12}$ (1.5).	6
Figure 1.6 – Transformation of the isomeric forms of icosahedral carboranes.	9
Figure 1.7 – Numbering system for <i>closo</i> and <i>nido</i> cage atoms.	10
Figure 1.8 – A) original and B) current proposals for the structure of <i>nido</i> -carborane.	14
Figure 1.9 – Structure representations of the <i>nido</i> - forms of <i>ortho</i> - (1.8), <i>meta</i> - (1.9) and <i>para</i> - (1.10) carboranes.	15
Figure 1.10 – Frontier orbital representation of $[\text{C}_5\text{H}_5]^-$ and $[\text{C}_2\text{B}_9\text{H}_{11}]^-$	16
Figure 1.11 – The boron-10 neutron capture reaction.	19
Figure 1.12 – Neutron capture event occurring within a cell.	19
Figure 1.13 – Neutron capture reactions of ^1H and ^{14}N .	21
Figure 1.14 – Sodium borates and boric acid. From left to right: Borax ($\text{Na}_2\text{B}_4\text{O}_7 \cdot 10\text{H}_2\text{O}$), Pentaborate ($\text{NaB}_5\text{O}_8 \cdot 4\text{H}_2\text{O}$) and Boric acid $[\text{B}(\text{OH})_3]$.	21
Figure 1.15 – Structures of BPA and BSH, current BNCT agents in clinical trials.	22

Figure 1.16 – Venus Flytrap cluster concept by Hawthorne and co-workers	26
Chapter 2 – Carborane Analogues of Tamoxifen	
Figure 2.1 – The chemical structures of estradiol (2.1), MER-25 (2.2), tamoxifen (2.3) and its metabolite, 4-hydroxytamoxifen (2.4).	35
Figure 2.2 – Molecular regions of tamoxifen responsible for pharmacological behaviour.	37
Figure 2.3 – Various Tamoxifen analogues, clockwise from top left: Idoxifen (2.5), Ferrocifen (2.6), Raloxifen (2.7) and Hawthorne's B ₂₀ tamoxifen derivative (2.8).	39
Figure 2.4 – X-ray structure of compound 2.9 showing the similarity in diameters between carborane and phenyl moieties.	40
Figure 2.5 – Carborane-based estrogen agonists and antagonists reported by Endo et al.	41
Figure 2.6 – Proposed carborane analogue of tamoxifen.	43
Figure 2.7 – ¹ H NMR spectrum of compound 2.23, showing the presence of both E and Z isomers.	47
Figure 2.8 – Diastereomer ratio as observed by the ethoxy peaks in the ¹ H NMR spectrum of 2.23.	47
Figure 2.9 – The ¹³ C NMR and ¹³ C DEPT NMR spectra of 2.23	48
Figure 2.10 – ORTEP representation of both crystallographic independent molecules of 2.25, with thermal ellipsoids shown at the 30% probability level.	55
Figure 2.11 – ¹¹ B NMR spectrum of 2.28.	58
Figure 2.12 – ¹ H NMR spectra of 2.25 and 2.28	59
Figure 2.13 – ¹ H NMR spectrum of 2.28 showing diastereomer peaks	60
Figure 2.14 – ORTEP representation of 2.29. Thermal ellipsoids shown at the 50% probability level. The NEt ₄ counter ion was removed for clarity	63

Figure 2.15 – η^5 carborane complexes of rhenium and technetium	64
Figure 2.16 – ESMS evidence for the formation of 2.31	65
Figure 2.17 – Proposed para-carborane analogue of tamoxifen 2.32 .	66
 Chapter 3 – Organometallic Analogues of Tamoxifen	
Figure 3.1 – Mechanism for the fluxional behaviour of the nido bipyramidal C_2Co_2	89
Figure 3.2 – 1H NMR spectra of 3.1 , 3.4 and 3.5 .	90
Figure 3.3 – ORTEP representation of 3.4 . Thermal ellipses are shown at the 50% probability level. Hydrogen atoms have been removed for clarity.	92
 Chapter 4 – <i>ortho</i>-Carborane Isonitriles and Their Rhenium Complexes	
Figure 4.1 – Illustration of proposed metal core BNCT/BNCS agents.	101
Figure 4.2 – $^{11}B\{^1H\}$ NMR of <i>ortho</i> -carborane and 3-amino <i>ortho</i> carborane.	104
Figure 4.3 – ORTEP representation of 4.2 . Thermal ellipsoids are shown at the 50% probability level.	108
Figure 4.4 – Packing diagram of 4.2 showing hydrogen bonding contacts.	108
Figure 4.5 – IR spectrum of 4.2 .	110
Figure 4.6 – ^{13}C NMR spectrum (150 MHz) of 4.3 in acetone- d_6	111
Figure 4.7 – X-ray crystal structure of 3-isonitrile- <i>ortho</i> -carborane (4.3) (50% thermal ellipsoids).	113
Figure 4.8 – Ball and stick representation for the solid-state packing of 4.3 .	113
Figure 4.9 – ORTEP representation of 4.19 , thermal ellipsoids shown at the 50% probability level.	130
Figure 4.10 – ^{13}C NMR of 4.14 and 4.18 .	134

Figure 4.11 – ORTEP representation of 4.21 . Thermal ellipsoids shown at 30% probability level.	143
Figure 4.12 – ORTEP representations of actual, and symmetry generated, solutions of 4.22 . Thermal ellipsoids are shown at the 30% probability level.	146
Figure 4.13 – $^{11}\text{B}\{^1\text{H}\}$ NMR of 4.22 before and after crystallization.	148
Figure 4.14 – ESMS spectrum of 4.23 .	150
Figure 4.15 – ^1H NMR spectrum of 4.24 .	153
Figure 4.16 – theoretical and actual ESMS spectrum of 4.24 .	153
Figure 4.17 – Re-Re bonding orbital interaction with LUMO of an isonitrile.	155
 Chapter 5 – The Synthesis and Coordination Chemistry of <i>para</i>-Carborane Isonitriles 	
Figure 5.1 – ORTEP representation of 5.4 . Thermal ellipsoids shown at the 50% probability level.	184
Figure 5.2 – Unit cell representation of 5.4 .	185
Figure 5.3 – IR spectrum of 5.5 .	187
Figure 5.4 – ORTEP representation of 5.5 showing 30% thermal ellipsoids.	188
Figure 5.5 – Packing representation of 5.5 down the b and c axes. Disordered solvent of crystallization was omitted for clarity.	189
Figure 5.6 – Infra-Red and ESMS spectra of 5.7 .	192
Figure 5.7 – ORTEP representation of 5.8 . Thermal ellipsoids are shown at the 30% probability level. H-atoms and a THF of crystallization have been omitted for clarity.	195
Figure 5.8 – Ball and stick representation of the disordered azetidine core. Both a) overlapping, face on and b) independent, edge-on solutions of 5.8 are shown. Carborane cages, hydrogen atoms and solvent have been omitted for clarity.	196

Figure 5.9 – ^{13}C NMR of 5.7 and 5.8 .	201
Figure 5.10 – ^1H NMR spectrum of 5.11 in acetone- d_6 .	204
Figure 5.11 – $^{11}\text{B}\{^1\text{H}\}$ NMR spectrum of 5.11 .	204
Figure 5.12 – Valence bond theory representation of metal back-donation.	205
Figure 5.13 – ORTEP representation of 5.11 with 30% thermal ellipsoids. Hydrogen atoms and counterions removed for clarity.	206
Figure 5.14 – ESMS spectrum of 5.11 prior to ion exchange.	208
Figure 5.15 – Class I and II complexes of $\text{Re}_2(\text{OAc})_4\text{Cl}_2\text{L}$.	209
Figure 5.16 – Possible coordination modes of 5.7 to $\text{Re}_2(\text{OAc})_4\text{Cl}_2$.	209
Figure 5.17 – Stacked VTNMR plot of 5.4 .	214
Figure 5.18 – Stacked VTNMR plot of 4.2 .	215

List of Schemes	Page
Chapter 1 – Introduction	
Scheme 1.1 – Synthesis of <i>ortho</i> -carborane.	7
Scheme 1.2 – Synthetic routes to substituted carboranes.	8
Scheme 1.3 – Formation of <i>nido-ortho</i> -carborane,	13
Scheme 1.4 – Proposed mechanism of cage degradation in an EtOH/KOH medium.	13
Scheme 1.5 – Generation of the dicarbollide dianion.	16
Chapter 2 – Carborane Analogues of Tamoxifen	
Scheme 2.1 – Retrosynthetic analysis of carborane analogue of tamoxifen.	43
Scheme 2.2 – The total synthesis of a <i>nido</i> -carborane analogue of tamoxifen.	45
Scheme 2.3 – Proposed mechanism for Friedel-Crafts acylation of 2-chlorethoxyphenol.	46
Scheme 2.4 – The reaction of a nucleophile with a prochiral ketone	50
Scheme 2.5 – Reactive conformers give <i>Z</i> -alkene with E2 elimination pathway	50
Scheme 2.6 – Isomerization of 4-hydroxy- <i>Z</i> -tamoxifen to the <i>E</i> isomer.	67
Scheme 2.7 – Attempted synthesis of 2.32 .	69
Scheme 2.8 – Attempted McMurry coupling of 2.34 with 4-methoxybenzophenone.	70
Scheme 2.9 – Attempted Wittig Olefination of benzylphosphonium bromide with 2.34 .	71

Chapter 3 – Organometallic Analogues of Tamoxifen

Scheme 3.1 – Synthesis of dicobalthexacarbonyl analogues of tamoxifen. 88

Chapter 4 – The Synthesis, Characterization and Coordination Chemistry of *ortho*-Carborane Isonitriles

Scheme 4.1 – The synthesis of a boron-linked *ortho*-carborane isonitrile. 102

Scheme 4.2 – Nucleophilic substitution of the third boron vertex of *ortho*-carborane. 103

Scheme 4.3 – Mechanism of asymmetric anhydride formation and subsequent formylation. 106

Scheme 4.4 – Mechanism of dehydration using the Burgess reagent. 111

Scheme 4.5 – A) Proposed mechanism for the formation of **4.4**. B) Mechanism of the Shapiro reaction. 115

Scheme 4.6 – Dehydration of 3-formyl-*ortho*-carborane with BOP-Cl 116

Scheme 4.7 – Retrosynthetic analysis for the formation of C-linked carboranyl isonitriles. 117

Scheme 4.8 – Synthesis of the tethered *ortho*-carborane isonitrile **4.10**. 120

Scheme 4.9 – Synthesis of aminopropyl-*ortho*-carborane **4.14**. 123

Scheme 4.10 – Synthesis of ω -amino-alkyl-*ortho*-carborane. 128

Scheme 4.11 – Attempted hydrogenation of **4.13** and formation of side products. 129

Scheme 4.12 – Proposed mechanism for the formation of **4.19** and **4.20** via hydrogenation. 132

Scheme 4.13 – Catalytic Transfer Hydrogenation of **4.17**. 133

Scheme 4.14 – Proposed mechanism for Catalytic Transfer Hydrogenation. 135

Scheme 4.15 – Attempted dehydration reactions of **4.18**. 137

Scheme 4.16 – Reaction of **4.15** and **4.16** with AgCN. 138

Scheme 4.17 – The formation of an intermediate complex with AgCN.	138
Scheme 4.18 – Synthesis of bis-3-isonitrile- <i>ortho</i> -carborane rhenium tricarbonyl (4.21).	141
Scheme 4.19 – Synthesis of tris-, tetrakis-, and hexakis-3-isonitrile- <i>ortho</i> -carborane rhenium carbonyl complexes.	144
Scheme 4.20 – Preparation of $\text{Re}_2(\text{O}_2\text{CR})_4\text{Cl}_2$ (R = Me, Ph) precursors.	152
Scheme 4.21 – Synthesis of the homoleptic Re(I) isonitrile complex 4.24 .	152
Scheme 4.22 – Proposed routes for the formation of 4.24 .	155
Scheme 4.23 – Proposed probes to determine the reactivity of pendent amino and formyl groups.	156
 Chapter 5 – The Synthesis and Coordination Chemistry of <i>para</i>-Carborane Isonitriles	
Scheme 5.1 – Synthesis of <i>para</i> -carborane formamide (5.4).	183
Scheme 5.2 – Formamide dehydration strategies.	187
Scheme 5.3 – Proposed mechanistic basis for the formation of 5.5 via the isocyanate 5.17 .	191
Scheme 5.4 – Hydrolysis and reaction of 5.7 in the presence of Re(I).	193
Scheme 5.5 – Proposed mechanism for the formation of 5.7 .	200
Scheme 5.6 – Synthesis of the hexacoordinate Re(I) <i>para</i> -carborane isonitrile complex (5.11).	201
Scheme 5.7 – Rotational isomers of 4.2 and 5.4 .	211

List of Abbreviations and Symbols

3c2e	Three-center two-electron (bond)
Å	Angstrom
AcOH	Acetic Acid
Anal.	Analysis (Elemental Analysis)
Asp	Aspartic acid
^{11}B NMR	Boron Nuclear Magnetic Resonance Spectroscopy
Bn	Benzyl
BNCT	Boron Neutron Capture Therapy
BOP-Cl	bis(2-oxo-3-oxazolidinyl)phosphinic chloride)
BPA	p-boronophenylalanine
br	Broad signal (^1H NMR, ^{11}B NMR)
BSH	Sodium mercaptoundecahydrododecaborate
^{13}C NMR	Carbon Nuclear Magnetic Resonance Spectroscopy
Calc.	Calculated
CI	Chemical Ionization Mass Spectrometry
Cp	Cyclopentadienyl
Cp ⁻	Cyclopentadienide
CTH	Catalytic Transfer Hydrogenation
d	Doublet (^1H NMR)
decomp.	Decomposed
DEPT	Distortionless Enhancement by Polarization Transfer
DMF	N,N Dimethyl formamide
DMSO	Dimethyl sulfoxide
DNA	Deoxyribonucleic acid
dsd	Diamond-Square-Diamond (rearrangement)
E	Entgegen
EI	Electron Impact Mass Spectrometry
equivs.	Equivalents
Et	Ethyl
EtOAc	Ethyl Acetate
EtOH	Ethanol
ER	Estrogen receptor
ESMS	Electrospray Mass Spectrometry
FID	Free Induction Decay
FTIR	Fourier Transform Infrared Spectroscopy

h	hour(s)
^1H NMR	Proton Nuclear Magnetic Resonance Spectroscopy
HOMO	Highest Occupied Molecular Orbital
HPLC	High Pressure Liquid Chromatography
HRFABMS	High-Resolution Fast Atom Bombardment Mass Spectrometry
HRESMS	High-Resolution Electrospray Mass Spectrometry
HRMS	High-Resolution Mass Spectrometry
Hz	Hertz
iPrOH	<i>iso</i> -propyl alcohol
IR	Infrared Spectroscopy
IUPAC	International Union of Pure and Applied Chemistry
K	Kelvins
LB	Lewis base
LBD	Ligand Binding Domain
LDA	Lithium diisopropylamide
LET	Linear Energy Transfer
m	Multiplet (^1H NMR)
Me	Methyl
MER-25	1-(<i>p</i> -2-diethylaminoethoxyphenyl)-1-phenyl-2- <i>p</i> -Methoxyphenylethanol
MHz	Megahertz
min.	Minute(s)
MO	Molecular Orbital
mp	Melting Point
MRI	Magnetic Resonance Imaging
MS	Mass Spectrometry
nBuLi	<i>n</i> -butyl lithium
NMR	Nuclear Magnetic Resonance Spectroscopy
NOE	Nuclear Overhauser Effect
NOESY	Nuclear Overhauser Effect Spectroscopy
OEt	Ethoxy
^{31}P NMR	Phosphorus Nuclear Magnetic Resonance Spectroscopy
PET	Positron Emission Tomography
Pet. Ether	Petroleum Ether

pK _a	log acidity constant (K _a)
Ph	Phenyl
ppm	Parts per million
PSEPT	Polyhedral Skeletal Electron Pair Theory
PT	Proton transfer
pyr.	Pyridine
q	quartet (¹ H NMR)
R _f	Retention Factor (TLC)
RBA	Relative Binding Affinity
s	Singlet (¹ H NMR)
SPECT	Single Photon Emission Computed Tomography
t	triplet (¹ H NMR)
TBAF	Tetrabutylammonium fluoride
tBu	<i>tert</i> -butyl
TEA	Triethylamine
Tf	Triflate
TFA	Trifluoroacetic acid
THF	Tetrahydrofuran
TLC	Thin Layer Chromatography
TMS	Trimethylsilyl
tol	Tolyl
VFC	Venus Flytrap Complex
VTNMR	Variable Temperature NMR
Z	Zusammen

Chapter 1 - Introduction

1.1 Introduction to Polyhedral Boranes

Early attempts to isolate the hydrides of boron were thwarted by the highly reactive nature of the compounds. Despite prophetic work by some,¹ such as the predicted existence of BH_3 as the dimeric B_2H_6 ($\text{B}_2\text{H}_4(\mu\text{-H})_2$), it took until 1933 for Stock and co-workers to isolate the first boron hydrides. Stock later prepared a series of boron hydrides including B_2H_6 , B_4H_{10} , B_5H_9 , B_5H_{11} , B_6H_{10} and $\text{B}_{10}\text{H}_{14}$. With the synthesis and isolation of these compounds, a new era in boron chemistry was launched.²

Stock proposed hydrocarbon-like chain structures for the boron hydrides, but was unable to adequately rationalize the electronic bonding interactions with what appeared to be an apparent electron deficiency. It was not until 1945 when Pitzer, while studying the bonding in diborane, proposed his concept of the “protonated double bond” that the nature of the chemical bonding in boranes began to become apparent.³ Pitzer’s work eventually led to Lipscomb and collaborators putting forth the concept of the three-center two-electron (3c2e) bond (Figure 1.1).⁴

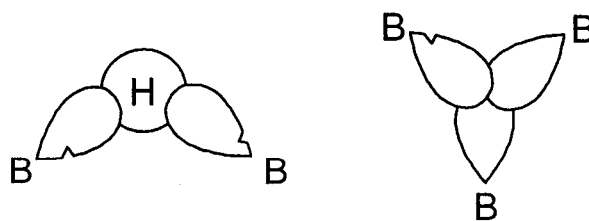


Figure 1.1 Three-centered B-H-B (left) and B-B-B (right) bonds.

Both two- and three-centered bonding models (classical and non-classical, Figure 1.1) give topological models for the structures of all the known boranes.⁵ Longuet-Higgins and Roberts were the first to use molecular orbital (MO) theory to show that the molecular structures of the borane family are polyhedral in nature.⁶ The MO's are comprised both of skeletal orbitals, responsible for maintaining the integrity of the cluster, in addition to outward directing external orbitals, for bonding to extrapolyhedral substituents.^{7,8}

Wade later published his theory on the nature of the bonding found in polyhedral boron clusters.⁹ Polyhedral Skeletal Electron Pair Theory (PSEPT), which complements Wade's rules, is a guide for correlating the total electron count in a polyhedral molecule with its shape.¹⁰ A summary of Wade's rules are as follows: 1) Clusters are comprised of units that contribute a designated number of electrons toward skeletal bonding in addition to those bonds already present within the unit itself 2) The cluster geometry is determined by the total number of skeletal bonding electron pairs, as each unit supplies three orbitals toward the construction of skeletal molecular orbitals. Thus, there are always $3n$ molecular orbitals in an n -vertex polyhedron, of which $n+1$ are designated as bonding molecular orbitals in a closed polyhedron, which are further divided into n tangential and

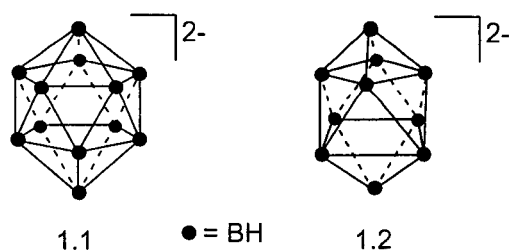


Figure 1.2 Structure of $[B_{12}H_{12}]^{2-}$ (1.1) and $[B_{10}H_{10}]^{2-}$ (1.2) polyhedra.

one inward directing 3) Removal of one or more vertices from the cage system does not affect the number of molecular orbitals. In light of this, the open-faced or *nido* polyhedra, which are missing one vertex, have $n+2$ molecular orbitals. Polyhedra missing two (*arachno*) and three (*hypho*) vertices have $n+3$ and $n+4$ orbitals respectively. This also accounts for the geometric likeness of the open clusters to that of fragments of the parent polyhedron (Figure 1.3). Wade's rules, which have been elaborated by others, have found a wide variety of applications beyond boron cluster chemistry, including correlating electron count and geometry for carbocations, metal clusters and other main group clusters.¹¹

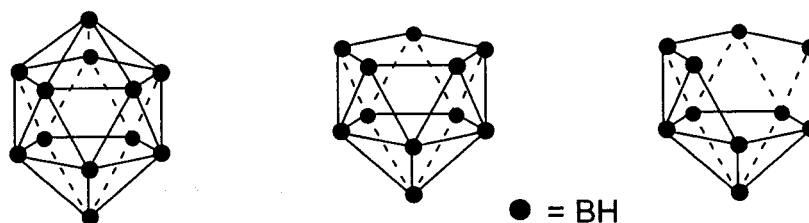


Figure 1.3 - Representations of dodecahedral-based closo (left), nido (center) and arachno (right) polyhedra. Charges and hydrogen atoms have been omitted for clarity.

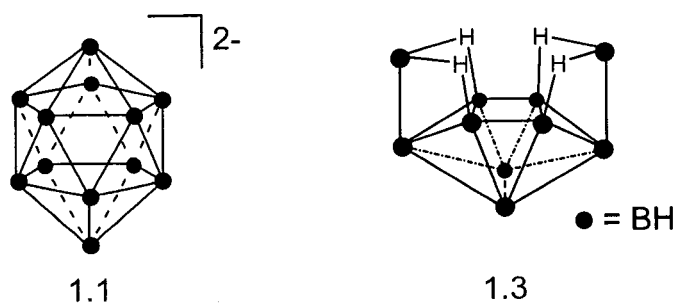


Figure 1.4 – Representations of $[B_{12}H_{12}]^{2-}$ (1.1) and $B_{10}H_{14}$ (1.3).

Considering $[B_{12}H_{12}]^{2-}$ (Figure 1.4, compound 1.3), it is apparent that the icosahedron is comprised of twelve BH units. For each BH unit there are two electrons

contributed toward the bonding skeletal molecular orbitals, as the remaining two are required to maintain the boron-hydrogen bonds. The double negative charge indicates the presence of two additional electrons, giving a total of 26 electrons (13 electron pairs) available for cage bonding. Wade's $n+1$ rule dictates that the cluster maintains a 12 vertex, or dodecahedral geometry. In the case of open clusters, there are other units to consider, such as extra terminal and bridging hydrogen atoms. These so-called "extra protons" contribute one electron toward cage bonding. In decaborane ($B_{10}H_{14}$) for example, 10 BH units and 4 bridging hydrogen atoms gives rise to 24 electrons (12 electron pairs) available for skeletal bonding MO's. Wade's rule indicates that an eleven-vertex geometry should exist and due to the presence of only ten, we deduce that decaborane is the ten vertex, *nido* form of the parent undecahedral polyhedron.

Lipscomb and co-workers noted that the structures of the lower boranes (B_4H_{10} , B_5H_{11} , B_6H_{12} , B_8H_{12} and B_9H_{15}) were essentially icosahedral fragments.^{12,13} This idea lead to the hypothesis for the existence of a parent $B_{12}H_{12}$ icosahedral cluster.⁶ The work, using MO arguments, went one step further and predicted that all clusters with the formula $[B_nH_n]$ existed as the dianion.¹⁴ It follows that the icosahedral $B_{12}H_{12}$ would exist as a dianion $[B_{12}H_{12}]^{2-}$ rather than a neutral species (Figure 1.2).¹⁵ Pitochelli and Hawthorne isolated the higher borane $[B_{10}H_{10}]^{2-}$ in 1959, which was followed by the synthesis of $[B_{12}H_{12}]^{2-}$ (**1.1**) in 1960 (Figure 1.2).¹⁶ The icosahedral shape of compound **1.1** was later confirmed by X-ray crystallography.¹⁷

The above section highlights the evolution of the polyhedral borane family, from the initial isolation of boranes by Stock to the eventual synthesis of dodecahedral forms

by Hawthorne and co-workers. In addition, a summary behind the remarkable bonding attributes of these clusters was discussed and an attempt to convey an understanding of the profound stability of these polyhedra given. The stability of the deltahedral cluster family compared to the quite unstable neutral boron hydrides has been the topic of a significant amount of research. The especially low reactivity of $[\text{B}_{12}\text{H}_{12}]^{2-}$ suggests that the concept of aromaticity may be extended to these three-dimensional polyhedral molecules. While the idea of aromaticity was originally proposed for flat polygonal molecules such as benzene, Aihara extended this concept into the field of cluster chemistry.¹⁸ A number of theories brought forth attempt to demonstrate the analogy between the electron delocalization in two-dimensional, planar polygonal aromatic hydrocarbons, and that found in three-dimensional deltahedral boranes and carboranes.¹⁹⁻

21

1.2 Dicarba-*closo*-dodecaboranes

With an increased understanding of the bonding and stability trends in the boron hydride family, it was reasoned that replacement of the cage boron atoms with isoelectronic units would give heterosubstituted cages of similar stability. Sure enough, some of the lower isoelectronic carbon substituted clusters, or carboranes, having the general formula $\text{C}_2\text{B}_{n-2}\text{H}_n$, were isolated by Keilin and Shapiro in the early 1960's.^{22,23} This work led to the synthesis of the icosahedral $\text{C}_2\text{B}_{10}\text{H}_{12}$ carboranes by two industrial groups in 1963.^{24,25}

It is convenient to regard carboranes as isoelectronic derivatives of boron hydrides in which a B^- or BH unit has been replaced with a neutral and isoelectronic

carbon or CH unit. The formal charge on the resulting cage decreases by one for every CH or CR unit added in place of a BH group. For example, replacement of one BH vertex with a CH moiety in $[B_{12}H_{12}]^{2-}$ would give $[CB_{n-1}H_n]^{1-}$, while a cage containing two CH vertices gives $C_2B_{n-2}H_n$ (Figure 1.5). Because of their unique properties and relevance to the work completed in this thesis, the remainder of the introduction will focus only on the chemistry of dicarba-*closo*-dodecaboranes ($C_2B_{10}H_{12}$).

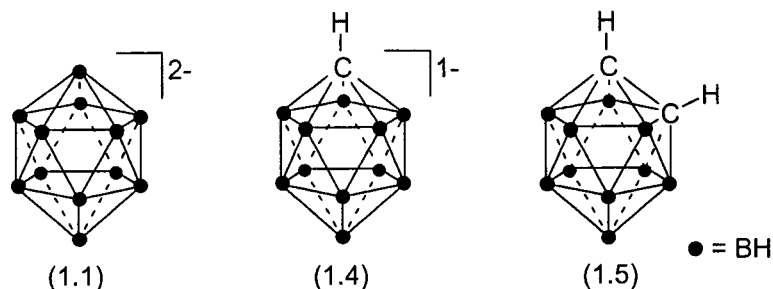
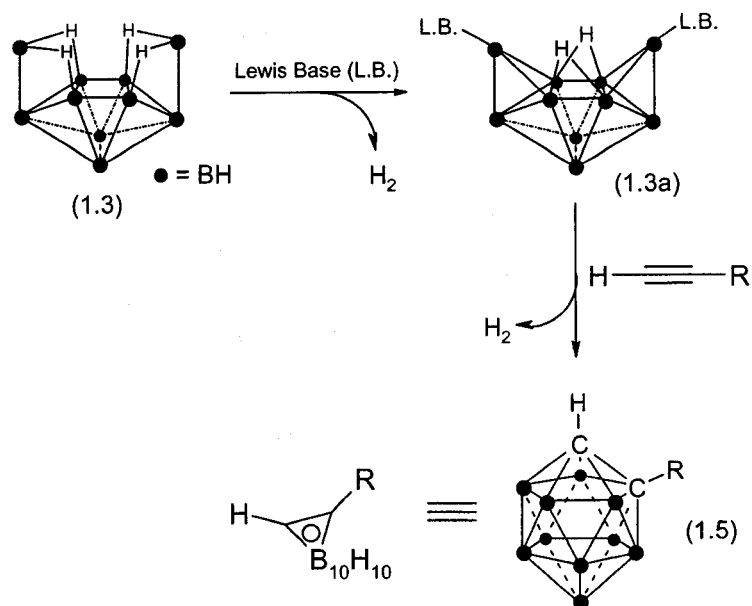


Figure 1.5 – Icosahedral structures of $[B_{12}H_{12}]^{2-}$ (1.1), $[CB_9H_{12}]^{1-}$ (1.4) and $C_2B_{10}H_{12}$ (1.5).

1.3 Synthesis of Carboranes

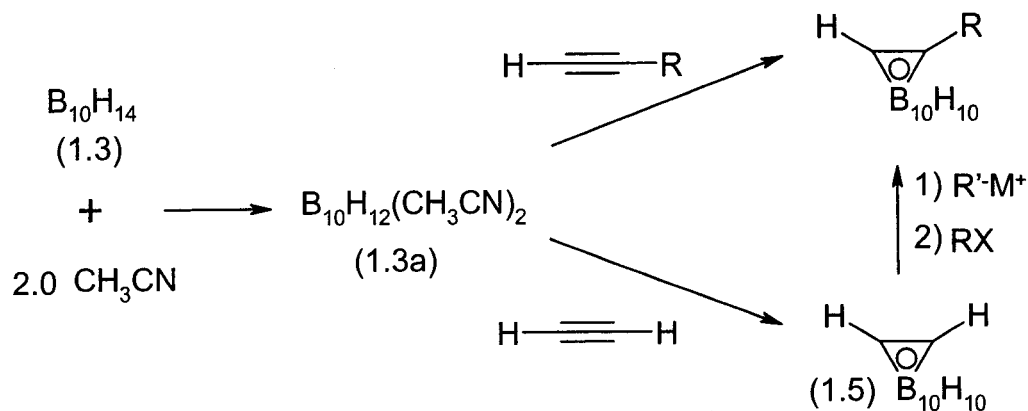
Synthesis of icosahedral neutral carboranes of the type $C_2B_{10}H_{12}$ proceeds from decaborane ($B_{10}H_{14}$). The process involves first “activating” decaborane by reacting it with a weak Lewis base (CH_3CN , R_3N , R_2S) to generate $B_{10}H_{12}L_2$ (Scheme 1.1). $B_{10}H_{12}L_2$ was first studied by Schaeffer in 1957 and the structure was later determined by Lipscomb.^{5,26,27} It was soon realized that the adduct was a good candidate for the synthesis of closed cage carboranes through insertion of an alkyne into the open face of the borane, replacing both Lewis bases and the two remaining bridging hydrogen atoms (Scheme 1.1).^{28,29} $B_{10}H_{12}L_2$, which can be prepared separately or generated in situ, when

heated to 80-110°C with an alkyne, will form the corresponding carborane in respectable yields.^{24,25}



Scheme 1.1 – Synthesis of ortho-carborane.

Having established a facile synthesis of carboranes from decaborane, two routes have since emerged and are used regularly in the preparation of C-substituted carborane derivatives (Scheme 1.2). The first approach involves generation of the carborane from the addition of acetylene to the Lewis base adduct of decaborane. Subsequent removal of a C-H proton by a base gives the conjugate base, and alkylation with the appropriate electrophile results in a C-substituted carborane.^{30,31} Alternatively, C-substituted carboranes can be prepared by reacting a substituted alkyne (terminal or internal) with B₁₀H₁₂L₂.³² The decision as to which procedure is best depends upon the nature of the functional groups present in the synthetic target.^{33,34}



Scheme 1.2 – Synthetic routes to substituted carboranes.

1.4 Isomerization of Dicarba-*closo*-dodecaboranes

1,2-Dicarba-*closo*-dodecaborane (1.5), otherwise referred to as *ortho*-carborane, can be converted to the 1,7- and 1,12- carborane isomers (herein referred to as *meta* (1.6) and *para* (1.7) carborane respectively) by thermal isomerization under an inert atmosphere. At 400°C (Figure 1.6), *ortho*-carborane converts to the *meta*-isomer, which in turn rearranges to the *para*-isomer at 750°C.

The mechanism of isomerization has been the subject of considerable interest.³⁵⁻³⁸ Lipscomb *et al.* were the first to propose a mechanism for the isomerization of *ortho*-carborane to *meta*-carborane.³⁹ This mechanism, which involves a cuboctahedral complementary geometry and a diamond-square-diamond (*dsd*) rearrangement, does not, however, explain the isomerization of *meta*-carborane to the *para*-isomer. More recently, Johnson *et al.* proposed a mechanism for the interconversion of the carboranes through anti-cuboctahedral complementary geometries.⁴⁰ Other theories have also been put forward, including the suggestion that the isomerization pathway involves the rotation of triangular faces on an unstable cuboctahedral intermediate, which is brought about by six

cooperative *dsd* processes.⁴¹ To date, there is no conclusive evidence as to the correct mechanism of isomerization. It is also interesting to note that the reverse isomerization of both *para* and *meta* carboranes is possible when the clusters are reduced to $[C_2B_{10}H_{12}]^{2-}$ (Figure 1.6).^{42,43}

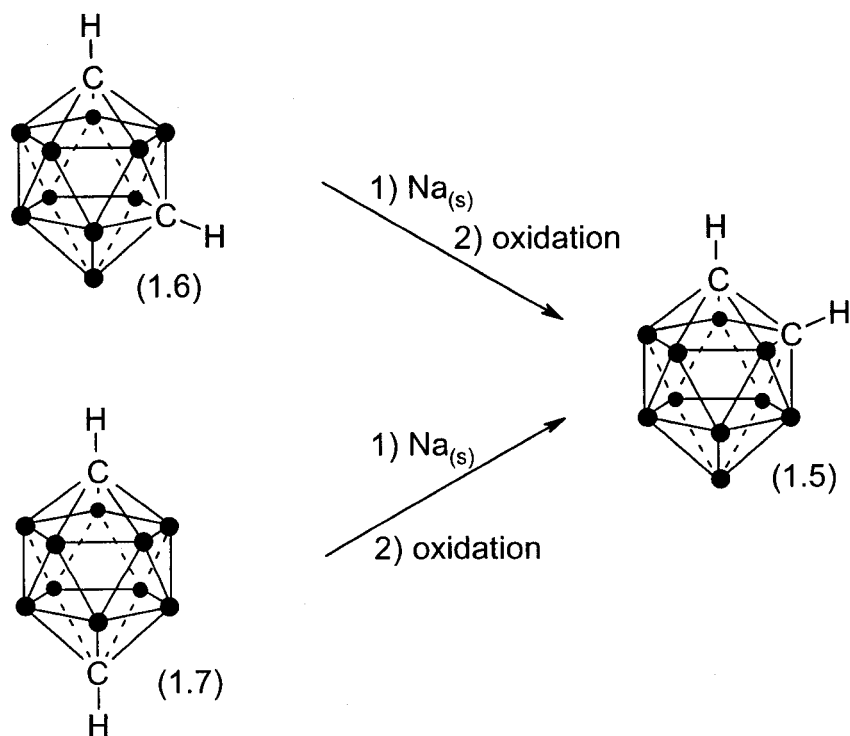
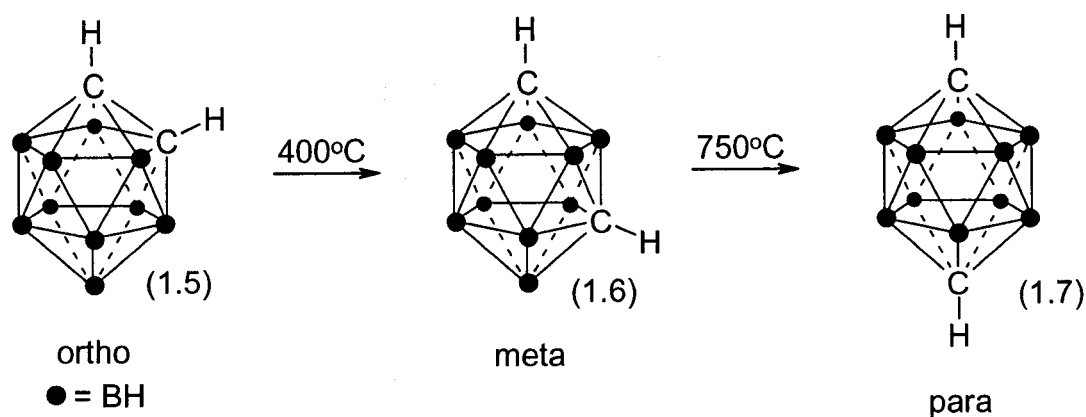


Figure 1.6 – Transformation of the isomeric forms of icosahedral carboranes.

1.5 Nomenclature of Carboranes

The term carborane originates from a contraction of the IUPAC approved designation of carbaborane. It is used to describe molecules composed as clusters of carbon and boron atoms. Polyhedra that contain all of the expected vertices, according to Wade's Rules, are designated with the prefix "closo". Numbering of the cage vertices in *closo*-carborane begins with an apex atom and the successive atoms are listed in "rings" in a clockwise direction (Figure 1.7). Carbon atoms are given the lowest numbers and are designated in front of the formula.¹ For example, the proper names for *ortho* and *para*-carborane are 1,2-dicarba-*closo*-dodecaborane and 1,12-dicarba-*closo*-dodecaborane respectively. Substitution off the cage is designated in the name by a numerical suffix (i.e. 1-(1,2-dicarba-*closo*-dodecaborane)-(pendant group name) for C-substituted *ortho*-carborane).^{44,45} Alternatively, the point of cage substitution can be indicated in a suffixal manner at the end of the polyhedral name (i.e. (1,2-dicarba-*closo*-dodecaboran-1-yl)-(pendant group name).

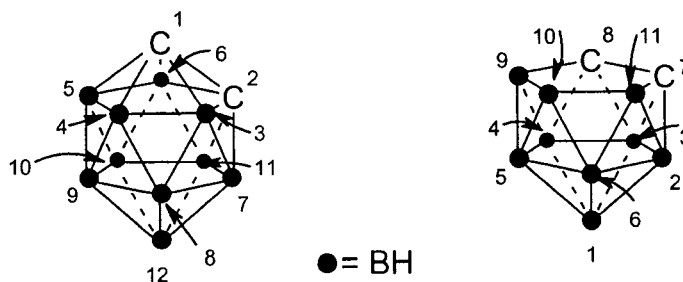


Figure 1.7 - Numbering system for *closo* and *nido* cage atoms.

Removal of a vertex from any member of the *closo*- polyhedral series generates, as mentioned previously, the related *nido*- system. The corresponding nomenclature for *nido-ortho*-carborane would be 7,8-dicarba-*nido*-undecaborane since the numbering of

the cage atoms begins at the vertex opposite to the open face and the carbon atoms are given the lowest possible numerical designation.

1.6 Derivatization of Icosahedral Carboranes

The carbon and boron vertices in carboranes exhibit orthogonal reactivity. The hydrogen atoms located off the carbon atoms of the cage are weakly acidic, with acidity constants comparable to those of alkynes (pK_a *ortho* = 22.0, pK_a *meta* = 25.6 and pK_a *para* = 26.8).^{46,47} In contrast, the hydrogen atoms on the boron vertices are removed by strong Lewis acids. The difference in reactivity between the two cage positions makes it possible to prepare a wide range of carbon and boron derivatives without the need to use complex protecting group strategies.⁴⁸⁻⁵⁰

The CH proton of *ortho*-carborane is more acidic than in *meta*- or *para*-carborane. This is as a consequence of the greater electronegativity of the adjacent carbon atom in *ortho*-carborane as compared to the other isomers, which only have boron vertices adjacent to the CH groups. As mentioned previously, deprotonation of the carbon vertex can be brought about through the use of strong, non-nucleophilic bases such as MeLi, PhLi and nBuLi. The resulting mono-lithiocarboranyl anions are sufficiently nucleophilic to react with a wide variety of electrophiles. The steric bulk of the carboranes, however, requires that the electrophile be unhindered and possess a good leaving group.

Derivatization of a boron vertex can be achieved using one of two fundamental strategies. One method involves reacting a carborane with a “hot” electrophile. Alternatively, BH groups can be derivatized by nucleophiles following two-electron reduction of the cage to the reactive dodecahedral dianion.⁵¹ Electrophilic substitution at

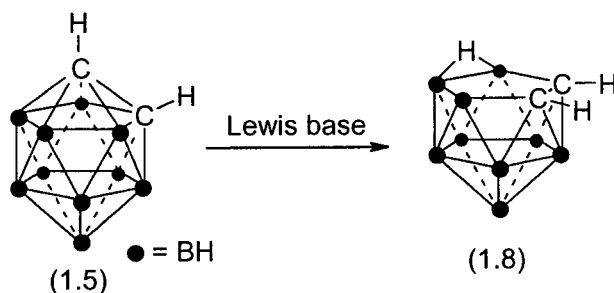
the BH vertices is analogous to the chemistry that is used to functionalize simple benzene derivatives. Halogenation of the boron vertices, for example, can be carried out using F₂ alone or Cl₂, Br₂ and I₂ in the presence of a Lewis acid. Reactions take place, at least initially, at the most electron rich boron vertex (ortho: B(9/12), meta B(9/10) and para: B(2-11)) however poly-substituted products are often observed.^{48-50,52,53} Notwithstanding, optimal reaction conditions have been reported so that it is possible to isolate mono-substituted halo-carboranes such as 9-iodo-*ortho*-carborane.⁵⁴

Reduction of carboranes by alkali metals has long been known, and was first described by Lipscomb.^{42,43} In the presence of a nucleophile, cage reduction of *ortho*-carborane is followed by nucleophilic attack at B(3) or B(6) positions. Subsequent reoxidation results in a boron-substituted carborane. This approach is often preferred over electrophilic reactions because of the greater regioselectivity.

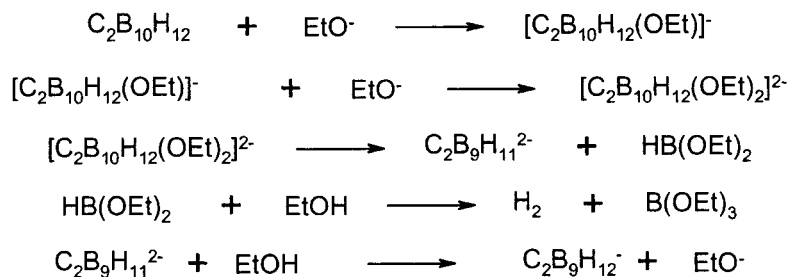
1.7 Degradation of Carboranes in Basic Solution

Although *closo*-carborane cages are highly resistant to chemical modification, Hawthorne and Wiesbock recognized that cage degradation can be brought about through nucleophilic attack on a cage boron atom.³³ The two adjacent carbon atoms present in the *ortho*-carborane cage framework are more electronegative than the cluster boron atoms. Consequently, the most electropositive boron atoms are those bonded directly to the two cage carbon atoms, namely boron atoms 3 and 6. Upon removal of one of these vertices, the resulting open face of the polyhedron consists of three boron atoms and two adjacent carbon atoms (Figure 1.7).

Cage degradation can be brought about in a range of solvents and with a variety of different bases. The most common strategy involves heating a carborane with ethoxide generated *in situ* from potassium hydroxide dissolved in ethanol (Scheme 1.3). The mechanism of the reaction involves nucleophilic attack at one of the electropositive boron vertices (B3 or B6) by ethoxide.⁵⁵ Addition of another ethoxide ion is followed by the loss of HB(OEt)_2 , which in turn, reacts with one more ethoxide ion to give triethoxyborane and molecular hydrogen (Scheme 1.4).³³



Scheme 1.3 – Formation of nido-ortho-carborane.



Scheme 1.4 - Proposed mechanism of cage degradation in an EtOH/KOH medium.

Upon formation of the *nido*-carborane, the open face of the degraded cage is protonated by a solvent molecule. The exact position of the proton has been debated for some time, and it was originally thought to occupy the vertex once occupied by a boron atom.^{12,13} This theory has since been modified based on solution state NMR data, which

suggests two possibilities, that the hydrogen atom transiently bridges two boron atoms on the open face of the polyhedral cage (Figure 1.8),^{56,57} or is located statically off of B(10) with minimal interaction with the adjacent boron atoms (B(9) and B(11)).^{58,59} Two-dimensional heteronuclear ^1H - ^{13}C (COSY) studies established early on that there were no interactions between the cage carbon atoms and the “extra” hydrogen atom.⁵⁸ X-ray diffraction studies performed by Wade and co-workers and neutron diffraction studies by Hughes et al. further confirmed that the hydrogen atom is in fact bridged between boron atoms on the open face.⁶⁰ Boron-hydrogen distances were determined to be 1.252(10)Å for H-B(10) and 1.469(11)Å for H-B(9)/H-B(11).

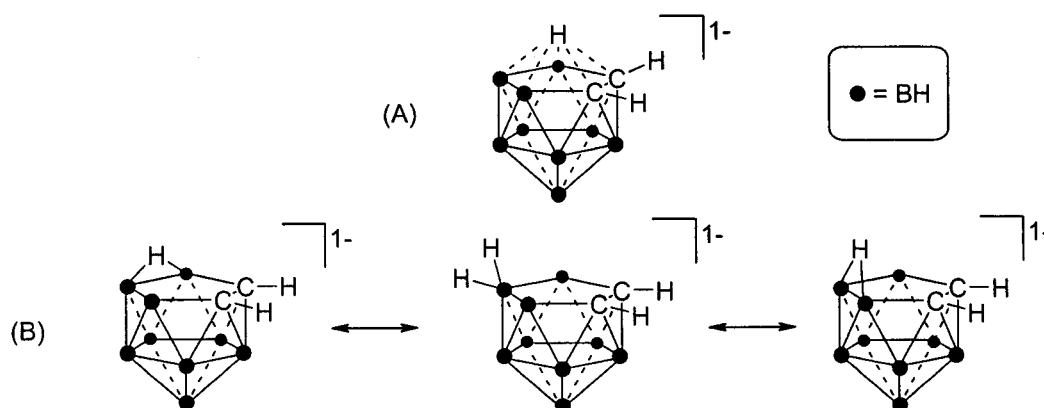


Figure 1.8 - A) original and B) current proposals for the structure of nido-carborane.

It is also possible to convert *meta*- and *para*-carboranes to the corresponding *nido*-anions (Figure 1.9). The *nido*-7,9- $[\text{C}_2\text{B}_{10}\text{H}_{12}]^-$ anion, obtained from *meta*-carborane, can be synthesized by heating the *closo* precursor to reflux in alcoholic KOH or aqueous solutions containing the fluoride ion.⁶¹⁻⁶⁴ Subsequent X-ray diffraction studies determined the location of the bridging hydrogen atom in a *nido-meta*-carborane to be located between atoms B(10) and B(11), again with no interaction of the bridging

hydrogen with the cage carbon atoms. Likewise, *para*-carborane can be converted to the corresponding *nido*-2,9-[C₂B₁₀H₁₂]⁻ by heating the cluster to reflux in KOH/isopropanol, tetraglyme or toluene. The solid-state structure of 2,9-[C₂B₁₀H₁₂]⁻, obtained by Hughes and co-workers, showed the bridging hydrogen to reside at the symmetrical site between cage atoms B(7) and B(11).⁶⁵

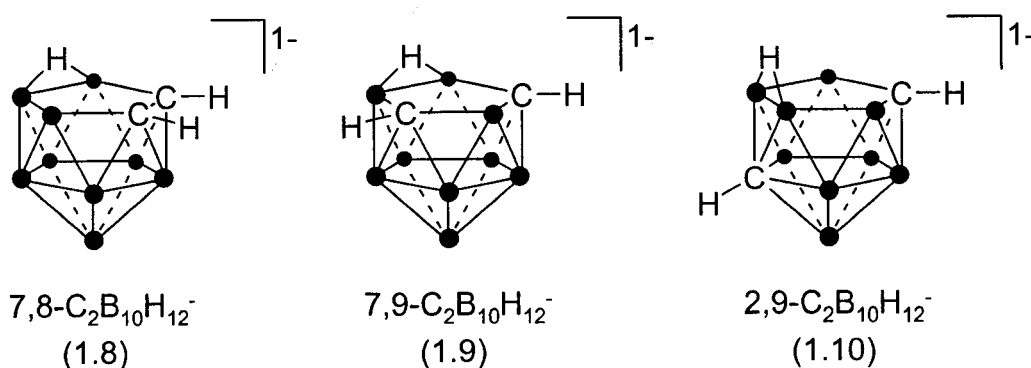


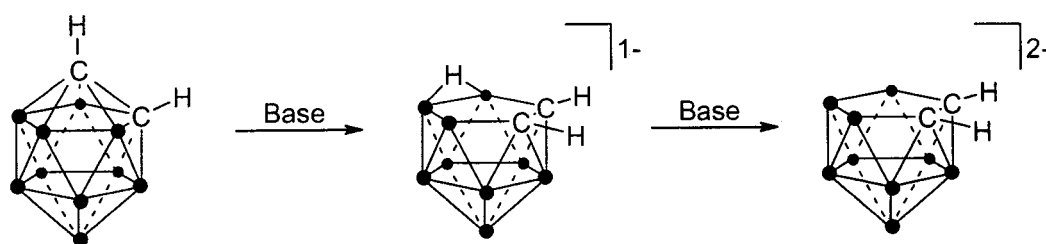
Figure 1.9 - Structure representations of the *nido*-forms of *ortho*- (1.8), *meta*- (1.9) and *para*- (1.10) carboranes.

1.8 The Dicarborollide Dianion

As mentioned previously, strong bases react with *ortho*- and *meta*- carborane to generate the corresponding hydrophilic *nido* (dicarbaundecaborate(1-)) ions. The *nido*-7,8 and 7,9-[C₂B₉H₁₂]⁻ ions each contain a bridging hydrogen atom on the open face of the cage, which can be readily removed with strong base (KH, nBuLi) to give the corresponding dicarborollide dianions (7,8 and 7,9-[C₂B₁₀H₁₁]²⁻) (Scheme 1.5).

The dicarborollide dianion is formally isolobal to cyclopentadienide (Cp⁻) and can therefore be used to prepare analogous metal complexes such as the carborane analogue of ferrocene (Figure 1.10).^{66,68} Both Cp⁻ and the dicarborollide dianion structures contain

six delocalized electrons in π -type orbitals.^{67,68} There are, however, a few features that serve to enhance the binding affinity of the carborane dianion toward metals compared to cyclopentadienide. These include the inward tilting of the frontier orbital,⁶⁸ the formal dinegative charge, and the presence of heteroatoms on the open face. Since the first report of a metallocarborane by Hawthorne and co-workers,⁶⁸ numerous carborane-based organometallic complexes have been prepared.⁶⁹



Scheme 1.5 – Generation of the dicarbollide dianion.

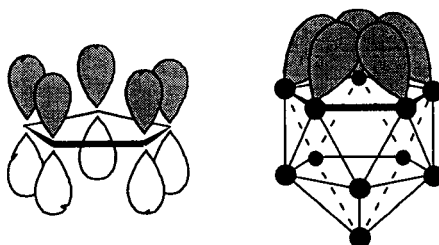


Figure 1.10 - Frontier orbital representation of $[C_5H_5]$ (left) and $[C_2B_9H_{11}]$ (right).

1.9 The Medicinal Chemistry of Carboranes

Due to their high boron content, size, lipophilicity, stability *in vivo*, and versatile synthetic chemistry, carboranes are attractive synthons for medicinal chemistry research. Some of the current and potential uses of carboranes in biological/medicinal chemistry are described herein. Additional details can be found in a review written by our group.⁷⁰

1.10 Boron Neutron Capture Therapy (BNCT)

Traditional methods for the destruction of cancerous tissue include surgery, radiotherapy, and chemotherapy, or a combination of these techniques. Surgical removal of a tumor is usually the method of choice, especially if the cancer is localized in a solitary mass and can be removed with minimal risk. Unfortunately, not all tumors are localized in one mass and it is also possible that during surgery some cells escape from the main tumor and serve as the foci for the formation of new post-operative tumors. As an alternative to physical removal, radiotherapy has been used as a non-invasive alternative to surgery in which a lethal dose of ionizing radiation is directed at the affected area. This technique is again only appropriate for tumors that are concentrated in a small number of primary masses.⁷¹ The third line of defence in cancer therapy is chemotherapy, in which a substance that is toxic to tumor cells is administered to patients. Drug therapy remains the most effective modality for widely metastasized tumors.⁷² In this scenario, the amount of drug administered is limited by normal tissue tolerance, which in turn raises concerns over the development of tumor resistance.

In order to circumvent the individual limitations of these treatment techniques the different therapy strategies are often used concomitantly, in the hope that the total effect of the combined modalities will be greater than the sum of their individual parts. The problem of selective tumor cell destruction still remains, and as a result, has brought about the development of a host of other potential treatment regimes including some that utilize binary treatment strategies. These two-component treatment methods are attractive alternatives to conventional therapies because each part of the treatment technique is not

harmful to biological tissue on its own. Each component can be manipulated independently and only the combination of the two components produces a cytotoxic effect. Binary treatment strategies currently include: radiation sensitization,^{73,74} photon activation therapy,⁷⁵ photodynamic therapy,^{76,77,78} gene therapy^{79,80} and neutron capture therapy.⁷⁰

With the discovery of the neutron by Chadwick⁸² in 1932, and the subsequent characterization of the boron-10 neutron capture reaction by Fermi⁸³ and Taylor⁸⁴ in 1935, Locher proposed the potential use of boron in the treatment of cancer in 1936.⁸⁵ Boron Neutron Capture Therapy (BNCT) is a binary radiation therapy that involves the capture of slow (thermal) neutrons by boron atoms selectively delivered to tumor cells.^{86,87} The nuclear event begins with the capture of a neutron by a boron-10 nucleus, producing an energetically excited boron-11 nucleus (Figure 1.11). This unstable intermediate undergoes fission, generating two daughter nuclei, (lithium-7 and helium-4 (alpha) particles), which possess a large amount of kinetic energy. The fission products travel through tissue creating ion tracks, which in the process, causes irreversible cellular damage. The daughter nuclides travel 5-7 μm before their kinetic energy is spent, which is approximately the diameter of a typical human cell.⁸⁸⁻⁹⁰ The result is a highly localized, cytotoxic event, capable of damaging the target cell without affecting the surrounding healthy tissue (Figure 1.12). The intracellular damage caused by the high linear energy transfer (LET) particles induces apoptosis.

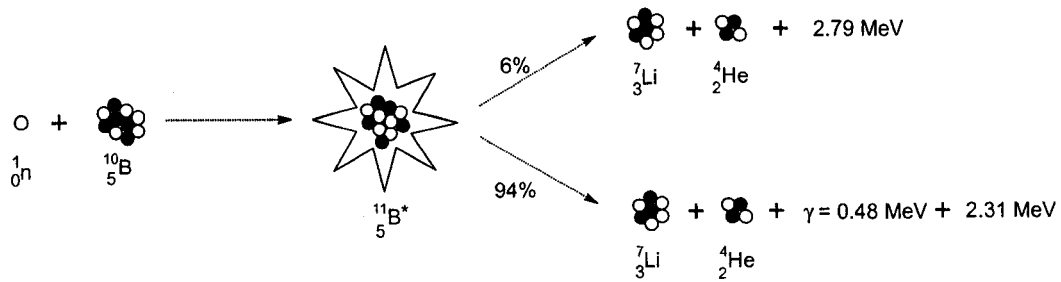


Figure 1.11 – The boron-10 neutron capture reaction.

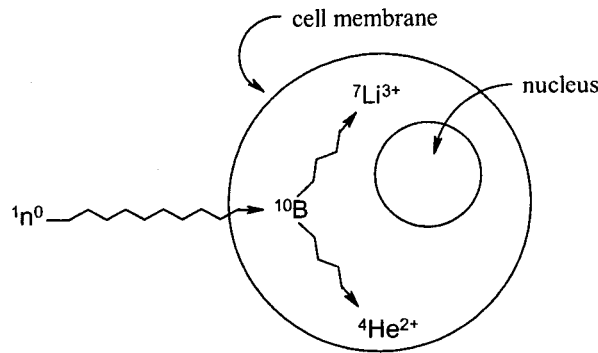


Figure 1.12 - Neutron capture event occurring within a cell.

In addition to the desired neutron capture event involving boron-10, one cannot ignore the possibility of neutron capture occurring with the more abundant endogenous elements. Table 1.1 shows the most abundant nuclei in healthy tissue, their relative natural isotopic and tissue abundance, and neutron capture cross-section. The development of a neutron capture therapy relies upon the fact that biological tissue contains elements with low capture cross-sections. Due to their high concentration however, it is evident that the radiation dose contribution from the ${}^1\text{H}(n,\gamma){}^2\text{H}$ and ${}^{14}\text{N}(n,p){}^{14}\text{C}$ reactions need to be considered when evaluating patient dose (Figure 1.13).

Sweet and co-workers calculated that 10 to 30 μg ${}^{10}\text{B}$ per gram of tumor, or approximately 1.0×10^9 ${}^{10}\text{B}$ atoms is needed to decrease the probability of activating

endogenous nuclei, thereby maximizing the radiation dose NCT delivers to the tumor.⁹¹⁻⁹⁵

The inability to achieve these therapeutic levels of boron was the main reason why the first BNCT clinical trials, held in the 1960's, failed to achieve any therapeutic value. In these trials, simple boron compounds such as ¹⁰B enriched sodium borate (Borax and pentaborate, Figure 1.14) and boric acid were used as delivery vehicles. Unfortunately a

nuclide	weight (% tissue)	nat. abund. (%)	cross section (barns)
¹ H	10.00	99.98	0.332
¹² C	18.0	98.89	0.0034
¹⁴ N	3.0	99.63	1.82
¹⁶ O	65.0	99.76	0.00018
²³ Na	0.11	100	0.43
²⁴ Mg	0.04	77.4	0.053
³¹ P	1.16	100	0.18
³² S	0.20	94.93	0.53
³⁵ Cl	0.16	75.53	32.68
³⁹ K	0.20	93.26	2.1
⁴⁰ Ca	2.01	96.94	0.4
⁵⁶ Fe	0.01	91.75	2.57

Table 1.1 – Neutron Capture Cross-Section and Relative Abundance⁹⁶ of Tissue Elements.

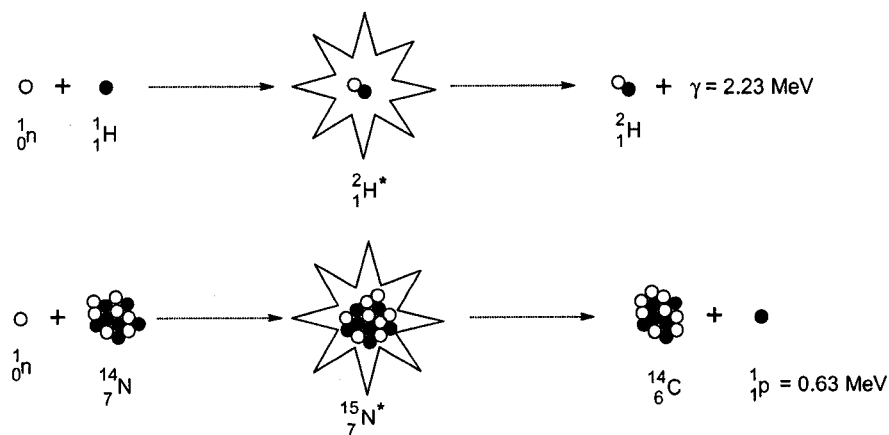


Figure 1.13 - Neutron capture reactions of ^1H and ^{14}N .

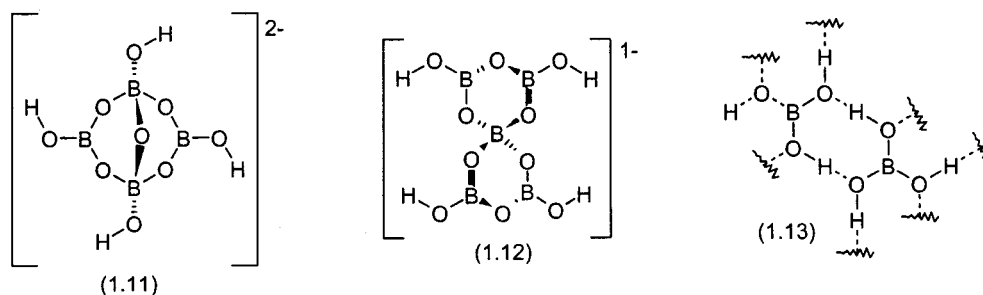


Figure 1.14 – Sodium borates and boric acid. From left to right: Borax ($\text{Na}_2\text{B}_4\text{O}_7 \cdot 10\text{H}_2\text{O}$) (1.10), Pentaborate ($\text{NaB}_5\text{O}_8 \cdot 4\text{H}_2\text{O}$) (1.11) and Boric acid [$\text{B}(\text{OH})_3$] (1.13).

number of patients suffered severe side effects (vascular necrosis), due primarily to the widespread distribution of the boron delivery vehicle in both cancerous and healthy tissue at the time of neutron irradiation.^{97,98}

The next generation of boron compounds for BNCT were analogues of simple biological substrates known to incorporate into tumors. For example, L-p-hydroxyphenylboronic acid (p-boronophenylalanine, BPA, compound 1.14), a boronic acid derivative of phenylalanine, was designed to mimic the *in vivo* behaviour of the

natural amino acid. Phenylalanine is a precursor to melanin, the pigment responsible for tumor colouration, and is present in higher concentrations in tumor cells. Discovered in 1958, BPA-BNCT has shown a great deal of promise in the treatment of skin cancer (Figure 1.15) and is currently undergoing clinical trials. Unfortunately one major limitation of BPA is that it delivers only one atom of boron per molecule, thereby requiring large doses to be administered to patients in order to achieve therapeutic levels of boron in the tumor.

Sodium mercaptoundecahydrododecaborate (BSH, $\text{Na}_2\text{B}_{12}\text{H}_{11}\text{SH}$, compound 1.15) (Figure 1.15) is another compound currently under investigation for its usefulness as a BNCT agent in the treatment of glioblastoma multiforme, a particularly aggressive and deadly form of brain cancer. Unfortunately this compound shows non-specific uptake in healthy brain tissue.

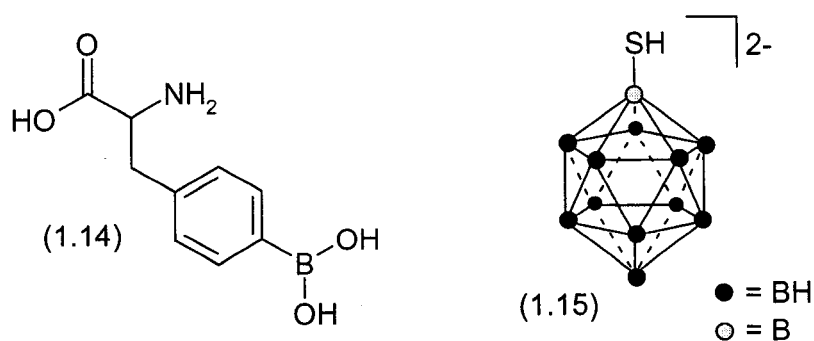


Figure 1.15 - Structures of a) BPA and b) BSH, current BNCT agents in clinical trials.

To compensate for the low weight percentage of boron in boronic acid derivatives (BPA), carboranes have been identified as ideal synthons for the construction of new agents because of their high boron content and the ease with which they can be linked to, or incorporated within, targeting agents.^{24,70} Consequently the third generation of BNCT

agents include carborane derivatives of carbohydrates,⁹⁹⁻¹⁰⁴ porphyrin (in both the porphyrin core,¹⁰⁵⁻¹⁰⁷ and as pendant groups),¹⁰⁸⁻¹¹¹ DNA intercalators,¹¹² polyamines,¹¹³ nucleosides,¹¹⁴⁻¹¹⁵ immunoconjugates,¹¹⁶ and liposomes.¹¹⁷ However, due to issues surrounding toxicity or lack of specificity, to date only a handful of these compounds have entered into clinical trials.⁷⁰

1.11 Carboranes in Drug Development

The initial attraction of carboranes to medicinal chemistry research was the result of their inherent high boron content (*vide supra*) and stability *in vivo* and hence their usefulness in BNCT. More recently, other uses of carboranes have begun to surface. For example, these polyhedra have been exploited for their hydrophobic nature, which can be used to enhance hydrophobic interactions between a drug substrate and the corresponding target receptor.¹¹⁸ A number of researchers have focused on the use of the polyhedral cage as a hydrophobic pharmacophore, and have synthesized a variety of anti-neoplastic agents,¹¹⁹ estrogen agonists and antagonists,¹²⁰ retinoids,^{121,122} protein kinase C modulators¹²³ and TNF- α modulators.¹²⁴ All are examples of compounds developed with carboranes used specifically as a hydrophobic entity to enhance receptor binding.

Carboranes have also been used as ligands for carrying both diagnostic and therapeutic, metallic and non-metallic radionuclides.⁹⁰ For example, previous studies have described the binding of different isotopes of iodine, hydrogen (tritium), astatine and cobalt to carboranes.

The labelling of carboranes with isotopes of iodine has garnered much attention because the most common method for the labelling of proteins is radioiodination. In this

approach, various aromatic moieties throughout the structure are iodinated using one of several possible techniques.¹²⁵ Thus, the radioiodination of *nido* 7,8 and 7,9-C₂B₉H₁₁ derivatives has been explored in which the polyhedral carborane was to be used as an inorganic carrier for the radionuclide. Advantages of this system over the traditional approach include the inherent *in vivo* stability of carboranes and the stronger B-I (381±21 KJ/mol) versus C-I (209±21 KJ/mol) bond strength, making the iodo-carborane less likely to undergo dehalogenation upon administration. The iodination of *nido*-carboranes was first reported by Hawthorne and co-workers in 1991;¹²⁶ since then, a number of other functionalized derivatives have been reported, including carboranes substituted with isothiocyanatophenyl groups,¹²⁷ 2-nitroimidazoles,^{128,129} amides,¹³⁰ oligomeric phosphate diesters and carboranyl peptides.^{131,132}

In biodistribution studies, the boron clusters were labelled using two different approaches. The first approach, biomolecules, such as epidermal growth factor or immunoproteins, were coupled with derivatized polyhedral boron clusters. Subsequent radioiodination of the whole conjugate occurs, placing the radioiodine on the boron cluster and on aromatic moieties throughout the protein structure. Typically, radioiodination occurs in the presence of an oxidizing agent which cause halogenation of one or many cage boron vertices. These conditions also induce electrophilic aromatic substitution with aromatic amino acids present. In the second approach, boron clusters are radioiodinated prior to being conjugated with the biomolecule, providing conjugates in which only the polyhedral cages are labelled.^{133,134}

This procedure has also been used in similar studies with various immunoconjugates radiolabelled with astatine-211 and tritium.^{90,135-137} Sjöberg et al. reported the use of polyhedral carboranes as ligands for the direct labelling of proteins (biotin) with astatine-211.¹³⁸ A *nido*-carboranyl propionate derivative was used and astatination was accomplished using a similar method to that reported for iodine. Electrophilic addition occurs in the presence of the oxidizing agent Chloramine-T. The use of a carborane as a carrier for astatine is critical, as direct astatination of biomolecules is generally unsuccessful due to the weak carbon-astatine bond.⁹⁰

1.12 Metallocarboranes and Medical Imaging

It was quickly realized that carboranes, or more specifically *nido*-carboranes, are ideal candidates for the binding of metal-based radionuclei. As mentioned previously, Hawthorne and co-workers reported the first organometallic complex of carboranes,^{68,69} and it was this group that also extended this concept to synthesize a novel radiometal ligand to bind isotopes of cobalt. The reported system, also known as the Venus Flytrap Cluster (VFC), is comprised of two *nido*-7,9-[C₂B₉H₁₁]²⁻ dicarbollide ions bridged with a bifunctional pyrazole molecule (Figure 1.17). A VFC complex of ⁵⁵Co, a positron emitting isotope, was used to determine the fate of an anti-CEA monoclonal antibody in small animal studies, and shows promise as a potential liver metastasis imaging agent.^{90,139}

The ability to radiolabel carboranes has implications in BNCT research. One of the greatest obstacles to the advancement of this field is associated with the inefficiencies of the methods used to determine the distribution of new boron-10 delivery vehicles. The

current strategy involves administering the compound to animals and then at set time points the subject is sacrificed and the boron distribution determined by elemental

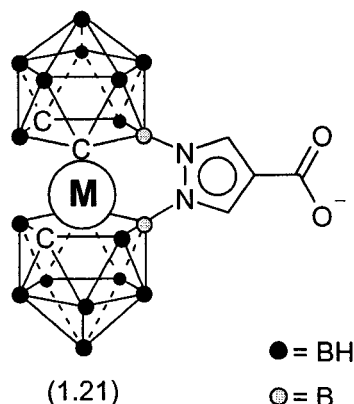


Figure 1.17 – Venus Flytrap cluster concept by Hawthorne and co-workers.

analysis following dissection.^{140,141} This approach is time consuming, expensive, and provides only a snapshot of the compound's distribution profile. It is also prone to error due to subject-to-subject variability.

Radioimaging techniques are currently being explored as a means to overcome the limitations associated with determining biodistribution profiles from excised tissue samples. Clinical imaging techniques such as PET, SPECT and ¹¹B/¹⁰B MRI are being used to evaluate the distribution of novel pharmaceuticals in animals and in humans. Consequently, radioimaging, so long as the appropriate radiolabelled compounds can be prepared, can similarly be used to evaluate novel BNCT agents accurately and rapidly. With a judiciously labelled boron compound, one can determine not only biodistribution and pharmacokinetics, but also information pertaining to the optimal duration of neutron bombardment, which is an important aspect of treatment planning exercises.

While several examples exist in which PET imaging is used to quantify boron uptake into specific tissue,¹⁴²⁻¹⁵⁵ only one involves the use of carboranes as a targeted radionuclide carrier. More specifically, those examples in which PET was used as a tool to aid in establishing BNCT treatment methods involve labelled derivatives of BPA, BSH and boric acid functionalized polyamines. However, one study by dos Santos et al. reports the synthesis of carborane benzimidazole derivatives that are labelled with ^{73}Se .¹⁵⁶ The strategy presented was to attach a carborane to a well known DNA binding ligand. While the total synthesis of a number of derivatives was reported, no clinical trials were performed.

1.13 Scope and Summary of Research

The overarching goal of the work reported in this thesis was to take advantage of the unique chemical and physical properties of carboranes to prepare a new generation of BNCT agents. Carboranes were chosen due to their substantial boron content, the fact that they can be radiolabelled and that they can be readily linked to a targeting entity. To this end two distinct strategies were investigated. The first approach, described in chapters 2 and 3, involved the synthesis of carborane analogues of the anti-estrogen tamoxifen. The addition of the carborane to the basic core of tamoxifen was designed to increase hydrophobic interactions between the anti-cancer agent and the ER receptor, thus increasing the drug potency while also serving as a source of boron for BNCT. Furthermore, a *nido*-carborane product could serve as a bifunctional ligand for the

binding of ^{99m}Tc . In turn it is hoped that the above mentioned compounds could also serve as a novel class of imaging agent for the detection of breast cancer tumors.

In parallel to the above research, an alternative boron delivery strategy was developed based on poly-substituted boron-transition metal complexes. To this end, two homoleptic Re(I) $[\text{ReL}_6]^+$ (L = *ortho* or *para*-carborane isonitrile) complexes of *ortho* and *para*-carborane isocyanide ligands were prepared as a new class of metal-based BNCT agents. These compounds are attractive agents for neutron capture therapy due to their exceptionally high boron content, the ease with which they can be targeted to specific receptors, and the fact that the biodistribution can be determined non-invasively using radioimaging techniques with the incorporation of the appropriate metal radionuclide. This research revealed some unexpected differences between the chemistry of *ortho*- and *para*-carboranes.

1.14 References

- ¹ Dilthey, W. Z. *Angew. Chem.* **1921**, 34, 596.
- ² Stock, A. *Hydrides of Boron and Silicon*; Cornell University Press: Ithaca, NY, 1933.
- ³ Pitzer, K.S. *J. Am. Chem. Soc.* **1945**, 67, 1126.
- ⁴ Eberhardt, W.H.; Crawford, B.; Lipscomb, W.N. *J. Chem. Phys.* **1954**, 22, 989.
- ⁵ Lipscomb, W.N. *Boron Hydrides*; W.A. Benjamin: New York, 1963.
- ⁶ Longuet-Higgins, H.C.; Roberts, M. de V. *Proc. Roy. Soc. (London)* **1955**, A230, 110.
- ⁷ Hoffman, R.; Lipscomb, W.N. *J. Chem. Phys.* **1962**, 36, 3489.
- ⁸ Hoffman, R.; Lipscomb, W.N. *J. Chem. Phys.* **1962**, 37, 520.
- ⁹ Mingos, D.M.P.; Wales, D.J. *Introduction to Cluster Chemistry*; Prentice Hall, Englewood Cliffs, N.J. 1990.
- ¹⁰ Gillespie, R.J.; Porterfield, W.W.; Wade, K. *Polyhedron* **1987**, 6, 2129.
- ¹¹ Williams, R.E. *Chem. Rev.* **1992**, 92, 177.
- ¹² Dobrott, R.D.; Lipscomb, W.N. *J. Chem. Phys.* **1962**, 37, 1779.
- ¹³ Wunderlich, J.A.; Lipscomb, W.N. *J. Am. Chem. Soc.* **1960**, 82, 4427.
- ¹⁴ O'Neill, M.E.; Wade, K.; Grimes, R.N. (ed.) *Metal Interactions with Boron Clusters*. Plenum Press. New York. (1982). pp.1-114.
- ¹⁵ Moore, E.B.; Lipscomb, W.N.; Lohr, L.L. *Journal of Chemical Physics.* **1963**, 35, 1329.
- ¹⁶ Hawthorne, M.F. *J. Am. Chem. Soc.* **1960**, 82, 3228.
- ¹⁷ Klanberg, F.; Eaton, D.R.; Guggenberg, L.J.; Muettterties, E.L. *Inorg. Chem.* **1967**, 6, 1271.
- ¹⁸ Aihara, J.-i. *J. Am. Chem. Soc.* **1978**, 100, 3339.
- ¹⁹ King, R.B.; Rouvray, D.H. *J. Am. Chem. Soc.* **1977**, 99, 7834.
- ²⁰ Stone, A.J.; Alderton, M.J. *Inorg. Chem.* **1982**, 21, 2297.
- ²¹ King, B.R. *Chem. Rev.* **2001**, 101, 1119.
- ²² Shapiro, I.; Good, C.D.; Williams, R.E. *J. Am. Chem. Soc.* **1962**, 84, 3837.
- ²³ Shapiro, I.; Keilin, B.; Williams, R.E.; Good, C.D. *J. Am. Chem. Soc.* **1963**, 85, 3167.
- ²⁴ Heying, T.L.; Ager, Fr., J.W.; Clark, S.L.; Mangold, D.J.; Goldstein, H.L.; Hillman, M.; Polak, R.J.; Szymanski, J.W. *Inorganic Chemistry* **1963**, 2, 1089.
- ²⁵ Fein, M.M.; Bobinski, J.; Mayes, N.; Schwartz, N.; Cohen, M.S. *Inorg. Chem.* **1963**, 2, 1111.
- ²⁶ Hawthorne, M.F.; Pilling, R.L.; Vasavada, R.C. *J. Am. Chem. Soc.* **1967**, 89, 1075.
- ²⁷ Schaeffer, R. *J. Am. Chem. Soc.* **1957**, 79, 1006.
- ²⁸ McKee, M. L. *J. Am. Chem. Soc.* **1995**, 117, 8001.
- ²⁹ McKee, M.L.; *J. Am. Chem. Soc.* **1996**, 118, 421.
- ³⁰ Cai, J.; Nemoto, H.; Singaram, B.; Yamamoto, Y. *Tetrahedron Lett.* **1996**, 37, 3383.
- ³¹ Gomez, F.A.; Hawthorne, M.F. *J. Org. Chem.* **1992**, 57, 1384.
- ³² Wu, Y.; Carroll, P. J.; Quintana, W. *Polyhedron* **1998**, 17, 3391.
- ³³ Hawthorne, M.F.; Wiesbock, R. A. *J. Am. Chem. Soc.* **1964**, 86, 1642.
- ³⁴ Lee, S.H.; Park, Y.J.; Yoon, C.M. *Tetrahedron Lett.* **1999**, 40, 6049.
- ³⁵ Hoffmann, R.; Lipscomb, W.N. *Inorg. Chem.* **1963**, 231.

- ³⁶ Kaesz, H.D.; Bau, R.; Beall, H.A.; Lipscomb, W.N. *J. Am. Chem. Soc.* **1967**, 89, 4218.
- ³⁷ Kaczmarczyk, A.; Dobrott, R.D.; Lipscomb, W.N. *Proc. Natl. Acad. Sci. U.S.A.* **1962**, 48, 729.
- ³⁸ Grafstein, D.; Dvorak, J. *Inorg. Chem.* **1963**, 2, 1128.
- ³⁹ Lipscomb, W.N. *Science* **1966**, 153, 373.
- ⁴⁰ Johnson, B.F.G.; Roberts, Y.V.; Parisini, E. *Inorg. Chim. Acta* **1993**, 211, 17.
- ⁴¹ Kaesz, H.D.; Bau, R.; Beall, H.A.; Lipscomb, W.N. *J. Am. Chem. Soc.* **1967**, 89, 4218.
- ⁴² Hoffmann, R.; Lipscomb, W.N. *J. Chem. Phys.* **1962**, 36, 3489.
- ⁴³ Hoffmann, R.; Lipscomb, W.N. *Inorg. Chem.* **1963**, 2, 231.
- ⁴⁴ Wu, Y.; Carrol, J.; Kang, S. O.; Quintana, W. *Inorg. Chem.* **1997**, 36, 4753.
- ⁴⁵ Nabakka, J.M.; Harwell, D.E.; Knobler, C.B.; Hawthorne, M.F. *J. Organomet. Chem.* **1998**, 550, 423.
- ⁴⁶ Kashin, A.N.; Butin, K.P.; Stanko, V.I.; Beletskaya, I.P. *Izv. Akad. Nauk. SSSR. Ser. Khim.* **1969**, 9, 1917.
- ⁴⁷ Leites, L.A. *Chem. Rev.* **1992**, 92, 279.
- ⁴⁸ Gomez, F.A.; Johnson, S.E.; Hawthorne, M.F. *J. Am. Chem. Soc.* **1991**, 113, 5915.
- ⁴⁹ Gomex, F.A.; Hawthorne, M.F. *J. Org. Chem.* **1992**, 57, 1384.
- ⁵⁰ Douglass, A.G.; Pakhomov, S.; Reeves, B.; Janousek, Z.; Kaszynski, P. *J. Org. Chem.* **2000**, 65, 1434.
- ⁵¹ Birch, A.J.; Nasipuri, D. *Tetrahedron* **1959**, 6, 148.
- ⁵² Hoffmann, R.; Lipscomb, W.N. *J. Chem. Phys.* **1962**, 36, 2179.
- ⁵³ Bragadze, V.I. *Chem. Rev.* **1992**, 92, 209.
- ⁵⁴ Andrews, J.S.; Zayas, J.; Jones, Jr. M. *Inorg. Chem.* **1985**, 24, 3715.
- ⁵⁵ Hawthorne, M.F. *J. Am. Chem. Soc.* **1968**, 90, 861.
- ⁵⁶ Howe, D.V.; Jones, C.J.; Wiersema, R.J.; Hawthorne, M.F. *Inorg. Chem.* **1971**, 10, 2516.
- ⁵⁷ Hermanek, S. *Chem. Rev.* **1992**, 92, 325.
- ⁵⁸ Fontaine, X.L.R.; Greenwood, N.N.; Kennedy, J.D.; Nestor, K.; Thornton-Pett, M.; Heřmánek, S.; Jelínek, T.; Štíbr, B. *J. Chem. Soc., Dalton Trans.* **1990**, 681.
- ⁵⁹ Štíbr, B. *Chem. Rev.* **1992**, 92, 225.
- ⁶⁰ Davidson, M.G.; Fox, M.A.; Hibbert, T.G.; Howard, J.A.K.; MacKinnon, A.; Neretin, I.S.; Wade, K. *Chem. Commun.* **1999**, 1649.
- ⁶¹ Fox, M.A.; Gill, W.R.; Herbertson, P.L.; MacBride, J.A.H.; Wade, K.; Colquhoun, H.M. *Polyhedron* **1996**, 15, 565.
- ⁶² Fox, M.A.; MacBride, J.A.H.; Wade, K. *Polyhedron* **1997**, 16, 2499.
- ⁶³ Fox, M.A.; Wade, K. *Polyhedron* **1997**, 16, 2517.
- ⁶⁴ Yoo, J.; Hwang, J.-W.; Do, Y. *Inorg. Chem.* **2001**, 40, 568.
- ⁶⁵ Fox, M.A.; Goeta, A.E.; Hughes, A.K.; Johnson, A.L. *J. Chem. Soc., Dalton Trans.* **2002**, 2132.
- ⁶⁶ Kang, H.C.; Lee, S.S.; Knobler, C.B.; Hawthorne, M.F. *Inorg. Chem.* **1991**, 30, 2024.
- ⁶⁷ Hanusa, T.P. *Polyhedron* **1982**, 1, 663.
- ⁶⁸ Hawthorne, M.F.; Young, D.C.; Wegner, P.A. *J. Am. Chem. Soc.* **1965**, 87, 1818.
- ⁶⁹ Grimes, R.N. *Chem. Rev.* **1992**, 92, 251.

- ⁷⁰ Valliant, J.F.; Guenther, K.J.; King, A.S.; Morel, P.; Schaffer, P.; Sogbein, O.O.; Stephenson, K.A. *Coord. Chem. Rev.* **2002**, 232, 173.
- ⁷¹ Sano, K. *Neurosurg. Rev.* **1986**, 9, 13.
- ⁷² Kornblith, P.L.; Walker, M. *J. Neurosurg.* **1988**, 66, 1.
- ⁷³ Kennedy, K.A. *Anti-Cancer Drug Des.* **1987**, 2, 181.
- ⁷⁴ Kennedy, K.A.; Teicher, B.A.; Rockwell, S.; Sartorelli, A.C. *Biochem. Pharmacol.* **1990**, 29, 1.
- ⁷⁵ Laster, B.H.; Thomlinson, W.C.; Fairchild, R.G. *Radiat. Res.* **1993**, 133, 219.
- ⁷⁶ Bonnet, R. *Chem. Soc. Rev.* **1995**, 19.
- ⁷⁷ Wainright, M. *Chem. Soc. Rev.* **1996**, 351.
- ⁷⁸ Diamond, I.; Granelli, S.; McDonagh, A.F.; Nielson, S.; Wilson, C.B.; Jaenicke, R. *Lancet* **1972**, ii, 1175.
- ⁷⁹ Caruso, M. *Mol. Med. Today* **1996**, May, 212.
- ⁸⁰ Culver, K.W. *CNS Drugs* **1996**, 6, 1.
- ⁸¹ Soloway, A.H.; Zhuo, J.-C.; Rong, F.G.; Lunato, A.J.; Ives, D.H.; Barth, R.F.; Anisuzzaman, A.K.M.; Barth, C.D.; Barnum, B.A. *J. Organomet. Chem.* **1999**, 581, 150.
- ⁸² Chadwick, J. *Nature* **1932**, 129, 312.
- ⁸³ Fermi, E.; Amaldi, E.; D'Agostino, O.; Rasetti, F.; Segre, E. *Proc. Roy. Soc.* **1934**, A146, 483.
- ⁸⁴ Taylor, H.J. *Proc. Phys. Soc. London* **1935**, A47, 873.
- ⁸⁵ Locher, G. L. *Am. J. Roentgenol. Radium Ther.* **1936**, 36, 1.
- ⁸⁶ Wiesboeck, R. A.; Hawthorne, M. F. *J. Am. Chem. Soc.* **1964**, 86, 1642.
- ⁸⁷ Zakharkin, L.I.; Kalinin, V.N.; Podvisotskaya, L.S. *Izv. Akad. Nauk. SSSR, Ser. Khim.* **1967**, 2310.
- ⁸⁸ Taylor, H.J. *Proc. Roy. Soc. London* **1935**, A150, 382.
- ⁸⁹ Taylor, H.J.; Goldhaber, M. *Nature* **1935**, 135, 341.
- ⁹⁰ Hawthorne, M. F.; Maderna, A. *Chem. Rev.* **1999**, 99, 3421.
- ⁹¹ Javid, M.; Brownell, G. L.; Sweet, W. H. *J. Clin. Invest.* **1952**, 31, 604.
- ⁹² Fairchild, R.G.; Bond, V.P. *Int. J. Radiat. Oncol. Biol. Phys.* **1985**, 11, 831.
- ⁹³ Zamenhof, R.G.; Kalend, A.M.; Bloomer, W.D. *J. Natl. Cancer Inst.* **1992**, 84, 1290.
- ⁹⁴ Hawthorne, M.F. *Mol Med. Today* **1998**, 4, 174.
- ⁹⁵ Tolpin, E.I.; Wellum, G.R.; Dohan, Jr., F.C.; Kornblith, P.L.; Zamenhof, R.G. *Oncology* **1935**, 32, 223.
- ⁹⁶ Isotope abundances were obtained from the Commission on Atomic Weights and Isotopic Abundances report for the International Union of Pure and Applied Chemistry in "Isotopic Compositions of the Elements 1989", *Pure and Applied Chemistry* **1998**, 70, 217.
- ⁹⁷ Brownell, G. L.; Murray, B. W.; Sweet, W. H.; Wellum, G. R.; Soloway, A. H. *Proc. Natl. Cancer Conf.* **1973**, 7, 827.
- ⁹⁸ Godwin, J.T.; Farr, L.E.; Sweet, W.H.; Robertson, J.S. *Cancer* **1955**, 8, 601.
- ⁹⁹ Sneath, Jr., R.L.; Wright, J.E.; Soloway, A.H.; O'Keef, S.M.; Dey, A.S.; Smolnycki, W.D. *J. Med. Chem.* **1976**, 19, 1290.

- ¹⁰⁰ Maurer, J.L.; Serino, A.J.; Hawthorne, M.F. *Organometallics*, **1988**, 7, 2519.
- ¹⁰¹ Maurer, J.L.; Berchier, F.; Serino, A.J.; Knobler, C.B.; Hawthorne, M.F. *J. Org. Chem.* **1990**, 5, 14123.
- ¹⁰² Tjarks, W.; Anisuzzaman, A.K.M.; Soloway, A.H. *Nucleosides Nucleotides* **1992**, 11, 1765.
- ¹⁰³ Dahlhoff, W.V.; Bruckmann, J.; Angermund, K.; Krüger, C. *Liebigs Ann. Chem.* **1993**, 8, 831.
- ¹⁰⁴ Giovenzana, G.B.; Lay, L.; Monti, D.; Palmisano, G.; Panza, L. *Tetrahedron* **1999**, 55, 14123.
- ¹⁰⁵ Dougherty, T.J. *Photochem. Photobiol.* **1983**, 38, 377.
- ¹⁰⁶ Murikami, H.; Nagasaki, T.; Hamachi, I.; Shinkai, S. *Tetrahedron Lett.* **1993**, 34, 6273.
- ¹⁰⁷ Toi, H.; Nagai, Y.; Aoyama, Y.; Kawabe, H.; Aizawa, K.; Ogoshi, H. *Chem. Lett.* **1993**, 58, 6273.
- ¹⁰⁸ Kahl, S.B.; Koo, M.-S. *Chem. Commun.* **1990**, 1769.
- ¹⁰⁹ Miura, M.; Gabel, D.; Oenbrink, G.; Fairchild, R.G. *Tetrahedron Lett.* **1990**, 31, 2247.
- ¹¹⁰ Oenbrink, G.; Jürgenlimke, P.; Gabel, D. *Photochem. Photobiol.* **1988**, 48, 451.
- ¹¹¹ Phadke, A.S.; Morgan, A.R. *Tetrahedron Lett.* **1993**, 34, 1725.
- ¹¹² Gedda, L.; Ghaneolhosseini, H.; Nilsson, P.; Nyholm, K.; Petterson, J.; Sjöberg, S.; Carlsson, J. *Anti-Cancer Drug Des.* **2000**, 15, 277.
- ¹¹³ Cai, J.; Soloway, A.H.; Barth, R.F.; Adams, D.M.; Harihara, J.R.; Wyzlic, I.M.; Radcliffe, K. *J. Med. Chem.* **1997**, 40, 3887.
- ¹¹⁴ Tjarks, W. *J. Organomet. Chem.* **2000**, 37, 614.
- ¹¹⁵ Schinazi, R.F.; Goudgaon, N.M.; Fulcrand, G.; el Katan, Y.; Lesnikowski, Z.; Ullas, G.; Moravek, J.; Liotta, D.C.; *Int. J. Radiat. Oncol. Biol. Phys.* **1994**, 28, 1113.
- ¹¹⁶ Kane, R.R.; Drechsel, K.; Hawthorne, M.F. *J. Am. Chem. Soc.* **1993**, 115, 8853.
- ¹¹⁷ Shelly, K.; Feakes, D.A.; Hawthorne, M.F.; Schmidt, P.G.; Krisch, T.A.; Bauer, W.F. *Proc. Natl. Acad. Sci. U.S.A.* **1992**, 89, 9039.
- ¹¹⁸ Yamamoto, K.; Endo, Y. *Bioorg. Med. Chem. Lett.* **2001**, 1, 2389.
- ¹¹⁹ Hall, I.H.; Elkins, A.; Powell, W.J.; Karthikeyan, S.; Sood, A.; Spielvogel, B.F. *Anticancer Res.* **1998**, 18, 2617.
- ¹²⁰ Endo, Y.; Iijima, T.; Yamakoshi, Y.; Kubo, A.; Itai, A. *Bioorg. Med. Chem. Lett.* **1999**, 9, 3313.
- ¹²¹ Kaneko, S.; Kagechika, H.; Kawachi, E.; Hashimoto, Y.; Shudo, K. *Med. Chem. Res.* **1991**, 1, 220.
- ¹²² Iijima, T.; Endo, Y.; Tsuji, M.; Kawachi, E.; Kagechika, H.; Shudo, K. *Chem. Pharm. Bull.* **1999**, 47, 398.
- ¹²³ Endo, Y.; Yoshimi, T.; Kimura, K.; Itai, A. *Bioorg. Med. Chem. Lett.* **1999**, 9, 2561.
- ¹²⁴ Tsuji, M.; Koiso, Y.; Takahashi, H.; Hashimoto, Y.; Endo, Y. *Biol. Pharm. Bull.* **2000**, 23, 513.
- ¹²⁵ Wilbur, D.S. *Bioconj. Chem.* **1992**, 3, 433.
- ¹²⁶ Varadarajan, A.; Sharkey, R.M.; Goldenber, D.M.; Hawthorne, M.F. *Bioconj. Chem.* **1991**, 2, 102.

- ¹²⁷ Olsen, F.P.; Hawthorne, M.F. *Inorg. Chem.* **1965**, 4, 1839.
- ¹²⁸ Wilbur, D.S.; Hamlin, D.K.; Liversey, J.C.; Srivastava, R.R.; Laramore, G.E.; Griffin, T.W. *Nucl. Med. Biol.* **1994**, 21, 601.
- ¹²⁹ Wilbure, D.S.; Hamlin, D.K.; Srivastava, R.R. *J. Labelled Cpd. Radiopharm.* **1994**, 35, 199.
- ¹³⁰ Primus, F.J.; Pak, R.H.; Rickard-Dickson, K.J.; Szalai, G.; Bolen, J.L.; Kane, R.R.; Hawthorne, M.F. *Bioconj. Chem.* **1996**, 7, 532.
- ¹³¹ Chen, C.-J.; Kane, R.R.; Primus, F.J.; Szalai, G.; Hawthorne, M.F.; Shively, J.E. *Bioconj. Chem.* **1994**, 5, 557.
- ¹³² Paxton, R.J.; Beatty, B.G.; Varadarajan, A.; Hawthorne, M.F. *Bioconj. Chem.* **1992**, 3, 241.
- ¹³³ Yamamoto, Y.; Seko, T.; Nakamura, H.; Nemoto, H.; Hojo, H.; Nukai, N.; Hashimoto, Y. *J. Chem. Soc. Chem. Commun.* **1992**, 157.
- ¹³⁴ Khaw, B.A.; Cooney, J.; Edington, T.; Strauss, H.W. *J. Nucl. Med.* **1986**, 27, 1293.
- ¹³⁵ Tolmachev, V.; Koziorowski, J.; Sivaev, I.; Lundqvist, H.; Carlsson, J.; Orlova, A.; Gedda, L.; Olsson, P.; Sjöberg, S.; Sundin, A. *Bioconj. Chem.* **1999**, 10, 338.
- ¹³⁶ Gedda, L.; Olsson, P.; Carlsson, J. *Bioconj. Chem.* **1996**, 7, 584.
- ¹³⁷ Mizusawa, E.; Dahlman, H.L.; Bennet, S.J.; Goldenberg, D.M.; Hawthorne, M.F. *Proc. Natl. Acad. Sci. U.S.A.* **1982**, 79, 3011.
- ¹³⁸ Orlova, A.; Lebeda, O.; Tolmachev, V.; Sjöberg, S.; Carlsson, J.; Lundqvist, H. *J. Labelled Cpd. Radiopharm.* **2000**, 43, 251.
- ¹³⁹ Beatty, B.G.; Paxton, R.J.; Hawthorne, M.F.; Williams, L.E.; Rickard-Dickson, K.J.; Do T.; Shively, J.E.; Beatty, J.D. *J. Nucl. Med.* **1993**, 34(8), 1294.
- ¹⁴⁰ Rupperecht, M.; Probst, T. *Anal. Chim. Acta* **1988**, 358, 205.
- ¹⁴¹ Barth, R.F.; Adams, D.M.; Soloway, A.H.; Mechetner, E.D.; Alam, F.; Annisuzzaman, A.K.M. *Anal. Chem.* **1991**, 63, 890.
- ¹⁴² Nicols, T.L.; Kabalka, G.W.; Miller, L.F.; Khan, M.K.; Smith, G.T. *Med. Phys.* **2002**, 29, 2351.
- ¹⁴³ Martin, B.; Posseme, F.; LeBarbier, C.; Carreaux, F.; Carboni, B.; Seiler, N.; Moulinoux, J.-P.; Deleros, J.-G. *Bioorg. Med. Chem.* **2002**, 10, 2863.
- ¹⁴⁴ Martin, B.; Posseme, F.; LeBarbier, C.; Carreaux, F.; Carboni, B.; Seiler, N.; Moulinoux, J.-P.; Deleros, J.-G. *J. Med. Chem.* **2001**, 44, 3653.
- ¹⁴⁵ Imahori, Y.; Ueda, S.; Ohmori, Y.; Sakae, K.; Kusuki, T.; Kobayashi, T.; Takagaki, M.; Ono, K.; Ido, T.; Fujii, R. *Clin. Cancer Res.* **1998**, 4, 1833.
- ¹⁴⁶ Imahori, Y.; Ueda, S.; Ohmori, Y.; Sakae, K.; Kusuki, T.; Kobayashi, T.; Takagaki, M.; Ono, K.; Ido, T.; Fujii, R. *Clin. Cancer Res.* **1998**, 4, 1825.
- ¹⁴⁷ Ishiwata, K.; Shiono, M.; Kubota, K.; Yoshino, K.; Hatazawa, J.; Ido, T.; Honda, C.; Ichihashi, M.; Mishima, Y. *Melanoma Research* **1992**, 2, 171.
- ¹⁴⁸ Ishiwata, K.; Ido, T.; Honda, C.; Kawamura, M.; Ichihashi, M.; Mishima, Y. *Nuc. Med. Biol.* **1992**, 19, 311.
- ¹⁴⁹ Ishiwata, K.; Ido, T.; Honda, C.; Kawamura, M.; Ichihashi, M.; Mishima, Y. *Nuc. Med. Biol.* **1992**, 19, 745.

- ¹⁵⁰ Ishiwata, K.; Ido, T.; Mejia, A.A.; Ichihashi, M.; Mishima, Y. *Appl. Radiation and Isotopes* **1991**, 42, 325.
- ¹⁵¹ Kabalka, G.W.; Nichols, T.L.; Smith, G.T.; Miller, L.F.; Khan, M.K.; Busse, P.M. *J. Neuro-Oncology* **2003**, 22, 187.
- ¹⁵² Imahori, Y.; Ueda, S.; Ohmori, Y.; Kusuki, T.; Ono, K.; Fujii, R.; Ido, T. *J. Nuc. Med.* **1998**, 39, 325.
- ¹⁵³ Arlinghaus, H.F.; Spaar, M.T.; Switzer, R.C.; Kabalka, G.W. *Anal. Chem.* **1997**, 69, 3169.
- ¹⁵⁴ Verbakel, W.F.A.R.; Stecher-Rasmussen, R. *Phys. Med. Biol.* **2001**, 46, 687.
- ¹⁵⁵ Verbakel, W.F.A.R.; Sauerwein, W.; Hideghety, K.; Stecher-Rasmussen, F. *Int. J. Radiation Oncol. Biol. Phys.* **2003**, 55, 743.
- ¹⁵⁶ dos Santos, D.F.; Argentini, M.; Weinreich, R.; Hansen, H.-J. *Helv. Chim. Acta* **2000**, 83, 2926.

Chapter 2 - Carborane Analogues of Tamoxifen

2.1 Overview

A carborane analogue of tamoxifen was synthesized as both a new type of BNCT agent and as a novel antiestrogen. This chapter describes the rationale for the design of the target compound, its potential uses, and the details of a unique synthetic strategy for incorporating a carborane into the basic skeleton of tamoxifen. The work described on the synthesis of compound **2.28** has been recently published.¹

2.2 Introduction to Antiestrogens

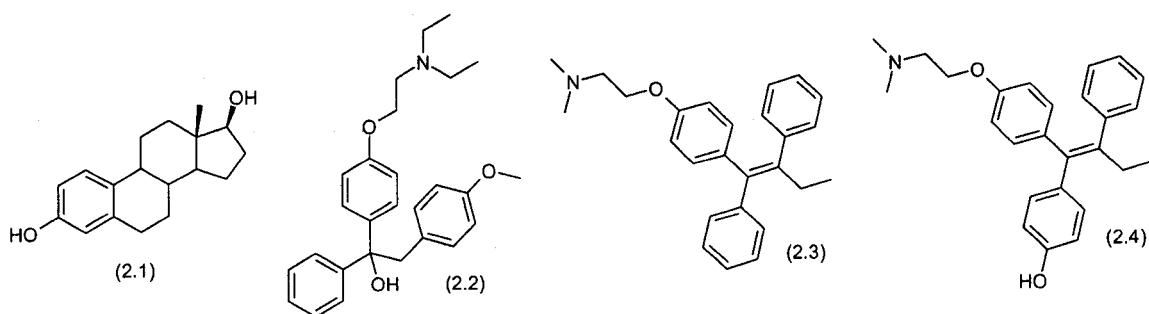


Figure 2.1 – The chemical structures of estradiol (2.1), MER-25 (2.2), tamoxifen (2.3) and its metabolite, 4-hydroxytamoxifen (2.4).

In 1923, Allen and Doisy first established the tissue specific actions of estrogen (Figure 2.1).² The mechanism by which this hormone produces its effects in the body remained a relative mystery, as there were no known methods to probe its behaviour *in vivo*. In response to this, a series of compounds were sought by which the mechanism of action for estrogen could be studied.³ In 1958, Lerner and co-workers published their landmark paper on the first non-steroidal anti-estrogen, 1-(*p*-2-

diethylaminoethoxyphenyl)-1-phenyl-2-*p*-methoxyphenylethanol (MER-25, Figure 2.1).⁴ They showed that the tri-aryl structure of MER-25 competitively inhibited the binding of estrogen to its receptor without exhibiting stimulatory properties in other organs expressing the estrogen receptor (ER). Further work by Jensen and co-workers demonstrated that MER-25 prevented the incorporation of estrogen into various tissues in rat models.^{5,6} Thus, a foundation had been established toward the molecular mechanism of estrogen action. Unfortunately, MER-25 exhibited high toxicity and low potency, inhibiting its development as a clinically useful agent. Despite this, anti-estrogens gained a great deal of attention as tools for investigating the physiological behaviour of the natural hormone. The research at the time of this discovery focused on the biochemistry of known anti-estrogens,⁷ and it was not until the discovery of tamoxifen in 1971 that the value of antiestrogens as anti-cancer agents became apparent.⁸

Tamoxifen (Figure 2.1) is a commonly prescribed drug for the treatment of hormone dependent breast cancer.⁹ Hormone dependent breast cancer, which accounts for approximately one third of all cases,¹⁰ relies on the binding of oestradiol (estrogen) to receptors on malignant cell surfaces. Once bound, the newly formed hormone-receptor complex dimerizes and attaches to a specific DNA sequence. DNA binding, along with the association of various co-factors, triggers protein synthesis (transcription) and eventually cell replication. Anti-estrogens such as tamoxifen exert their effect by preventing optimal conformational shifts of the ER thereby compromising the ability of the receptor dimer from initiating transcription.⁷

There are several structural features of Tamoxifen that contribute to its pharmacological properties, some of which are highlighted in Figure 2.2. The three phenyl rings (A, B and C) each participate in hydrophobic contacts and/or non-polar interactions with a variety of amino acids around the ligand binding domain (LBD) of the estrogen receptor. While the presence of bulky substituents on ring A show little influence on the binding affinity,^{11,12} modifications to ring B dramatically decrease the affinity of the drug to the ER. X-ray crystallography has shown that there is sufficient space around the region where ring A interacts with the ER to accommodate groups that are larger than unsubstituted benzene rings.¹³

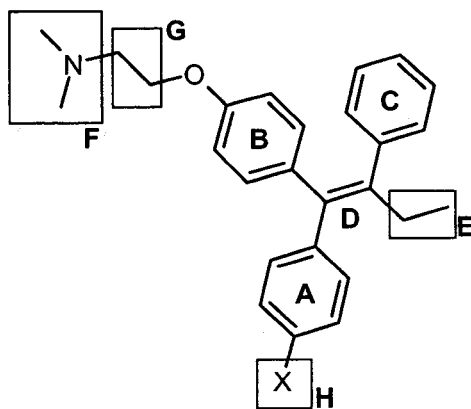


Figure 2.2 – Molecular regions of tamoxifen responsible for pharmacological behaviour.

While these features aid in the binding to the LBD, the most important structural feature required for antiestrogenic action lies in the pendant amino group (Group F, Figure 2.2). The basic amine functionality interacts with one key amino acid (ASP³⁵¹) of the ER-LBD. Interactions at this position prevent key structural shifts of the estrogen receptor upon ligand binding. Changes in the basicity, distance from, or position of the

amine all dramatically affect binding affinity.¹⁴ The ethyl group (Group E, Figure 2.2) also facilitates binding to the ER by “pushing” the amino functionality deeper into the receptor. While small changes at this location are tolerated, large changes to the size of the ethyl group have a detrimental impact on anti-estrogen activity.⁷

2.3 Analogues of Tamoxifen

Many different analogues of tamoxifen have been prepared in order to increase the efficacy of the drug and to reduce the development of drug resistance. Most compounds retain the pharmacophores of the parent drug in order to maintain affinity for the ER (Figure 2.3). Examples include derivatives such as Idoxifen (**2.5**), synthesized by McCague and co-workers,¹⁵ Ferrocifen (**2.6**), as reported by Top *et al.*,¹¹ and Raloxifene (**2.8**) originally synthesized by Jones and co-workers.¹⁶ Boron containing analogues of tamoxifen have also been prepared as novel delivery vehicles for BNCT. Hawthorne and co-workers reported the attachment of a polyhedral borane onto the triphenyl arene core of tamoxifen through the pendant amino group (compound **2.7**, Figure 2.3).¹³ It is well known, however, that substitution at this position has a detrimental impact on the relative binding affinity (RBA) for the ER (*vide infra*).¹⁷ In addition, N-dealkylation at this position occurs rapidly *in vivo*, which may limit the efficacy of the reported compounds.¹⁸ In order to use tamoxifen as a BNCT targeting agent, an alternative conjugation strategy is needed.

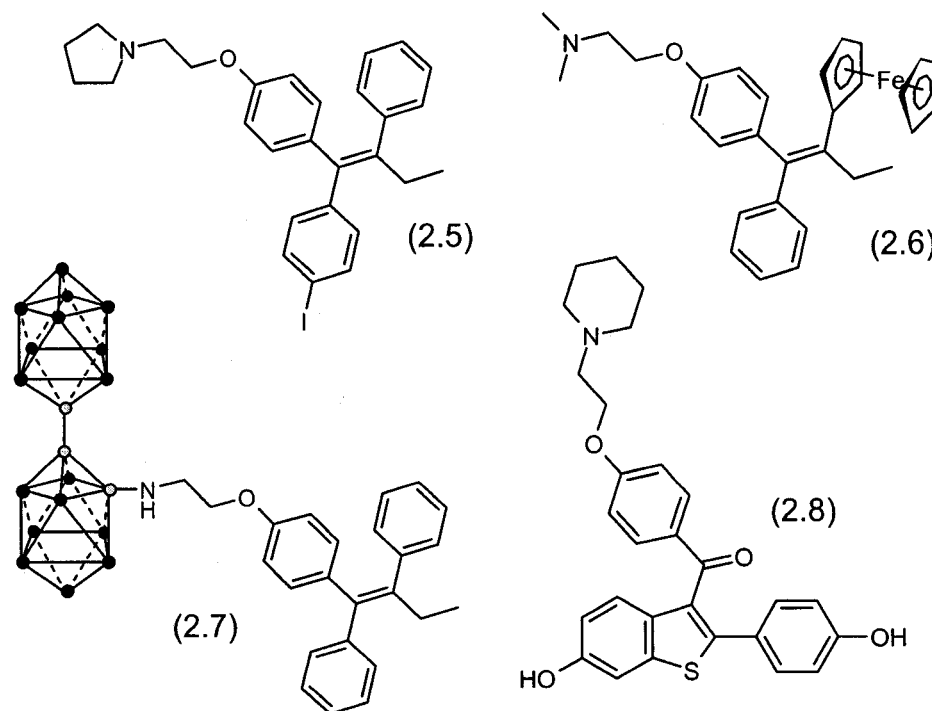


Figure 2.3 - Various Tamoxifen analogues, clockwise from top left: Idoxifen (2.5), Ferrocifen (2.6), Raloxifen (2.7) and Hawthorne's B₂₀ tamoxifen derivative (2.8).

2.4 Carboranes as Pharmacophores

The initial attraction to carboranes for medicinal chemistry research was a result of their high boron content and stability to catabolism, which are important criteria for BNCT agents. More recently, it has been demonstrated that carboranes can be used to enhance hydrophobic interactions between pharmaceuticals and their receptors and to increase the *in vivo* stability, and hence bioavailability, of compounds that are normally rapidly metabolized. These properties, coupled with their diverse chemistry, including the opportunity to 'tag' the clusters with diagnostic radionuclides, make carboranes attractive

synthons from which to construct novel pharmaceuticals, radiopharmaceuticals and biological probes.

Bioconjugation strategies for carboranes can follow a number of different strategies. In addition to direct conjugation to a pendant functionality on the biomolecule, carboranes can be introduced in place of a specific aryl group. The volume occupied by a carborane is similar to the 3-dimensional sweep of a phenyl aromatic ring.¹⁹ To illustrate this point, the X-ray structure of the benzamide derivative (2.9) of 3-amino-*ortho*-carborane, which was solved in our laboratory, is shown in Figure 2.4. The diameter of the cluster (without standard deviations from atomic centroids) is 5.25Å while that of the phenyl ring is 4.72Å. In light of this and the space available in the ER around where ring A is situated, the increase in size in changing ring A in tamoxifen to a carborane should have no effect on receptor binding.²⁰⁻²⁴

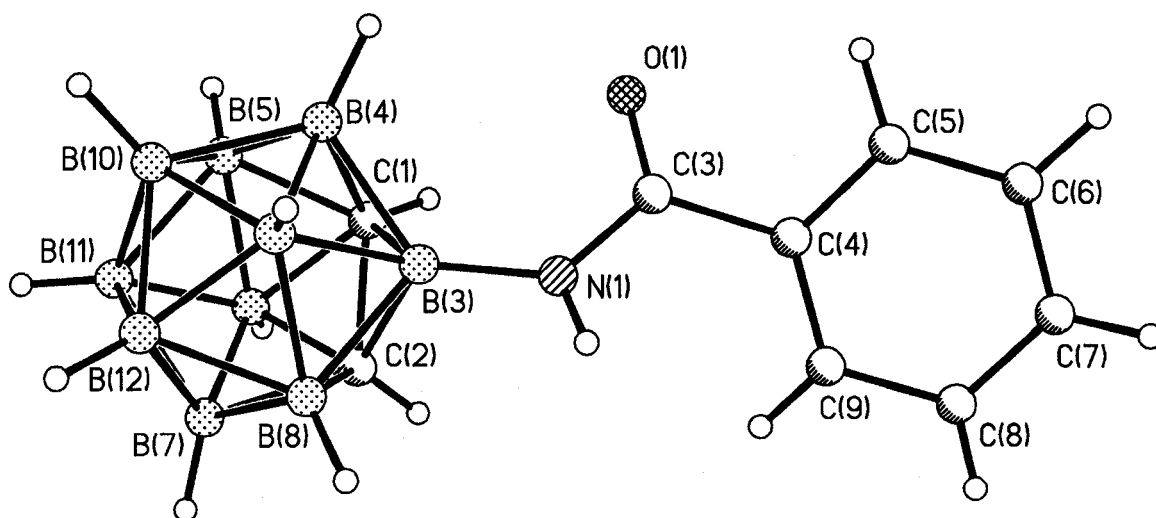


Figure 2.4 – X-ray structure of compound 2.9 showing the similarity in the diameters of carborane and phenyl moieties.

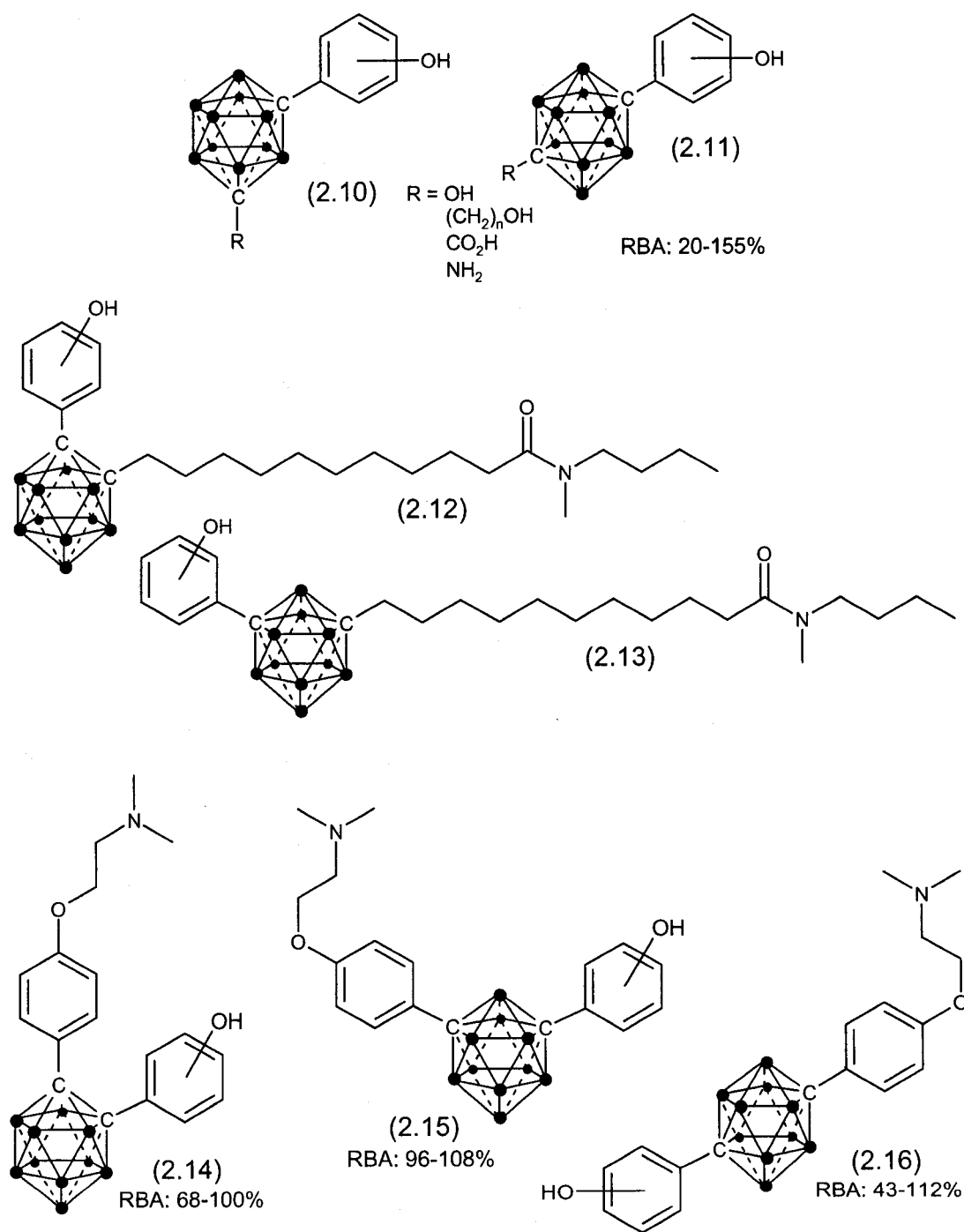


Figure 2.5 – Carborane-based estrogen agonists and antagonists reported by Endo et al.

2.5 Carborane-Derived Antiestrogens

Endo *et al.* reported the discovery of a series of estrogen agonists based on simple carborane derivatives (Figure 2.5). The affinity of these compounds for the ER was surprising because the corresponding aryl analogues had low RBA values. Their hypothesis was that the carborane moiety acts as a hydrophobic pharmacophore thereby enhancing the interactions between the carborane substrate and the hydrophobic regions of the ER.^{23,24} In some cases, the reported binding affinity of these carborane derivatives was greater than that of estrogen itself.

In light of the increased affinity of Endo's carborane derivatives for the ER compared to the corresponding phenyl counterparts, we were interested in preparing a carborane analogue of tamoxifen as a novel and potent anti-estrogen and as a boron delivery vehicle for BNCT. The target compound is one in which a carborane is substituted for ring A of tamoxifen.

2.6 Target Molecule and Retrosynthetic Analysis

The initial target involved replacing ring A with an *ortho*-carborane cage (Figure 2.6). As mentioned previously, substitution of a bulky group at this position does not have a significant impact on the RBA. The *closo*-carborane target compound can also be converted to the corresponding *nido*-carborane, thereby providing the opportunity to radiolabel the product.²⁵

The general strategy for preparing the target compound involved a stereoselective synthesis of the ene-yne **2.24** from the ketone **2.21**. The ketone in turn is synthesized

from three commercially available precursors. Once the ene-yne **2.24** is generated, the desired target can be prepared by reacting the alkyne **2.24** with $B_{10}H_{12}L_2$ followed by conversion to the corresponding amine.

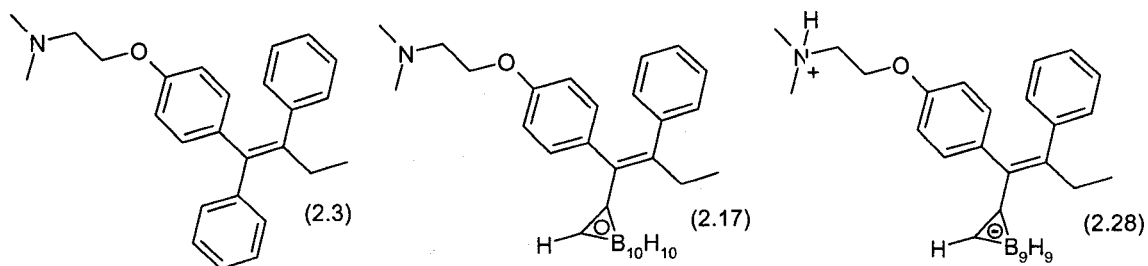
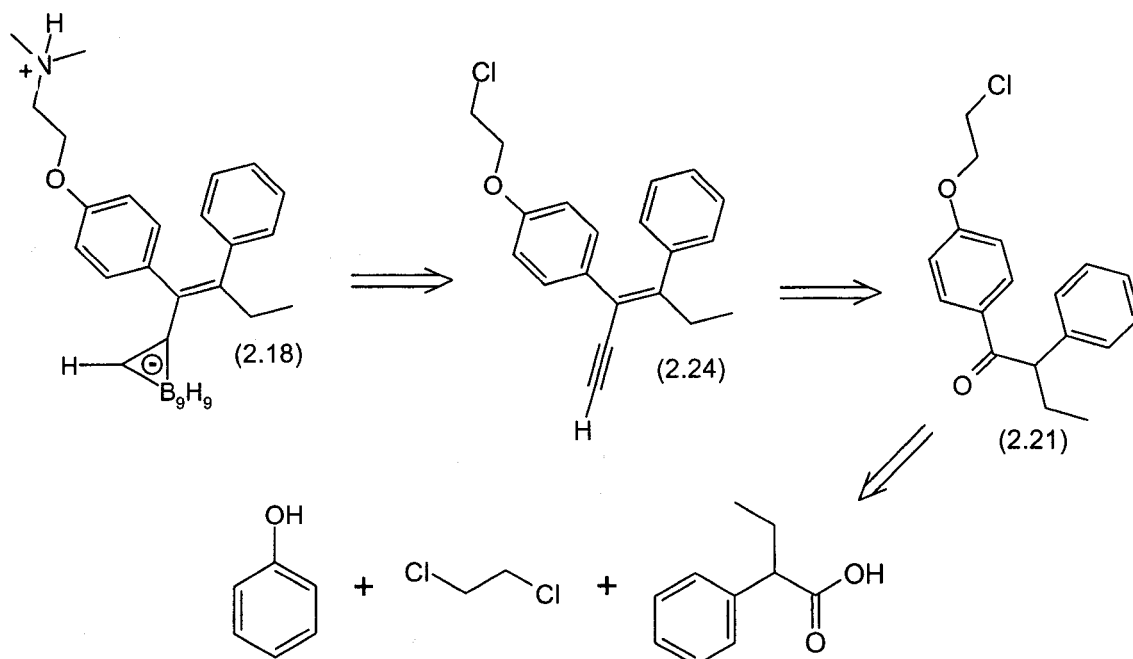


Figure 2.6 – Proposed carborane analogue of tamoxifen.



Scheme 2.1 – Retrosynthetic analysis of carborane analogue of tamoxifen.

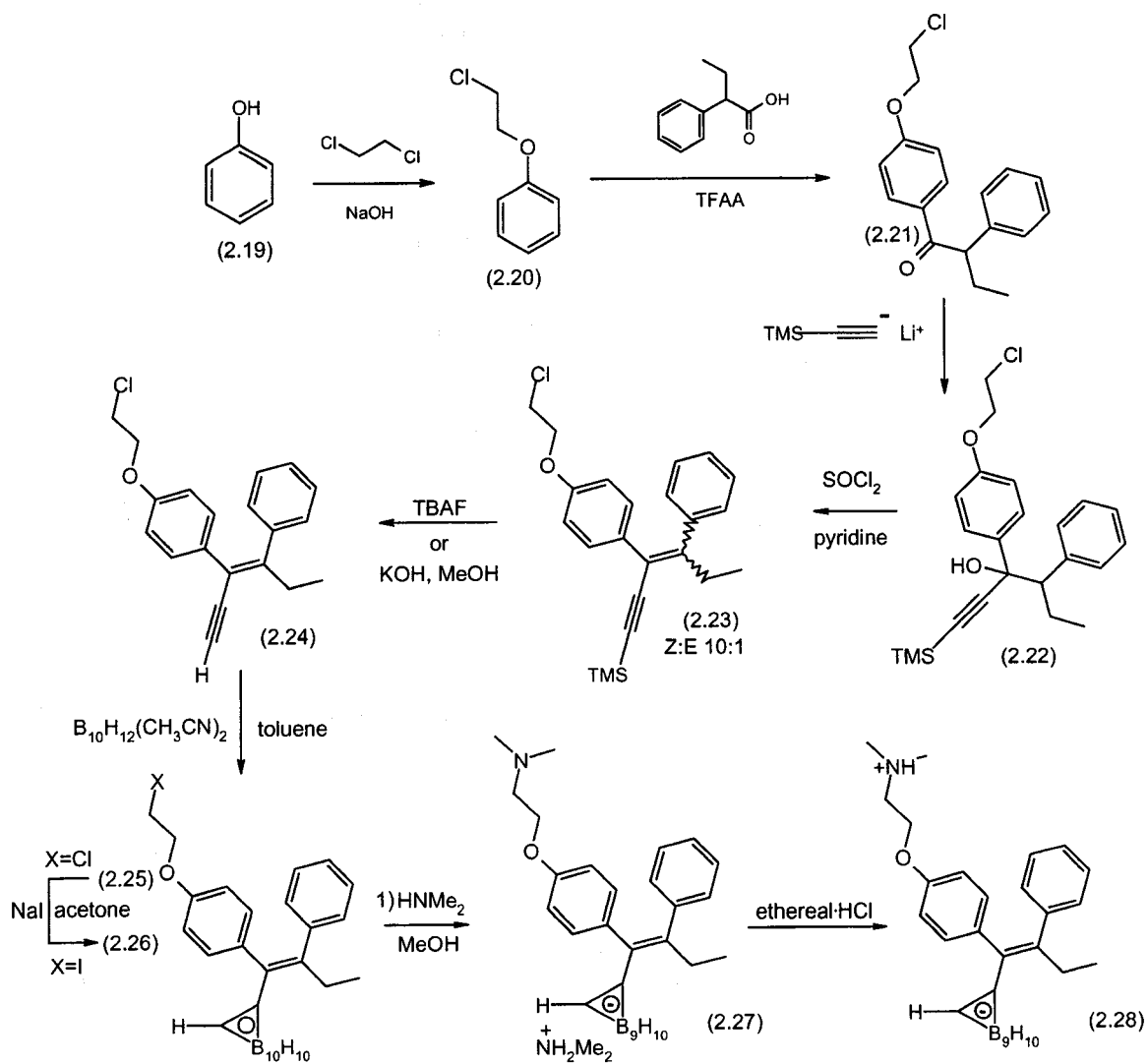
2.7 The Total Synthesis of a *nido*-Carborane Analogue of Tamoxifen

The preparation of the Tamoxifen alkyne follows the path shown in Scheme 2.2. and was derived from the synthesis of tamoxifen reported by McCague and co-workers.²⁶

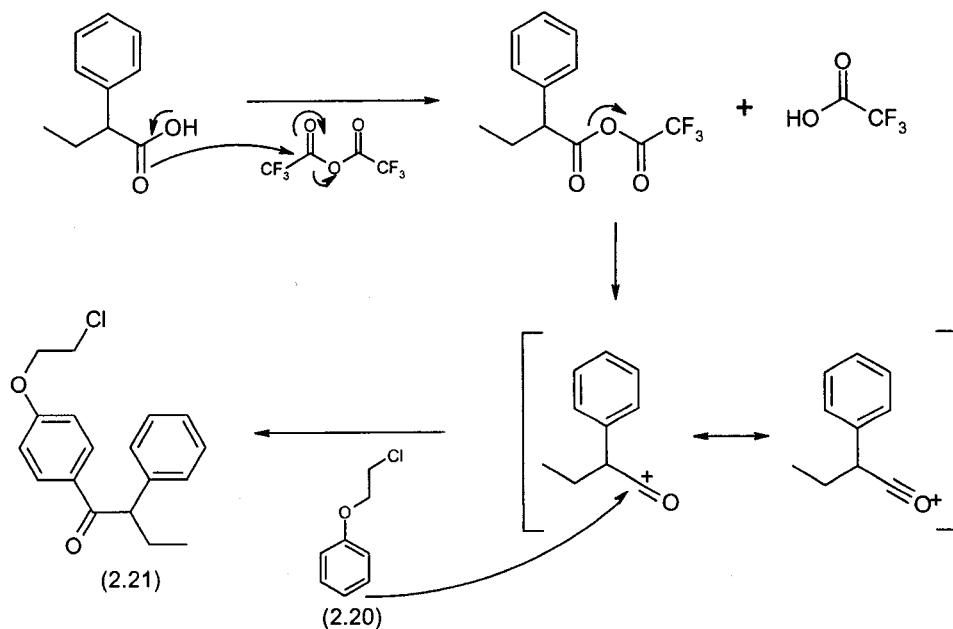
Synthesis began with the preparation of 2-chloroethoxybenzene (**2.20**) in which phenol (**2.19**) was dissolved in a solution of sodium hydroxide, in the presence of a phase transfer catalyst, dimethyldioctadecylammonium bromide, and excess 1,2-dichloroethane. Subsequent nucleophilic attack on 1,2-dichloroethane generated 2-chloroethoxybenzene in good yields. Formation of the monosubstituted product is thought to be favoured due to the use of a biphasic reaction mixture and a large excess of dichloroethane; the phase transfer catalyst establishes a transport mechanism between the organic and aqueous layers, thereby transferring a small amount of the phenoxide from the aqueous phase to the organic phase. Purification of the product **2.20** was performed by vacuum distillation, which afforded the product, a clear colourless oil, in reasonable yield (53%).

Preparation of the ketone **2.21** involved a Friedel-Crafts acylation of 2-chloroethoxy benzene (**2.20**) with 2-phenyl butyric acid (Scheme 2.3). Since the aromatic ring is activated by the electron donating ethoxy substituent, both the *ortho* and *para* positions are favoured for acylation. The *para* isomer was selectively obtained in greater yield due to the steric influence exhibited by the pendant ethoxy group at the *ortho* position. The product was purified by recrystallization from petroleum ether.

The alkyne derivative **2.23** was prepared by nucleophilic attack of lithium trimethylsilylacetylide on the ketone **2.21** giving the tertiary alcohol **2.22**. Compound **2.22** was immediately dehydrated using thionyl chloride and pyridine, giving the desired compound as a mixture of stereoisomers.



Scheme 2.2 – The total synthesis of a nido-carborane analogue of tamoxifen.



Scheme 2.3 – Proposed mechanism for Friedel-Crafts acylation of 2-chloroethoxyphenol

The two isomers of compound **2.23** were difficult to separate using column chromatography, so they were collected together as a viscous oil. The 1H NMR spectrum of the mixture showed two identical sets of peaks for each of the unique protons in *Z*-**2.23** and *E*-**2.23** (Figure 2.7). Integration of complimentary pairs of peaks indicated that one isomer was ten times more abundant than the other (Figure 2.8). The ^{13}C NMR spectrum further supported the presence of the expected product, and was assigned with the aid of a ^{13}C DEPT experiment. The TMS methyl peaks were quite clear at 0.07 ppm, while the protons on the remaining methyl group gave rise to a peak at 7.96 ppm. The methylene hydrogen signals due to the pendant chloroethoxy group were evident at 63.53 and 37.49 ppm while the CH_2 of the ethyl group appeared at 27.09 ppm. Five peaks were also observed in the region of the spectrum in which aromatic carbon atoms typically reside,

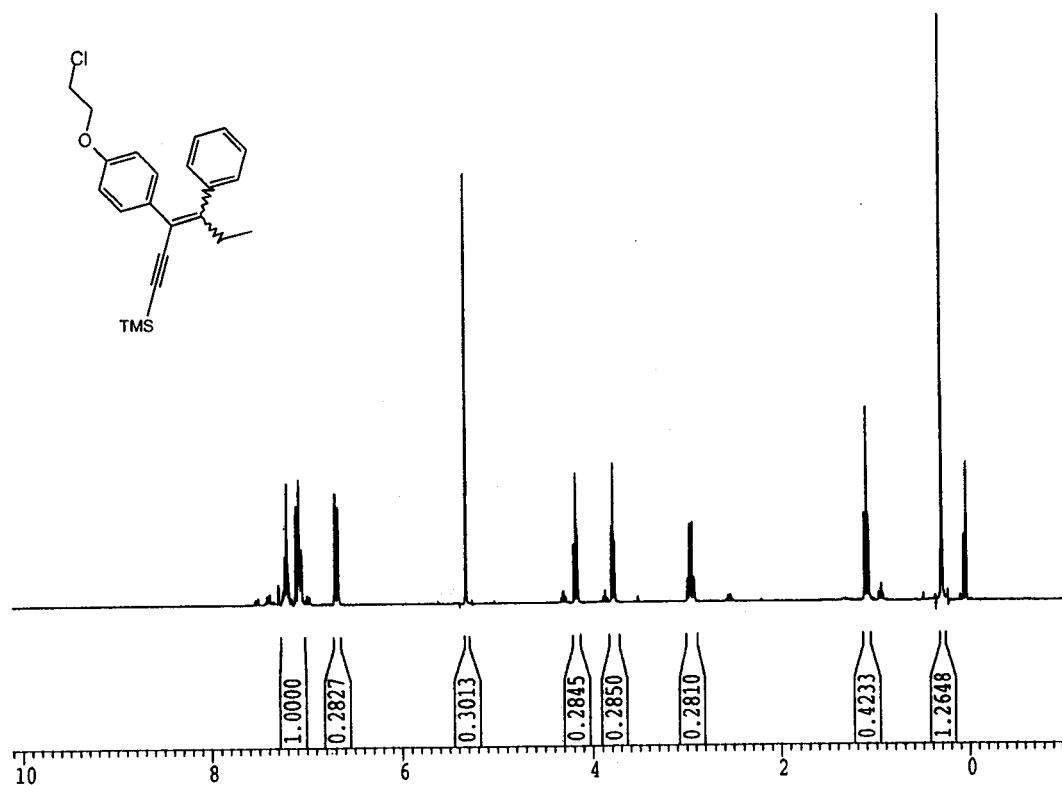


Figure 2.7 – ¹H NMR spectrum of compound 2.23, showing the presence of both *E* and *Z* isomers.

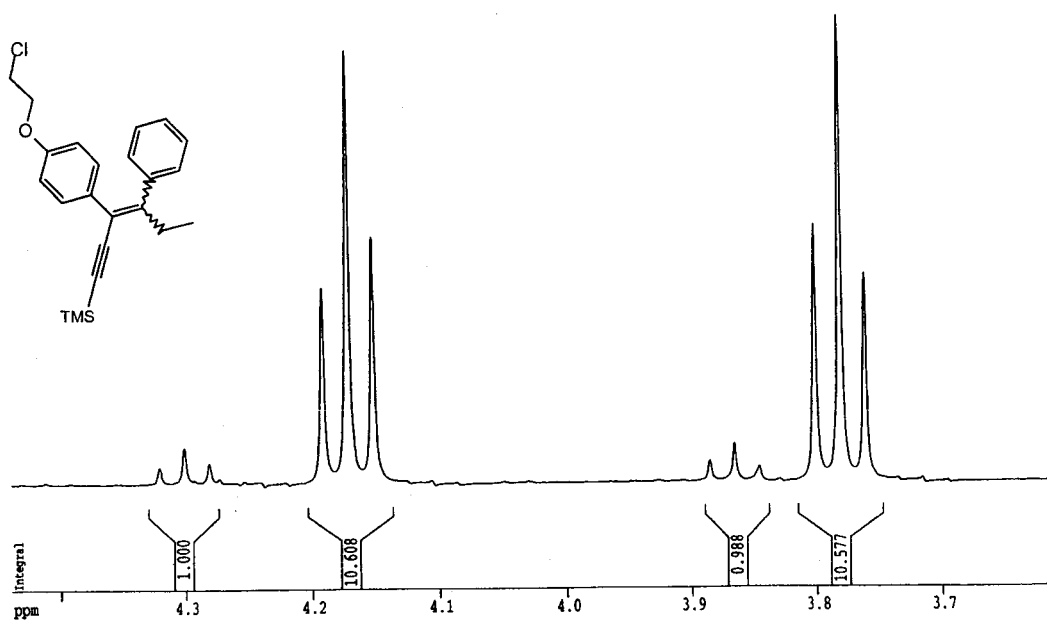


Figure 2.8 – Diastereomer ratio as observed by the ethoxy peaks in the ¹H NMR spectrum of 2.23.

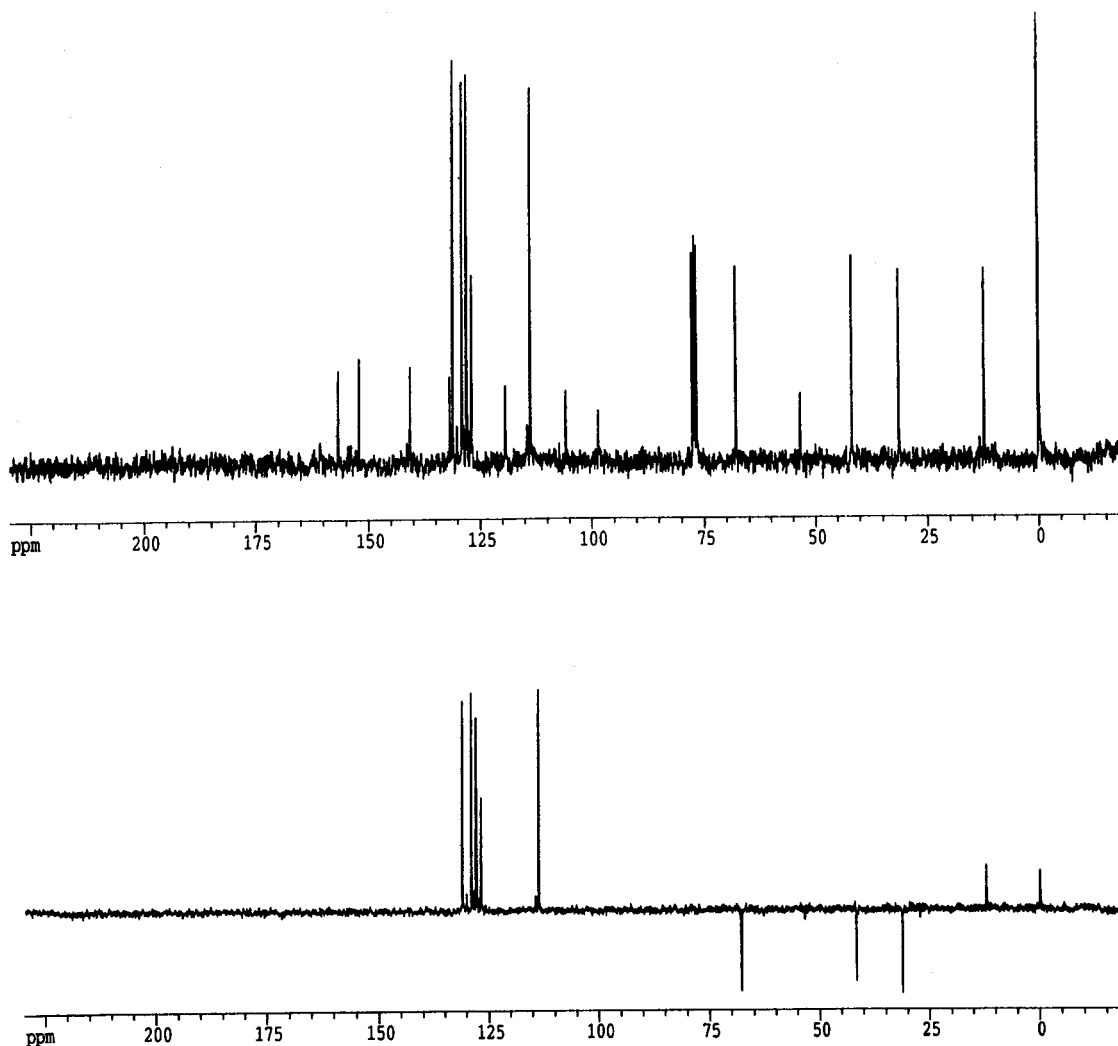


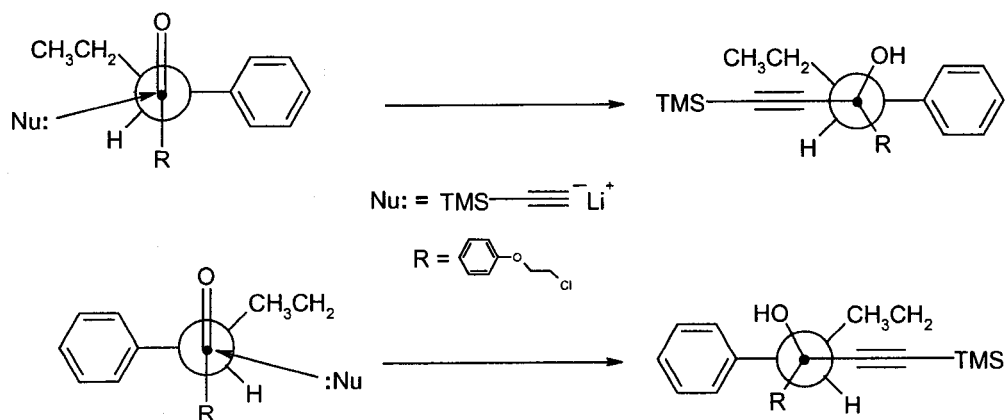
Figure 2.9 – The ^{13}C NMR (above) and ^{13}C DEPT (below) NMR spectra of 2.23.

and were therefore assigned to the five aromatic CH groups present in the molecule. Ternary carbon atoms do not appear in the ^{13}C DEPT experiment, and are thus responsible for the remaining peaks in the standard 1-D ^{13}C NMR spectrum. An infrared analysis of the TMS protected alkyne 2.23 showed absorbances corresponding to all the expected functional groups. Aliphatic CH stretches were observed between 3056 cm^{-1} and 2874 cm^{-1} in addition to a $\text{C}\equiv\text{C}$ stretch at 2134 cm^{-1} . A strong C-O stretching

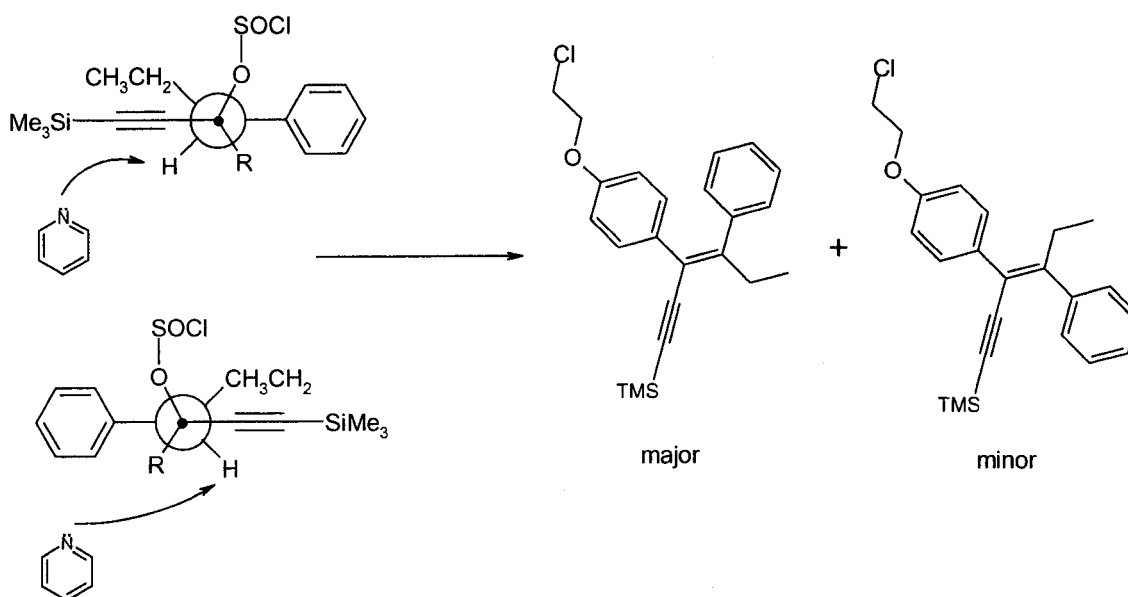
frequency is also observed at 1247 cm^{-1} . High resolution mass spectrometric analysis of **2.23** gave a molecular mass peak of 382.1537 m/z which was in excellent agreement with the calculated mass of 382.1520 m/z .

The stereoselectivity observed for the conversion of **2.22** to **2.23** can be rationalized using the Felkin-Ahn model^{27,28} for the prediction of the stereochemical outcome of the addition of a nucleophile to a prochiral carbonyl group. The theoretical foundation of this model is found in the Curtin-Hammett principle, which states that the relative energy of the transition states, and not the difference in energies of the ground states, control the selectivity of the reaction.^{29,30} Thus, according to the Felkin-Ahn model, the incoming nucleophile will react with the conformers shown in Scheme 2.4, at the Bürgi-Dunitz angle (107°).³¹ The preferred pathway is the one in which the nucleophile encounters the least amount of steric hindrance. As a result, the nucleophile reacts as shown in Scheme 2.4 where it passes closest to the smallest substituent on the adjacent carbon center, the H atom.

The mechanism for the dehydration reaction used to prepare **2.23** is shown in Scheme 2.5. Regardless of which enantiomer is obtained upon attack of the acetylide anion on the ketone (**2.21**), the formation of the desired Z-isomer is favoured so long as the subsequent elimination reaction proceeds via the E2 mechanism (Scheme 2.5). Thionyl chloride activates the alcohol, generating a good leaving group, which is followed by abstraction of the proton attached to the adjacent carbon atom and loss of SO_2 and HCl to yield the alkene **2.23**.



Scheme 2.4 – The reaction of a nucleophile with a prochiral ketone.



Scheme 2.5 – Reactive conformers give *Z*-alkene with *E2* elimination pathway.

While the reaction is, to a significant degree stereoselective (10:1 *Z*:*E*), the formation of small amounts of the *E* isomer cannot be entirely avoided (Figure 2.8). Separation of these isomers is necessary because it has been well established that the geometric isomers of tamoxifen show significantly different biological activity. The *Z*

isomer is antiestrogenic while the *E* isomer is estrogenic.^{32,33} While separation of the two isomers of **2.23** was difficult, it was found that after removal of the TMS group, the deprotected *E*- and *Z*- isomers could be separated by radial chromatography. Removal of the trimethylsilyl group was performed using potassium hydroxide, producing the terminal alkyne in good yield (60%) (Scheme 2.2).

The alkyne **2.24** was characterized using ¹H and ¹³C NMR spectroscopy, mass spectrometry and Fourier transform infrared analysis. As expected, the ¹H NMR spectrum of **2.24** was very similar to that of the TMS derivative. One notable feature was the absence of peaks corresponding to the minor *E* isomer. While the peaks corresponding to the phenyl protons (7.16 – 6.64 ppm) were complicated due to second order effects, those from the pendant ethoxy (4.12 ppm, 3.73 ppm) and ethyl groups (2.91 ppm, 1.03 ppm) were characteristic of compound **2.24**. The terminal alkyne proton appeared as a singlet at 3.29 ppm.

The ¹³C NMR spectrum of compound **2.24** was much simpler in the absence of a second isomer, displaying a total of sixteen peaks, six in the aliphatic region of the spectrum accounting for the non-aromatic carbon atoms, and ten remaining peaks in the 115-170 ppm range in accordance with the presence of aromatic carbon nuclei. A ¹³C DEPT experiment helped determine the chemical shift of the methyl group, which was found to be 12.40 ppm. The methylene carbon peaks were observed at 67.80, 41.77 and 31.16 ppm respectively with the more deshielded peaks belonging to the pendant chloroethoxy group.

Infrared, mass spectrometric and elemental analysis further supported the identification of **2.24**. The IR spectrum of the terminal alkyne exhibited a strong, highly diagnostic peak at 3301 cm^{-1} . In addition, a number of other peaks corresponding to aliphatic C-H stretching frequencies ($3055\text{-}2875\text{ cm}^{-1}$) were observed. High resolution mass spectrometry showed a molecular ion at 310.1136 m/z , which is in good agreement with the calculated mass of 310.1124 m/z . A combustion analysis enabled the determination of elemental composition, with observed carbon and hydrogen percentages at 77.66% and 6.34% respectively. Each of these values agree acceptably with the calculated values of 77.29% and 6.16% for carbon and hydrogen.

Conversion of the deprotected terminal alkyne **2.24** to the carborane **2.25** was brought about by the addition of $\text{B}_{10}\text{H}_{12}(\text{CH}_3\text{CN})_2$ across the carbon-carbon triple bond. The structure of **2.25** was established by FTIR, MS spectrometry and multi-NMR spectroscopy. The infrared spectrum of **2.25** contained a strong B-H stretching frequency at 2579 cm^{-1} which is characteristic of a carborane derivative. In addition, the ^1H NMR spectrum of **2.25** showed that the C-H peak associated with the carborane was broadened relative to the corresponding peak in **2.24**. This broadening is caused by the proximity of this proton to the quadrupolar boron nuclei in the carborane cage; the hydride-like hydrogen atoms of the cage are affected similarly. The carborane B-H units were observed as a characteristic broad and undulating baseline between 1 and 4 ppm. The remainder of the ^1H NMR spectrum was similar to that of the ene-yne precursor **2.24**.

Incorporation of the boron cage across the terminal alkyne also brought about changes in the ^{13}C NMR spectrum. The carborane peaks appear at 67.82 and 62.98 ppm

respectively, which is similar to values reported for other carborane-containing products.³⁴⁻³⁹ The ¹¹B NMR spectrum showed four discernable peaks at -3.51, -8.99, -12.67 and -13.95 ppm which indicate the cage is *closo* in nature.⁴⁰⁻⁴² Mass spectroscopic analysis gave a molecular ion peak consistent with the isotopic distribution pattern expected for **2.25**.

The yield of the reaction was quite poor (7%), possibly due to steric hindrance and/or the highly delocalized nature of the ene-yne. There are only a few reported examples of the synthesis of carboranes from ene-ynes,⁴³⁻⁴⁵ the first being 1-isopropenyl carborane.⁴⁶ The yield of **2.25** was not affected by changing the nature of the Lewis base decaborane adducts (B₁₀H₁₂L₂, L = CH₃CN, Me₂S), the reaction solvent (benzene, acetonitrile, toluene and acetonitrile-toluene mixtures), or the molar ratio of alkyne to decaborane employed (1:1, 1:3, 1:10).

2.8 X-ray Structural Characterization of Compound 2.25

X-ray quality crystals of **2.25** were grown from a petroleum ether solution at -10°C. There were two independent molecules in the asymmetric unit (Z = 8), both with the expected Z-geometry. The major difference between the two molecules was the orientation of the ethyl groups, which had torsion angles of -122.7° and 112.1° for molecules 1 and 2 respectively. The molecules adopt a propeller-like conformation, similar to that reported for the solid-state structure of tamoxifen. Having such a conformation is reported to be an important feature for retaining affinity for the estrogen receptor.⁴⁷

The boron-carbon bond lengths in the carborane cage ranged from 1.692(4) Å to 1.746(3) Å (average = 1.713(4) Å) in molecule 1 and 1.683(4) Å to 1.749(3) Å (average = 1.713(4) Å) in molecule 2 (Figure 2.10). The boron-boron bond distances in both molecules ranged from 1.763(4) Å to 1.790(4) Å. These distances are within the normal range for carboranes.^{48,49} The alkene C-C distances C3 to C4 and C3' to C4' were 1.353(3) Å for molecule 1 and 1.347(3) Å for molecule 2, while the alkene carborane distances C2-C3 and C2' to C3' were 1.518(3) Å and 1.524(3) Å respectively. Both of these bond distances are similar to the corresponding bond lengths found between the alkene and the ternary aromatic carbon atom of ring A in tamoxifen (1.34 Å and 1.50 Å).⁵⁰

The angles between the planes defined by the phenyl rings B and C (Figure 2.2) and the alkene group demonstrate that the B-ring in molecule 1 is nearly perpendicular to the alkene plane (89.27(7)°). An analysis of the second molecule shows a slightly different orientation (79.27(7)°) of the conjugated system, a characteristic that is most likely a result of solid-state packing effects. The angles between the planes defined by the atoms of rings B and C are marginally different (53.44(8)° and 55.17(7)°) than those reported for tamoxifen itself (~ 57°),⁵⁰ which may be ascribed to the size of the carborane and the apparent preference for the orientation of the carborane C-H group toward the centroid of ring B. The interaction of the π -systems of aromatic rings with the carborane C-H groups has been previously documented.⁵¹⁻⁵⁵ This interaction does not appear to affect the number of preferred orientations in solution at room temperature.

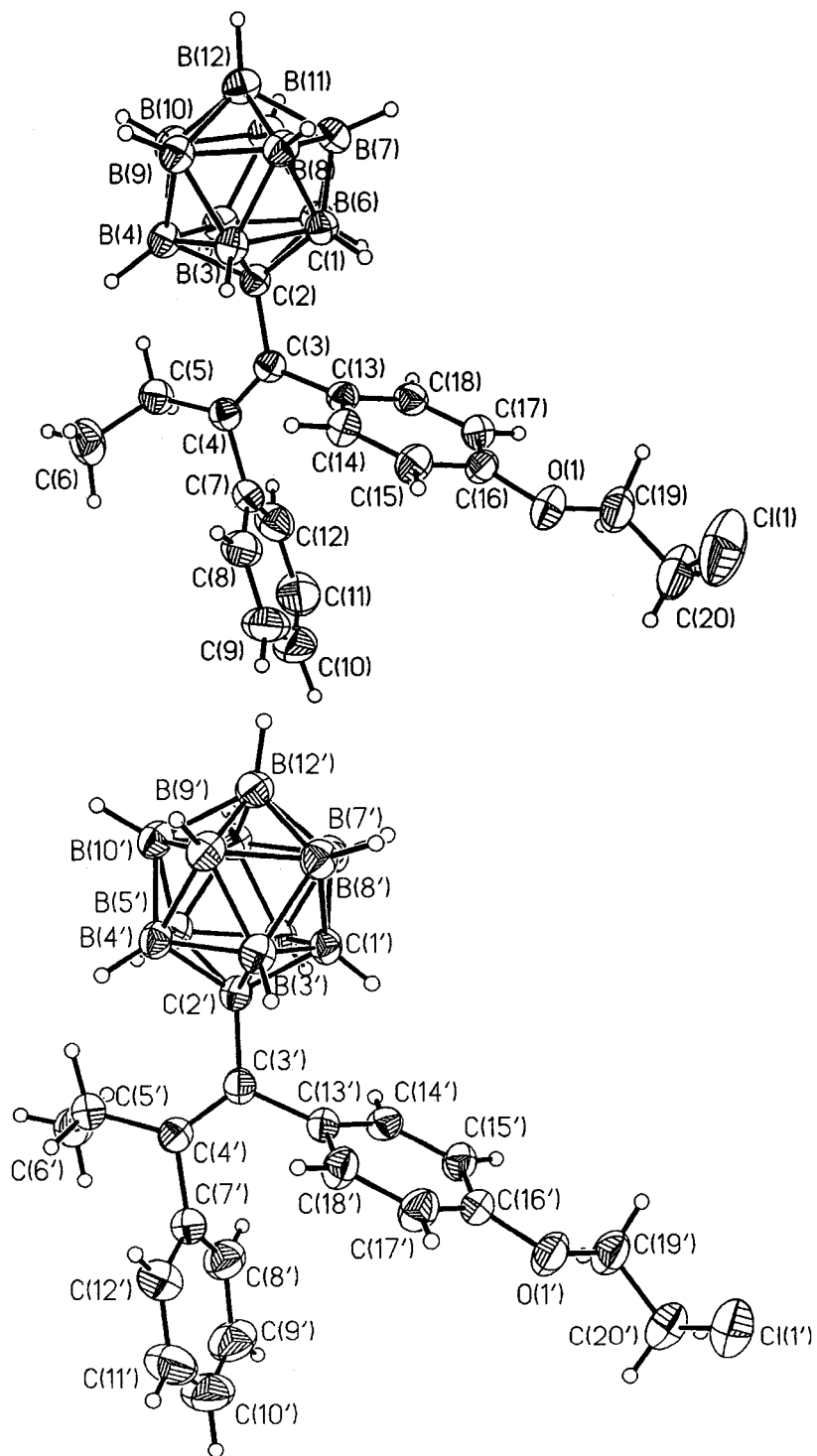


Figure 2.10 – ORTEP representation of both crystallographic independent molecules of 2.25, with thermal ellipsoids shown at the 30% probability level.

2.9 Synthesis of a *nido*-Carborane Analogue of Tamoxifen (2.28)

The chloro group of **2.25** was subsequently converted to the corresponding dimethylamino derivative (**2.27**) by heating **2.25** in an alcoholic solution of dimethylamine (*vide infra*). However, the yield of the product was low, which is attributed to the low reactivity of the pendant chloro group toward S_N2 substitution. In order to improve the yields of **2.27**, the chloride was first converted to the iodide **2.26**.⁵⁶

Compound **2.25** was converted to the iodide **2.26** by reaction with sodium iodide in acetone, giving the desired product in 65% isolated yield. The proton NMR spectrum of the iodide **2.26** was nearly identical to that of the chloride precursor (**2.25**) except for the upfield shift of the CH₂X-proton triplet from 3.71 to 3.32 ppm. The ¹³C NMR spectrum of **2.26** showed a dramatic upfield shift of the CH₂X-carbon peak from 41.67 ppm in the chloride **2.26** to 0.63 ppm in the iodide product. The mass spectrum of **2.26** did contain a molecular ion at m/z = 521 ([M]⁺), however fragmentation of the iodoethoxy group was evident with the base peak being 155 m/z ([CH₂CH₂I]⁺), which, in addition to a B₁₀ isotopic distribution at 365 m/z [M-CH₂CH₂I]⁺, give the combined mass of the parent ion (521 m/z). The ¹¹B NMR and IR spectrum of **2.26** were not significantly different from those of compound **2.25** and do not warrant further discussion.

The iodide **2.26** was successfully converted to the target compound **2.27** using a similar procedure to that used with the chloride; however, heating at reflux was unnecessary. The iodide was displaced with dimethylamine at ambient temperature, which gave the same product as obtained from **2.25**, but in better yield (20%). The ammonium salt of the *nido*-carborane (**2.27**) product proved to be relatively unstable,

degrading slowly even when stored at low (-10°C) temperature under argon. Alteration of the counter ion was performed in an attempt to stabilize the product, with little effect. The source of degradation was hypothesized to be associated with the free tertiary amine reacting with the anionic *nido*- cage. This problem was alleviated by protonation of the dimethylamino group with ethereal HCl, resulting in the formation of the internal salt **2.28**. Compound **2.28**, which showed vastly improved stability, was readily isolated by radial chromatography. Reverse phase HPLC analysis of compound **2.28** under several different solvent conditions exhibited only one peak.

Degradation of the cage also introduced a second stereocenter into the structure, producing diastereotopic protons throughout the remainder of the structure. This is observed in the 500 MHz ^1H NMR spectrum of **2.28** from the presence of closely associated peaks for all splitting patterns observed (Figure 2.13). The two different enantiomers that form upon conversion of **2.26** to **2.27** are not separable by HPLC. As a whole, the ^1H NMR experiments indicated that compound **2.28** behaved, in solution, much like **2.25** and tamoxifen itself. The ^1H NMR spectrum of **2.28** showed a peak at 2.83 ppm due to the six equivalent methyl protons associated with the dimethylamino functionality (Figure 2.12). The allylic protons in the ethyl group of both **2.25** and **2.28** were found to be magnetically equivalent, suggesting that at room temperature neither compound exists as a discrete atropisomer. This is in contrast to the observations made in the X-ray structure analysis of **2.25**.⁵⁷ The protons on ring B of both **2.25** and **2.28** appear as AA'BB' systems, which is identical to that for tamoxifen. This is further evidence to

suggest that the presence of the carborane cage does not impede the number of possible orientations of the B and C rings in solution.

The ^{11}B NMR spectrum of **2.28** was more complex than that of **2.25**, which is consistent with the loss of symmetry brought about by degradation of the carborane cage.⁴⁰ The proton-decoupled spectrum for **2.28** consisted of resonances between -7.90 and -35.20 ppm occurring in a 1:1:1:2:1:1:1 ratio. The resonance at -31.58 in the proton-coupled spectrum (Figure 2.11), exhibited coupling to the bridging hydrogen atom. The IR spectrum of compound **2.28** exhibits a strong B-H stretch at 2514 cm^{-1} , which is shifted from the corresponding stretch in the spectrum of the *closo* precursor **2.25** (2579 cm^{-1}), but within the range expected for a *nido*-carborane.

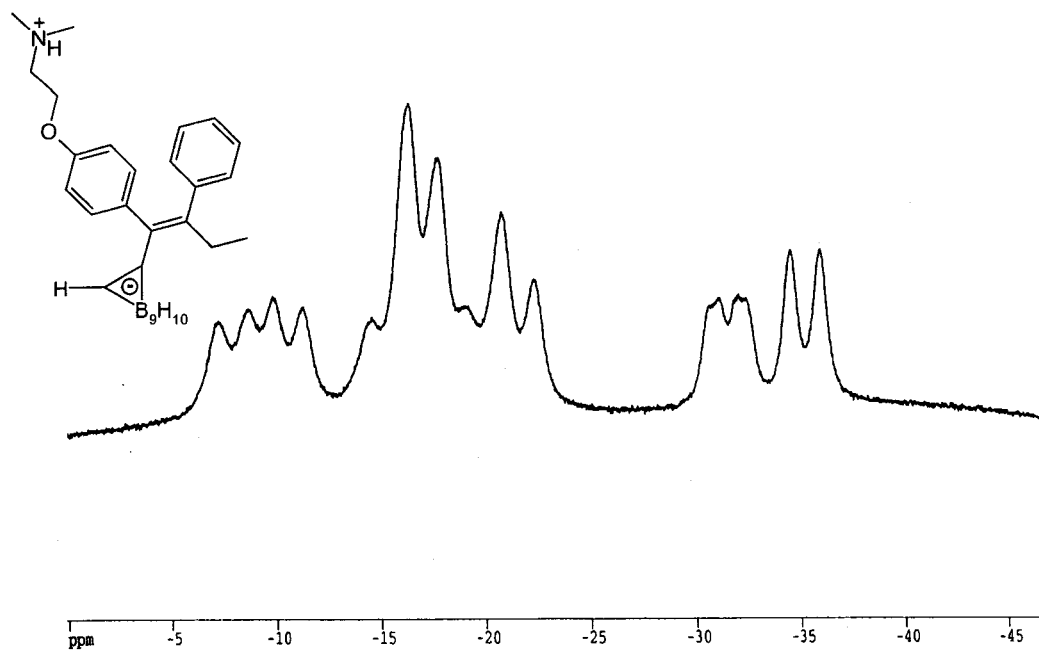


Figure 2.11 – ^{11}B NMR spectrum of **2.28**

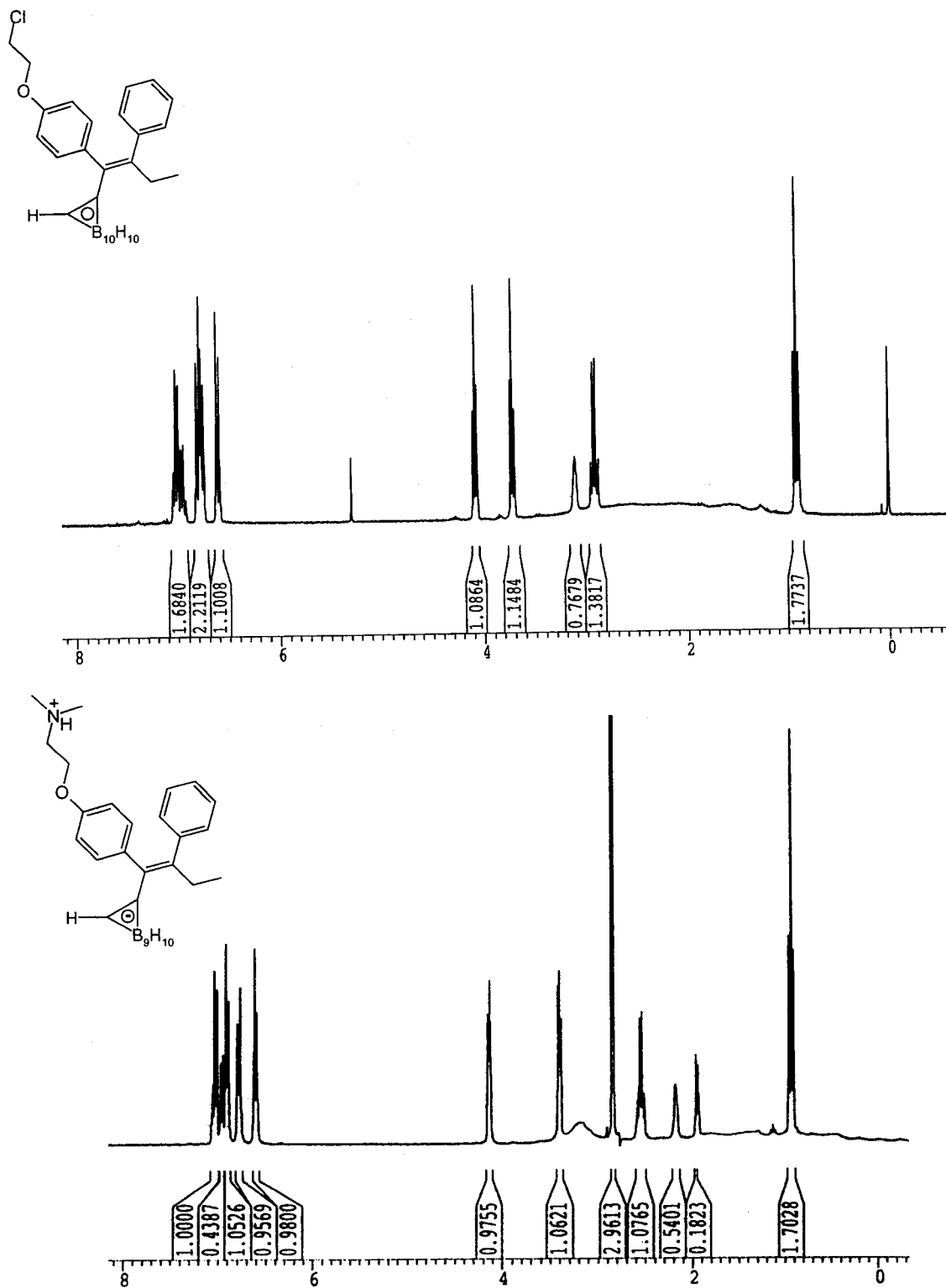


Figure 2.12 – ^1H NMR spectra of 2.25 and 2.28.

The major peak in the electrospray mass spectrum of compound **2.28** was that of the molecular ion (427 m/z). The parent peak also displayed the expected isotopic distribution pattern. High resolution positive ion ESMS gave a molecular mass peak at 430.374 m/z, in close agreement with the calculated value of 430.371 m/z.

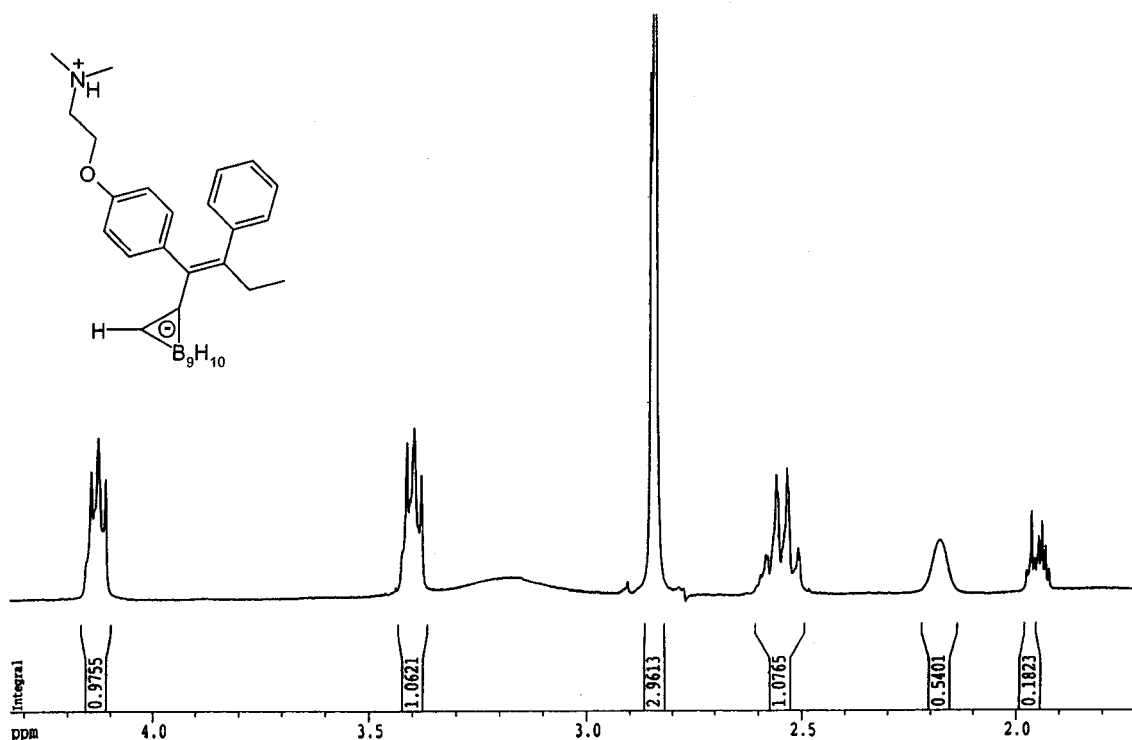


Figure 2.13 ^1H NMR spectrum of **2.28** showing diastereomer peaks.

2.10 Relative Binding Affinity Study

With the successful generation of the tamoxifen analogues **2.25** and **2.28**, we collaborated with Drs. Gerard Jaouen and Anne Vessières-Jaouen (Ecole Nationale Supérieure de Chimie de Paris) in order to determine the relative binding affinities (RBA)

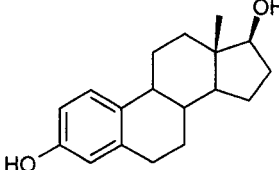
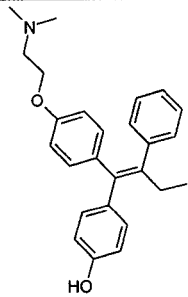
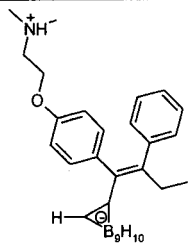
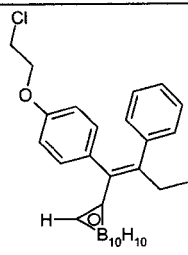
Compound	RBA on ER α (%)	RBA on ER β (%)
	100 (by definition)	100 (by definition)
	38.5	20
	0.03	No competition
	No competition	No competition

Table 2.1 – Relative binding affinities for some tamoxifen analogues.

of compounds **2.25** and **2.28** (Table 2.1).⁵⁸ Compound **2.28** showed less than 0.1% of the RBA of estradiol while **2.25** exhibited no ability to displace the same hormone from either ER α or ER β .

The fact that compound **2.28** showed some affinity for the ER, albeit low, suggests that the proposed strategy holds some promise. The reported synthetic methodology was designed to allow facile variation in the basic structure in order to optimize the RBA. The synthesis of other analogues of compound **2.28** will be the subject of future research in an effort to increase the binding of the carborane analogue to the ER.

2.11 Synthesis of a Rhenium Complex of Tamoxifen-Carborane

Having successfully developed a novel synthesis of a *nido*-carborane analogue of tamoxifen, emphasis was shifted toward demonstrating the feasibility of attaching a $[\text{Re}(\text{CO})_3]^+$ core to the open face of the *nido*-cage in **2.28**. The rhenium carbonyl core serves as a model for the $^{99\text{m}}\text{Tc}$ analogue, which can be used to evaluate the compound *in vivo*.

Previous work performed in our research laboratory established a method for the synthesis of η^5 -carborane complexes of rhenium and technetium.⁵⁹ The X-ray structure of **2.29** (Figure 2.14) was obtained and is the first reported structure of a technetium-carborane complex. Compound **2.29** is, as expected, nearly iso-structural with the previously reported rhenium complex.⁶⁰ The average distance between the bonding face of the carborane and the metal center is 2.32 Å, which is nearly identical to the corresponding distance reported for the Re complex. The carborane cage itself appears to be a slightly irregular icosahedron with the average B-B, B-C and C-C bond distances being 1.76(2) Å, 1.71(2) Å and 1.60(2) Å, respectively.

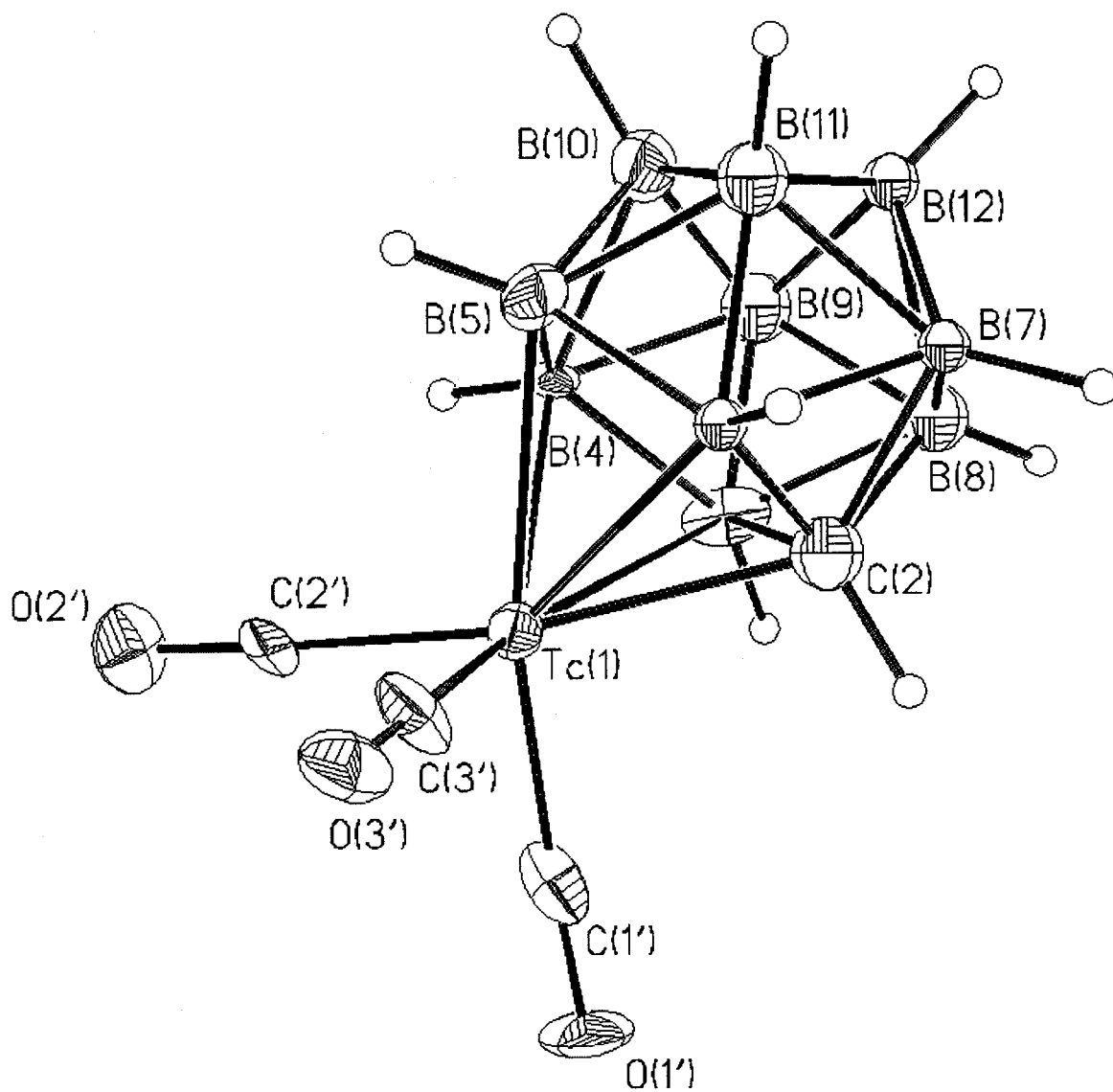


Figure 2.14 – ORTEP representation of 2.29. Thermal ellipsoids are shown at the 50% probability level. The NEt₄ counter ion was removed for clarity.

The resistance of these complexes to substitution by biological ligands was evaluated using a cysteine challenge experiment.⁶¹ It was shown that the complex, when incubated with excess cysteine under physiological conditions, remained largely intact as determined by HPLC, FTIR and ESMS experiments. This stability, which is essential if

carboranes are to be used as carriers of radionuclides, was expected because the 18-electron system exhibits electron delocalization between the transition metal and carborane orbitals of appropriate symmetry.⁶²

Building on these results, we attempted to prepare the rhenium complex of the *nido*-carborane tamoxifen **2.3** (Figure 2.15). The synthesis of **2.31** was attempted using the internal salt precursor **2.28** by reacting the *nido*-carborane derivative with $[\text{NEt}_4]_2[\text{Re}(\text{CO})_3\text{Br}_3]$ under either organic (THF) or aqueous conditions. Using aqueous media, no reaction was observed to occur and ESMS analysis of the crude reaction mixture showed only the presence of the deprotonated *nido*-tamoxifen ($m/z = 427$, Figure 2.16) starting material and a number of peaks corresponding to “ $\text{Re}(\text{CO})_3$ ” clusters.⁶³ With THF as the reaction solvent, TIOEt was used as a base in hopes of stabilizing the dicarbollide dianion as a weakly bound complex with thallium.⁶⁴ Once in the presence of $\text{Re}(\text{I})$ or $\text{Tc}(\text{I})$, transmetallation would yield the desired complex. The desired product

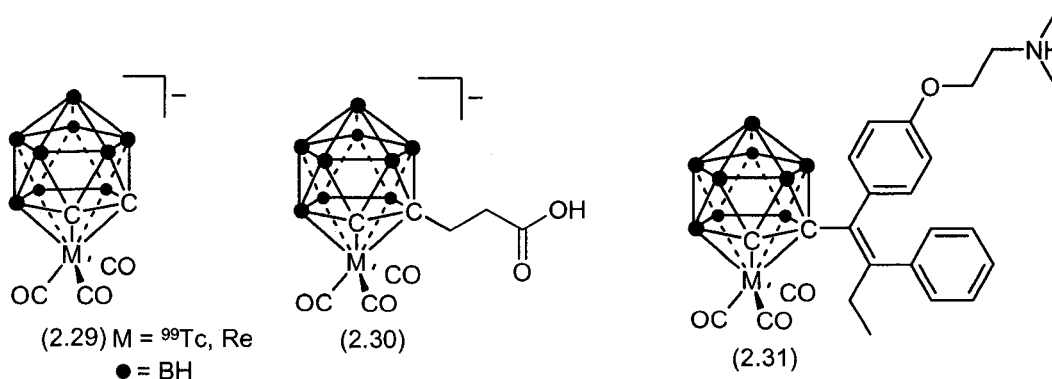


Figure 2.15 - η^5 carborane complexes of rhenium and technetium.

was observed by LCMS ($m/z = 647.9$, Figure 2.16), however we were unable to isolate an appreciable amount of the complex by HPLC.

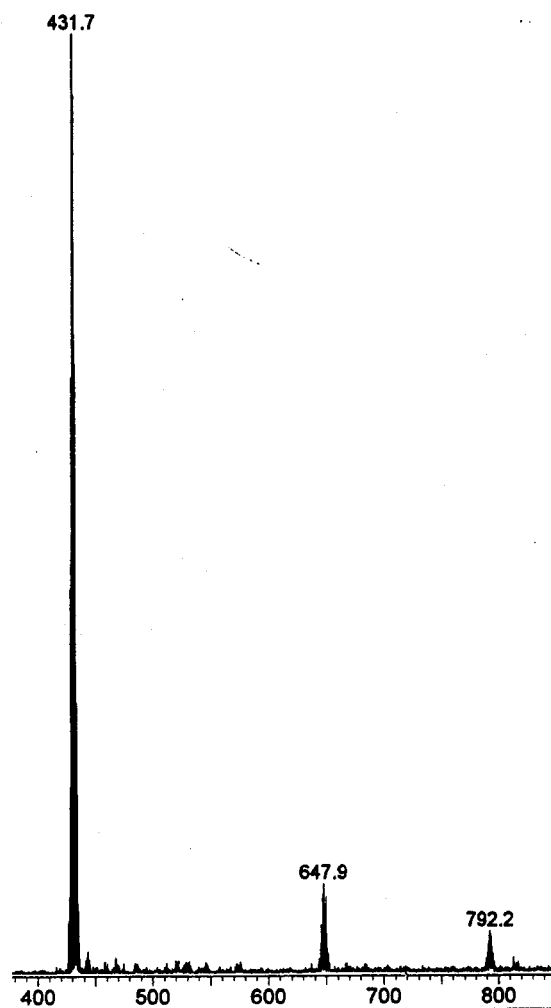


Figure 2.16 – ESMS evidence for the formation of 2.31.

2.12 Attempted Synthesis of a *para*-Carborane Analogue of Tamoxifen

Given the inherent reactivity of the *ortho*-carborane cage toward bases, and the subsequent formation of the *nido*-carborane in the aforementioned synthesis of 2.28,⁶⁵

attempts were made to prepare a *para*-carborane analogue of tamoxifen (Figure 2.17).^{66,67} The more robust *para*-structural isomer is highly resistant to degradation and should yield the *closo*-carborane product **2.32**, even when exposed to alkaline reaction conditions. An additional advantage to using the *para* isomer is that the remaining C-H vertex can be readily derivatized.⁶⁸ This would enable the exploration of structure-activity relationships for a variety of functionalities, including the *para*-hydroxyl derivative, which is analogous to 4-hydroxy-tamoxifen **2.4**, an active metabolite of tamoxifen.⁶⁹

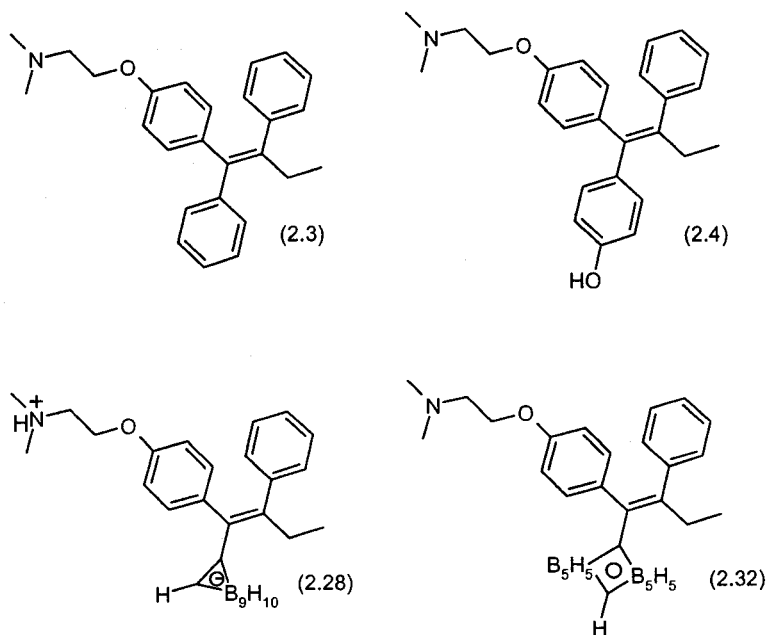
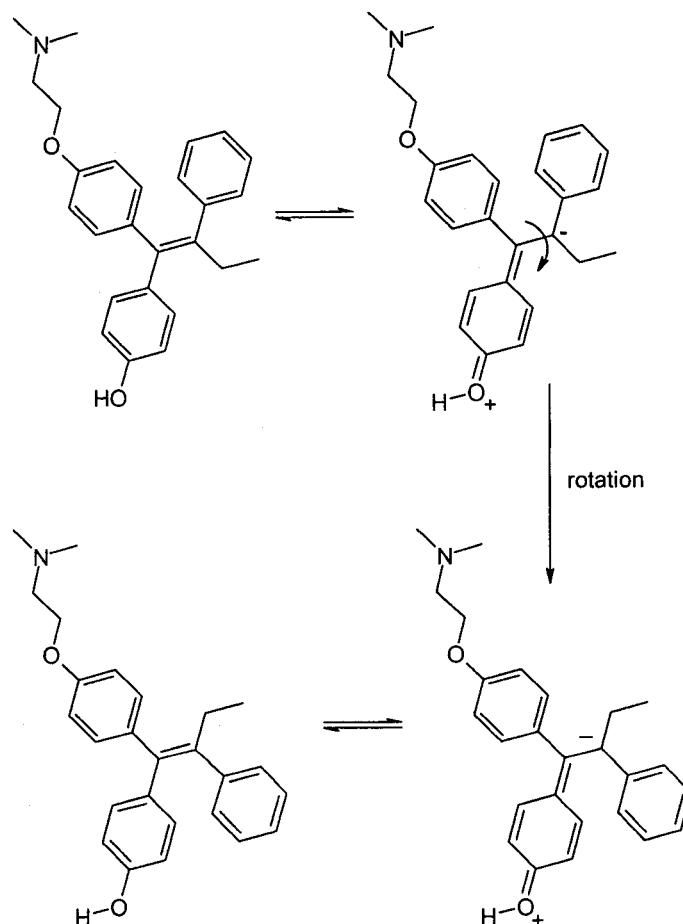


Figure 2.17 – Proposed *para*-carborane analogue of tamoxifen **2.32**.

2.13 Rationale

It is known that 4-hydroxytamoxifen (**2.4**), exhibits a 100-fold higher affinity for the estrogen receptor than tamoxifen itself.⁷⁰ Unfortunately, the hydroxylated form undergoes isomerization *in vivo*, yielding *E*-tamoxifen, which is known to be estrogenic.

Generation of an oestrogen agonist *in vivo* is not desirable, because it can promote rather than inhibit tumor growth (Scheme 2.6).⁷¹



Scheme 2.6 – Isomerization of 4-hydroxy-Z-tamoxifen to the E isomer. Not all canonical forms are shown.

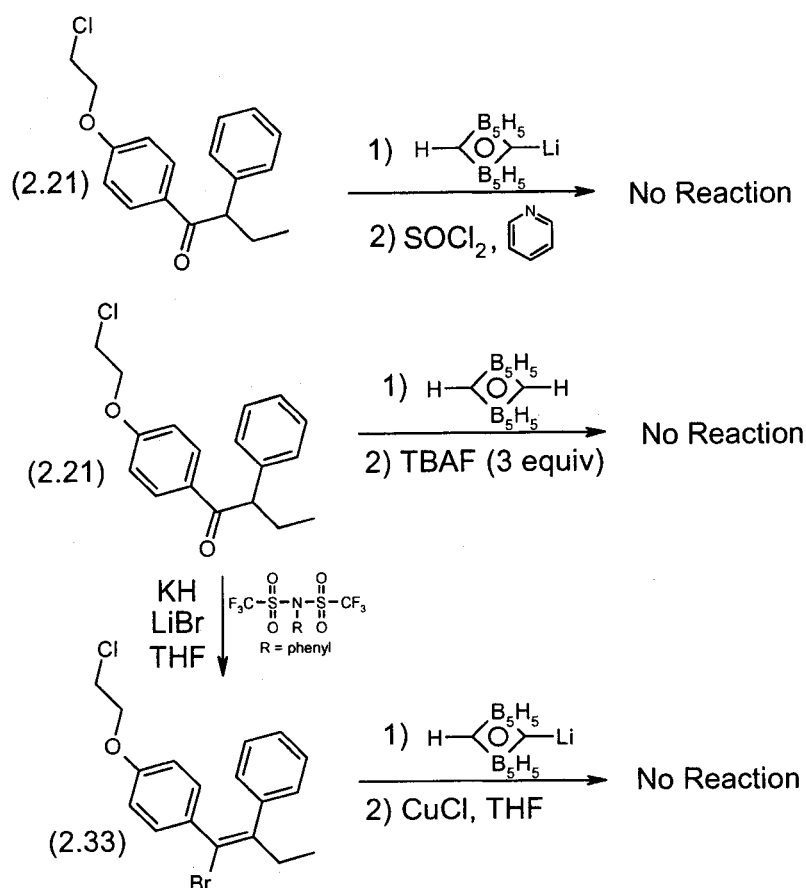
Many studies have been devoted toward the development of a tamoxifen derivative that exhibits the same binding affinity as **2.4**, but do not undergo the detrimental isomerization process *in vivo*. In order to avoid resonance isomerization, all derivatives reported to date significantly alter the basic structure of tamoxifen, thereby reducing their affinity for the ER.⁷²⁻⁷⁷

Because carboranes are resistant to catabolism, formation of the hydroxylated analogue *in vivo* is highly improbable. Furthermore, the hydroxylated derivative of *para*-carborane, which should have a high affinity for the ER, would not be able to isomerize owing to the clusters unique electronic structure. Consequently the corresponding *para*-carborane analogue **2.32** and the *para*-carborane hydroxy analogue should not only have enhanced affinity to the ER compared to compound **2.28**, but could potentially act as metabolically resilient antiestrogen.

2.14 Attempted Synthesis of 2.32 by Carbon-Carbon Single Bond Formation

Several strategies were undertaken to prepare **2.32** (Figure 2.17). The first involved nucleophilic attack of mono-lithio *para*-carborane on the previously prepared ketone **2.21**. Despite the inherent steric bulk introduced by the icosahedral carborane cage, these polyhedra have been previously shown to react with ketones and aldehydes.⁷⁸ Unfortunately, despite the use of excess nucleophile and vigorous reaction conditions, it was found that the desired product could not be formed (Scheme 2.7).

Yamamoto and co-workers⁷⁹ have previously shown that the C-H bond of the polyhedral carborane is highly activated due to the delocalized electronic nature inherent to the cage, and can thus be deprotonated easily using a weak base such as the F⁻ anion from tetrabutylammonium fluoride (TBAF). The resulting carbanion has been coupled with a variety of electrophiles, including aldehydes and ketones, without the need for strongly basic reaction conditions. Unfortunately, this approach also failed to yield **2.32**.

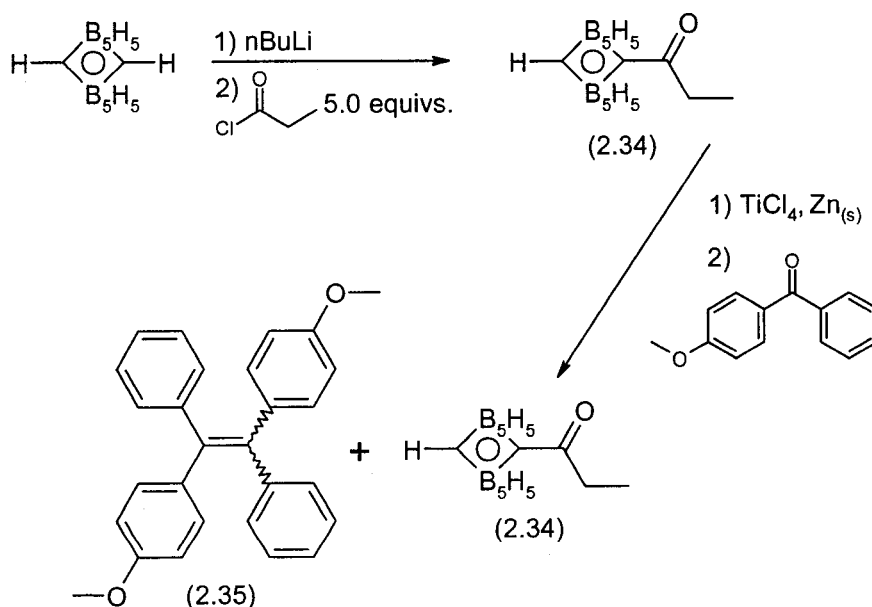


Scheme 2.7 – Attempted synthesis of 2.32.

With the lack of reactivity exhibited between the *para*-carborane anion and the ketone (2.21), the possibility of generating 2.32 using a metal-mediated cross coupling reaction was explored (Scheme 2.7). The vinyl bromide 2.33 was prepared following the method of Potter et al. in 51% yield.³³ Using a method first reported by Coult and co-workers⁸⁰ the *para*-carborane anion was subjected to a reaction with the vinyl bromide 2.33 in the presence of CuCl. Unfortunately the starting material remained intact regardless of solvent, temperature or reaction time.

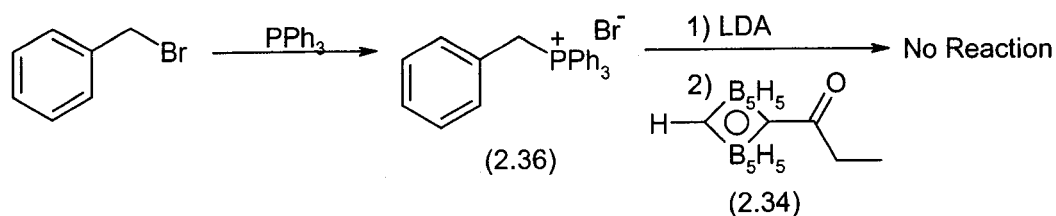
2.15 Attempted Synthesis of 2.32 by Carbon-Carbon Double Bond Formation

A number of methods have been used to generate tamoxifen analogues through carbon-carbon double bond forming reactions. Examples include the McMurry coupling with Ti(II)^{81,82} and the traditional dehydration of 1,1,2-triarylbutan-1-ols.⁸³ These strategies were followed as a means of preparing 2.32. The ethyl ketone 2.34 was generated directly from the lithio-salt of *para*-carborane in the presence of an excess of propionyl chloride. The ketone 2.34 was combined with 4-methoxybenzophenone in hopes of generating a mixture of diastereomeric mixture of cross-coupled products. Unfortunately, it was found that the ethyl ketone did not undergo a reaction at all, while the homo-coupling of 4-methoxybenzophenone to generate 2.35 took place readily (Scheme 2.8).



Scheme 2.8 – Attempted McMurry coupling of 2.34 with 4-methoxybenzophenone.

Following a more classical approach, the phosphonium salt **2.36** was generated from benzyl bromide and triphenylphosphine. Deprotonation of the phosphonium to the corresponding ylide with lithium diisopropylamide (LDA) was followed by the addition of compound **2.34**. Again, the desired alkene did not form (Scheme 2.9).



Scheme 2.9 – Attempted Wittig Olefination of benzylphosphonium bromide with **2.34**.

2.16 Summary and Future Work

A novel, stereoselective strategy for the synthesis of a *nido*-carborane analogue of tamoxifen **2.28** was developed, and a key intermediate **2.25** was characterized by X-ray crystallography. The reported synthetic approach yielded the carborane derivative of tamoxifen having the appropriate stereochemistry to act as an estrogen antagonist. The *nido*-carborane **2.28**, which formed upon reaction of compound **2.25** or **2.26** with dimethylamine, showed modest affinity for the ER. With this encouraging result in hand, future work is set on developing the synthetic methodology for other carborane analogues of tamoxifen.

The fact that compound **2.28** showed some affinity for the ER suggests that the inclusion of a carborane into the basic core of tamoxifen is a viable strategy for developing new antiestrogens and BNCT agents. The lower than optimal RBA may be a result of the reduced lipophilicity of the anionic *nido*-carborane.

In an attempt to generate a new class of radioimaging agent for breast cancer, the synthesis of the model η^5 -complex of $\text{Re}(\text{CO})_3$, compound **2.31**, was accomplished. Having previously established the synthetic methodology for attaching a $[\text{Tc}(\text{CO})_3]^+$ and $[\text{Re}(\text{CO})_3]^+$ core to the open face of an unsubstituted *nido*-carborane, the next logical step was to extend this method toward a bifunctional derivative. This derivative, while enabling the attachment of a radionuclide, also contained a targeting entity. To this end the $[\text{Re}(\text{CO})_3]^+$ core was attached to the open face of the *nido*-carborane analogue of tamoxifen (**2.28**) to give **2.31**, as a test toward the feasibility of this approach. While the yield of the reaction was low, it was accompanied by the formation of a significant quantity of “ $\text{Re}(\text{CO})_3$ ” clusters, which left mostly unreacted starting material **2.28** as the major reaction component. Future research efforts include the development of synthetic methods capable of generating greater yields for the desired metal complexes.

Attempts were also made to synthesize the *para*-carborane analogue of tamoxifen **2.32**, in the hopes of eventually enabling the synthesis of a *para*-hydroxylated analogue of 4-hydroxytamoxifen. One method involved was the reaction of a C-lithio carboranyl anion on the ketone **2.21**, while another involved TBAF mediated deprotonation of *para*-carborane in the presence of the same ketone **2.21**. Both methods were unsuccessful at generating any of the target compound. It is clear from the current work that the *para*-carborane moiety is too sterically hindered to react with the ketone **2.21** carbonyl.

Additional attempts to synthesize **2.32** included a number of metal-mediated cross coupling reactions using Cu(I) and Pd(0) based catalysts. Attempts in our research laboratory to couple vinyl halides with the corresponding carborane halide using a variety

of palladium catalysts were unsuccessful. In the future, other variations of metal-mediated cross coupling reactions should be attempted. These should include exploring the effectiveness of using different vinyl substituents (I, Tf) and carboranyl organometallic reagents (Li, Mg, Zn, etc.) in an effort to optimize the reaction.

A second strategy used to generate **2.32** employed carbon-carbon double bond forming reactions, including an attempted McMurry coupling and Wittig olefination. The cross coupling of the *para*-carboranyl ketone **2.34** with 4-methoxybenzophenone and triphenylphosphonium bromide **2.36** were both unsuccessful.

Consequently, future work should focus on completing the synthesis of the *para*-carborane analogue, which as mentioned will not degrade under the stated reaction conditions. In addition, substitution of the remaining CH vertex with a hydroxyl group will allow the generation of analogues of 4-hydroxyl tamoxifen, the active metabolite of tamoxifen in humans. Furthermore, replacing the dimethylamine with other amines could potentially optimize binding of the carborane-tamoxifen analogues. These strategies have been used successfully in other tamoxifen analogues to improve affinity for the ER.

2.17 Experimental

Synthesis of 2-Chloroethoxybenzene (2.20)²⁶

Distilled, deionized water (225 mL) and 1,2-dichloroethane (225 mL) were added to a 1L round bottom flask. The biphasic solution was stirred rapidly while phenol (29.05g, 309 mmol), NaOH (24.9 g, 622.5 mmol) and dimethyldioctadecylammonium bromide (1.7 g, 3.09 mmol) were all added in single portions. The reaction mixture was maintained at reflux for 48 hours. After allowing the mixture to cool to room temperature, the organic layer was separated and washed with 3M NaOH (5 x 200 mL). The organic portion was subsequently dried over Na₂SO₄ and filtered giving a transparent yellow solution. Concentration *in vacuo* gave a crude yellow oil, which was purified by vacuum distillation (60°C, < 1mm Hg) affording a clear colourless distillate (25.5 g, 53%).

Synthesis of 1-(4-(2-chloroethoxy)phenyl)-2-phenyl-butanone (2.21)²⁶

A dry round bottom flask was charged with 2-chloroethoxybenzene (25.5 g, 162.8 mmol) and 2-phenylbutyric acid (25.46g, 155.07 mmol). Stirring was initiated under dry N₂ as the reaction mixture was cooled to 0°C. Trifluoroacetic anhydride (34.52 g, 23.21 mL, 164.38 mmol) was added dropwise to the cold stirring solution. The reaction was allowed to warm to room temperature and maintained under an inert atmosphere for 72 hours. The resulting red solution was poured into distilled deionized water (175 mL) and extracted with CH₂Cl₂ (3 x 100 mL). The organic fractions were pooled, dried over Na₂SO₄ and gravity filtered giving a dark filtrate. The solvent was removed by rotary

evaporation giving a red solid. The product, a white crystalline solid was obtained upon recrystallization from ether (41.42 g, 84%). m.p. 62-64°C

Synthesis of Z-3-(4-(2-Chloroethoxy)phenyl)-4-phenyl-hex-3-ene-1-(2-trimethylsilylacetylene) (2.23)

Four equal portions of fresh n-butyllithium (80 mL, 1.6 M hexanes) were added to (trimethylsilyl)acetylene (18 mL, 0.13 mol) in dry THF (100 mL), which had been previously cooled to -78°C under a nitrogen atmosphere. After five minutes, the ketone **2.21** (33 g, 0.11 mol) dissolved in dry THF (50 mL) was added dropwise. The reaction was allowed to warm to room temperature overnight. Saturated ammonium chloride (20 mL) was slowly added to the reaction followed by distilled water (100 mL) and the resulting solution extracted with ether (4 x 100 mL). The organic fractions were combined, dried over Na_2SO_4 , filtered through a fritted funnel and the filtrate evaporated to dryness. The resulting yellow oil was dissolved in a mixture of freshly distilled pyridine (50 mL) and ether (50 mL) and cooled to 0°C under nitrogen. Thionyl chloride (16 mL) was added dropwise over five minutes. The reaction was allowed to warm to room temperature overnight whereupon distilled water (100 mL) was added slowly while cooling the solution over ice. Aqueous HCl (1M, 100 mL) was added and the layers separated. The dark aqueous layer was extracted with ether (3 x 200 mL) and combined with the original organic fraction. The organic solution was further extracted with 1M HCl (3 x 100 mL), dried over sodium sulfate and the solvent evaporated, leaving an orange/red oil. The product, a yellow oil (27.2 g, 65%), was isolated by column

chromatography (100% hexanes). Compound 2.23 showed: TLC (70:30 hexanes:ether): $R_f = 0.71$; $^1\text{H NMR}$ (200 MHz, CDCl_3): δ 7.14-6.60 (m, 9H, aryl-H), 4.11 (t, 2H, OCH_2), 3.72 (t, $^3J_{\text{HH}} = 6.0$ Hz, 2H, CH_2Cl), 2.89 (q, 2H, CH_2CH_3), 1.03 (t, $^3J = 7.4$ Hz, 3H, CH_2CH_3), 0.24 (s, 9H, SiMe_3); $^{13}\text{C NMR}$ (50 MHz, CDCl_3): δ 152.41, 147.77, 136.42, 126.73, 125.82, 124.30, 123.71, 122.53, 115.04, 109.47, 101.49, 94.16, 63.53, 37.49, 27.09, 7.96, 0.07; IR (neat, cm^{-1}): 3056, 2967, 2929, 2874, 2134, 1608, 1247; MS (CI, NH_3): m/z 383 (M+H); HRMS (EI): Calcd for $\text{C}_{23}\text{H}_{27}\text{ClOSi}$ (M^+) 382.153. Found 382.152.

Synthesis of Z-3-(4-(2-chloroethoxy)phenyl)-4-phenyl-hex-3-ene-1-yne (2.24)²⁶

The protected alkyne 2.23 (26.5 g, 69.1 mmol) was dispensed as a solution in absolute methanol and to it was added potassium hydroxide (4.26 g, 76.0 mmol) as a solid. The reaction was maintained at ambient temperature overnight. After the addition of distilled water (100 mL) the mixture was extracted with ether (3 x 50 mL). The organic fractions were pooled, dried over sodium sulfate and gravity filtered and the solvent removed by rotary evaporation giving a yellow-coloured solid. The product was initially purified by flash silica gel chromatography (4% ether in pet. ether) and recrystallized once from petroleum ether giving pure product, compound 2.24 (0.122 g, 60%) which showed: mp 53-55°C; TLC (8% Ether:Hexanes): R_f 0.59; $^1\text{H NMR}$ (200 MHz, CDCl_3): δ 7.16-6.64 (m, 9H, Ar-H), 4.12 (t, $^3J_{\text{HH}} = 6.0$ Hz, 2H, OCH_2), 3.73 (t, 2H, CH_2Cl), 3.29 (s, 1H, CH), 2.91 (q, 2H, CH_2CH_3), 1.03 (t, $^3J_{\text{HH}} = 7.5$ Hz, 3H, CH_3); $^{13}\text{C NMR}$ (50 MHz, CDCl_3): δ 156.76, 152.49, 140.37, 131.63, 130.93, 128.96, 128.01,

126.90, 118.24, 113.82, 84.24, 81.38, 67.80, 41.77, 31.16, 12.40; IR (CH₂Cl₂, cm⁻¹): 3301, 3055, 2974, 2935, 2874, 1607, 1508; MS (EI): m/z 310 [M⁺]; HRMS (EI): Calcd for C₂₀H₁₉ClO (M⁺) 310.114. Found 310.112; Anal. Calculated for C₂₀H₁₉ClO: C, 77.29; H, 6.16. Found: C, 77.66, H, 6.34.

Synthesis of Z-1-(1,2-dicarba-closo-dodecaboran-1-yl)-1-(4-(2-chloroethoxy)phenyl)-2-phenyl-but-1-ene (2.25)

The alkyne **2.24** (14.43 g, 46.43 mmol) was dissolved in dry toluene (150 mL) followed by the addition of the decaborane-acetonitrile adduct (10.31 g, 51.07 mmol) was added in one portion. The reaction mixture was brought to reflux for 24 hour upon which completion was noted by TLC. (9:1 pet. ether: ether) and IR spectroscopy. After 24 h, the solvent was removed by rotary evaporation leaving a yellow oil. The oil was taken up in ethylene chloride (100 mL) and washed with 0.1 N NaOH (3 x 50 mL). The aqueous fractions were combined and further extracted with CH₂Cl₂ (3 x 50 mL). All organic fractions were pooled and dried over sodium sulfate and gravity filtered. The solvent was removed by rotary evaporation, leaving a crude yellow solid. The product, compound **2.25** (2.0 g, 10%) was purified by flash silica gel chromatography with 4% ether in petroleum ether as the eluent. Recrystallization from petroleum ether gave X-ray quality crystals. mp 55-57°C; TLC (8% Ether:Hexanes): R_f 0.50; ¹H NMR (500 MHz, CDCl₃): δ 7.16-6.64 (m, 9H, Ar-H), 4.09 (t, ³J_{HH} = 6.0 Hz, 2H, OCH₂), 3.90-0.90 (br m, 10H, BH), 3.71 (t, 2H, CH₂Cl), 3.13 (br s, 1H, CH), 2.92 (q, ³J_{HH} = 7.5 Hz, 2H, CH₂CH₃), 0.91 (t, 3H, CH₃); ¹³C NMR (50 MHz, CDCl₃): δ 157.14, 151.13, 142.40, 132.73, 131.73,

128.99, 128.24, 127.39, 126.00, 114.24, 67.82, 62.98, 41.67, 27.49, 12.56; ^{11}B NMR (96 MHz, CDCl_3): δ -3.51, -8.99, -12.67, -13.95; IR (Unroll, cm^{-1}): 3303, 3055, 2970, 2935, 2579, 1607; MS (EI): m/z observed boron isotopic distribution at 429 (M^+). HRMS (EI): Calcd for $\text{C}_{20}\text{H}_{29}\text{B}_{10}\text{ClO}$ (M^+) 429.290. Found 429.292. Anal. Calculated for $\text{C}_{20}\text{H}_{29}\text{B}_{10}\text{ClO}$: C, 55.81; H, 6.74. Found: C, 55.78; H, 6.36. X-ray Crystallography: Space group: $\text{P}2_1/c$, $a = 13.0341(5)$ Å, $b = 30.6131(9)$ Å, $c = 13.4514(2)$ Å, $\alpha = \gamma = 90^\circ$, $\beta = 116.6400(10)^\circ$, $V = 4797.5(2)$ Å³, $Z = 8$, data/parameters: 9509/810, $R = 0.0505$, $R_w = 0.1228$, GOF = 0.911.

Synthesis of Z-1-(1,2-dicarba-closo-dodecaboran-1-yl)-1-(4-(2-iodoethoxy) phenyl)-2-phenyl-but-1-ene (2.26)

Compound **2.25** (0.200 g, 0.46 mmol) was dissolved in freshly distilled acetone (20 mL). Sodium iodide (0.350 g, 2.34 mmol) was added and the reaction heated under refluxing conditions for 2 days. The reaction was cooled and the solvent removed by rotary evaporation giving a colourless solid, which was taken up in methylene chloride and extracted with distilled water (2 x 25 mL). The organic layer was then dried over sodium sulfate, gravity filtered and the excess solvent removed using a rotary evaporator. The crude iodide was purified by radial chromatography with 3% ether in petroleum ether. The purified product, compound **2.26**, a white crystalline solid (0.156 g, 65%) showed: TLC (5% Ether:Petroleum Ether): R_f 0.37; ^1H NMR (200 MHz, CDCl_3): δ 7.01-6.60 (m, 9H, Ar-H), 4.10 (t, $^3J_{\text{HH}} = 6.6$ Hz, 2H, OCH_2), 3.90-0.80 (br m, 10H, BH), 3.32 (t, 2H, CH_2Cl), 3.13 (br s, 1H, CH), 2.92 (q, $^3J_{\text{HH}} = 7.3$ Hz, 2H, CH_2CH_3), 0.91 (t, 3H,

CH₃); ¹³C NMR (50 MHz, CDCl₃): δ 156.86, 151.10, 142.38, 131.98, 131.73, 128.95, 128.24, 127.39, 125.99, 114.31, 68.42, 62.96, 27.49, 12.59, 0.63; ¹¹B NMR (160 MHz, CDCl₃): δ -3.50, -8.97, -12.67, -13.96; IR (CHCl₃, cm⁻¹): 3020, 2971, 2579; MS (EI): m/z observed boron isotopic distribution at 521 m/z (M+H); HRMS (EI): Calcd for C₁₈H₂₅B₁₀ (M-OCH₂CH₂I) 365.2929. Found 365.2918.

Synthesis of Z-1-(1,2-dicarba-*nido*-undecaboran(-1)-1-yl)-1-(4-(2-dimethylammoniummethoxy) phenyl)-2-phenyl-but-1-ene. Inner salt. (2.28)

The iodide **2.26** (0.136 g, 0.261 mmol) was dissolved in a solution of dimethyl amine (10 mL, 30% solution in EtOH) whereupon gas evolution was immediately evident. The reaction mixture was stirred at ambient temperature under dry nitrogen for 3 hours. The excess amine was removed by rotary evaporation resulting in a viscous yellow oil. The oil was triturated with ethereal HCl and allowed to stand at -10°C for 48 hours. The excess ether was removed by rotary evaporation leaving a yellow semi-solid, which was subsequently dissolved in a minimal amount of CH₂Cl₂. The crude product was purified by radial chromatography (10% methanol in methylene chloride), yielding a colourless solid (**2.28**) (0.021 g, 19 %) showed: mp 260°C (decomp.); TLC (20% MeOH in CH₂Cl₂): R_f 0.53; ¹H NMR (300 MHz, CD₃CN): δ 7.03-6.58 (m, 9H, Ar-H); 4.12 (t, ³J = 5.0 Hz, 2H, CH₂NMe₂); 3.90-1.10 (br m, 9H, BH), 3.39 (t, 2H, OCH₂); 2.83 (s, 6H, N(CH₃)₂); 2.55 (q, ³J = 7.4 Hz, 2H, CH₂CH₃); 2.17 (br s, 1H, CH); 0.92 (t, 3H, CH₃); ¹³C NMR (50 MHz, CD₃CN): δ 154.99, 144.49, 143.58, 141.32, 137.14, 132.03, 129.65, 127.29, 125.36, 117.45, 112.32, 61.08, 57.04, 43.47, 28.84, 12.22; ¹¹B NMR (96 MHz,

CD₃CN): δ -7.90, -10.47, -15.37, -18.36, -21.47, -31.58, -35.20; IR (nujol, cm⁻¹): 3119, 2963, 2927, 2854, 2752, 2514, 1603; MS (ES, positive): m/z observed boron isotopic distribution at 427.3 (M⁺); HRMS (ES, positive): Calcd for C₂₂H₃₆B₉NO (M⁺) 430.371. Found 430.374. Anal. Calculated for C₂₂H₃₆B₉NO: C, 61.92; H, 8.26. Found: C, 61.93; H, 8.96.

Synthesis of (E)-1-Bromo-1-[4-(2-chloroethoxy)phenyl]-2-phenyl-1-butene (2.33)

Compound **2.21** (3.00 g, 10.00 mmol) was added to a stirred suspension of potassium hydride (1.70g of 50 wt % dispersion in mineral oil, 15.0 mmol) in dry THF (10 mL). After 1h, a solution of anhydrous lithium bromide (1.76 g, 20 mmol) in dry THF (10 mL) was added to the yellow enolate solution, followed by a solution of N-phenyltrifluoromethanesulfonimide (3.60 g, 10 mmol) in dry THF (10 mL), and the mixture was stirred for 4 h. After addition of 2-propanol (1 mL), the mixture was poured in distilled deionized water (100 mL) and extracted with ether (3 × 25 mL). The combined extracts were dried over Na₂SO₄ and concentrated *in vacuo* giving a crude oil. Compound **2.33** was purified by flash silica gel chromatography giving a white amorphous solid (1.87 g, 51%). TLC (30% Ether in Hexanes): R_f 0.54; ¹H NMR (200 MHz, CDCl₃): δ 7.14-6.98 (m, 7H, ArH), 6.71 (d, ³J = 8.8Hz, 2H, ArH), 4.12 (t, ³J = 5.9 Hz, 2H, OCH₂), 3.74 (t, 2H, CH₂Cl), 2.78 (q, ³J = 7.5 Hz, 2H, CH₂CH₃), 1.03 (t, 3H, CH₂CH₃); ¹³C NMR (50 MHz, CDCl₃): δ 157.00, 143.81, 140.47, 134.21, 131.44, 128.96, 127.85, 126.50, 120.63, 113.59, 67.70, 41.60, 33.11, 11.52; MS (CI, NH₃): m/z 366.02 (M⁺), 285.1 (M⁺-Br).

Synthesis of (1,12-dicarba-closo-dodecaboran-1-yl) ethyl ketone (2.34)

para-Carborane (1.00 g, 6.93 mmol) was dissolved in diethyl ether (50 mL). nBuLi (1.6 M in hexanes, 4.33 mL, 6.93 mmol) was added dropwise to the solution at room temperature, becoming cloudy upon complete addition. The reaction was maintained for 0.5 h at which time the reaction vessel was cooled to -78°C . Propionyl chloride (3.21 g, 3.01 mL, 34.67 mmol) was added slowly to the cold solution. The reaction was allowed to warm to room temperature (4 hours) and a white precipitate formed. The reaction was quenched with distilled, deionized water (20 mL), becoming homogeneous immediately upon addition of the water. The biphasic solution was transferred to a separatory funnel and the aqueous layer diluted to 50 mL. The organic phase was washed with distilled water (2 x 50 mL) and the resulting aqueous layers combined and further washed with ether (1 x 50 mL). All organic fractions were pooled, dried over Na_2SO_4 and gravity filtered. The clear, colourless filtrate was concentrated *in vacuo* and the crude solid purified by silica chromatography (100% hexanes, then 100% ether) The product (1.08 g, 79%) showed: TLC (1:1 Ether in Hexanes): R_f 0.25; ^1H NMR (200 MHz, CDCl_3): δ 3.90 – 0.7 (br m, 10H, BH), 2.82 (br s, 1H, CH), 2.38 (q, $^3J = 7.1$ Hz, 2H, CH_2), 0.90 (t, 3H, CH_3); ^{13}C NMR (50 MHz, CDCl_3): δ 195.37, 87.69, 62.50, 32.61, 7.82; ^{11}B NMR (160 MHz, acetone- d_6): δ -13.05, -14.50; IR (CH_2Cl_2 , cm^{-1}): 3068, 2987, 2944, 2618, 1727.

Synthesis of Benzyltriphenylphosphonium bromide (2.35)

Benzyl bromide (1.0 g, 0.695 mL, 5.84 mmol) was mixed with diethyl ether (10 mL). Vacuum dried triphenylphosphine (1.53 g, 5.85 mmol) was added as a solid in one portion, dissolving quickly. The reaction was maintained overnight at room temperature, becoming increasingly heterogeneous with time. The white precipitate was isolated by suction filtration. The product (2.1 g, 83 %) showed: ^1H NMR (200 MHz, CD_3OD): δ 7.90-7.01 (m, 20H, Ar-H), 4.97 (d, $^2J_{\text{HP}} = 14.9$ Hz, 2H, CH_2); ^{13}C NMR (50 MHz, CD_3OD): δ 136.41, 135.49, 135.29, 132.29, 132.18, 131.46, 131.22, 130.06, 129.56, 128.91, 128.74, 120.01, 118.30, 31.28, 30.33; ^{31}P NMR (81 MHz, CD_3OD): δ 23.80.

2.18 References

- ¹ Valliant, J.F.; Schaffer, P.; Stephenson, K.A.; Britten, J.F. *J. Org. Chem.* **2002**, 67, 383.
- ² Allen, E.; Doisy, E.A. *J.A.M.A.* **1923**, 81, 810.
- ³ MacGregor, J.I.; Jordan, V.C. *Pharm. Rev.* **1998**, 50, 151.
- ⁴ Lerner, L.J.; Holthaus, J.F.; Thompson, C.R. *Endocrinology* **1958**, 63, 295.
- ⁵ Jenson, E.V. *Recent Prog. Horm. Res.* **1962**, 18, 418.
- ⁶ Jenson, E.V.; Jacobson, H.I. *Recent Prog. Horm. Res.* **1962**, 18, 387.
- ⁷ MacGregor, J.I.; Jordan, V.C. *Pharm. Rev.* **1998**, 50, 151.
- ⁸ Jordan, V.C. *J. Steroid Biochem.* **1974**, 5, 354.
- ⁹ Furr, B.J.A.; Jordan, V.C. *Pharmacol. Ther.* **1984**, 25, 127.
- ¹⁰ Theobald, A.J. *Int. J. Clin. Pract.* **2000**, 54, 665.
- ¹¹ Top, S.; Dauer, B.; Vaissermann, J.; Jaouen, G. *J. Organomet. Chem.* **1997**, 541, 355.
- ¹² Hunter, D.H.; Payne, N.C.; Rahman, A.; Richardson, J.F.; Ponce, Y.Z. *Can. J. Chem.* **1983**, 61, 421.
- ¹³ Hawthorne, M.F.; Groudine, M.T. PCT Int. Appl. 9600090, **1996**; Chem. Abstr. **1996**, 125, 460006.
- ¹⁴ Carter, C. L.; Allen, G.; Henderson, D. E. *Cancer*, **1989**, 63, 181.
- ¹⁵ McCague, R.; Leclercq, G.; Legros, N.; Goodman, J.; Blackburn, G.M.; Jarman, M.; Foster, A.B. *J. Med. Chem.* **1989**, 32, 2527.
- ¹⁶ Jones, C.D.; Jevnikar, M.G.; Pike, A.J.; Peters, M.K.; Black, L.J.; Thompson, A.R.; Falcone, J.F.; Clemens, J.A. *J. Med. Chem.* **1984**, 27, 1057.
- ¹⁷ Jordan, V.C. *J. Natl. Cancer Inst.* **1998**, 1, 967.
- ¹⁸ Adam, H.K.; Douglas, E.J.; Kemp, J.V. *Biochem. Pharmacol.* **1979**, 27, 145.
- ¹⁹ Heying, T.L.; Ager, J.W., Jr.; Clark, S.L.; Mongold, D.J.; Goldstein, H.L.; Hillman, M.; Plak, R.J. *Inorg. Chem.* **1963**, 2, 1089.
- ²⁰ Leukart, O.; Caviezel, M.; Eberle, A.; Tun-Kyi, A.; Schwyzer, R. *Helv. Chim. Acta.* **1976**, 59, 546.
- ²¹ Endo, Y.; Yoshimi, T.; Yamakoshi, Y. *Chem. Pharm. Bull.* **2000**, 48, 312.
- ²² Endo, Y.; Yoshimi, T.; Iijima, T.; Yamakoshi, Y. *Bioorg. Med. Chem. Lett.* **1999**, 9, 3387.
- ²³ Endo, Y.; Iijima, T.; Yamakoshi, Y.; Fukasawa, H.; Miyaura, C.; Inada, M.; Kubo, A.; Itai, A. *Chem. Biol.* **2001**, 8, 341.
- ²⁴ Endo, Y.; Iijima, T.; Yamakoshi, Y.; Kubo, A.; Itai, A. *Bioorg. Med. Chem. Lett.* **1999**, 9, 3313.
- ²⁵ Hawthorne, M.F.; Maderna, A. *Chem. Rev.* **1999**, 99, 3421.
- ²⁶ Lewis, W. R.; Lin, B.; Khan, M. S.; Al-Mandhary, M. R. A.; Raithby, P. R. J. *Organomet. Chem.* **1994**, 48, 161.
- ²⁷ Cherest, M.; Felkin, H.; Prudent, N. *Tetrahedron Lett.* **1968**, 2199.
- ²⁸ Ahn, N. J. *Top. Curr. Chem.* **1980**, 88, 145.
- ²⁹ Curtin, D.Y. *Record Chem. Prog.* **1954**, 15, 111.
- ³⁰ Carrol, F.A. *Perspectives on Structure and Mechanism in Organic Chemistry*, Brooks/Cole: Toronto, **1998**.

- ³¹ Bürgi, H.B.; Dunitz, J.D.; Shefter, E. *J. Am. Chem. Soc.* **1973**, 95, 5065.
- ³² McCaugue, R. *J. Chem. Research (S)*, **1986**, 58.
- ³³ Potter, G.A.; McCague, R. *J. Org. Chem.* **1990**, 55, 6184.
- ³⁴ Clouse, A.O.; Doddrell, D.M.; Kahl, S.B.; Todd, L.J. *J. Chem. Soc. Chem. Commun.* **1969**, 13, 729.
- ³⁵ Siedle, A.R.; Bodner, G.M.; Garber, A.R.; Beer, D.C.; Todd, L.J. *Inorg. Chem.* **1974**, 13, 2321.
- ³⁶ Stanko, V.I.; Babushkina, T.A. *Zh. Struk. Khim.* **1975**, 16, 681.
- ³⁷ Zakharkin, L.I.; Kalinin, V.N.; Antonovich, V.A.; Rys, E.G. *Izv. Akad. Nauk. SSSR., Ser. Khim.* **1976**, 5, 1036.
- ³⁸ Reynhardt, E.C.; *J. Magn. Res.* **1986**, 69, 337.
- ³⁹ Diaz, M.; Jaballs, J.; Arias, J.; Lee, H.; Onak, T. *J. Am. Chem. Soc.* **1996**, 118, 4405.
- ⁴⁰ Heřmánek, S. *Chem Rev.* **1992**, 92, 325.
- ⁴¹ Reynhardt, E.C. *J. Mag. Res.* **1986**, 69, 337.
- ⁴² Leites, L.A. **1992**, 92, 279.
- ⁴³ Zakharkin, L.I.; Ponomarenko, A.A.; Okhlobystin, O.Y. *Izv. Akad. Nauk. SSSR, Ser. Khim.* **1964**, 2210.
- ⁴⁴ Zakharkin, L.I.; Kazanstev, A.V. *Izv. Akad. Nauk. SSSR, Ser. Khim.* **1965**, 2190.
- ⁴⁵ Gafstein, D.; Bobinski, J.; Dvorak, J.; Smith, H.F.; Schwach, N.N.; Cohen, M.S.; Fein, M.M. *Inorg. Chem.* **1963**, 2, 1120.
- ⁴⁶ Fein, M.M.; Bobinski, J.; Mayes, N.; Schwartz, N.; Cohen, M.S. *Inorg. Chem.* **1963**, 2, 1111.
- ⁴⁷ McCague, R.; Kuroda, R.; Leclercq, G.; Stoessel, S. *J. Med. Chem.* **1986**, 29, 2053.
- ⁴⁸ Wu, Y.; Carrol, P.J.; Quintana, W. *Polyhedron*, **1998**, 17, 3391.
- ⁴⁹ Potenza, J.A.; Lipscomb, W.N. *J. Am. Chem. Soc.* **1964**, 86, 1874.
- ⁵⁰ Precigoux, P.G.; Courseille, C.; Geoffre, S.; Hospital, M. *Acta Crystallogr.* **1979**, B35, 3072.
- ⁵¹ Hardie, M.J.; Raston, C.L. *Eur. J. Inorg. Chem.* **1999**, 195.
- ⁵² Hardie, M.J.; Raston, C.L. *Chem. Comm.* **1999**, 13, 1153.
- ⁵³ Blanch, R.J.; Williams, M.; Fallon, G.D.; Gardiner, M.G.; Kaddour, R.; Raston, C.L. *Angew. Chem. Int. Ed. Engl.* **1997**, 36, 504.
- ⁵⁴ Davison, M.G.; Hibbert, T.G.; Howard, J.A.K.; Mackinnon, A.; Wade, K. *Chem. Comm.* **1996**, 2285.
- ⁵⁵ Godfrey, P.D.; Grigsby, W.J.; Nichols, P.J.; Raston, C.L. *J. Am. Chem. Soc.* **1997**, 119, 9283.
- ⁵⁶ Finkelstein, H. *Ber.* **1910**, 43, 1510.
- ⁵⁷ McCaugue, R. *Tetrahedron Asymmetry* **1990**, 2, 97.
- ⁵⁸ Top, S.; Kaloun, E.B.; Vessières, A.; Leclercq, G.; Laios, I.; Ourevitch, M.; Deuschel, C.; McGlinchey, M.J.; Jaouen, G. *ChemBioChem* **2003**, 4, 754.
- ⁵⁹ Valliant, J.F.; Morel, P.; Schaffer, P.; Kaldis, J.H. *Inorg. Chem.* **2002**, 41, 628.
- ⁶⁰ Zalkin, A.; Hopkins, T.E.; Templeton, D.H. *Inorg. Chem.* **1966**, 5, 1189.
- ⁶¹ Stalteri, M.A.; Bansal, S.; Hider, R.; Mather, S.J. *Bioconj. Chem.* **1999**, 10, 130.

- ⁶² Varadarajan, A.; Johnson, S.E.; Gomez, F.A.; Chakrabarti, S.; Knobler, C.B.; Hawthorne, M.F. *J. Am. Chem. Soc.* **1992**, 114, 9003.
- ⁶³ Alberto, R.; Egli, A.; Abram, U.; Hegetschweiler, K.; Grumlich, V.; Schubiger, P.A. *J. Chem. Soc. Dalton Trans.* **1994**, 2815.
- ⁶⁴ Spencer, J.L.; Green, M.; Stone, F.G.A. *Chem. Commun.* **1972**, 1178.
- ⁶⁵ Wiesboek, R.A.; Hawthorne, M.F. *J. Am. Chem. Soc.* **1964**, 86, 1642.
- ⁶⁶ Drechsel, K.; Lee, C.S.; Leung, E.W.; Kane, R.R.; Hawthorne, M.F. *Tetrahedron Letters*, **1994**, 34, 6217.
- ⁶⁷ Gill, R.W.; Herbertson, J.A.; MacBride, J.A.H.; Wade, K. *J. Organomet. Chem.* **1996**, 507, 249.
- ⁶⁸ Malan, C.; Morin, C. *Tetrahedron Lett.* **1997**, 38, 6599.
- ⁶⁹ Jaouen, G. *Chem. Britain* **2001**, 37, 36.
- ⁷⁰ Shani, J.; Gazit, A.; Livshitz, T.; Biran, S. *J. Med. Chem.* **1985**, 28, 1504.
- ⁷¹ MacGregor, J.I.; Jordan, V.C. *Pharm. Rev.* **1998**, 50, 151.
- ⁷² Goldberg, I.; Becker, Y. *J. Pharm. Sci.* **1987**, 76, 259.
- ⁷³ Hunter, D.H.; Payne, N.C.; Rahman, A.; Richardson, J.F.; Ponce, Y.Z. *Can. J. Chem.* **1983**, 61, 421.
- ⁷⁴ Kuroda, R.; Cutcush, S.; Neidle, S.; Leung, O.-T. *J. Med. Chem.* **1985**, 28, 1497.
- ⁷⁵ Blackburn, G.M.; Goodman, J.; Smith, A.J. *Acta. Cryst. Sec. C.* **1988**, 44, 1632.
- ⁷⁶ Precieux, G.; Courseille, C.; Geoffre, S.; Hospital, M. *Acta. Cryst. Sec. B.* **1979**, 35, 3072.
- ⁷⁷ Kilbourn, B.T.; Owston, P.G. *J. Chem. Soc. B.*, **1970**, 1.
- ⁷⁸ Nakamura, H.; Aoyagi, K.; Yamamoto, Y. *J. Org. Chem.* **1997**, 62, 780.
- ⁷⁹ Nakamura, H.; Aoyagi, K.; Yamamoto, Y. *J. Am. Chem. Soc.* **1998**, 120, 1167.
- ⁸⁰ Coult, R.; Fox, M.A.; Gill, W.R.; Herbertson, P.L.; MacBride J.A.H.; Wade, K. *J. Organomet. Chem.* **1993**, 462, 19.
- ⁸¹ Gauthier, S.; Mailhot, J.; Labrie, F. *J. Org. Chem.* **1996**, 61, 3890.
- ⁸² Jaouen, G.; Top, S.; Vessières, A.; Pigeon, P.; Leclercq, G.; Laios, I. *Chem. Commun.* **2001**, 383.
- ⁸³ McCaughey, R. *J. Chem. Soc. Perkin Trans. 1* **1987**, 1011.

Chapter 3 - Organometallic Analogues of Tamoxifen

3.1 Introduction to Dicobalthexacarbonyl Analogues of Tamoxifen

The formation of compound **2.25** from the ene-yne **2.24** proceeded in very low yield (Chapter 2). This chapter describes experiments designed to probe the reactivity of the alkyne as a means of rationalizing the low yield. To this end, dicobalthexacarbonyl complexes of **2.24** were prepared and characterized.

The proposed research holds two potential goals. One is to probe the reactivity of the alkyne toward other electrophiles in order to determine the reason behind the poor yield of the carborane **2.25**. In addition, the introduction of an organometallic fragment across the alkyne could serve to generate a novel class of antiestrogen compounds capable of *in vivo* detection using carbonylmetalloimmunoassay (CMIA), a versatile technique that utilizes Fourier transform infrared (FT-IR) spectroscopy for *in vivo* quantification of a variety of analytes.¹ This methodology can be used to simultaneously determine the uptake and biodistribution of multiple carbonyl containing analytes *in vivo*. For our purposes, we sought to use the dicobalt metal core as a means of exploring the potential for this marker to determine the uptake of various tamoxifen-alkyne analogues into the estrogen receptor. Concern as to how the presence of the cobalt core may affect the binding affinity of the target molecule for the natural receptor is real. However, it has been previously established by Endo *et al.* that bulky tamoxifen analogues can retain, and in some cases outperform, the affinity of estrogen itself.²⁻⁵

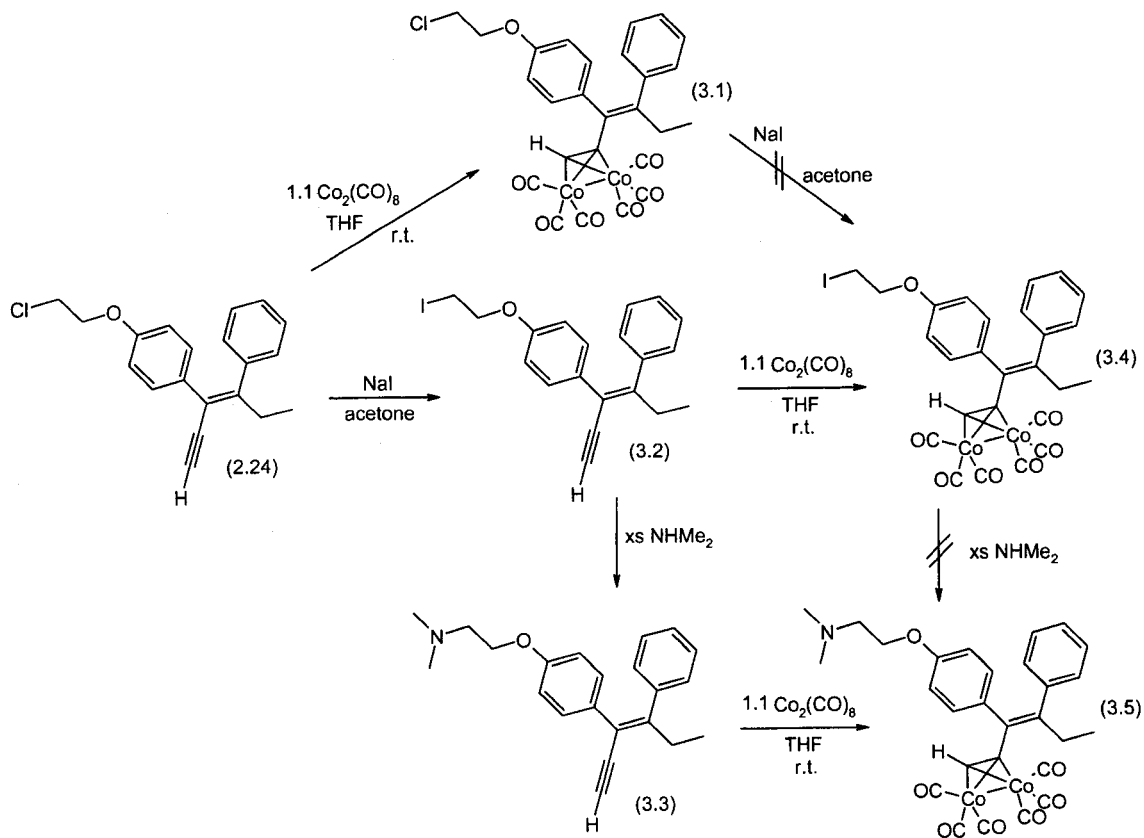
3.2 Probing the Reactivity of Alkyne 2.24.

Initially, the dicobalt metal core was to be used as a sterically hindered electrophile in order to probe the reactivity of the alkyne **2.24** to gain insight into the low reactivity of this compound with bis(acetonitrile)decaborane. Two potential reasons for the low yield are steric hindrance around the alkyne and reduced reactivity of the alkyne due to conjugation. To probe these factors, the reactivity of **2.24** towards an alternative electrophile, dicobaltoctacarbonyl, was examined.

3.3 Dicobalthexacarbonyl Analogues of Tamoxifen

The ene-yne **2.24**, **3.2** and **3.3** were mixed with dicobaltoctacarbonyl (Scheme 3.1) in THF solution at room temperature. The corresponding dicobalthexacarbonyl alkyne adducts (**3.1**, **3.4** and **3.5**) were isolated in 88%, 92% and 54% yields, respectively. The superior yields of the cobalt complexes compared to that of **2.25** suggest that steric interference cannot explain the low reactivity of alkyne **2.24** toward bis(acetonitrile)decaborane.

The coordination of the alkynes to $\text{Co}_2(\text{CO})_6$ was evident from the notable downfield shift of the alkyne C-H proton in the ^1H NMR spectra of compounds **3.1** and **3.4** (Figure 3.2). The ^{13}C chemical shifts of the carbonyl groups in both complexes appear as one signal at 199.74 and 199.76 ppm respectively, suggesting rapid exchange on the NMR timescale.⁶ The IR spectra of both **3.1** and **3.4** exhibited the characteristic strong CO absorption peaks. More specifically, these complexes exhibit a characteristic pattern for terminal carbonyl stretches as has been reported elsewhere.^{6,7} These complexes also



Scheme 3.1 – Synthesis of dicobalthexacarbonyl analogues of tamoxifen.

displayed satisfactory mass spectrometric data and, in both cases, showed the molecular ion with a number of other peaks consistent with the consecutive loss of CO fragments.

Attempts to convert the halo complexes **3.1** and **3.4** to the amine cobalt complex **3.5**, a novel tamoxifen analogue, were unsuccessful. Conversion of the chloride **3.1** to the iodide **3.4** and subsequent reaction of **3.4** with compound **3.5**, led to complex reaction mixtures. The preparation of **3.5** was successfully carried out by direct reaction of the dimethylamino precursor **3.3** with $\text{Co}_2(\text{CO})_8$. The product was isolated in 54% yield.

The IR spectrum of compound **3.5** shows aliphatic C-H stretching frequencies around 3311 and 2727 cm^{-1} , and characteristic carbonyl stretching peaks at 2091 , 2052

and 2028 cm^{-1} . The ^1H NMR spectrum of **3.5** shows line broadening for those protons located on the pendant ethoxy group, as well as the alkyne C-H group. Broadening of the alkyne C-H proton signal may be the result of the dynamic behaviour associated with the metal carbonyl cluster. On the other hand, the poor lineshape exhibited by the ethoxy group is likely to be associated with intermolecular coordination of the amine to a cobalt metal center of another molecule.⁸

Using Wade's approach, one can justify the above arguments of coordination and dynamic behaviour. With six skeletal electron pairs, the tetrahedral cobalt clusters can be viewed as *nido* trigonal bipyramids (Figure 3.1) with low barriers to rearrangement. Thus the coordination of the amine to a vacant metal site is justified and the broad lineshape of the ^1H NMR spectrum can be accounted for by a low barrier to rearrangement.⁸⁻¹¹

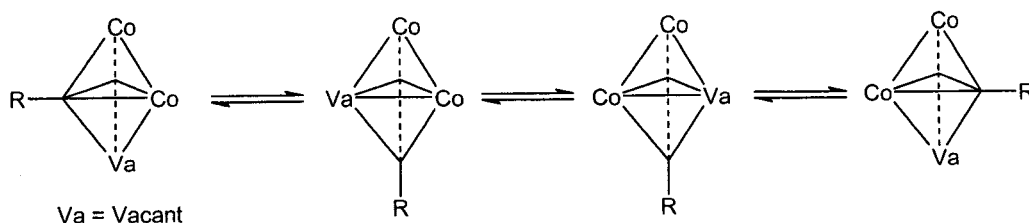


Figure 3.1 – Mechanism for the fluxional behaviour of the nido bipyramidal C_2Co_2 .

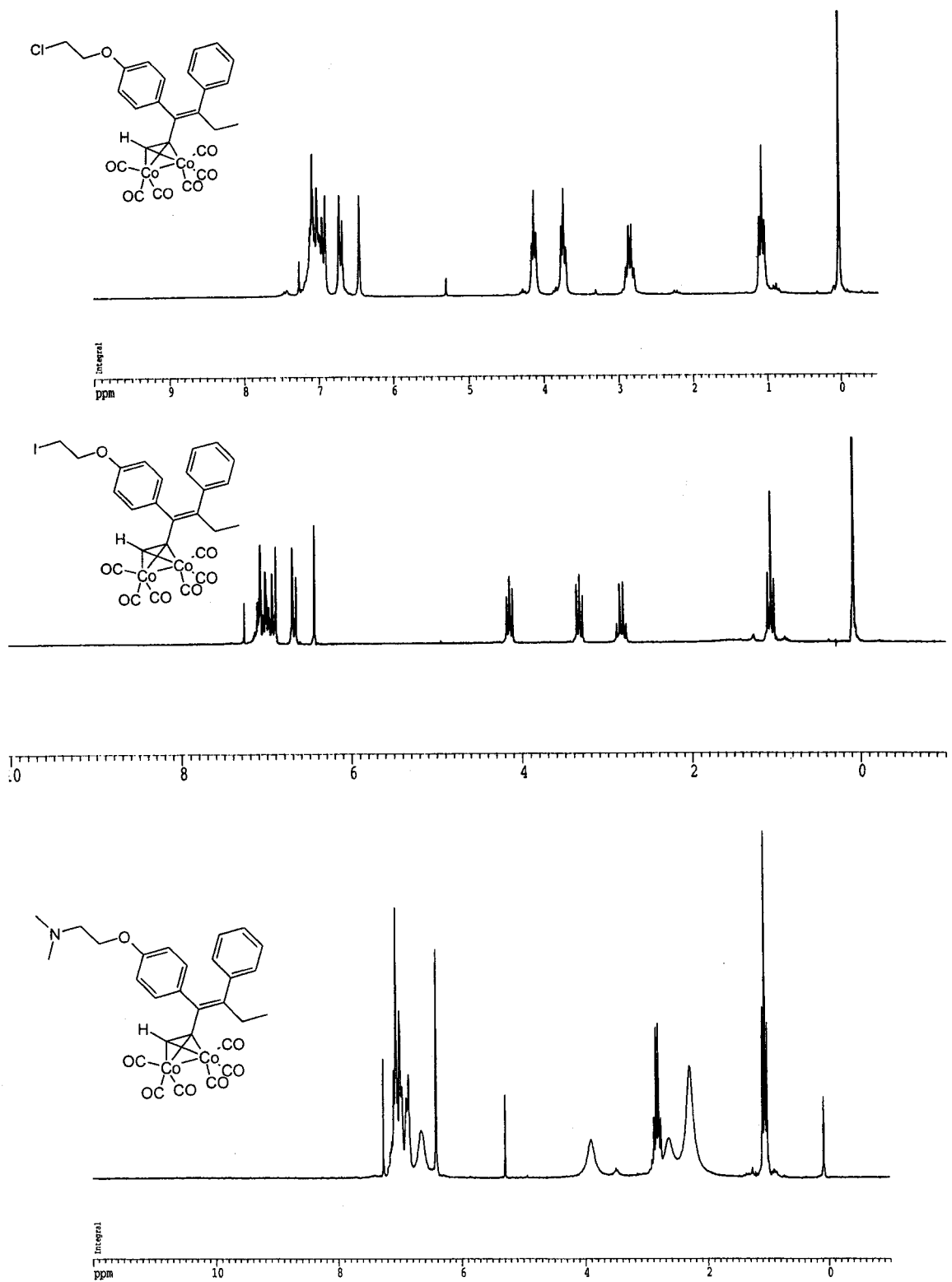


Figure 3.2 – ^1H NMR spectra of 3.1, 3.4 and 3.5.

3.4 Single Crystal X-ray Analysis of Compound 3.4

Single crystals of **3.4** were obtained by slow evaporation of hexanes at -10°C under an inert Ar atmosphere. X-ray diffraction analysis revealed the structure of the dicobalt tamoxifen iodide (Figure 3.3). The compound crystallized in the monoclinic $P2_1/c$ space group with one molecule in the asymmetric unit ($Z = 4$). The molecular geometry exhibited by this system shows many similarities to those of other conjugated dicobalthexacarbonyl systems.⁷ The Co-Co bond distance is $2.480(3) \text{ \AA}$, while the average Co-C_{alkyne} distance is $1.968(14) \text{ \AA}$ and the eclipsed carbonyl ligands exhibit similar distances to reported values (Co-C_{carbonyl}: $1.79(2) \text{ \AA}$, C-O: $1.136(17) \text{ \AA}$).¹² Perhaps the most important feature of this structure is that the diaryl moiety adopts the propeller orientation observed for other solid-state tamoxifen structures.^{13,14-18} Table 3.1 highlights the pertinent bond angles observed for the solid-state packing of **3.4** relative to those measured for the carboranyl analogue **2.25**.

	tamoxifen	2.25	2.25'	3.4
alkene – B(ring)	50.4	89.27(7)	79.27(7)	78.74(34)
alkene – C(ring)	56.9	70.81(9)	77.26(7)	64.43(35)
B(ring) – C(ring)	56.9	53.44(8)	55.17(7)	66.33(4)
ethyl (dihedral angle)	114.0	-122.7	112.1	96.2

Table 3.1 – Interplanar and dihedral angle comparison for tamoxifen analogues.^{18,19}

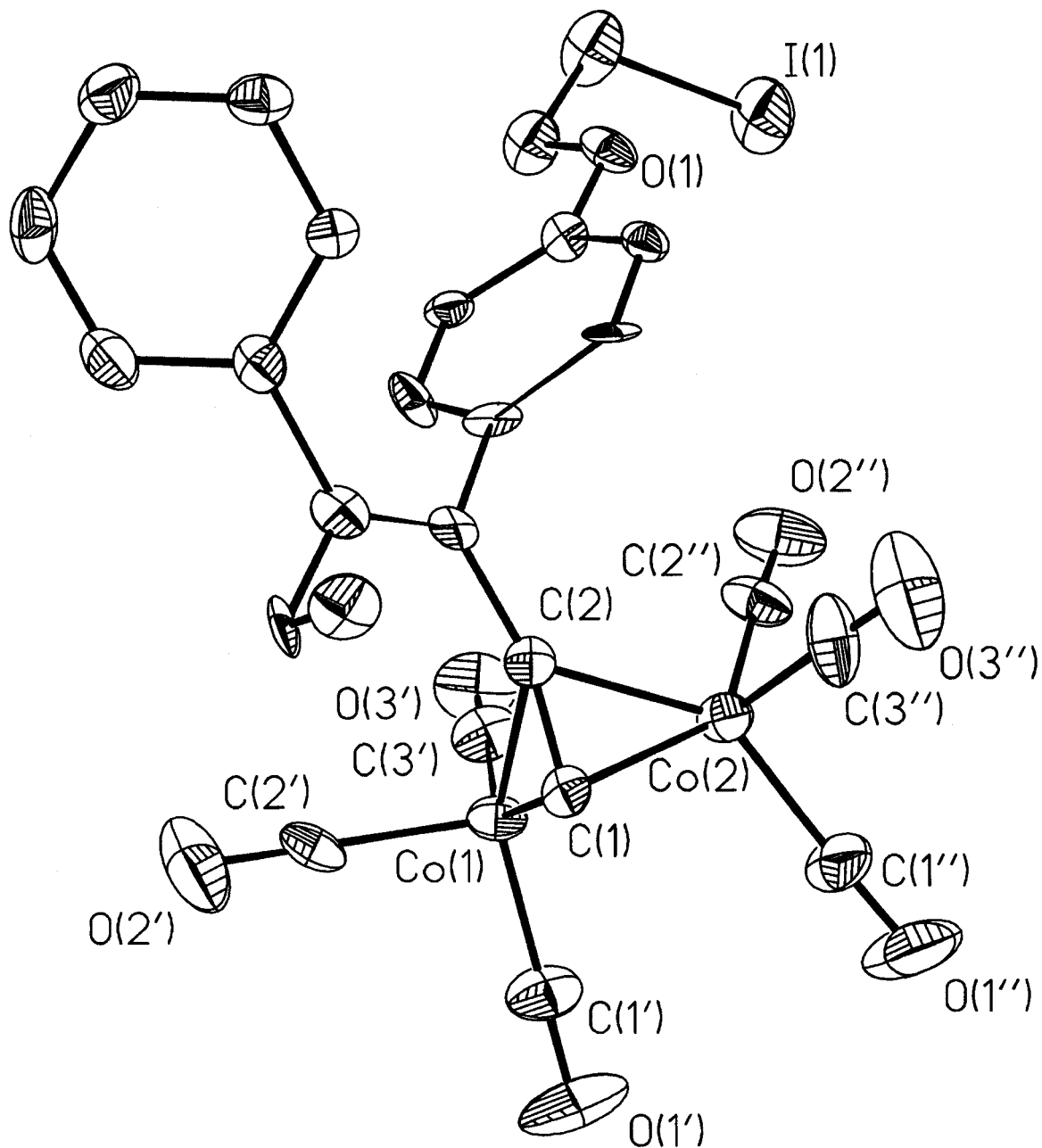


Figure 3.3 - ORTEP representation of 3.4. Thermal ellipsoids are shown at the 50% probability level. Hydrogen atoms have been removed for clarity.

3.5 Summary and Conclusions

The main purpose of this work was to probe the reactivity of the alkyne functionality of a number of tamoxifen analogues in response to the poor reactivity of these same alkynes toward $B_{10}H_{12}(CH_3CN)_2$. In the course of this work, a novel class of antiestrogens with the capability of undergoing *in vivo* detection using CMIA were prepared.

The high yielding syntheses of three different dicobalthexacarbonyl complexes suggests that the low yield of the carborane **2.25** is associated with electronic, rather than steric effects. In the process of probing the reactivity of these alkynes, a new class of potential antiestrogen was synthesized. Future work will involve the testing of these compounds for their binding affinity toward the estrogen receptor.

In addition, the potential for compound **3.5** to serve as a substrate for CMIA was also discussed. This depends upon the cluster possessing high affinity for the estrogen receptor. Determination of the RBA for compound **3.5** remains, therefore, a goal for future research.

3.6 Experimental

Synthesis of {Z-3-(4-(2-chloroethoxy)phenyl-4-phenyl-hex-3-ene-1-yne}Co₂(CO)₆ (3.1)

The alkyne **2.24** (0.250 g, 0.804 mmol) was combined with dicobaltoctacarbonyl (0.303 g, 0.885 mmol) in dry THF (5 mL). The opaque, dark red reaction mixture was maintained at ambient temperature under argon for 12 hours. The solvent was removed *in vacuo* giving a dark red paste. The crude product was immediately purified by flash silica gel chromatography (100 % Hexanes). The product, a dark red oil (0.424 g, 88%), showed: T.L.C. (8% ether in petroleum ether) $R_f = 0.65$; ¹H NMR (200 MHz, CDCl₃); δ 7.14 – 6.67 (m, 9H, ArH), 6.44 (s, 1H, CH), 4.12 (t, ³J_{HH} = 5.9 Hz, 2H, OCH₂), 3.73 (t, 2H, CH₂Cl), 2.84 (q, ³J_{HH} = 7.5 Hz, 2H, CH₂CH₃), 1.07 (t, 3H, CH₂CH₃); ¹³C NMR (50 MHz, CDCl₃): δ 199.74, 156.76, 147.83, 142.23, 136.57, 132.53, 131.44, 128.99, 127.68, 126.41, 114.11, 89.86, 76.90, 68.07, 41.93, 29.61, 12.41; IR (CH₂Cl₂, cm⁻¹): 3315, 3080, 3054, 3034, 2970, 2935, 2875, 2091, 2051, 2024, 1979(sh), 1948(sh); MS (ES, positive): m/z 614 (M + NH₄), 619 (M + Na), 634 (M + K).

Synthesis of Z-3-(4-(2-iodoethoxy)phenyl)-4-phenyl-hex-3-ene-1-yne (3.2)

Compound **2.24** (0.500 g, 1.61 mmol) was combined with sodium iodide (2.41 g, 16.09 mmol) in freshly distilled acetone (10 mL). The reaction was maintained under refluxing conditions for 14 days, at which time TLC analysis showed the consumption of the starting alkyne. Excess acetone was removed by rotary evaporation giving a yellow solid. The crude solid was suspended in CH₂Cl₂ (50 mL) and washed with distilled

deionized water (3 x 50 mL). All aqueous portions were combined and further washed with methylene chloride (1 x 50 mL). The organic fractions were pooled, dried over Na_2SO_4 and gravity filtered. Excess solvent was removed and the product purified by silica gel chromatography (gradient: 100% pet. ether to 10% ether in pet. ether, 1% intervals). The product (0.641 g, 99%), a clear colourless oil showed: TLC: (5% Ether:Petroleum Ether): R_f 0.49; ^1H NMR (200 MHz, CDCl_3): δ 7.23-7.03 (m, 7H, Ar-H), 6.68-6.63 (m, 2H, Ar-H), 4.18 (t, $^3J_{\text{HH}} = 6.9$ Hz, 2H, OCH_2), 3.38 (t, 2H, CH_2Cl), 3.34 (s, 1H, CH), 2.94 (q, 2H, $^3J_{\text{HH}} = 7.5$ Hz, CH_2CH_3), 1.07 (t, 3H, CH_3); ^{13}C NMR (50 MHz, CDCl_3): δ 156.66, 152.70, 140.53, 131.81, 131.12, 129.13, 128.17, 127.07, 118.35, 114.08, 84.41, 81.45, 68.64, 34.26, 31.32, 12.56; IR (CHCl_3 , cm^{-1}): 3294, 3055, 2971, 2933, 2873, 2088; MS (EI): m/z 402 (M⁺); HRMS (CI, NH_3): Calculated for $\text{C}_{20}\text{H}_{19}\text{IO}$ (M⁺) 402.0481. Found 402.0465.

Synthesis of Z-3-(4-(2-dimethylaminoethoxy)phenyl)-4-phenyl-hex-3-ene-1-yne (3.3)

The chloro-alkyne (2.24) (0.100 g, 0.322 mmol) was dissolved in a solution of dimethylamine (5 mL) (33% solution in EtOH, ~ 5.6 M). The reaction was maintained under refluxing conditions for 2 hours. Subsequent additions of dimethylamine solution (2 mL) were performed on an hourly basis for 8 hours. The reaction was then heated to reflux overnight, at which time thin layer chromatography (10% ether in petroleum ether) showed the complete consumption of starting material. The heat source was removed and the dark brown reaction mixture was allowed to cool to room temperature. The solvent was removed by rotary evaporation and the resulting dark oil was taken up in CH_2Cl_2 (25

mL) and washed with distilled water (2 x 25 mL). The aqueous layers were pooled and further washed with CH₂Cl₂ (25 mL). All organic fractions were combined, dried over Na₂SO₄ and gravity filtered. The filtrate was concentrated *in vacuo* and the crude product purified by radial chromatography (20% MeOH in Ether). The product, a yellow semi-solid (0.100 g, 97%) showed: T.L.C. (20% MeOH in Ether) R_f = 0.28; ¹H NMR (200 MHz, CDCl₃): δ 7.16-6.61 (m, 9H, ArH), 4.08 (t, ³J_{HH} = 7.5 Hz, 2H, OCH₂), 3.27 (s, 1H, CH), 2.93 (m, 4H, overlap CH₂NMe₂ and CH₂CH₃), 2.49 (s, 6H, N(CH₃)₂), 1.00 (t, ³J = 7.5 Hz, 3H, CH₂CH₃); ¹³C NMR (50 MHz, CDCl₃): δ 156.78, 152.53, 140.34, 131.50, 130.90, 128.95, 128.03, 126.93, 118.17, 113.77, 84.26, 81.41, 64.40, 57.55, 45.09, 31.15, 12.40; IR (CH₂Cl₂, cm⁻¹): 3289, 2971, 2936, 2873, 2823, 2774, 2710, 2087, 1607, 1509, 1244, 1033; MS (CI, NH₃): m/z 320 (M+H); HRMS (CI, NH₃): Calculated for C₂₂H₂₅NO (M+) 319.1898. Found 319.1936.

Synthesis of {Z-3-(4-(2-iodoethoxy)phenyl-4-phenyl-hex-3-ene-1-yne)Co₂(CO)₆ (3.4)

Using a similar procedure for that of the chloro analogue **2.24**, the iodo-alkyne **3.2** (0.100 g, 0.249 mmol) was combined with dicobalt octacarbonyl (0.094 g, 0.274 mmol). Dry THF (10 mL) was added, and stirring initiated, giving a dark red opaque reaction mixture. The reaction was maintained at ambient temperature for 6 hours whereby the excess solvent was removed by rotary evaporation. The resulting dark red oil was suspended in a minimal amount of hexanes and purified by flash silica gel chromatography (100% Hexanes). X-ray quality crystals were obtained by the slow evaporation of a hexanes solution of **3.4** at -10°C. The product, a red solid (0.157 g,

92%) showed: T.L.C. (8% ether in pet. ether): $R_f = 0.66$; $^1\text{H NMR}$ (200 MHz, CDCl_3): δ 7.11-6.65 (m, 9H, ArH), 6.43 (s, 1H, CH), 4.14 (t, $^3J_{\text{HH}} = 6.8$ Hz, 2H, OCH_2), 3.33 (t, 2H, CH_2I), 2.82 (q, $^3J_{\text{HH}} = 7.5$ Hz, 2H, CH_2CH_3), 1.06 (t, 3H, CH_2CH_3). $^{13}\text{C NMR}$ (50 MHz, CDCl_3): δ 199.76, 156.52, 147.84, 142.23, 136.62, 132.55, 131.45, 128.98, 127.66, 126.40, 114.30, 89.86, 76.91, 68.86, 29.56, 12.37; IR (cm^{-1} , CH_2Cl_2): 3317, 3081, 3057, 3032, 2973, 2938, 2877, 2826, 2090, 2051, 2026; MS (ES, positive): m/z 706 ($\text{M}+\text{NH}_4$), 711 ($\text{M}+\text{Na}$), 727 ($\text{M}+\text{K}$). X-ray Crystallography: Space group: $\text{P2}_1/\text{c}$, $a = 18.959(8)$ Å, $b = 9.512(4)$ Å, $c = 15.617(7)$ Å, $\alpha = \gamma = 90^\circ$, $\beta = 106.977(8)^\circ$, $V = 2693(2)$ Å³, $Z = 4$, data/parameters: 3877/315, $R = 0.0892$, $R_w = 0.2187$, GOF = 1.003.

Synthesis of {Z-3-(4-(2-dimethylaminoethoxy)phenyl-4-phenyl-hex-3-ene-1-yne)Co₂(CO)₆ (3.5)

The alkyne **3.3** (0.05 g, 0.157 mmol) and dicobalt octacarbonyl (0.059 g, 0.172 mmol) were combined in dry THF (5mL), giving a dark red opaque reaction mixture. The reaction was maintained at ambient temperature for 2 hours. Excess solvent was removed by rotary evaporation giving a dark red oil. The crude product was taken up in a minimal amount of CH_2Cl_2 and subjected to flash silica gel chromatography. The product, a dark red oil (0.051 g, 54%), showed: T.L.C. (10% MeOH in CH_2Cl_2): $R_f = 0.70$; $^1\text{H NMR}$ (200 MHz, CDCl_3): δ 7.15-6.66 (m, 9H, ArH), 6.42 (s, 1H, CH), 3.90 (br s, 2H, OCH_2), 2.82 (q, $^3J_{\text{HH}} = 7.5$ Hz, 2H, CH_2CH_3), 2.63 (br s, 2H, CH_2NMe_2), 2.29 (br s, 6H, $\text{N}(\text{CH}_3)_2$), 1.05 (t, 3H, CH_2CH_3); $^{13}\text{C NMR}$ (50 MHz, CDCl_3): δ 199.51, 157.17, 147.54, 142.09, 135.80, 132.45, 131.05, 128.82, 127.49, 126.19, 113.92, 97.27, 89.85, 76.75,

29.38, 12.24; IR (neat, cm^{-1}): 3311, 3082, 3062, 3035, 2973, 2938 2875, 2824, 2775, 2727 (sh), 2527, 2474, 2091, 2052, 2028; MS (ES, positive): m/z 606 (M + H), 578 (M-CO), 550 (M-(CO)₂).

3.7 References

- ¹ Salmain, M.; Vessières, A.; Varenne, A.; Brossier, P.; Jaouen, G. *J. Organomet. Chem.* **1999**, 589, 92.
- ² Endo, Y.; Yoshimi, T.; Yamakoshi, Y. *Chem. Pharm. Bull.* **2000**, 48, 312.
- ³ Endo, Y.; Yoshimi, T.; Iijima, T.; Yamakoshi, Y. *Bioorg. Med. Chem. Lett.* **1999**, 9, 3387.
- ⁴ Endo, Y.; Iijima, T.; Yamakoshi, Y.; Fukasawa, H.; Miyaura, C.; Inada, M.; Kubo, A.; Itai, A. *Chem. Biol.* **2001**, 8, 341.
- ⁵ Endo, Y.; Iijima, T.; Yamakoshi, Y.; Kubo, A.; Itai, A. *Bioorg. Med. Chem. Lett.* **1999**, 9, 3313.
- ⁶ Draper, S.M.; Delamesiere, M.; Champeil, E.; Twamley, B.; Byrne, J.J.; Long, C. *J. Organomet. Chem.* **1999**, 589, 157.
- ⁷ Malisza, K.L.; Girard, L.; Hughes, D.W.; Britten, J.F.; McGlinchey, M.J. *Organometallics* **1995**, 14, 4676.
- ⁸ Jaouen, G.; Marinetti, A.; Saillard, J.-Y.; Sayer, B.G.; McGlinchey, M.J. *Organometallics* **1982**, 1, 225.
- ⁹ Hanson, B.E.; Mancini, J.S. *Organometallics* **1983**, 2, 126.
- ¹⁰ Dickson, R.S.; Pain, G.N. *J. Chem. Soc. Chem Commun.* **1979**, 277.
- ¹¹ Boag, N.M.; Green, M.; Stone, F.G.A. *J. Chem. Soc. Chem. Commun.* **1980**, 1281.
- ¹² Adams, R.D.; Bunz, U.H.F.; Fu, W.; Nguyen, L. *J. Organomet. Chem.* **1999**, 578, 91.
- ¹³ Hunter, D.H.; Payne, N.C.; Rahman, A.; Richardson, J.F.; Ponce, Y.Z. *Can. J. Chem.* **1983**, 61, 421.
- ¹⁴ Cutbush, S.D.; Neidle, S.; Foster, A.B.; Leclercq, F. *Acta Cryst. Sec. B.* **1982**, 38, 1024.
- ¹⁵ Goldberg, I.; Becker, Y. *J. Pharm. Sci.* **1987**, 76, 259.
- ¹⁶ Huroda, R.; Cutcush, S.; Neidle, S.; Leung, O.-T. *J. Med. Chem.* **1985**, 28, 1497.
- ¹⁷ Blackburn, G.M.; Goodman, J.; Smith, A.J. *Acta. Cryst. Sec. C.* **1988**, 44, 1632.
- ¹⁸ Precieux, G.; Courseille, C.; Geoffre, S.; Hospital, M. *Acta. Cryst. Sec. B.* **1979**, 35, 3072.
- ¹⁹ Weeks, C.M.; Griffin, J.F.; Duax, W.L. *Am. Cryst. Assoc., Ser. 2.* **1977**, 5, 69.

Chapter 4 – The Synthesis, Characterization and Coordination Chemistry of *ortho*-Carborane Isonitriles

4.1 Introduction

Much research has been done on the development of boron containing molecules that are capable of delivering significant quantities of ^{10}B to diseased tissue for Boron Neutron Capture Therapy (BNCT).^{1,2} It is important that BNCT³ agents possess favourable biological properties, including high uptake into the targeted cells, rapid clearance from the blood and short retention times in non-target tissues. In order to achieve these requirements, a number of research groups have begun using clinical imaging techniques, including positron emission tomography (PET),⁴ magnetic resonance imaging (MRI)^{5,6} and single photon emission tomography (SPECT)⁷ as methods of determining and optimizing the *in vivo* biodistribution of potential agents. As mentioned previously, imaging offers several advantages over the arduous and expensive method of evaluating boron concentrations in excised animal tissue samples. The radioimaging approach, although attractive, suffers from the limitation that radiolabelling can significantly alter the distribution of the BNCT agent under investigation.⁷

Our goal was to develop a novel class of BNCT agents that could be radiolabelled without changing the physical or chemical properties of the target compound. The proposed strategy (Figure 4.1), which is different for that used in Chapter 2, involves the preparation of metal-based BNCT agents in which a bifunctional carborane is linked to a

targeting agent and coordinated to a metal (M) through a donor group (X). By increasing the coordination number through the judicious choice of M and X, the number of boron atoms in a given molecule can be increased, and furthermore, the metal can be conveniently substituted with a radioactive isotope without altering the structure of the complex. Having multiple biomolecules in one complex (i.e. for values $n > 1$) also presents the opportunity for achieving enhanced receptor selectivity through multi-valent binding.

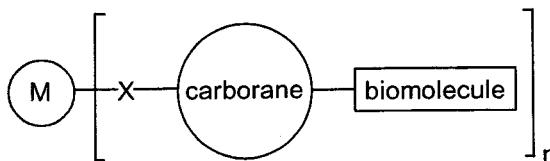


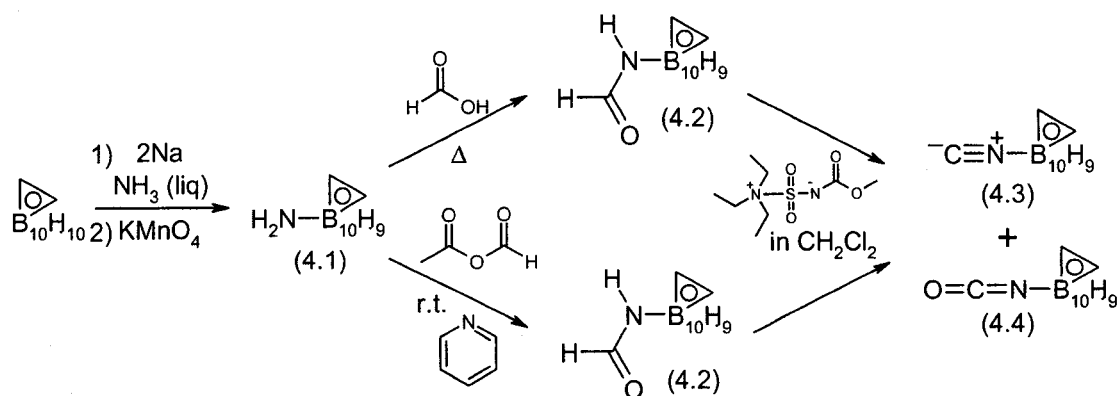
Figure 4.1 – Illustration of proposed metal core BNCT/BNCS agents

Because several stable, bifunctional, and poly-substituted isonitrile organometallic and transition metal complexes are known,⁸⁻¹² we were interested in preparing the carborane analogue as a model system. This particular system was selected because technetium isonitrile complexes are already widely used for clinical cardiac imaging and are therefore known to be stable *in vivo*.^{13,14} Furthermore, for $n = 6$, the resulting carborane complex would have a substantial boron content (60 boron atoms per molecule) and could be made to target specific receptors through derivatization of the remaining C-H vertices with a biomolecule. To this end, it was necessary to develop a methodology for the preparation of carborane-isonitrile derivatives. The work described

for the synthesis of the isonitrile ligand and the corresponding rhenium metal complexes has been published.¹⁵⁻¹⁷

4.2 Synthesis of *ortho*-Carborane Isonitriles

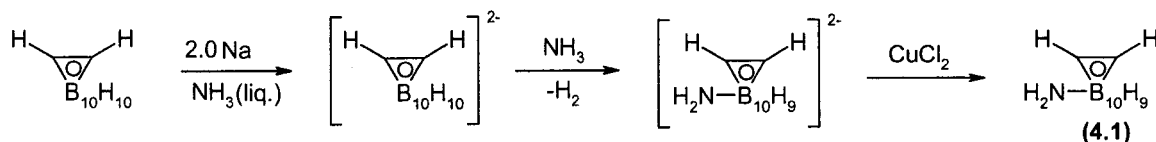
Zakharkin and co-workers originally reported the synthesis of the boron-linked isonitrile **4.3** in 1971 (Scheme 4.1).¹⁸ The isonitrile was reported as an intermediate en route to 3-*ortho*-carborane carboxylic acids. The strategy was to first synthesize the 3-amino-*ortho*-carborane (**4.1**) followed by formylation to give compound **4.2**. Subsequent dehydration with POCl₃ reportedly led to high yields of the target isonitrile **4.3**. Following Zakharkin's procedure, the 3-amino-*ortho*-carborane (**4.1**) was prepared by reacting *ortho*-carborane with sodium in liquid ammonia (Scheme 4.1). Oxidation of the



Scheme 4.1 – The synthesis of a boron-linked *ortho*-carborane isonitrile.

resulting dianion, using the reported hydrated copper(II) chloride method, afforded very low yields of the product when working at a modest scale (0.5-2 g). Kasar et al.¹⁹ recently reported a successful modification of the original method in which permanganate was

used as the oxidant. We found that reoxidation was also accomplished efficiently with oven dried cupric chloride. Using this procedure the product, compound **4.1**, was isolated in 56% yield.



Scheme 4.2 – Nucleophilic substitution of the third boron vertex of *ortho*-carborane.

The mechanism of reduction is thought to involve the addition of two electrons to the carborane cage, followed by substitution of the activated boron vertex with ammonia (Scheme 4.2). The addition of two electrons to the carborane cage occurs to regions of lowest electron density (boron atoms 3 and 6), which are those boron atoms closest to the electronegative carbon atoms. These added electrons dramatically increase the electron density around B-3 and B-6 as well as the exoskeletal H-atoms bound to them. Following the reaction of ammonia with the *nido*-carborane, hydrogen gas is evolved yielding 3-amino-*nido*-dodecaborane.¹⁸ Substitution at the third position results in a lower electron density at the sixth cage position, which in turn draws electron density from the adjacent exoskeletal H-atom. This decrease in electron density reduces the reactivity of the 3-substituted carborane, thereby preventing formation of any disubstituted product. Oxidation of the resulting dianion results in the formation of the 3-amino-*ortho*-carborane (**4.1**).¹⁸

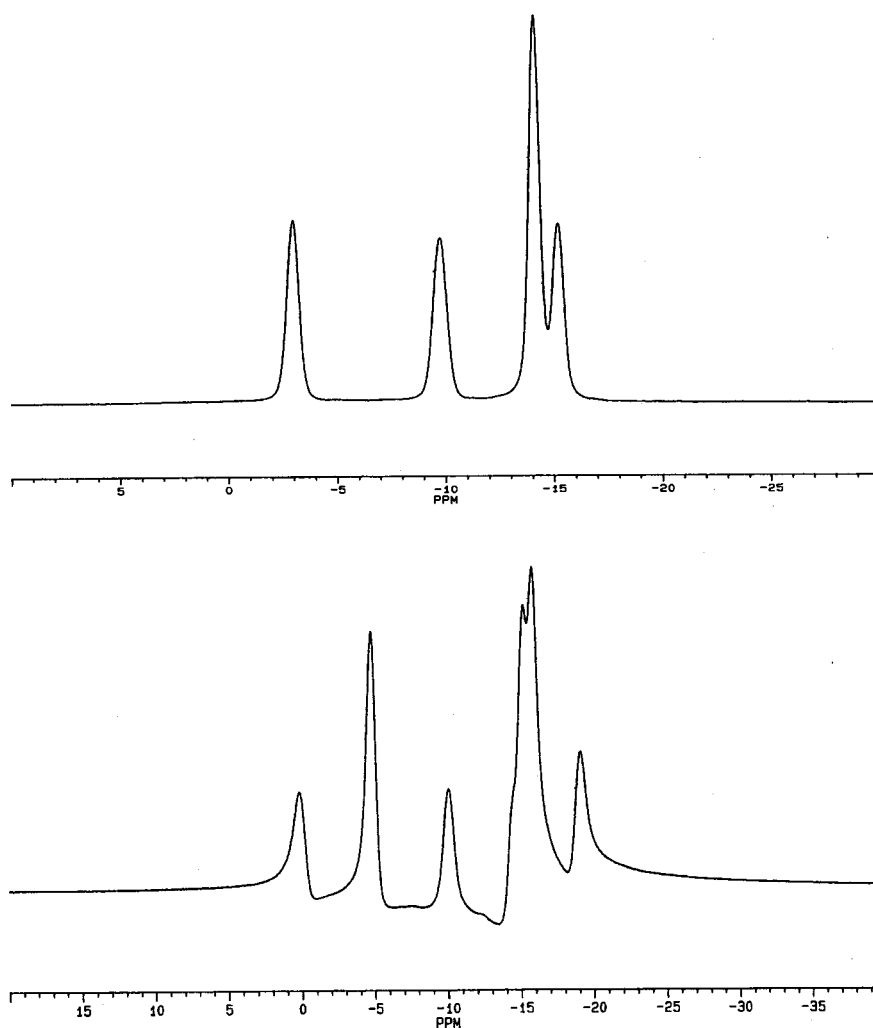


Figure 4.2 - $^{11}\text{B}\{^1\text{H}\}$ NMR of *ortho*-carborane (top) and **4.1** (bottom)

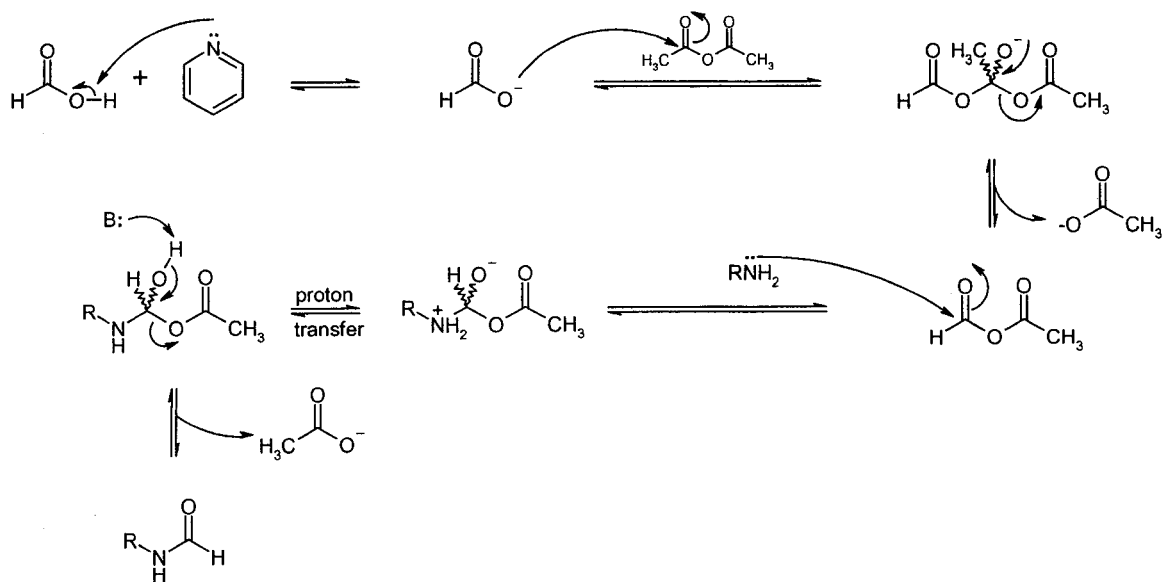
Characterization of compound **4.1** was accomplished using multi-NMR, IR and MS experiments. The ^{11}B NMR spectrum clearly reflects the changes in the symmetry of **4.1** compared to *ortho*-carborane (Figure 4.2). The proton-decoupled ^{11}B spectrum of *ortho*-carborane gave four peaks with the expected 1:1:2:1 ratio,²⁰ while the ^{11}B spectrum of **4.1** was much more complicated, which is a result of the lower symmetry in **4.1**.

Several approaches were evaluated for the conversion of the amine **4.1** to the corresponding formamide. Zakharkin originally succeeded by heating the amino-

carborane in formic acid to reflux for two hours, obtaining 3-formyl-*ortho*-carborane (**4.2**) in 80% yield.^{41,49} Repeating this reaction, the desired product **4.2** was isolated in good yield (74%). While acceptable for this approach, these conditions are most likely too harsh for applications in which a biomolecule is also attached to the carborane, leading to the investigation of a milder procedure (Scheme 4.3). To this end, a mixed anhydride was prepared from formic acid and acetic anhydride in the presence of pyridine at 0°C, which was then combined with the carborane-amine. Using this approach, formylation occurred in 60% isolated yield, and the product was readily purified by recrystallization.

The ¹H NMR spectrum of **4.2** contained a broad, undulating baseline between 1 and 3 ppm, indicative of the carborane B-H protons. The carborane C-H vertices are responsible for a slightly broadened singlet at 4.44 ppm while a very broad singlet centered at 5.79 ppm was assigned to the formamide N-H proton. The formamide C-H proton was observed as a singlet at 8.27 ppm. The ¹³C NMR spectrum exhibits carbon resonances at 165.95 ppm and 59.70 ppm, which are in the appropriate spectral region for carbonyl and *closo*-carborane carbon atoms, respectively. The ¹¹B NMR spectrum shows a series of peaks ranging from -4.5 to -15.1 ppm which is consistent with the presence of a closed *ortho*-carborane cage. An infrared analysis of **4.2** shows typical stretching frequencies for N-H (3300 cm⁻¹), C-H (3058 – 2901 cm⁻¹), B-H (1602 cm⁻¹) and C=O (1693 cm⁻¹) functional groups. Mass spectrometric analysis (CI) shows a characteristic isotopic distribution pattern centered at 186 m/z, which is the mass expected for **4.2**.

The mechanism of formylation using the asymmetric anhydride involves initial formation of the formylating reagent *in situ*, by first mixing a two-fold excess of formic acid with acetic anhydride in the presence of pyridine. Following the establishment of a series of equilibria, in which one portion of acetic anhydride is displaced by a formate anion, the amine **4.1** reacts at the least hindered, more electron deficient carbonyl carbon atom (Scheme 4.3). Care was taken to ensure that the reaction mixture always remained close to 0°C, especially during the mixing of the two reagents at which point heat evolution was evident. If the reaction was allowed to warm, a discoloured solution resulted and the overall reaction yield dropped.



Scheme 4.3 – Mechanism of asymmetric anhydride formation and subsequent formylation.

4.3 X-ray Crystal Structure of 3-Formyl-*ortho*-carborane

Single crystals of **4.2** were obtained by the evaporation of an acetone solution at room temperature and subjected to X-ray diffraction analysis. Compound **4.2** contained a slightly distorted icosahedron in which the carborane cage is oriented *cis* to the formamide oxygen (Figure 4.3). The average B-C bond length is 1.707(4)Å, ranging between a maximum of 1.749(4)Å and a minimum of 1.691(4)Å. The B-B bond lengths range from 1.758(4)Å to 1.800(5)Å with an average distance of 1.774(5)Å. The carborane carbon atoms were located based on the slightly shorter C-C bond distance (1.632(4) Å) than for the surrounding B-C and B-B bond lengths. The solid-state packing of **4.2** (Figure 4.4) shows that intermolecular hydrogen bonding plays a significant role in the formation of the three-dimensional lattice. Adjacent molecules along the c-axis interact with the carborane cages packing opposite to each other about the hydrogen bond axes. Along the b-axis, the carborane cages of adjacent molecules are situated next to each other. The lattice is composed of an infinite number of pleated layers along the a-axis.

The absolute structure shown has been arbitrarily chosen, and the correct solution may be that of the symmetry-inverted counterpart. Because compound **4.2** is not chiral, this inversion would not result in a chemically different product. The need to solve the X-ray structure of compound **4.2** in a chiral (Pna₂) space group was due to the overall packing mode of the formamide. The preference for compound **4.2** to pack in the manner shown gave the bulk crystal chiral symmetry, which in turn resulted in the chiral space group designation.

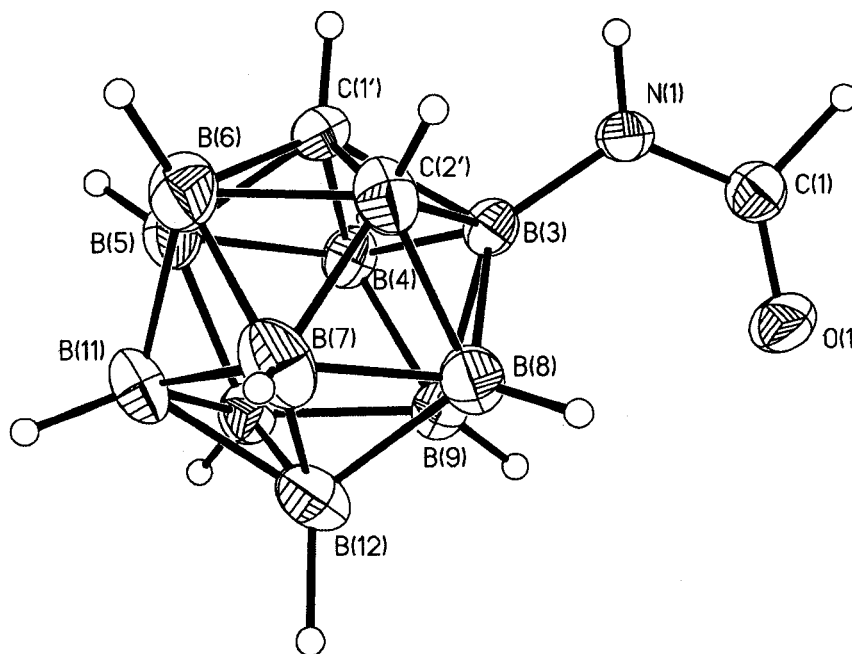


Figure 4.3 - ORTEP representation of 4.2. Thermal ellipsoids are shown at the 50% probability level.

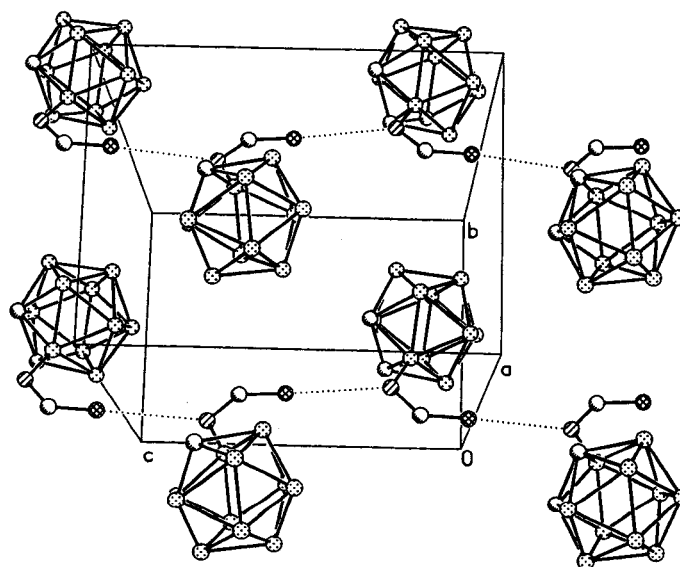


Figure 4.4 - Packing diagram of 4.2. Dotted lines indicate hydrogen-bond contacts.

4.4 Dehydration of 3-Formyl-*ortho*-carborane

Dehydration of formamide **4.2** was attempted using Zakharkin's procedure involving a reaction of **4.2** with POCl₃ and pyridine.⁴⁰ This yielded a complex product mixture, of which only a small fraction was the isonitrile. Consequently, an alternative approach was investigated in which compound **4.2** was treated with methyl(carboxysulfamoyl)triethylammonium hydroxide inner salt, otherwise known as the Burgess reagent.^{21,22} Creedon et al.²³ showed that the Burgess reagent efficiently dehydrates simple formamides under mild conditions, giving the corresponding isonitriles in respectable yields. Mixing the formamide (**4.2**) with the Burgess reagent in dichloromethane at room temperature for five hours yielded two products (Scheme 4.4), which were isolated chromatographically. Mass spectral analysis (EI) of the isonitrile gave a characteristic boron isotopic distribution at M+16. The presence of the isonitrile group was confirmed by the IR spectrum, which showed a strong R-N≡C stretch at 2139 cm⁻¹ (Figure 4.5).

The ¹¹B NMR spectrum of **4.3** contains five peaks ranging from -3.1 to -13.9 ppm, which is consistent with a *closo*-carborane cage substituted at the B-3 vertex. The ¹H NMR spectrum of **4.3** contained a broad, undulating baseline between 1 and 4 ppm, indicative of the carborane B-H protons, while the carborane C-H vertex was responsible for a slightly broadened singlet at 3.88 ppm. The ¹³C NMR spectrum was relatively simple and showed only one carbon resonance at 59.70 ppm, the region in which *closo*-carborane carbon atoms typically appear. The reason for the absence of a resonance from the isonitrile carbon was not immediately apparent, but was attributed to the lack of

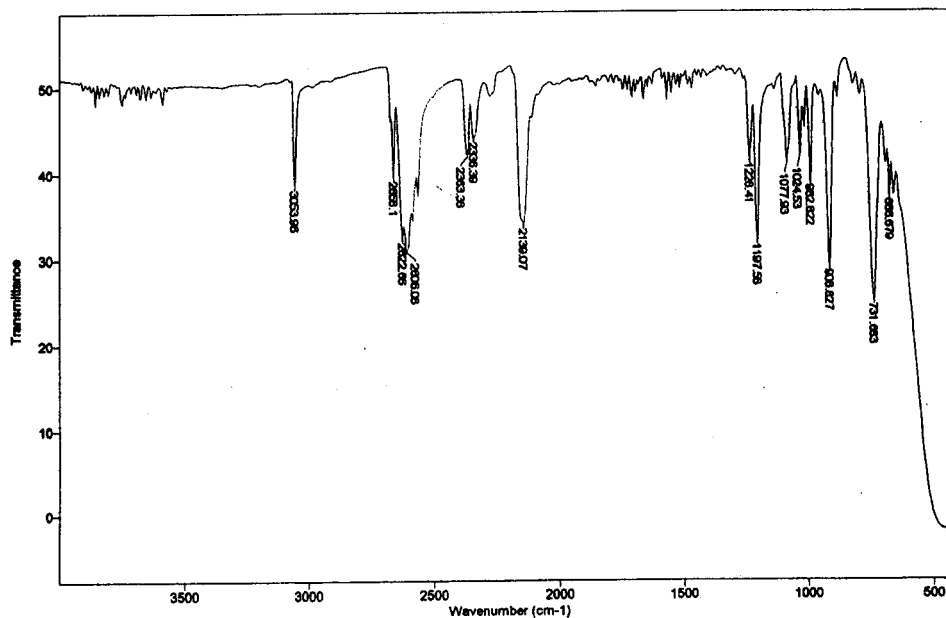


Figure 4.5 - IR spectrum of 4.2.

sufficient hetero-Nuclear Overhauser Enhancement (NOE) to intensify the carbon resonance peak. The experimental delay time between scans was increased from 0.5 seconds to 3 seconds, but did not reveal any additional peaks. Some ternary carbon nuclei have been known to exhibit relaxation times on the order of minutes, thereby not allowing for the complete Free Induction Decay (FID) signal to be collected before continuing with the next experimental scan.²⁴ More recently, however, the ^{13}C NMR spectrum of 4.3 was re-acquired at 150 MHz with a pulse delay of 0.5 seconds and an accumulation of nearly 97,000 scans (Figure 4.6). Under these conditions two peaks are observed: the previously recorded carborane carbon resonance at 59.70 ppm and a less intense peak at 181.83 ppm, which is associated with the carbon atom of the isonitrile group. This resonance frequency is much higher than that of any previously reported isonitrile.²⁵⁻²⁷

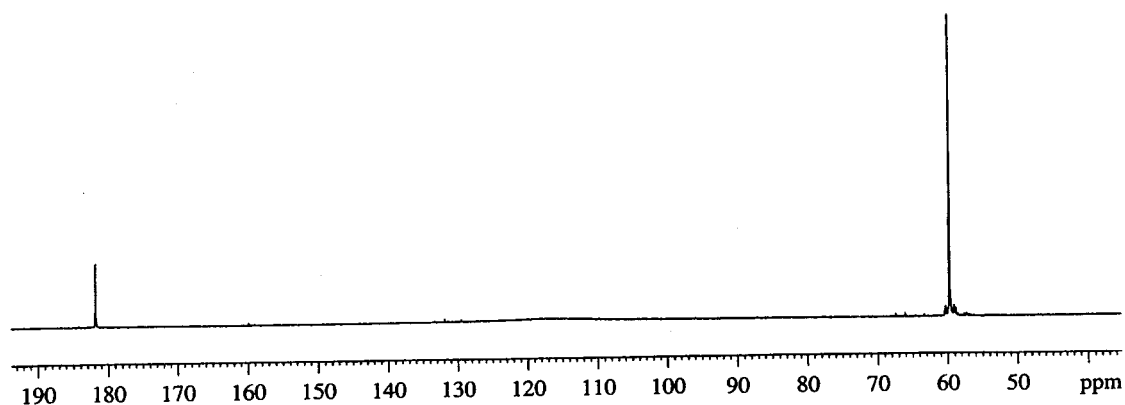
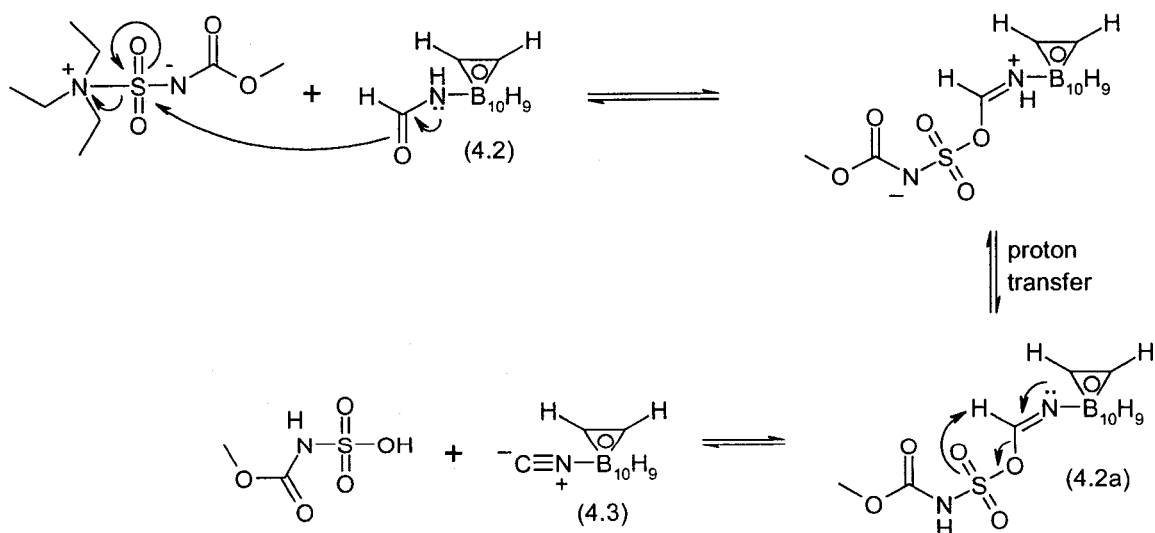


Figure 4.6 – The ^{13}C NMR spectrum (150 MHz) of 4.3 in acetone- d_6

The mechanism of dehydration involves reaction of the oxygen atom of the formyl group with the electrophilic sulfone group of the Burgess reagent (Scheme 4.4). Following proton transfer, the carbon-nitrogen triple bond is generated by the displacement of the sulfamoyl moiety. The resulting sulfamic acid is sequestered *in situ*, thereby preventing the acid catalyzed hydrolysis of the desired isocyanide.²⁸



Scheme 4.4 – Mechanism of dehydration using the Burgess reagent. Not all canonical forms are given for the sake of clarity.

4.5 X-ray Crystal Structure of 3-Isonitrile-*ortho*-carborane

The structure of the B-substituted isonitrile carborane was confirmed by single crystal X-ray crystallography. Crystals were grown by the slow evaporation of an ethanolic solution of **4.3** at room temperature (Figure 4.7). The carbon vertices were discernible in the crystal packing, and are not disordered about five cage atoms adjacent to the functionalized vertex. The two carbon atoms were identified by the shorter C-C bond distance (1.638(4)Å) relative to the average B-B (1.774(5) Å) and B-C (1.704(4) Å) bond lengths. The B-B bond distances ranged from 1.752(5) Å to 1.785(5)Å and the B-C bond lengths ranged between a minimum value of 1.683(5)Å to a maximum distance of 1.719(4)Å. The solid-state structure of **4.3** confirmed substitution at the third cage position, with the N1-C1 bond length being 1.157(4) Å. The N1-B3 bond length was 1.467(4) Å, which is similar to the distances reported for the rhodium complex of **4.3**.²⁹ The B3-N1-C1 bond angle was, as expected, nearly linear (178.2(3)°).

The solid-state crystal packing of the isonitrile appears to be governed primarily by the carborane cages themselves, which pack in a columnar fashion (Figure 4.8). The linear isonitrile functionalities project orthogonally within each lattice column and are related by inversion of molecules in adjacent (alternating) columns.

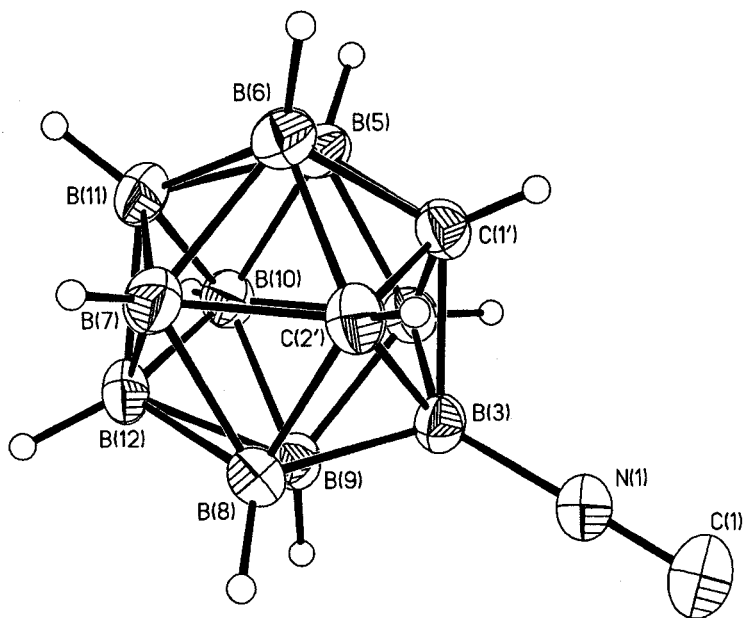


Figure 4.7 – X-ray crystal structure of 3-isonitrile-ortho-carborane (4.3) (50% thermal ellipsoids).

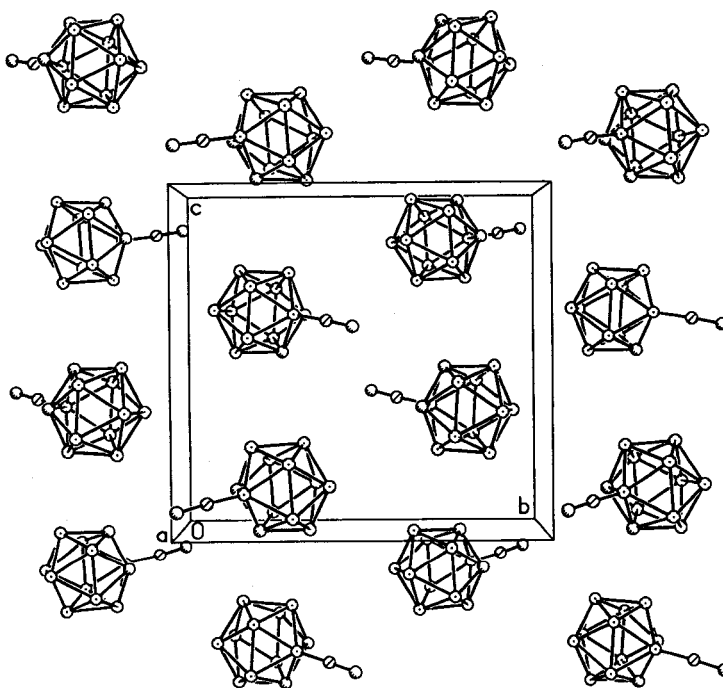


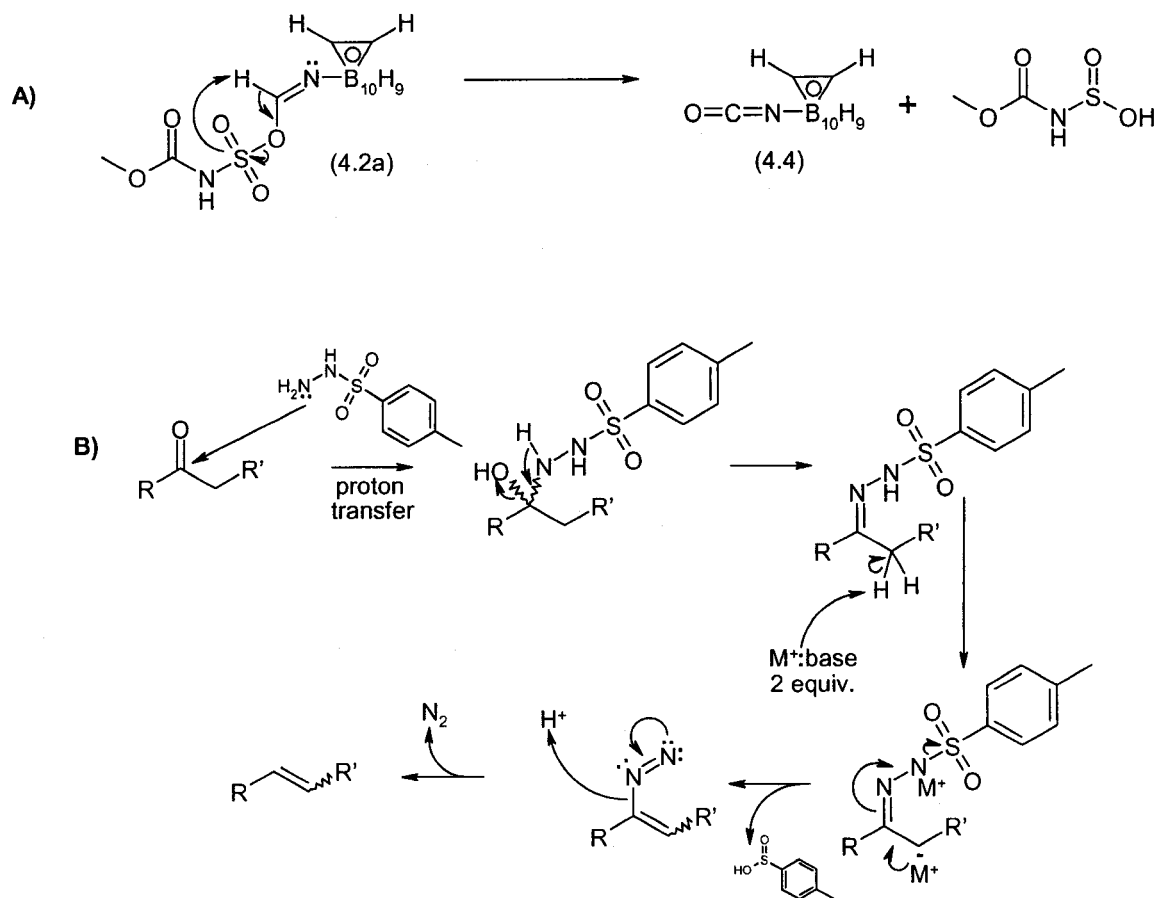
Figure 4.8 – Ball and stick representation for the solid-state packing of 4.3.

4.6 Formation of an Isocyanate from Burgess Reagent Dehydration of 4.3

A second product was obtained in the Burgess reagent mediated dehydration of 4.2, and was determined to be the isocyanate 4.4. IR analysis of the product indicated the presence of the R-N=C=O functionality through the very intense absorption band present at 2307 cm^{-1} . The mass spectrum of 4.4 was nearly identical to that of the isonitrile 4.3, with the base peak and molecular ion at 184 m/z . The ^1H , ^{13}C and ^{11}B NMR spectra are all consistent with the proposed structure of compound 4.4. In addition to the broad undulating baseline between 1 and 4 ppm, a broad singlet at 3.67 ppm was the only other peak present in the ^1H NMR spectrum. This singlet is in the typical chemical shift range for the C-H vertex of a mono-substituted *ortho*-carborane. The ^{13}C NMR spectrum contained two peaks, one at 56.57 ppm from the carborane carbon atoms, and another at 135.14 ppm from the isocyanate carbonyl carbon. The 160 MHz ^{11}B NMR spectrum of 4.4 shows a series of peaks between -3.92 and -15.43 ppm, which is consistent with the *closo* cage structure.

The mechanism for formation of the isocyanate likely resembles the accepted pathway followed by the Shapiro reaction (Scheme 4.5). In the Shapiro reaction, elimination of an arylsulfinate from an aryl sulfonylhydrazone intermediate occurs to generate a carbon-carbon double bond.³⁰ A similar mechanism is proposed for the formation of 4.4. Due to the electron accepting properties of the carborane, the conjugation of the formamide nitrogen and the adjacent carbonyl group is reduced. As a result, the reaction proceeds along a different pathway than that previously discussed for the formation of 4.3 (Scheme 4.4). Intramolecular elimination of the sulfamoyl group (via

reduction of the sulphur) competes and subsequently yields the isocyanate (**4.4**) (Scheme 4.5).

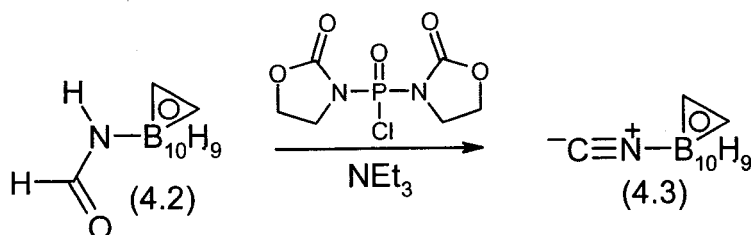


Scheme 4.5 – A) Proposed mechanism for the formation of **4.4**. B) Mechanism of the Shapiro reaction.

4.7 Dehydration of **4.2** with BOP-Cl

Despite the successful dehydration of **4.2** with the Burgess reagent (*vide supra*), formation of the isonitrile **4.3** was always accompanied by the formation of the isocyanate **4.4** regardless of the reaction conditions used. In an attempt to minimize the yield of **4.4**, **4.3** was dehydrated with BOP-Cl (bis(2-oxo-3-oxazolidinyl)phosphinic

chloride) in the presence of triethylamine (Scheme 4.6). While complete consumption of the starting material was never achieved, yields were comparable to those obtained previously (49% vs. 51%) and the unreacted starting material was easily separated and recycled for future use. The BOP-Cl mediated dehydration of an N-formyl group, which to the best of our knowledge has not been previously reported, is thus a useful method for the preparation of the desired carborane-isonitrile (4.3).



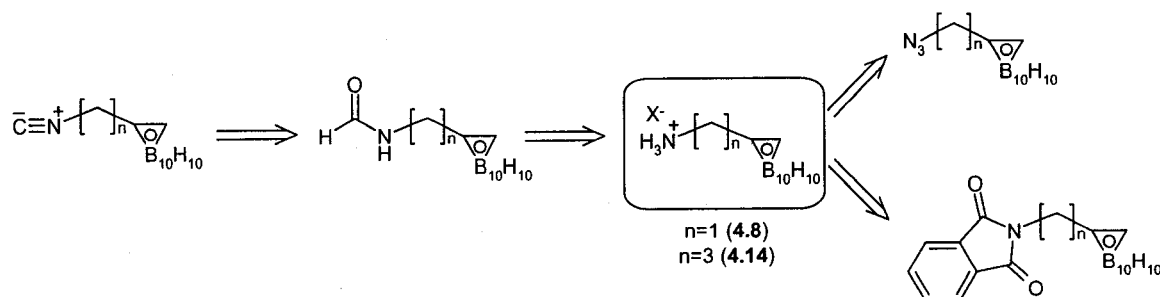
Scheme 4.6 – Dehydration of 3-formyl-ortho-carborane with BOP-Cl.

4.8 Tethered C-Substituted *ortho*-Carborane Isonitriles

In addition to boron-linked isonitriles, the previously described method was also used in an attempt to prepare carbon-linked isonitrile derivatives. In particular, a method was sought that would allow the introduction of a spacer between the carborane cage and the isonitrile unit. It was hoped that this spacer unit would reduce the influence of the bulky carborane cage during the synthesis of poly-substituted metal complexes.

A retrosynthetic analysis suggested that the key synthetic intermediates are the amino-alkyl-carboranes 4.8 and 4.14 (Scheme 4.7). A search of the literature uncovered two fundamental approaches for the synthesis of tethered amino-carboranes. One approach involved a modified Gabriel amine synthesis,³¹ while the second method

involved introducing the amino functionality by the reduction of an azide.³² Both strategies were investigated.



Scheme 4.7 - Retrosynthetic analysis for the formation of C-linked carboranyl isonitriles.

Phthalimido-carboranes were originally used by Nakagawa and co-workers to prepare the corresponding amino-alkyl-*closo*-carboranes.³³ Their procedure calls for deprotection of the phthalimide with hydrazine hydrate, which is surprising given the sensitivity of the *ortho*-carborane cage toward strong Lewis bases. Twenty years later, Soloway and co-workers assigned the product of the identical reaction to be the amino-alkyl-*nido*-carborane, and postulated that the degradation of the *closo* cage to the *nido* cage occurs during the deprotection of the phthalimide with hydrazine.³² Clarification of this discrepancy was reported one decade later by Hughes and co-workers.³⁴ The phthalimide mask was removed with hydrazine hydrate under varying conditions and it was determined that the cage remained intact if deprotection was carried out under mild conditions, while the *nido* product was obtained only upon heating the reaction mixture.

Propargyl phthalimide **4.5** was prepared by the procedure of Soloway et al. This was followed by introduction of the carborane cage to give **4.6** in 60% isolated yield. The solubility of **4.6** is extremely poor in most solvents, which makes characterization

difficult. Despite this, the ^1H NMR spectrum of **4.6** was obtained and showed a prominent and characteristic AA'BB' multiplet at 7.86 ppm due to the phthalimide aromatic protons. That, in addition to the broad singlets at 4.38 and 4.00 ppm, was helpful in assigning the structure of **4.6**. The ^{13}C NMR spectrum showed peaks at 167.13 ppm as would be expected from the C=O group as well as two peaks at 73.15 and 59.99 ppm which are in the usual range for the carbon nuclei of *ortho*-carborane polyhedra. The ^{11}B NMR spectrum shows peaks ranging from -1.39 to -13.16 ppm, which is indicative of the *closo* nature of the cage. EI mass spectrometry gave a peak containing a ten boron atom isotopic distribution at 303 m/z (M^+), while the IR spectrum of the phthalimido-carborane gave characteristic stretching frequencies for the carborane ($\nu_{\text{BH}} = 2598 \text{ cm}^{-1}$) and carbonyl ($\nu_{\text{CO}} = 1723 \text{ cm}^{-1}$) functional groups.

In order to avoid *nido*-carborane formation and the uncertainty associated with the deprotection procedure, compound **4.6** was treated with NaBH_4 to give the amide **4.7** which in turn was hydrolyzed using concentrated HCl to give **4.8** (Scheme 4.8).³²

Both **4.7** and **4.8** were isolated and fully characterized by ^1H , ^{13}C and ^{11}B NMR, MS and IR spectroscopy. The ^1H NMR spectrum of **4.7** was, as expected, more complicated than that of the phthalimide precursor. A characteristically broad peak due to the amide N-H proton was observed at 9.10 ppm. Aromatic multiplets at 7.48 ppm were also present in addition to peaks at 5.29 ppm (OH), 4.62 and 4.03 (methylene protons), 3.35 (br s, 1H, CH) and the broad undulating baseline between 3.9 and 0.9 ppm from the cage B-H vertices. The ^{13}C NMR spectrum of **4.7** was equally complicated, while the ^{11}B NMR spectrum gave a range of peaks between -1.19 and -12.99 ppm, consistent with the

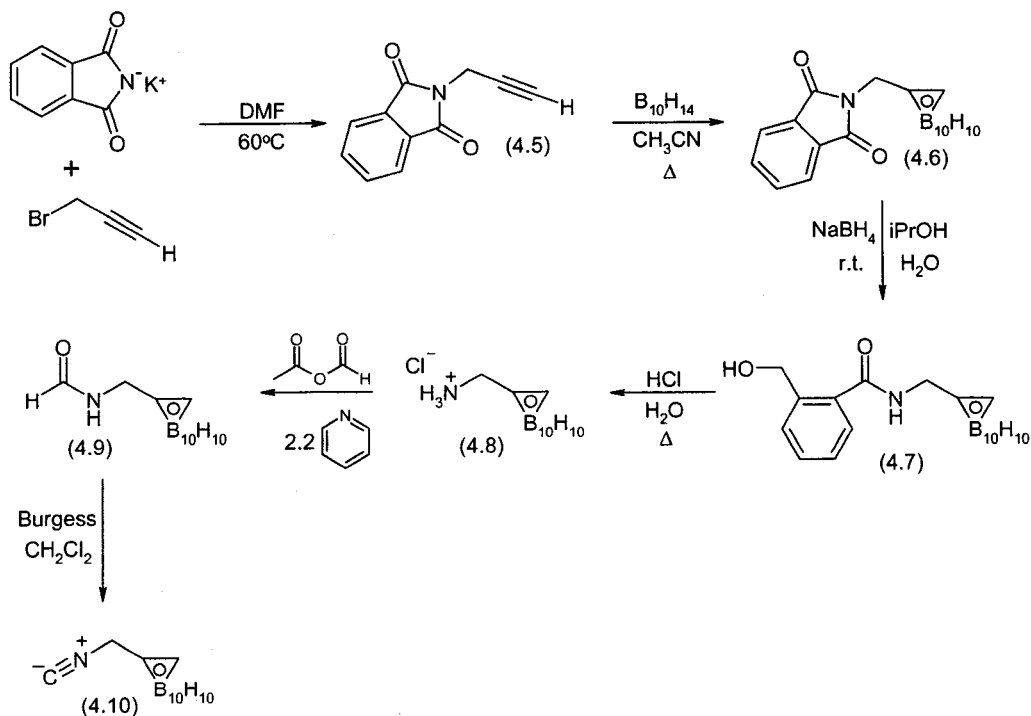
presence of a *closo*-carborane. The infrared spectrum shows a broad OH stretch at 3247 cm^{-1} , in addition to C-H stretching peaks between 3092 and 3048 cm^{-1} . A characteristic B-H peak was visible at 2578 cm^{-1} as well as a carbonyl stretch at 1632 cm^{-1} , consistent with an amide C=O group. The CI mass spectrum shows a peak at 308 m/z (M^+), consistent with the ten-boron atoms in **4.7**.

Compound **4.8** showed a broad ^1H NMR spectrum, due in part, to poor solubility and the need to use $\text{DMSO-}d_6$. A broad NH_3 peak was observed at 8.86 ppm while the methylene protons were visible at 3.80 ppm. The carborane cage gave the characteristic broad singlet at 3.51 ppm from the C-H group, as well as the broad series of peaks between 1 and 4 ppm from the B-H vertices. The ^{11}B NMR spectrum of **4.8** gave a range of peaks between -1.20 and -11.14 ppm, however after several hours in solution peaks as low as -37.5 began to appear. This is consistent with the conversion of the *closo* cage to the corresponding *nido* product. If characterized shortly after isolation, the ESMS spectrum of **4.8** showed one boron isotopic distribution pattern at an m/z of 174 (M^+). To simplify the reaction, the amine **4.8** was not stored for long periods of time, and when synthesized, promptly converted to the formamide. The synthesis and isolation of compound **4.9** was accomplished in reasonable yield (66%) through the use of the mixed anhydride strategy.

Complete characterization of the formamide **4.9** was accomplished by multi-NMR and IR spectroscopy in addition to mass spectrometry. The ^1H NMR spectrum of **4.9** showed a peak at 8.21 ppm corresponding to the formyl proton, a broad NH peak at 6.39 ppm, and overlapping resonances due to the methylene and carborane CH protons at 3.97

ppm and 3.91 ppm respectively. The ^{13}C NMR spectrum shows four peaks at 161.74, 74.05, 60.28 and 43.18 ppm, which is consistent with the presence of one carbonyl, two carboranyl and one methylene carbon nuclei. The ^{11}B NMR spectrum confirms that the carborane cage in **4.9** has a *closo* structure.

Chemical ionization mass spectrometry showed two sets of peaks containing a ten-boron isotopic distribution pattern at m/z values of 200 (M^+) and 218 ($M+\text{NH}_4$). The IR spectrum of **4.9** was also consistent with the functional groups present, such as the NH stretching peak at 3290 cm^{-1} , the aliphatic C-H peaks at 3064 and 3042 cm^{-1} , the strong B-H stretch at 2585 cm^{-1} and a carbonyl peak at 1672 cm^{-1} .



Scheme 4.8 – Synthesis of the tethered ortho-carborane isonitrile **4.10**.

The synthesis of isonitrile **4.10** was attempted following the procedure used to dehydrate 3-formyl-*ortho*-carborane **4.2**. Dehydration of **4.9** using the Burgess reagent yielded the desired isonitrile (**4.10**), which was isolated in 22% yield.³⁵

Electrospray mass spectrometric and NMR analysis supported the formation of **4.10**. The negative ion mode ESMS showed a molecular ion at 182.1 m/z, the molecular mass of the expected product, with the anticipated isotopic distribution pattern for a molecule containing ten boron atoms. The ¹H NMR spectrum of **4.10** was also relatively simple and showed no formyl proton peak, providing strong evidence that the desired transformation took place. In addition, a broad singlet at 4.14 ppm contained twice the area as another broad singlet at 3.88 ppm, allowing us to assign these peaks as those corresponding to the methylene spacer and carborane C-H group respectively. The undulating baseline between 1 and 3 ppm is also characteristic for the presence of carborane B-H vertices.

Infrared spectroscopic analysis of the purified product proved to be the definitive method in the characterization of **4.10**, as a peak at 2151 cm⁻¹, corresponding to the R-N≡C group, was observed. The higher frequency of the isonitrile functionality for **4.10** compared to that observed for the untethered derivative (**4.3**, 2139 cm⁻¹) is indicative of the insulating effect of the methylene spacer.

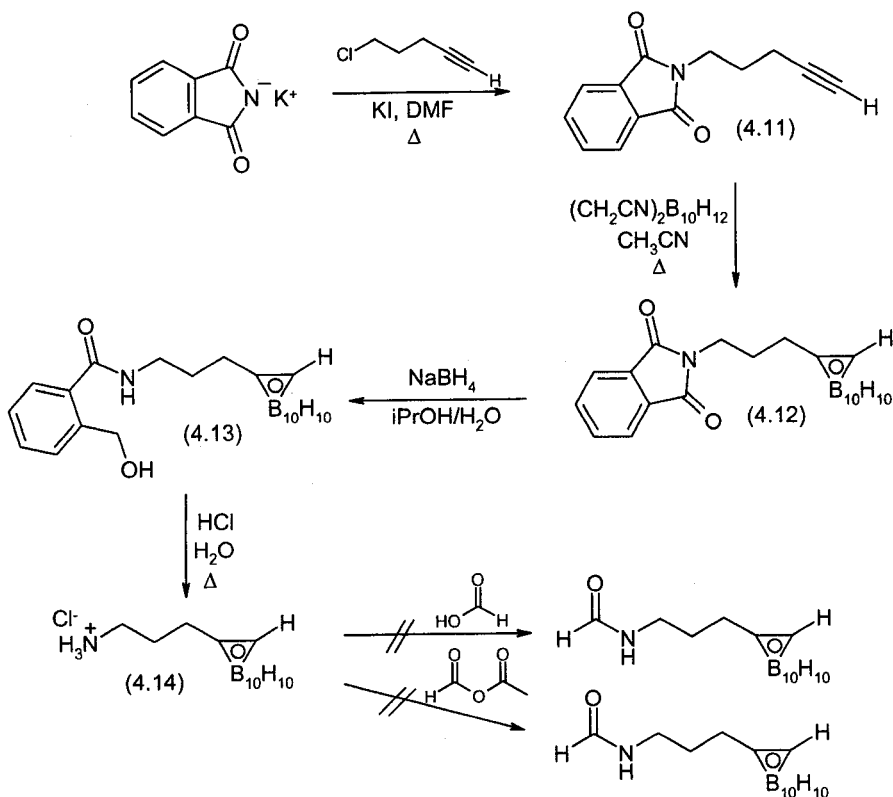
4.9 Synthesis of Isonitrile Carboranes Containing Longer Alkyl Tethers

With the successful synthesis of the isonitrile **4.10**, in which the N≡C functionality was separated from the cage by one methylene spacer, and in light of the low yield, a method for the synthesis of carboranyl isonitriles containing longer tethers

was investigated. Following a similar procedure as that used to prepare **4.8**, a Gabriel synthesis yielded the alkyne **4.11** in good yield (80%) by heating 5-chloropentyne with potassium phthalimide in a DMF solution at reflux (Scheme 4.9).^{31,36} Carborane **4.12** was synthesized in low yield (20%) by reacting the bis(acetonitrile) Lewis base adduct of decaborane with the alkyne **4.11**.

The ¹H NMR spectrum of **4.12** exhibited peaks consistent with the proposed structure. A multiplet of peaks showing an AA'BB' substitution pattern centered at 7.78 ppm is consistent with the presence of the phthalimide group. A triplet at 3.65 ppm contained a broad shoulder which was characterized as an overlap of the carborane C-H proton with an aliphatic methylene group. The remaining methylene groups were observed at 2.28 and 1.87 ppm, while the undulating baseline between 1 and 4 ppm was indicative of the cage B-H vertices. The ¹³C NMR spectrum of **4.12** contained nine peaks with the phthalimide carbonyl atoms appearing at 168.31 ppm and the carborane carbon atoms at 61.35 and 36.97 ppm. A series of peaks in the ¹¹B NMR spectrum of **4.12**, ranging from -1.51 ppm to -12.22 ppm indicate that the cage is of the *closo* structure.

Infrared and mass spectrometric analysis also both confirmed the identity of product **4.12**. The infrared spectrum showed a number of peaks characteristic of the various functional groups present in the carborane phthalimide **4.12**. Aliphatic C-H stretching frequencies were observed between 3058 cm⁻¹ and 2968 cm⁻¹. The prominent carborane B-H peak at 2597 cm⁻¹ was also present, while two carbonyl stretches were observed at 1773 cm⁻¹ and 1716 cm⁻¹. The electron impact mass spectrum exhibited a molecular ion containing a ten-boron isotopic distribution pattern at 331 m/z.



Scheme 4.9 – Synthesis of aminopropyl-ortho-carborane (4.14).

Removal of the phthalimide group then proceeded as described for 4.8, by first reducing of one phthalimide carbonyl with NaBH_4 in $i\text{-PrOH}$ to give amide 4.13. Isolation and characterization of 4.13 was carried out in order to confirm the formation of the desired product. Despite the fact that characterization of 4.13 was tedious due in part to the poor solubility of this compound in most solvents, reasonable quality spectra were obtained.

The ^1H NMR spectrum of 4.13 showed a broad singlet at 7.96 ppm and 4.83 ppm for the amide N-H and alcohol O-H groups, respectively. A multiplet between 7.58 and 7.33 ppm for the phenyl protons was observed, in addition to the undulating baseline between 0.6 and 3.8 ppm due to the carborane B-H units. Other multiplets observed in the

aliphatic region of the spectrum were assigned to the six methylene protons. The ^{13}C NMR spectrum was much more complex than that of the phthalimide precursor **4.12**, which is consistent with the loss of symmetry in **4.13**. The ^{11}B NMR spectrum confirmed that the integrity of the *closo* cage had not been compromised, with five peaks observed between -1.73 and -11.84 ppm.

Isolation and characterization of compound **4.13** was followed by acid hydrolysis to give the ω -substituted aminoalkyl ortho-carborane **4.14**. Hydrolysis was accomplished in a similar fashion to the method used for the synthesis of **4.8**; a 3N solution of hydrochloric acid was added to the benzoylamide **4.13** in isopropanol. The reaction was allowed to continue for 18 hours at ambient temperature, giving the desired amine in greater than 99%.

The electrospray mass spectrum of **4.14** showed a molecular ion with a typical ten-boron isotopic distribution at an m/z value of 202. The ^1H NMR spectrum of **4.14** showed a broad singlet at 5.90 ppm corresponding to the amine protons. Other peaks, such as a broad singlet at 3.46 ppm from the carborane C-H vertex, and three multiplets in the aliphatic region, confirmed the successful isolation of **4.14**. The ^{13}C NMR spectrum showed five peaks, of which two (74.59 and 61.56 ppm) are in the region typically found for the C-vertices of a *closo*-carborane cage. The ^{11}B NMR spectrum of **4.14** once again indicated the presence of a *closo* cage.

It was found that working with phthalimido-carborane derivatives was cumbersome particularly with regard to solubility of intermediates and removal of the last traces of phthalimide by-products that form during deprotection reactions. It was apparent

that a simpler and more robust methodology was needed.³⁷ The obvious alternative route to carboranyl-amines is the hydrogenation of the corresponding azide substituted carborane. Soloway and co-workers reported that hydrogenation of carboranyl azides in the presence of Pd/C led to the corresponding *nido*-carborane.³² Because of the ease with which a wide variety of carboran-1-yl-alkyl azides have been synthesized in the past, we were interested in re-investigating this approach using different conditions, in an attempt to isolate *ortho*-carboranyl amines without degradation of the cage. Studies were therefore carried out on the reduction of 3-azido-1-(1,2-dicarba-*closo*-dodecaboran-1-yl)propane as a model substrate (Scheme 4.10).³²

The chloro-carborane **4.15** was synthesized by reaction of 5-chloro-1-pentyne with decaborane in an acetonitrile solution. The reaction mixture was heated at reflux until complete consumption of the starting material was noted by thin layer chromatography (72 hours). Compound **4.15** was purified by chromatography and fully characterized.

A ¹H NMR spectrum of **4.15** showed a broad singlet at 3.58 ppm due to the carborane C-H vertex, overlapped with a triplet due to one of the aliphatic methylene groups at 3.50 ppm. The remaining methylene peaks were located further upfield at 2.38 and 1.95 ppm, respectively. All peaks were superimposed on the undulating baseline between 3.9 and 0.8 ppm, arising from the cage B-H vertices.

The ¹³C, ¹¹B NMR and IR spectra of **4.15** were also consistent with the assigned structure, with the ¹³C spectrum exhibiting five peaks and the ¹¹B spectrum showing the typical range and pattern consistent with a mono-substituted 1,2-dicarba-*closo*-

dodecaborane cage. The infrared spectrum of **4.15** was relatively simple, containing some aliphatic C-H stretching peaks around 3000-2900 cm^{-1} in addition to a strong B-H stretch at 2595 cm^{-1} . The peak corresponding to the C-Cl stretching frequency was also discernable in the fingerprint region of the spectrum at 723 cm^{-1} . The electron impact mass spectrum showed both the molecular ion mass peak at 220 m/z as well as a fragment at 185 m/z. This fragment peak is consistent with the loss of chloride from the parent ion.

Compound **4.15** and sodium iodide were combined in acetone to give **4.16** in nearly quantitative yield.³⁸ Two of the aliphatic methylene peaks at 2.33 and 1.99 ppm in the ^1H NMR spectrum of **4.16** were similar to those values obtained for the chloride precursor. As expected, the triplet at 3.50 ppm in **4.15** was now further upfield at 3.13 ppm, due to the replacement of chloride with iodide. The chemical shift of the carborane C-H group, a singlet at 3.59 ppm, remained unchanged between the two derivatives. One notable chemical shift difference was observed in the ^{13}C NMR spectrum of **4.16**. A new peak at 3.69 ppm was significantly further upfield than any in the spectrum of the chloride precursor, owing to the change in electronic environment at the carbon atom bound to the iodide substituent. The ^{11}B NMR spectrum of **4.16** once again showed a range of peaks between -2.67 and -13.50 ppm consistent with the structure of the desired product.

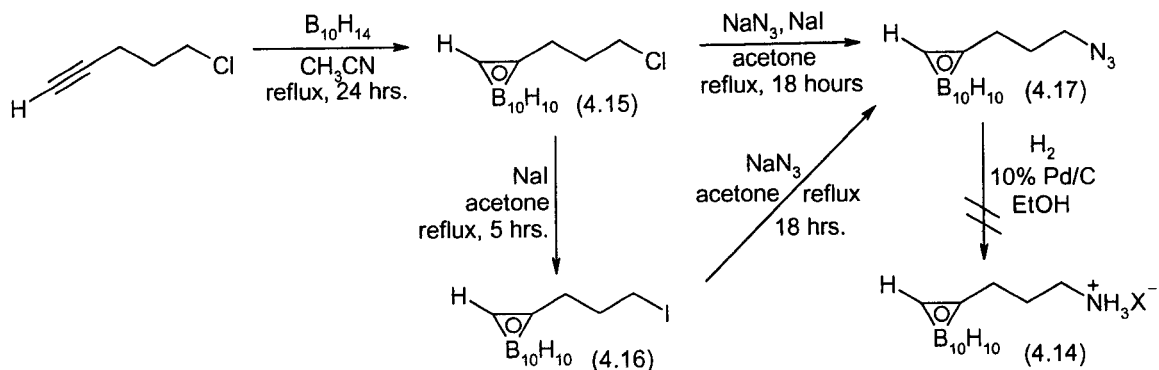
An interesting aspect of the CI mass spectrum for the iodo-carborane **4.16** was the presence of a very intense peak at 494 m/z in addition to the expected molecular ion at 311 m/z. Upon closer examination of this high molecular weight peak, it was apparent

from the isotope distribution pattern that the contributing ion contained twenty boron atoms. This molecular weight is also consistent with a compound of the chemical formula $C_{10}H_{34}B_{20}I$, and is likely an artifact of the mass spectrometry experiment. A subsequent EI experiment gave a molecular ion at 183 m/z which is consistent with the loss of I from the parent ion. A low intensity, ten-boron distribution peak was observed at 311 m/z in addition to an equally intense peak at 494 m/z.

Conversion of iodide **4.16** to the azide **4.17** was accomplished by treating **4.16** with sodium azide in acetone, thus yielding the desired product in greater than 99% yield. Similarly, chloride **4.15** could be directly converted to **4.17** in the presence of a catalytic amount of sodium iodide, in comparable yield (86%).

The NMR spectra of **4.17** resembled those of the chloro and iodo precursors, **4.15** and **4.16**. A series of overlapping peaks at 3.26, 2.27 and 1.71 ppm in the 1H NMR spectrum are consistent with the presence of six methylene protons, in addition to the broad carborane C-H peak at 3.58 ppm. The ^{13}C NMR spectrum was very similar to that of **4.15**, with only minor chemical shift differences noted between the two. The ^{11}B NMR showed that the carborane cage remained intact during the nucleophilic displacement of the chloride or iodide with azide.

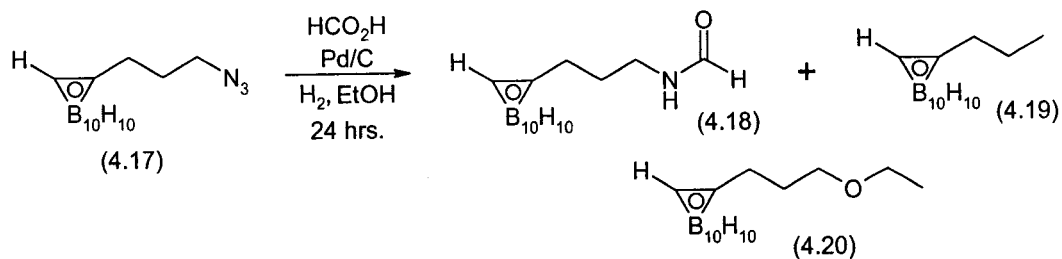
The base peak observed in the electron impact mass spectrum of **4.17** was at 198 m/z, which is consistent with the loss of N_3^- from the parent ion. The infrared spectrum of **4.17** showed a highly characteristic N_3 stretching frequency at 2102 cm^{-1} , in addition to a series of peaks corresponding to the presence of C-H groups and a B-H stretch at 2595 cm^{-1} .



Scheme 4.10 – Synthesis of ω -amino-alkyl-ortho-carborane.

Attempts were then made to generate the amine **4.14** by hydrogenation of **4.17** in the presence of 10% Pd/C as catalyst. Following the procedure established by Soloway and co-workers, hydrogenation in the presence of acetic acid was performed. An analysis of the reaction mixture showed that the azide was reduced to the ammonium acetate salt. However, isolation of **4.14** proved to be difficult, which is consistent with the results reported by Soloway and co-workers.³²

In order to determine if the nature of the acid affected the reaction outcome, hydrogenation was attempted in the presence of formic acid. Surprisingly, the reaction did not yield any of the desired product **4.14**. The main products were the formamide **4.18** (9%), the alkane **4.19** (2.5%) and the ethyl ether **4.20** (13%) (Scheme 4.11), which were separated by column chromatography. The alkane **4.19**, being the most non-polar, eluted first, followed by the ethyl ether **4.20** and finally the formamide **4.18**.



Scheme 4.11 – Attempted hydrogenation of 4.13 and formation of side products.

The ^1H NMR spectrum of compound **4.18** showed a N-H proton peak as a singlet at 8.03 ppm in addition to three sets of multiplets corresponding to the methylene groups at 4.14, 3.60 and 2.31 ppm. The carborane C-H vertex gave rise to a singlet at 3.60 ppm on the edge of the broad B-H resonances. The ^{13}C NMR spectrum showed six peaks, one at 160.59 ppm corresponding to the formyl carbonyl group. The infrared spectrum showed several peaks in the aliphatic region between 3068 and 2872 cm^{-1} in addition to a prominent B-H stretch at 2598 cm^{-1} and a carbonyl stretch at 1726 cm^{-1} . The CI mass spectrum exhibited a molecular ion at 229 m/z and a fragment ion peak at 198 m/z corresponding to the loss of the formyl group.

The proton NMR spectrum of alkane **4.19** is consistent with the proposed structure, with three methylene multiplets observed at 2.17, 1.49 and 0.91 ppm. The triplet at 0.91 ppm was determined to be from the protons of the terminal methyl group, due to the relative peak area when compared to the other two multiplets. The ^{13}C NMR spectrum showed five peaks, two of which were in the characteristic chemical shift range for carbon atoms belonging to the polyhedral cage. The remaining peaks were all located in the aliphatic region of the spectrum.

Conclusive evidence for the structure of alkane **4.19** was obtained by X-ray diffraction, using single crystals grown by slow evaporation of an ethanol solution at room temperature (Figure 4.9). The compound crystallized in the orthorhombic $Pna2_1$ space group, with two independent molecules in the asymmetric unit ($Z = 8$). Compound **4.19** was a slightly distorted icosahedron in which the carborane was oriented $146.6(9)^\circ$ and $67.9(9)^\circ$ to the alkyl chain in each case. The average boron-carbon bond lengths in each of the molecules were $1.729(12) \text{ \AA}$ and $1.700(12) \text{ \AA}$, ranging between a maximum

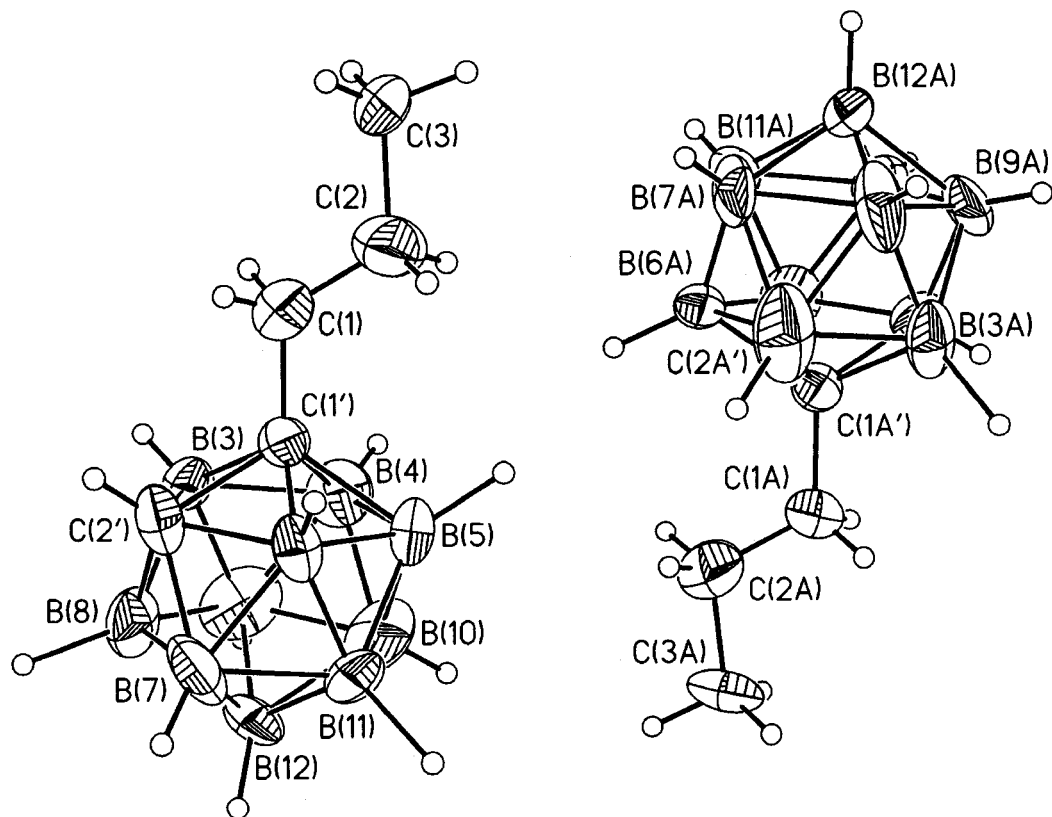


Figure 4.9 - ORTEP representation of **4.19**, thermal ellipsoids shown at the 50% probability level.

of $1.754(12) \text{ \AA}$ and a minimum of $1.628(12) \text{ \AA}$. The boron-boron bond lengths ranged from $1.644(14) \text{ \AA}$ to $1.833(15) \text{ \AA}$ with an average distance of $1.756(14) \text{ \AA}$ and $1.738(14)$

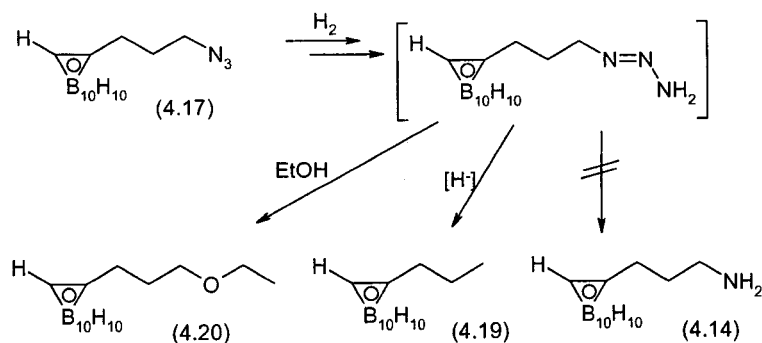
Å for both molecules respectively. The two carbon atoms of the cage were clearly identifiable based on their shorter carbon-carbon bond lengths of 1.670(10) Å and 1.660(12) Å and by their proximity to the cage substituent. The solid-state packing of the alkane appeared to be governed primarily by the association of the spherical cages with the alkyl chains of adjacent molecules interacting through simple van der Waals forces.

The ethyl ether **4.20** was isolated as a viscous, colourless oil. The ^1H NMR spectrum of **4.20** exhibited a similar set of peaks to those observed in compound **4.19**, including signals associated with the three methylene units, carborane C-H groups and the broad baseline peaks due to the B-H protons. In addition to these however, another spin system was evident and is associated with the ethyl ether group. While one quartet is significantly overlapped with the peak from another CH_2 group, the triplet at 1.17 ppm was quite distinctive. Integration of the peak area gave a ratio consistent with the proposed structure. The presence of two additional carbon peaks in the ^{13}C NMR spectrum, compared to that of alkane **4.19**, was evident as well. In all, seven peaks were observed, two of which occurred at chemical shifts characteristic of carborane carbon atoms (75.14 and 61.29 ppm), while another two were in the correct region of the spectrum for those carbon atoms adjacent to the electron withdrawing oxygen atom (68.78 and 66.29 ppm). The ^{11}B NMR spectrum showed a number of peaks ranging between -2.49 ppm and -13.41 ppm, which is consistent with that expected for a *closo*, mono-substituted, *ortho*-carborane cage. Chemical ionization mass spectrometry further confirmed the nature of the product. The spectrum showed a peak corresponding to the parent ion at 230 m/z (M^+) and at 248 m/z ($\text{M} + \text{NH}_4^+$). Fragmentation of the molecular

ion was also apparent with the observation of a peak at 198 m/z, consistent with the loss of ethoxide.

4.10 Mechanisms for the Formation of 4.19 and 4.20

To the best of our knowledge, the direct reduction of an azide to an alkane under the specified reaction conditions has not been previously reported (Scheme 4.12). The formation of **4.19** is likely the result of the displacement of the triazene intermediate by a hydride from the activated palladium surface. Formation of the ether **4.20** is possibly the result of reaction of the triazene intermediate being with ethanol, present as the reaction solvent. The formation of both side products, in addition to the lack of reactivity of **4.17**, was surprising in light of the successful hydrogenation of the bulkier undecamethylated analogue of **4.17** (1-(1,2-dicarba-closo-undecamethyl-dodecaboran-1-yl)-3-azidopropane), as reported by Hawthorne and co-workers.³⁹

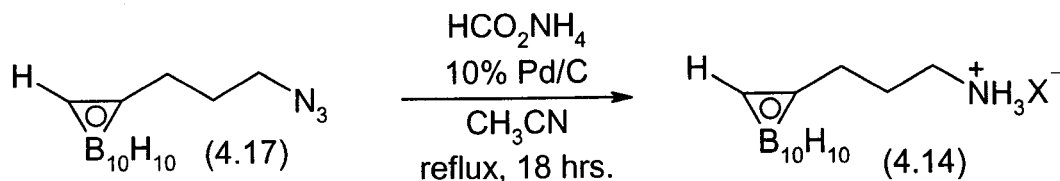


Scheme 4.12 - Proposed mechanism for the formation of 4.19 and 4.20 via hydrogenation.

4.11 Alternative Methods for the Synthesis of 4.14

A method for the reduction of azides directly to the corresponding formamide using Catalytic Transfer Hydrogenation (CTH) has recently been reported.⁴⁰ This method

employs ammonium formate as an *in situ* source of hydrogen gas, and employs an aprotic solvent (acetonitrile), which should eliminate the formation of the ethyl ether **4.20** side product.



Scheme 4.13 – Catalytic Transfer Hydrogenation of **4.17**.

Reaction of the azide **4.17** with ammonium formate, by heating to reflux in the presence of palladium on carbon, gave a mixture of three products. The formamide **4.18** was isolated in 16% yield, while the formyl salt of **4.14** was more abundant at 80%. The alkane side product **4.19** was also formed, but only in 4% yield.

Multi-NMR spectroscopy proved to be crucial for the characterization and differentiation between the formyl and chloride salts of **4.14**. The key difference between the formyl salt of **4.14** and the previously characterized chloride salt is the presence of a singlet at 8.15 ppm in the ^1H NMR spectrum, corresponding to the formate C-H proton. The broad singlets at 5.90 and 3.46 ppm, due to the N-H and carborane C-H protons, respectively, occur at almost exactly the same chemical shifts as exhibited by the chloride salt. Additionally, the presence of a carbonyl peak in the ^{13}C NMR spectrum at 161.63 ppm is indicative of the formate counterion. The ^{11}B NMR spectra of the two salts were virtually indistinguishable.

NMR spectroscopy also proved useful in the characterization of, and differentiation between, the formyl salt **4.14** and the formamide **4.18**. The difference in

chemical shifts of the formyl carbonyl carbon atoms in the two compounds is not significant (161.63 ppm for **4.14**, and 160.59 ppm for **4.18**). The chemical shifts of the carbon atoms alpha to the nitrogen atoms, on the other hand, were quite different,

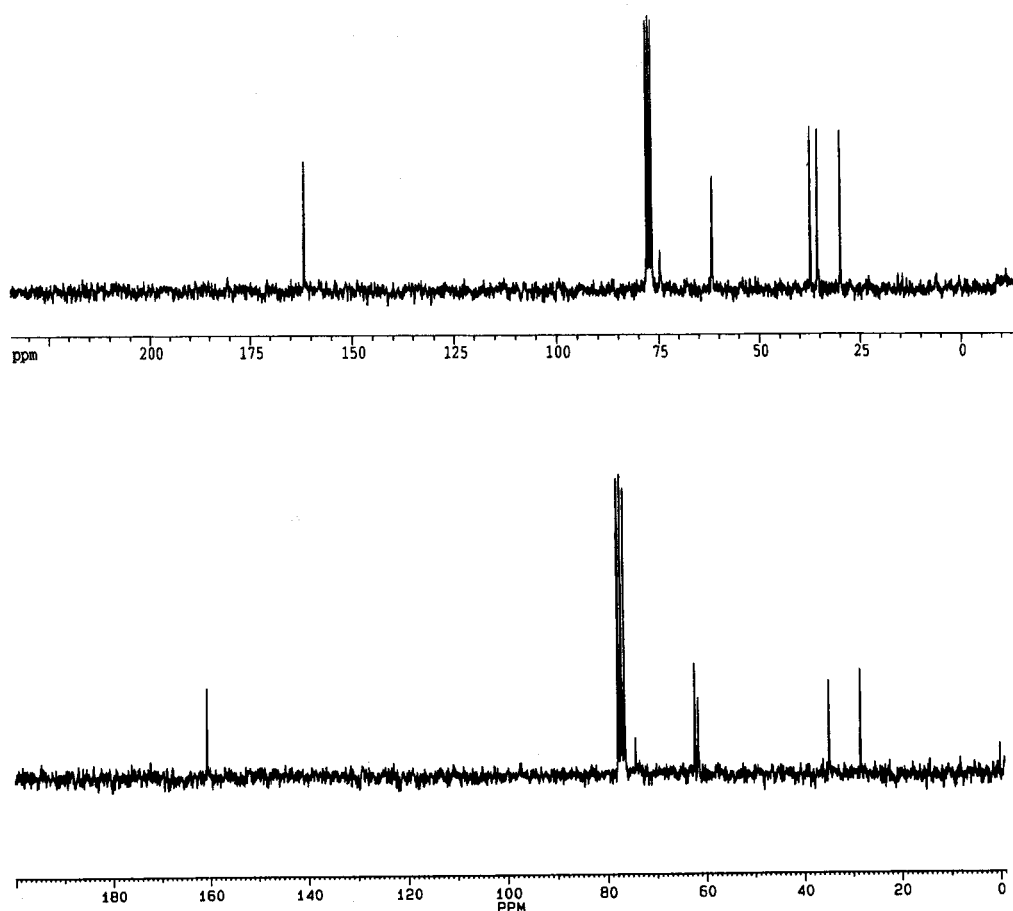


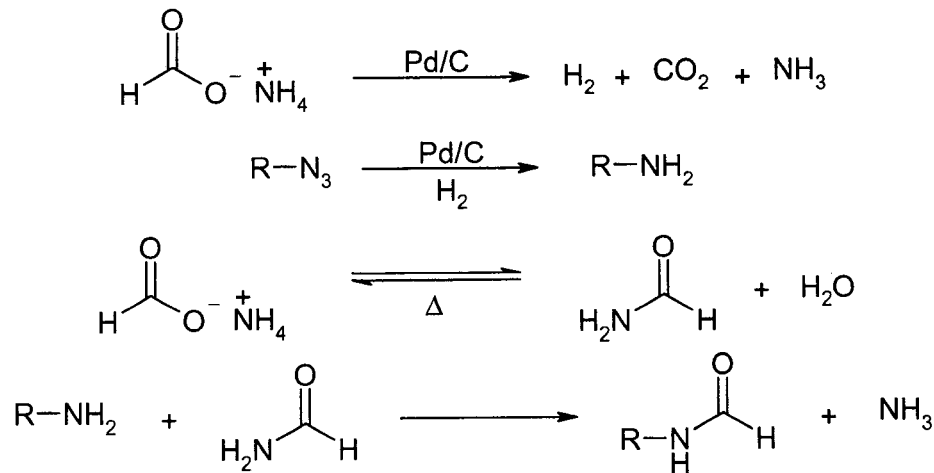
Figure 4.10 - ^{13}C NMR of **4.14** (top) and **4.18** (bottom).

occurring at 37.16 ppm in **4.14** and 62.13 ppm in formamide **4.18**. Deshielding of this carbon atom would be expected in light of the electron withdrawing effect of the neighbouring formyl group. The ^{11}B NMR spectra of **4.18** and **4.14** were only slightly different. However, the presence of *closo*-carborane cages in both compounds was still

apparent with peaks appearing between -2.49 ppm to -13.41 ppm and -1.99 ppm to -12.66 ppm respectively.

Further differentiation between **4.14** and **4.18** was observed in the IR spectra of the two compounds. In particular, a significant shift in the C=O stretching frequency between the formate salt (**4.14**, 1673 cm^{-1}) and the formamide (**4.18**, 1726 cm^{-1}) was observed.

Chemical ionization mass spectrometry of **4.18** supported the structural assignment with a molecular ion at 229 m/z (M^+) and the corresponding $M+18$ ($M+\text{NH}_4$) peak at 246 m/z . Fragmentation of the formyl group was evident with a much smaller mass ion observed at 198 m/z .



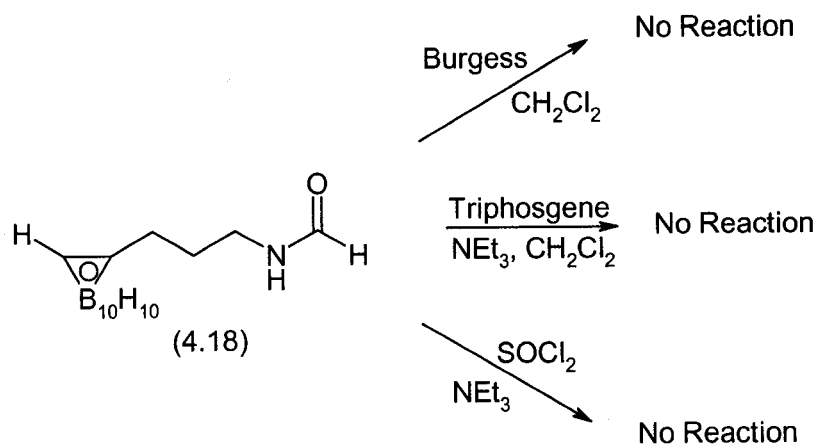
Scheme 4.14 - Proposed mechanism for Catalytic Transfer Hydrogenation.

The mechanism of CTH is thought to involve decomposition of ammonium formate to H_2 and CO_2 in the presence of Pd/C (Scheme 4.14).⁴⁰ Reduction of the carbonyl azide takes place in the presence of the activated Pd/C and the resulting amine then reacts with ammonium formate to generate the formamide.⁴¹⁻⁴⁵

4.12 Attempted Dehydration of the Tethered Formamide 4.18

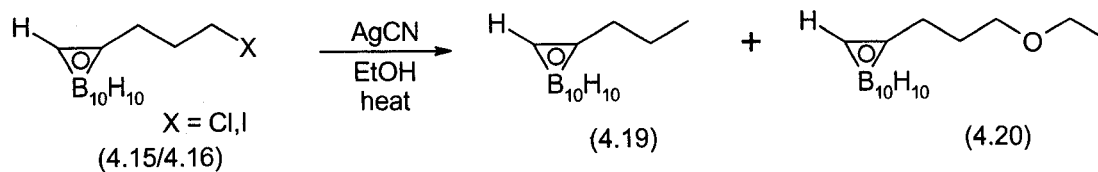
With the formamide **4.18** in hand, we attempted to prepare the corresponding isonitrile. Attempts were made to dehydrate the formamide to the isonitrile following the previously established method utilizing the Burgess Reagent. Much to our surprise, no reaction was observed at room or elevated temperatures. Compound **4.18** was subsequently treated with other dehydrating agents including triphosgene⁴⁶ and thionyl chloride with triethylamine.⁴⁷ In both cases, the main reaction constituent was unreacted starting material.

The poor reactivity of **4.18** may be the result of Newman's Rule of Six,⁴⁸ which simply states that the greater the number of atoms in the sixth position away from the functional group under nucleophilic attack, the greater the steric hindrance to addition. Newman also stated that "...when considering steric factors in a reaction, it is well to emphasize the point that the overall effects are a result of all reagents and participants in the reaction."⁴⁸ For the reaction under consideration, it is conceivable that the bulky carborane cage is partly responsible for the low reactivity of the azide toward the palladium catalyst. However, the heterogeneous hydrogenation catalyst itself could be held accountable. Whether the use of a soluble (homogeneous) catalyst would have an effect on the outcome of the reaction remains to be determined.



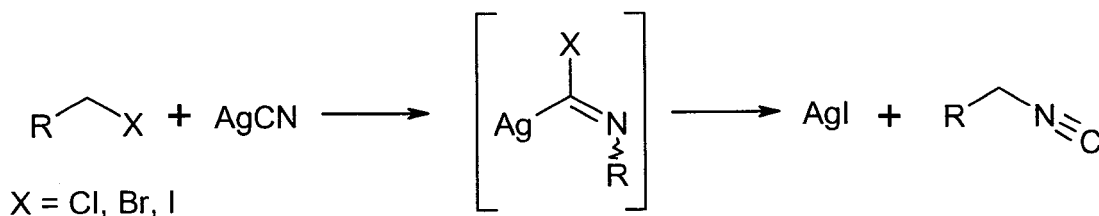
Scheme 4.15 – Attempted dehydration reactions of 4.18.

As an alternative strategy, and as a means to probe the reactivity at the ω -position, generation of the isonitrile was attempted by heating halide **4.15** and silver cyanide in absolute ethanol. Group 11 cyanide salts have traditionally been used to generate isonitriles from their corresponding halide precursors.⁴⁹ Nevertheless, reaction of chloride **4.15** with AgCN was inefficient, and a significant amount of starting material was recovered (Scheme 4.16). Two minor products were also observed, the alkane **4.19** and the ethyl ether **4.20**. None of the desired isonitrile product could be isolated. In order to determine if changing the nature of the halide may enhance the reactivity of the carborane halide, the iodide **4.16** was subjected to the same reaction. In this situation, reaction led almost exclusively to alkane **4.19** and ethyl ether **4.20**. In order to probe the effect of solvent on the formation of the observed products, the reaction was attempted in isopropyl alcohol, *tert*-butyl alcohol and acetone. In other alcoholic solvents, complex mixtures were obtained, while an attempted hydrogenation in acetone yielded only starting material.



Scheme 4.16 – Reaction of 4.15 and 4.16 with AgCN.

The reaction of alkyl halides with silver cyanide is generally accepted as a nucleophilic displacement of the halide by cyanide, using the lone pair formally located on the nitrogen of CN^- .⁵⁰ The metal cation modifies the electron density around the electrophilic carbon atom through interactions with the halide substituent. Alternatively, others have suggested that participation of a species other than CN^- is responsible for isonitrile formation.⁴⁹ Regardless of the true mechanism, it is apparent in our system that the reaction of cyanide or isocyanide nucleophiles is highly disfavored over reaction with the ethanol solvent or a hydride source.⁵¹ The only plausible hydride source in this reaction is the B-H of the polyhedral cage.



Scheme 4.17 – The formation of an intermediate complex with AgCN.

4.13 Summary

Two synthetic strategies for boron- and carbon-substituted carborane-isocyanides were successfully developed. As a result, 3-isocyanocarborane **4.3**, and 1-

methylisocyanocarborane **4.10**, were prepared and fully characterized. Attempts to generate the isonitrile from the corresponding formamide using previously established methods were unsuccessful. However, the boron-substituted carborane-isonitrile was successfully generated from the corresponding formamide **4.2** using a novel methodology employing the Burgess reagent. The C-linked isonitrile **4.10** was generated using a similar procedure to that used for **4.3**, although the desired product was obtained in lower yield.

Unfortunately, attempts to synthesize carbon-linked isonitriles more distal to the carborane cage were not successful. The reactivity of the carboranyl amine **4.14**, containing a longer alkyl tether, was very different from that of the more compact carborane amine **4.8**. Attempts to hydrogenate the azide **4.17** with Pd/C gave complex reaction mixtures containing the alkane **4.19** and ethyl ether **4.20**. Attempts to hydrogenate **4.17** in the presence of formic acid gave the amine **4.14**, and subsequent attempts to derivatize this amine proved to be unsuccessful. Attempts to formylate **4.14**, using both formic acid and the asymmetric anhydride did not yield any of the desired formamide **4.18**, and led only to the isolation of starting material. Alternative methods of hydrogenation were explored (CTH) and were successful in generating the formamide **4.18**. Despite the use of an aprotic solvent, the formation of **4.19** and **4.20** was still observed.

Having successfully isolated some of the formamide **4.18**, its dehydration to the corresponding isonitrile was attempted. Despite numerous attempts with a variety of known dehydrating reagents, none of the desired compound was obtained.

Nonetheless, with the successful generation of two isonitrile derivatives (4.3 and 4.10) the focus of research shifted toward the synthesis of a number of carborane-isonitrile metal complexes. The remainder of this chapter discusses the synthesis and characterization of the proposed model system, which utilizes rhenium as the core metal and 3-isonitrile-*ortho*-carborane as the boron containing ligand. This particular system was selected because analogous isonitrile complexes of ^{99m}Tc are widely used in clinical nuclear medicine, and therefore have some of the intrinsic properties that are needed to construct metal-based BNCT agents. Hence, the goal of this work was to study the coordination chemistry of the carborane-isonitrile ligand in comparison to aliphatic isonitriles as a means of evaluating the suitability of this ligand system for the synthesis of Re / ^{99m}Tc -derived BNCT agents.

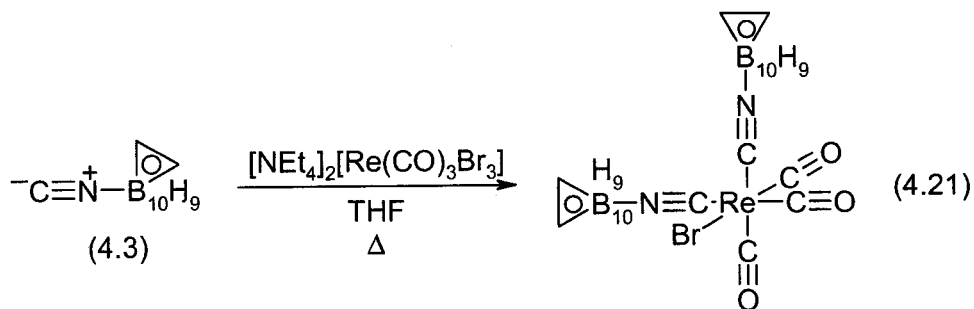
4.14 3-Isonitrile-*ortho*-carborane Complexes of Rhenium(I)

4.14.1 Disubstituted Rhenium(I) Complex

Zakharkin and co-workers investigated the coordination chemistry of 3-isonitrile-1,2-dicarba-*closo*-dodecaborane (4.3) with a variety of metals,⁵² however the extent of characterization of the resulting products was typically limited to elemental analysis and IR spectroscopy. A complex of the general formula $[\text{Re}(\text{CO})_3\text{L}_2\text{Br}]$ was prepared from $\text{Re}(\text{CO})_5\text{Br}$, which is an unsuitable starting material for our purposes because the ^{99m}Tc analogue, which is the isotope to be used for future imaging studies, is not currently available in these forms. We therefore sought to investigate the reaction of 3-

isonitrilecarborane with $[\text{Re}(\text{CO})_3\text{X}_3]^n$ ($\text{X} = \text{Br}$, $n = -2$; $\text{X} = \text{solvent}$, $n = +1$),⁵³ for which the analogous $^{99\text{m}}\text{Tc}$ complexes are readily available and frequently used for labelling biomolecules.⁵⁴⁻⁵⁶

The isonitrile ligand **4.3** was heated with $[\text{NEt}_4]_2[\text{Re}(\text{CO})_3\text{Br}_3]$ in THF overnight (Scheme 4.18), and the resulting complex **4.21** isolated by radial chromatography. While the yield was low (20%), it was still possible to unambiguously characterize **4.21** by ESMS, IR, ^1H , ^{13}C and ^{11}B NMR as well as X-ray crystallography.



Scheme 4.18 – Synthesis of bis-3-isonitrile-ortho-carborane rhenium tricarbonyl (**4.21**).

The IR of compound **4.21** showed a series of CO stretches at 2042, 2004, 1956 cm^{-1} , which are consistent with the expected symmetry of the product. These values are in reasonable agreement with those reported for *fac*- $[\text{Re}(\text{CO})_3(\text{CNMe})_2\text{Br}]$.⁵⁷ The BH stretch is observed at 2602 cm^{-1} , while the CN stretches are within expected values, appearing at 2183 and 2132 cm^{-1} . The negative ion ESMS spectrum of the product exhibited a molecular ion peak at an m/z value of 687.5. Simulation of the spectrum is consistent with the isotopic distribution pattern expected for **4.21**.

A 96 MHz, ^1H decoupled ^{11}B NMR spectrum of **4.21** exhibited resonances at

-1.76, -8.53, -12.22 and -13.29 ppm, which is consistent with the compound containing two *closo*-carborane cages. The ^{13}C NMR spectrum shows two peaks shifted downfield at 183.94 ppm and 181.54 ppm, corresponding to the CO ligands. The ^{13}C NMR spectrum also indicates the presence of the carborane CH groups at 57.47 and 57.23 ppm. Unfortunately, the carbon atoms of the isonitrile ligands functionality to give any peaks in the carbon-NMR spectrum. The ^1H NMR spectrum exhibited a broad peak associated with the BH protons in addition to one other resonance corresponding to the carborane CH proton.

Single crystals of **4.21** were isolated and the studied by X-ray crystallography. The resulting solution is shown in Figure 4.11. In the crystal structure, compound **4.21** was confirmed to have two isonitrile, one bromine, and three CO ligands arranged in the expected facial geometry. Additional peaks in the difference map were modelled as disordered oxygen atoms, most likely the result of THF solvent or water present in the crystal lattice. The average Re-(CO) distance was 1.976(6)Å ranging from 1.958(5)Å to 1.985(6)Å, the shortest being the ligand *trans* to the bromine. The C-O bond distances were 1.088(5)Å, 1.134(5)Å and 1.132(6)Å, while the bromine-metal distance, 2.6351(6)Å, is in the upper portion of the accepted Re-Br bond length of 2.606(39)Å.⁵⁸ This increase in bond length between the rhenium and bromine atoms clearly demonstrates the strong *trans* influence of the opposing CO ligand. The Re-CNR bond distances were similar (2.075(5)Å and 2.063(5)Å) and only slightly shorter than the corresponding distances in $\text{Tc}(\text{CO})_3(\text{CN}^t\text{Bu})_2\text{Cl}$.⁵³ The $\text{C}\equiv\text{N}$ bond distances were 1.164(6)Å and 1.161(6)Å and very

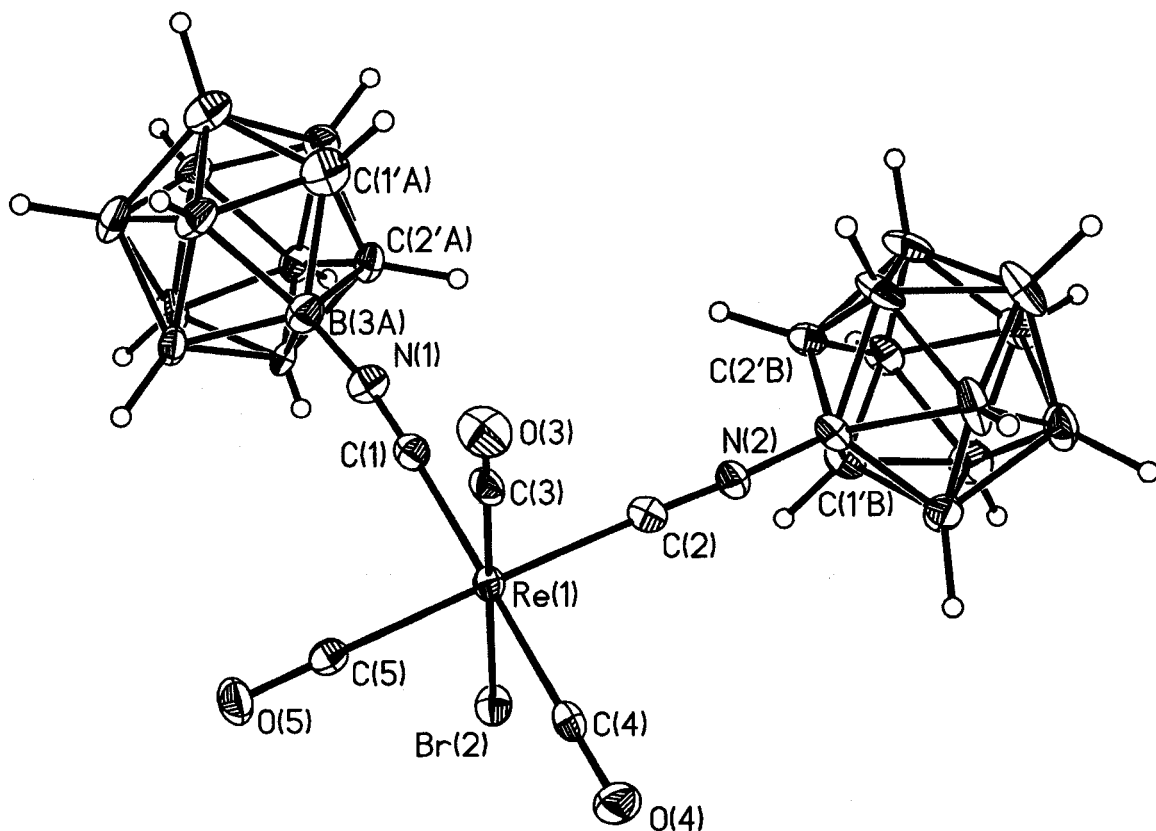


Figure 4.11 – ORTEP representation of 4.21. Thermal ellipsoids shown at 30% probability level.

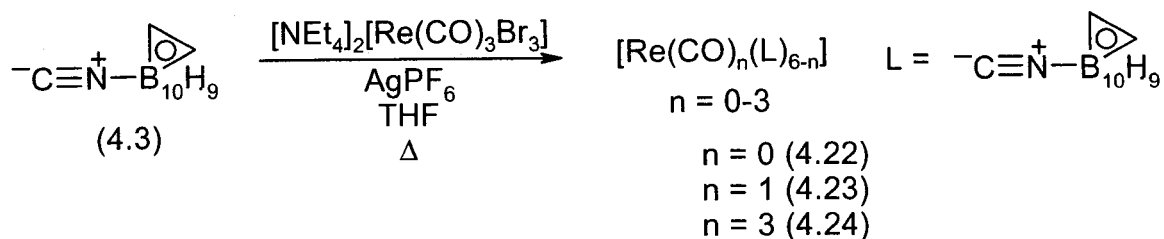
similar to those of the free ligand ($1.157(4)\text{\AA}$)³⁵ indicating little π -back donation from the metal to the isonitrile ligand. The N(1)-C(1)-Re(1) and N(2)-C(2)-Re(1) bond angles were nearly linear ($178.1(5)^\circ$ and $177.0(4)^\circ$ respectively). In addition, the distances between the nitrogen of the isonitrile and the boron atom of the carborane were very similar to the same distance for the free ligand.

The dimensions of the carborane icosahedra are similar to those reported for other structures. Both cages exhibited an average boron-boron bond length of $1.767(9)\text{\AA}$ and boron-carbon bond lengths of $1.705(8)\text{\AA}$. The carbon atoms of the cage were readily

identified by the shorter bond length (1.647(7) Å) between these atoms compared to all other distances between atoms in the cage.

4.14.2 Trisubstituted Rhenium(I) Complexes

Alberto and co-workers demonstrated that it is possible to bind three isocyanides to the $[\text{Re}(\text{CO})_3]^+$ core by first replacing the halide ligands of $[\text{Re}(\text{CO})_3\text{Br}_3]^{2-}$ with solvent molecules.⁵⁹ Using a similar method, $[\text{NEt}_4]_2[\text{Re}(\text{CO})_3\text{Br}_3]$ was pre-treated with AgPF_6 in THF to replace the halide substituents, followed by the introduction of the isocyanide **4.3** (Scheme 4.19). The reaction was heated to reflux overnight giving a complex mixture of products, which were subsequently separated and isolated by radial chromatography.



Scheme 4.19 – Synthesis of tris-, tetrakis-, and hexakis-3-isocyanide-ortho-carborane rhenium carbonyl complexes.

The main reaction product was the trisubstituted metal complex, compound **4.22**, which is consistent with the observations reported by Alberto.⁵⁹ The ESMS of **4.22** showed a molecular ion at an $m/z = 792.3$ having a ReB_{30} isotopic distribution pattern. The IR spectrum showed ν_{CN} and ν_{CO} stretches at 2178 cm^{-1} , 2122 cm^{-1} , 2098 cm^{-1} , 2038 cm^{-1} , 2007 cm^{-1} , and 1948 cm^{-1} respectively, which are consistent with literature values for analogous alkyl-isocyanide complexes.⁵⁷ The ^{11}B NMR spectrum of **4.22**, having peaks

at -2.45 , -3.69 , -7.37 , -9.76 , and -13.56 ppm, indicated that all cages were *closo* (Figure 4.12).

Single crystals of **4.22** were isolated and the structure determined by X-ray crystallography (Figure 4.12). This complex crystallized in the highly symmetrical rhombohedral $R\bar{3}m$ space group ($Z = 3$). The Re-(CO) distance in **4.22** was $2.01(2)\text{\AA}$ which is slightly longer than the corresponding distance in $[\text{Tc}(\text{CO})_3(\text{CNtBu})_3][\text{NO}_3]$.⁵⁹ The Re-CNR distance is $2.08(2)\text{\AA}$ while the $\text{C}\equiv\text{N}$ distance is $1.19(2)\text{\AA}$, which is similar to the same distance in **4.22**, within experimental error. The distance between the isonitrile nitrogen atom and the carborane cage is $1.451(19)\text{\AA}$ while the ligands themselves project in a near linear fashion from the rhenium center (C(1)-N(1)-B(3): $173.4(18)^\circ$, C(2)-Re(1)-C(1): $178.6(11)^\circ$).

Upon refinement it was noted that the thermal occupancy for atom B(6) appeared to deviate from the accepted value for boron. This suggests either an incorrect atomic assignment, or that one of the three carborane cages underwent degradation to the *nido* product during recrystallization. The presence of a *nido* cage explains the absence of a counter-ion in the lattice as the complex would possess an overall neutral charge. When the degree of occupancy was given a free variable, it converged to 66% upon least-squares refinement. Similar treatment of other non-restrained atoms B(7), B(8) and B(12), confirmed complete (100%) occupancy at these sites. Thus, it was determined that only $2/3$ of a boron atom was present at the B(6) position and, given the symmetry of the

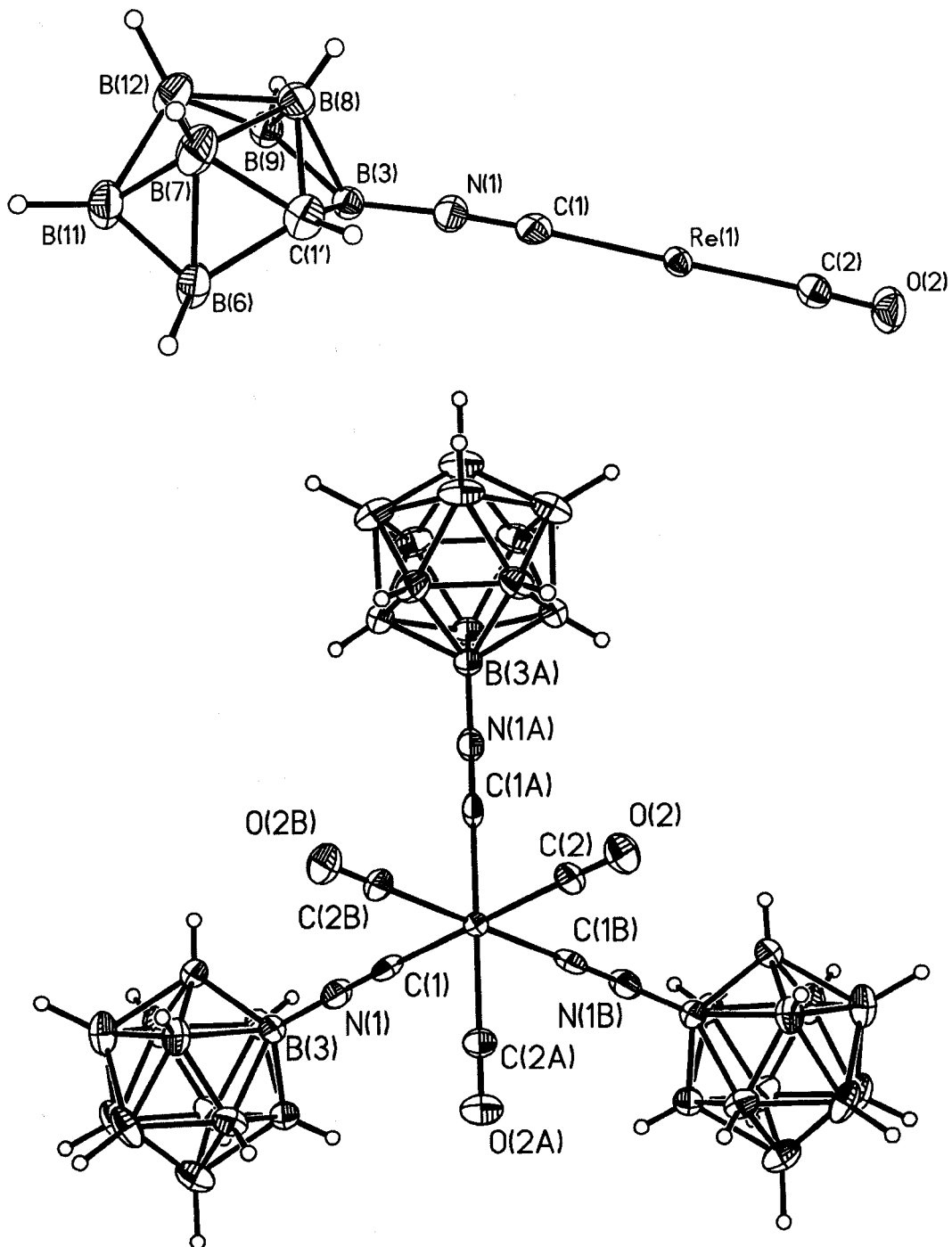


Figure 4.12 - ORTEP representations of actual and symmetry generated solutions of 4.22. Thermal ellipsoids are shown at the 30% probability level.

system, is consistent with degradation of one cage to the *nido* species. The initial solution appeared to contain three *closo* cages, a result of the delocalization of the missing vertex over all three icosahedra. Since the *nido* cage was disordered evenly over three possible orientations, it seems that the presence of an open-faced cage did not influence the overall packing mode of the complex in the crystal lattice.

The ^{11}B NMR spectrum of **4.22** obtained after isolation clearly indicates that all three carborane cages are *closo* (Figure 4.13). However, the ^{11}B spectrum of the recrystallized material shows a substantially more complicated pattern; clearly indicating that at least one of the clusters was converted to the *nido*-carborane during the crystallization process. The conversion of dicarba-*closo*-dodecaboranes to the corresponding *nido*-carboranes is typically brought about through the use of strong bases such as alkoxides,⁶⁰ amines,^{61,62} or fluoride ion.⁶³ There have been reports of seemingly spontaneous cage degradation reactions under very mild conditions,⁶⁴ however, the same reaction for carboranes substituted at the 3-position have not, to the best of our knowledge, been previously reported. It is clear that coordination of the metal influences the compound to convert to the *nido*-cluster under mild conditions. The free ligand does not readily convert to the *nido*-carborane and is stable in solution for prolonged periods of time.

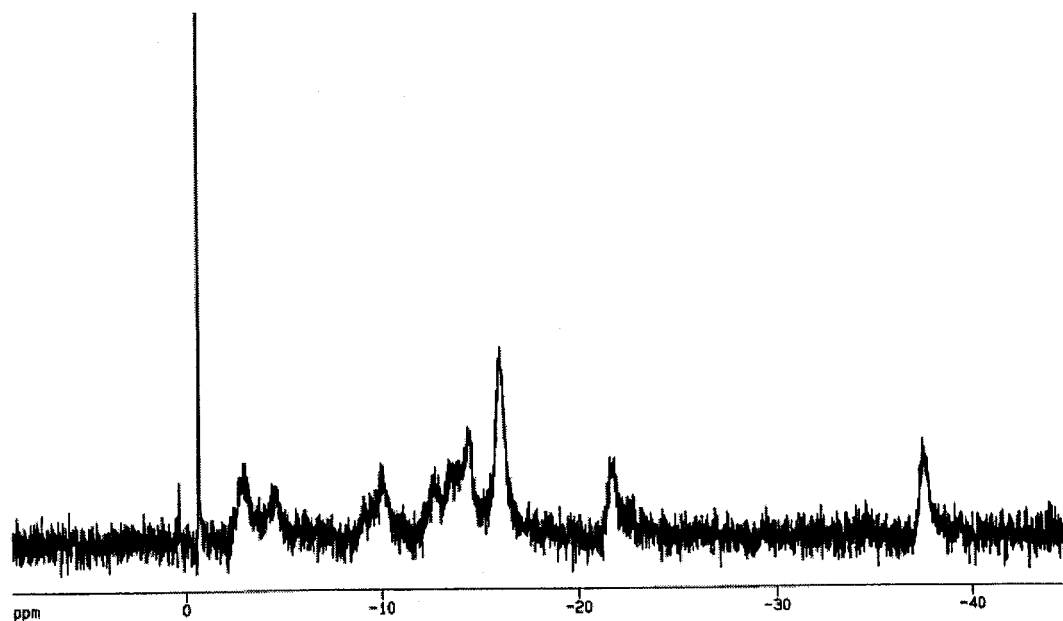
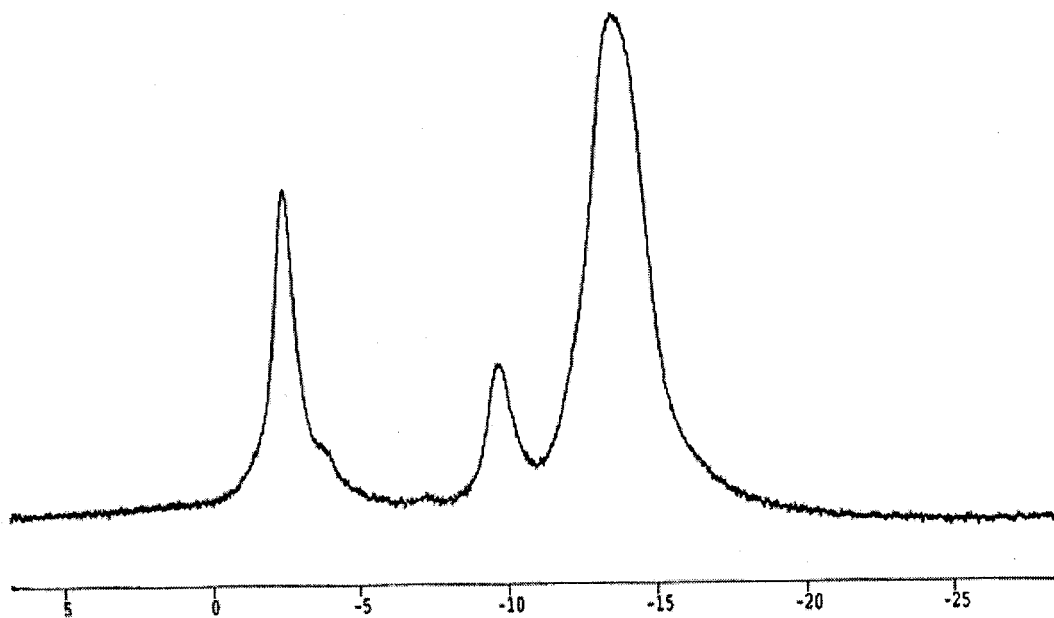


Figure 4.13- $^{11}\text{B}\{^1\text{H}\}$ NMR of 4.22 before (above) and after (below) crystallization.

4.14.3 Tetrasubstituted Rhenium(I) Complex

During the reaction of **4.3** with $[\text{Re}(\text{CO})_3(\text{solvent})_3]^+$ an additional product was isolated from the reaction mixture. The ESMS spectrum of the product showed an m/z value of 919.7, which is consistent with a product having the formula $[\text{Re}(\text{CO})_2(\text{CNR})_4]^+$ (**4.23**) (R = 3-ortho-carborane) (Figure 4.14). The observed isotopic distribution pattern is also consistent with a ReB_{40} composition. The IR spectrum of **4.23** shows peaks at 2604 cm^{-1} (ν_{BH}), 2210 cm^{-1} , 2140 cm^{-1} and 2095 cm^{-1} (ν_{CN}) and 2025 cm^{-1} and 2002 cm^{-1} (ν_{CO}). The pattern observed for the CN and CO stretches suggests that the product is the *cis* isomer.

The ^1H NMR spectrum of **4.23** showed all four carborane CH protons overlapped in a broad peak at 4.49 ppm. The undulating baseling between 1 and 4 ppm was indicative of the B-H protons in the cages of the complex. The ^{13}C NMR spectrum exhibited one peak at 171.65 ppm from the carbonyl ligands, and four distinct resonances at 64.95, 64.38, 63.97 and 62.26 ppm for the carborane C-H groups. There was no observed peak for the isonitrile carbon atoms, which is consistent with the spectra of compounds **4.21** and **4.22**. An ^{11}B NMR spectrum of **4.23** showed that all *ortho*-carborane cages maintained a *closo* geometry, with peaks ranging between -2.12 ppm and -13.27 ppm.

The substitution of a CO ligand directly from the $[\text{Re}(\text{CO})_3]^+$ core is not typically observed when using simple isonitrile ligands and relatively mild reaction conditions. It has been reported however that $[\text{Re}(\text{CO})_2(\text{CNtol})_4][\text{PF}_6]$ can be prepared from $\text{Re}(\text{CO})_3(\text{CNtol})_2\text{Br}$ under relatively benign reaction conditions.⁵⁷ Unfortunately, despite

numerous attempts, single crystals of **4.23** could not be obtained in order to unambiguously determine its structure.

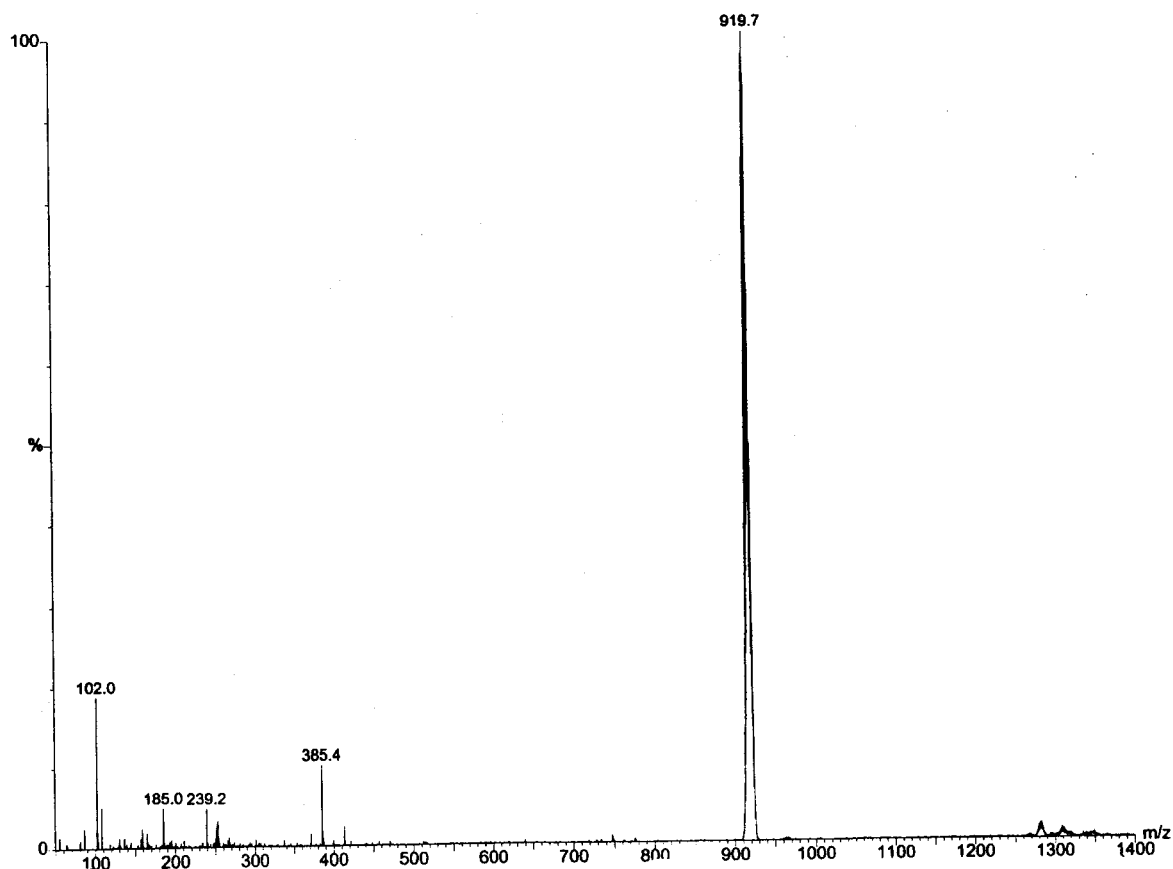


Figure 4.14 - ESMS spectrum of **4.23**.

4.14.4 *ortho*-Carborane Homoleptic-Isonitrile Complexes of Rhenium(I)

The isolation of **4.23** motivated us to examine the ESMS spectrum of the crude reaction mixture in order to determine if there were any other derivatives of the type $[M(CO)_n(L)_{6-n}]$ ($L = 3\text{-isonitrile-}ortho\text{-carborane}$; $n = 0\text{-}3$). Surprisingly, the positive ion ESMS also showed a peak at 1202 m/z having a ReB_{60} isotopic distribution pattern, which is consistent for the formation of the homoleptic derivative $[\text{Re}(\text{CNR})_6]^+$ (**4.24**) (R

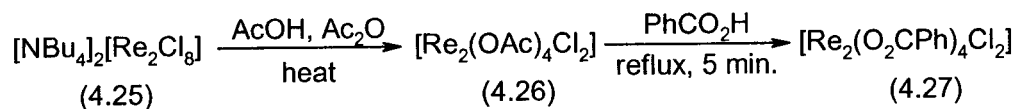
= 3-*ortho*-carborane). Despite repeated efforts, an appreciable quantity of **4.24** could not be isolated, however, the fact that this product was observed in the mass spectrum suggested that it was possible to prepare a Re(I) complex containing six carborane ligands around the metal center. This compound, which is the rhenium-carborane analogue of the homoleptic(isocyanide) technetium complex, prepared nearly 20 years ago,¹³ has 60 boron atoms and would be an attractive platform from which to construct novel visible BNCT and BNCS agents.

In order to prepare an appreciable amount of **4.24**, we combined the ligand **4.3** with the dirhenium species $\text{Re}_2(\text{OAc})_4\text{Cl}_2$. This approach had been used by Allison et al. to prepare hexacoordinate Re(I) aryl and alkyl isonitrile complexes.⁶⁵

The synthesis of **4.24** began by preparing the rhenium(III) starting material, using the method established by Cotton *et al.*^{66,67} $[\text{NBu}_4]_2[\text{Re}_2\text{Cl}_8]$ (**4.25**) was heated to reflux in freshly distilled glacial acetic acid and acetic anhydride for 1 hour yielding the red product $[\text{Re}_2(\text{OAc})_4\text{Cl}_2]$ (**4.26**) in 85% yield (Scheme 4.20).

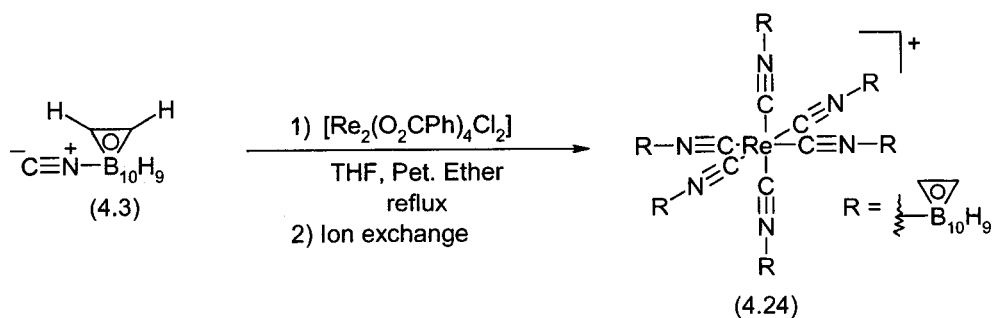
Reaction of the tetracarboxylato-dirhenium complex **4.26** with an excess (8.5 equiv.) of 3-isonitrile-1,2-dicarba-*closo*-dodecaborane (**4.3**) in dry ethyl ether or THF resulted in a poor yield of the homoleptic rhenium isonitrile complex (**4.24**, < 1%, Scheme 4.17). Thinking that the apparent lack of reactivity was a direct result of the poor solubility of the rhenium starting material in organic solvents, **4.26** was converted to the more soluble benzyl tetracarboxylato complex (**4.27**) by heating the tetraacetate at reflux in a benzoic acid melt for five minutes.⁶⁶ Isolation of **4.27** proved to be problematic, as the higher carboxylates are known to be more sensitive toward oxidation. Despite this,

4.27 was isolated by filtration from a cold and degassed solution of CHCl_3 and used promptly thereafter.



Scheme 4.20 – Preparation of $\text{Re}_2(\text{O}_2\text{CR})_4\text{Cl}_2$ ($R = \text{Me, Ph}$) precursors.

Reaction of **4.27** with excess 3-isonitrile-1,2-dicarba-*closo*-dodecaborane gave the desired hexacoordinate rhenium(I) complex **4.24** in 10% isolated yield following ion exchange and precipitation from a 1:1 solution of THF and deionized water (Scheme 4.21).



Scheme 4.21 - Synthesis of the homoleptic $\text{Re}(\text{I})$ isonitrile complex **4.24**.

Compound **4.24** exhibited relatively simple ^1H , ^{13}C and ^{11}B NMR spectra (Figure 4.15), with only one major proton and carbon peak present at 5.10 ppm and 59.20 ppm respectively. The low intensity peaks present at 5.25 and 4.90 ppm in the ^1H NMR are believed to be a result of perturbations in the octahedral structure, thereby eliminating magnetic equivalence between the six cage CH protons. As expected, the isonitrile carbon atoms were not observed in the ^{13}C NMR spectrum. The proton-decoupled ^{11}B NMR spectrum indicated that all carborane cages were *closo*, with peaks appearing at -1.99, -8.06, and -11.66 ppm.

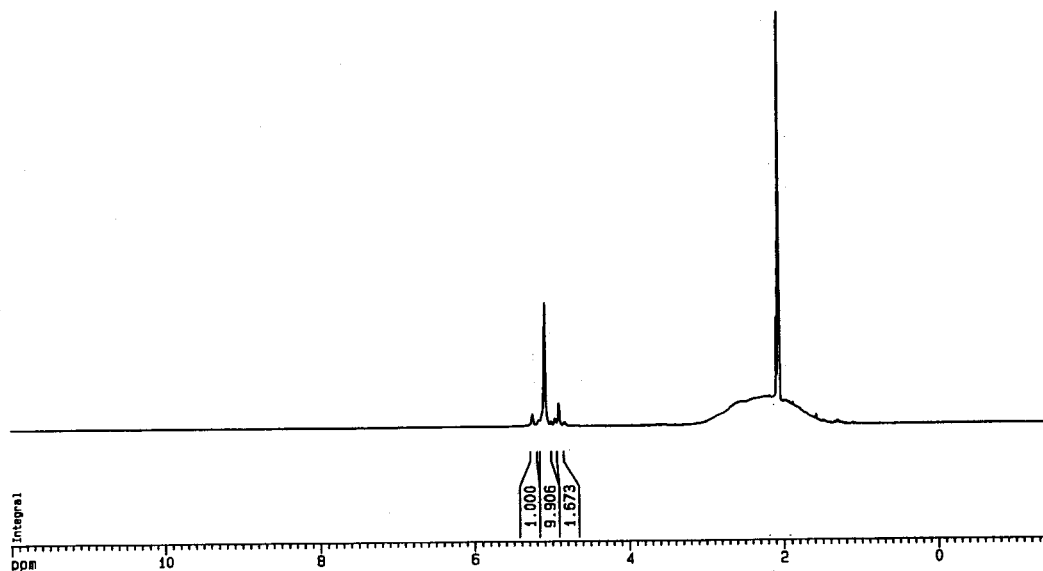


Figure 4.15 - ^1H NMR spectrum of 4.24.

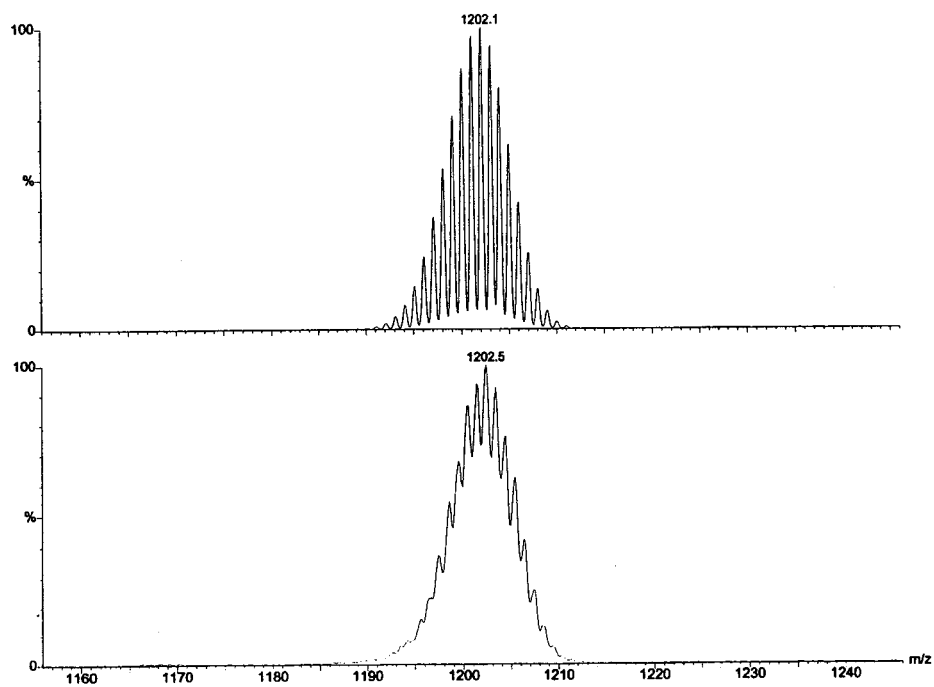


Figure 4.16 - theoretical (top) and experimental (bottom) ESMS spectra of 4.24.

In addition to low resolution mass spectrometry (Figure 4.16), high resolution mass spectrometry (HRMS) was performed in order to confirm the molecular formula. High resolution FAB mass spectrometry exhibited a peak at 1202.087 m/z, which is in excellent agreement with the mass calculated for $[C_{18}H_{66}B_{60}N_6Re]$ (1202.091 m/z). Despite repeated attempts with different counter ions and recrystallization conditions, single crystals of **4.24** could not be formed.

The mechanism by which isonitriles react with **4.26** or **4.27** is not completely understood. Much work has been done to determine this mechanism by analyzing the reactivity of the isoelectronic molybdenum and ruthenium analogues with varying numbers of equivalents of the isonitrile ligand. Mononuclear complex formation proceeds by one of two possible pathways, either by the dissociation of an axial bound chloride ligand, or through the attack of the incoming isonitrile at an equatorial position with resulting opening of the carboxylate bridge (Scheme 4.22).⁶⁷ Due to the inherent steric bulk associated with the carborane cage, it is likely that axial coordination is favourable. Metal-metal bond rupture in the dirhenium and dimolybdenum complexes is facilitated by the binding of π -acceptor ligands (Figure 4.17). The bonding d- π orbitals of $Re_2(OAc)_4Cl_2$, upon coordination of good π -acceptor ligands such as isonitriles, results in weakening of the metal-metal bonds. Reduction in metal-metal bond strength ultimately leads to the desired mononuclear product.

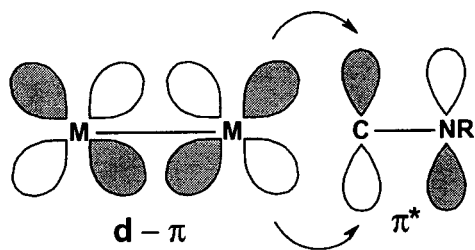
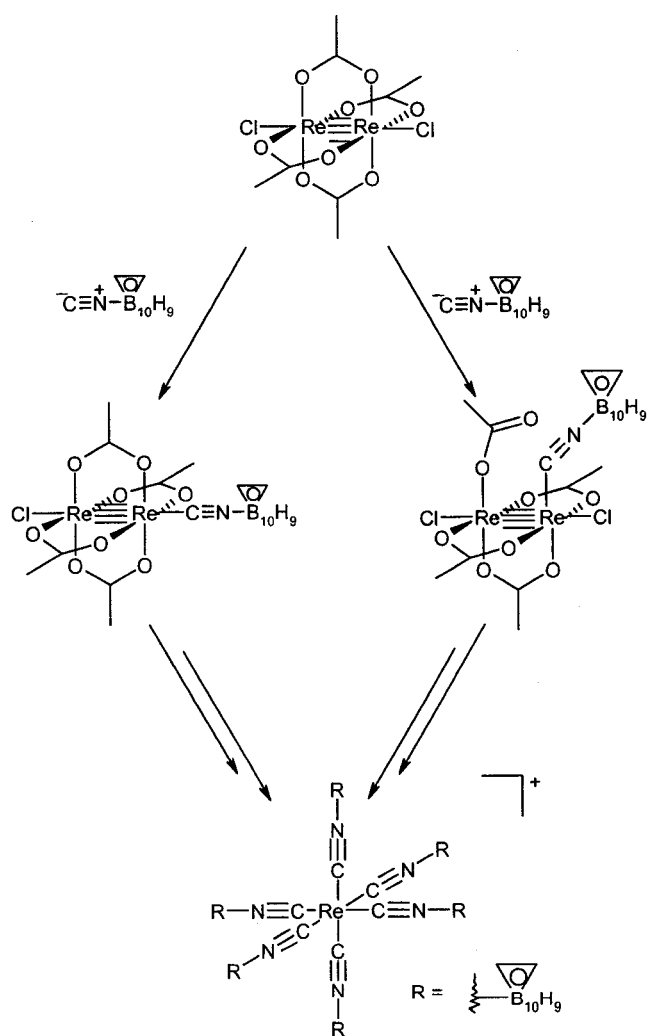


Figure 4.17 - Re-Re bonding orbital interaction with the LUMO of an isonitrile.

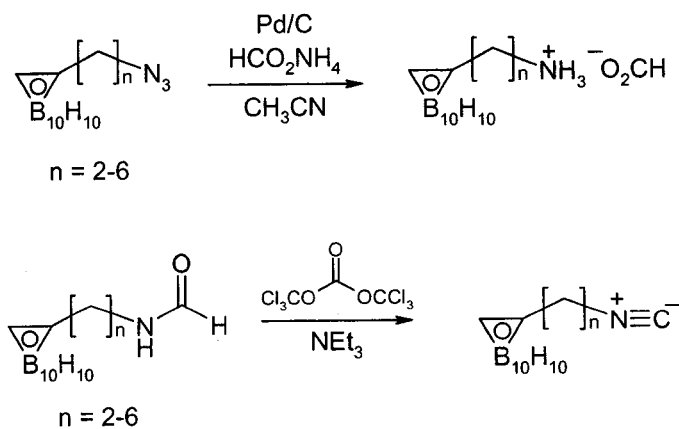


Scheme 4.22 – Proposed routes for the formation of 4.24.

4.15 Summary and Future Work

A method for the synthesis of two novel carborane-isonitrile ligands, compounds **4.3** and **4.10**, was developed. Compound **4.3** was isolated in reasonable yield by dehydrating the formamide precursor with the Burgess reagent. Unfortunately, this reaction was also accompanied by the formation of the isocyanate **4.4**, which arises as a result of the electron accepting property of the *ortho*-carborane cage in **4.2**. This was circumvented by using a different dehydration technique, in which the formamide was reacted with BOP-Cl in a basic solution. However, the different reaction conditions were accompanied by increased reaction times and lower yields of the desired product.

Due to the surprising lack of reactivity of the 3-aminopropyl-1,2-dicarba-*closo*-dodecaborane **4.14** and the corresponding formamide **4.18** with electrophilic reagents, additional work is required to generate isonitrile ligands having longer spacer groups. One approach to probing the role of Newman's Rule of Six in the poor reactivity of compound **4.18** would be to synthesize a series of tethered



Scheme 4.23 - Proposed probes to determine the reactivity of pendant amino and formyl groups.

formamides (Scheme 4.23) and then determine the relative reactivity of each toward various dehydrating reagents.

Despite the difficulties encountered, a new and efficient method for the synthesis of 3-amino-1-(1,2-dicarba-*closo*-dodecaboran-1-yl)propane, through the reduction of the corresponding azide, using catalytic transfer hydrogenation (CTH), was developed. This methodology was discovered through product studies of more conventional hydrogenation methods. Efforts are currently underway to expand the applicability of the methodology while also evaluating the procedure for the synthesis of more highly functionalized amino alkylcarboranes.

With the successful synthesis of 3-isonitrile-*ortho*-carborane **4.3**, the coordination chemistry of the ligand was investigated. Compound **4.3** and $[\text{NEt}_4]_2[\text{Re}(\text{CO})_3\text{Br}_3]$ were combined, resulting in compounds of the general formulae $\text{Re}(\text{CO})_3\text{L}_2\text{Br}$, $[\text{Re}(\text{CO})_3\text{L}_3]^+$ and $[\text{Re}(\text{CO})_3\text{L}_2\text{L}']$ ($\text{L} = 3\text{-isonitrile-ortho-carborane}$, $\text{L}' = 3\text{-isonitrile-nido-carborane}$). Two of these compounds were characterized by X-ray crystallography. In addition, the isolation of **4.23** and **4.24** from this same reaction mixture indicates that compound **4.3** has the unique ability to displace CO ligands from $[\text{Re}(\text{CO})_3(\text{solvent})_3]^+$, which led to the formation of $[\text{Re}(\text{CO})_2\text{L}_4]^+$ and $[\text{ReL}_6]^+$.

The detection of **4.24** from the reaction between the ligand **4.3** and the $[\text{Re}(\text{CO})_3]^+$ intermediate, prompted the synthesis of the homoleptic complex using other methods. Allison et al. reported the synthesis of homoleptic complexes $\text{Re}(\text{I})$ from $\text{Re}_2(\text{O}_2\text{CPh})_4\text{Cl}_2$ as a source of $\text{Re}(\text{I})$. An analogous reaction with our ligand was successful in generating the target complex, albeit in poor yield. While $\text{Re}_2(\text{O}_2\text{CPh})_4\text{Cl}_2$ and other reported ReL_6

(L = isonitrile) precursors (KReI_6 or $\text{Re}(\text{CO})_5\text{X}$ (X=Br,Cl))^{57,68} are not suitable starting materials for use in radiopharmaceutical development as their $^{99\text{m}}\text{Tc}$ counterparts are not readily available, their use was necessary to synthesize and fully characterize the rhenium(I) analogues of the target technetium complex. Synthesis of the TcL_6 (L = isonitrile) analogues can be attempted using the method established by Abrams et al.¹³

With the successful generation of the $[\text{ReL}_6]^+$ (L= 3-isonitrile-*ortho*-carborane) complex, the next step in this research would be to synthesize the technetium analogue and to then evaluate the biodistribution in animal models. This research will require the development of a strategy to prepare the homoleptic technetium(I) complex in water.

4.16 Experimental

Synthesis of 3-amino-1,2-dicarba-*closo*-dodecaborane (4.1)

Ammonia (20 mL) was condensed into a flask containing *ortho*-carborane (1.0 g, 6.93 mmol) cooled to -50°C under nitrogen. Freshly pressed sodium metal (0.64 g, 27.73 mmol) was added in small portions, forming wisps of blue solution that quickly disappeared eventually taking to a blue coloured solution. The reaction was maintained at -50°C for two hours at which time the condenser was removed and oven dried cuprous chloride (4.73 g, 35.52 mmol) was added in small portions to the liquid ammonia solution. The cold bath was removed and the liquid ammonia allowed to evaporate leaving a blue slurry. Distilled water (20 mL) then toluene (20 mL) was carefully added to the reaction vessel, turning the reaction mixture brown/blue. The mixture was transferred to a separatory funnel and the aqueous layer extracted with toluene (3 x 25 mL). All organic fractions were pooled, dried over sodium sulfate and filtered giving a clear colourless filtrate. The solvent was removed by rotary evaporation giving an oily semi-solid. The crude product was purified by silica gel chromatography with 40% ether in hexanes as the eluent. The product (0.623 g, 56%) showed: mp 220°C ; TLC: (100% CH_2Cl_2) R_f 0.40; ^1H NMR (200 MHz, CDCl_3): δ 4.00-0.60 (br m, 9H, BH), 3.57 (br s, 2H, CH), 1.43 (br s, 2H, NH_2); ^{13}C NMR (50 MHz, CDCl_3): δ 57.98; ^{11}B NMR (96 MHz, CDCl_3): δ 0.14, -4.80, -10.10, -15.23, -15.84, -19.14; IR (CHCl_3 , cm^{-1}): 3421, 3078, 3020, 2603; MS (ES, positive): m/z observed boron isotopic distribution at 160 (M^+).

Synthesis of 3-formyl-1,2-dicarba-*closo*-dodecaborane (4.2)

Method A: Compound **4.1** (0.500 g, 3.13 mmol) was dissolved in formic acid under nitrogen and the solution brought to reflux for 4 h. The solvent was removed by rotary evaporation and the resulting solid dissolved in ether (30 mL) and extracted with NaHCO₃ (2 x 10 mL). The aqueous fractions were combined and extracted with ether (25 mL). All organic fractions were pooled, dried over sodium sulfate and filtered. The solvent was removed by rotary evaporation and the crude product was purified by silica gel chromatography with 20% hexanes in dichloromethane as the eluent. Slow evaporation of an acetone solution produced X-ray quality single crystals. The product, compound **4.2** (0.435 g, 74%), showed: mp 147-148°C; TLC (5% MeOH in CH₂Cl₂): R_f 0.37; ¹H NMR (200 MHz, CDCl₃): δ 8.27 (s, 1H, CHO), 5.79 (br s, 1H, NH), 4.44 (s, 1H, CH), 3.90-0.60 (br m, 9H, BH); ¹³C NMR (50 MHz, CDCl₃): δ 164.95, 55.11; ¹¹B NMR (96 MHz, CDCl₃): δ -4.49, -7.92, -11.21, -13.18, -15.08; IR (CH₂Cl₂, cm⁻¹): 3300, 3058, 2989, 2901, 2602, 1693; MS (CI, NH₃): m/z observed boron isotopic distribution at 186 m/z (M⁺). X-ray Crystallography: Space group: Pna2₁, a = 15.892(3) Å, b = 7.0124(14) Å, c = 9.3974(4) Å, α = β = γ = 90°, V = 1047.3(4) Å³, Z = 4, data/parameters: 2167/189, R = 0.0488, R_w = 0.1079, GOF = 0.881.

Method B⁶⁹: Formic acid (1.42 mL, 1.73 g, 37.68 mmol) and acetic anhydride (1.91 mL, 2.07 g, 20.26 mmol) were combined dropwise at 0°C. Pyridine (1.17 mL, 1.15 g, 14.52 mmol) was added over 5 minutes to the cold mixture, followed by the amine (0.100 g,

0.628 mmol) in dry acetonitrile (~1 mL). The reaction was maintained for 4 hours while warming to room temperature. The excess anhydride and pyridine were removed by rotary evaporation leaving a yellow oil. The crude product was taken up in distilled water (25 mL) and acidified with 5 drops of conc. HCl. The aqueous layer was extracted with dichloromethane (3 x 15 mL) and the organic fractions combined and further washed with 0.1N HCl (2 x 25 mL). The organic layer was collected, dried over sodium sulfate and gravity filtered. Excess solvent was removed *in vacuo* giving a white solid, which was purified by flash silica gel chromatography with 20% hexanes in dichloromethane as the eluent. The product, compound **4.2** was isolated as a white solid (71 mg, 60%)

Synthesis of 3-isonitrile-1,2-dicarba-*closo*-dodecaborane (4.3)⁷⁰

Method A: The formamide **4.2** (0.422 g, 2.25 mmol) and Burgess reagent (1.07 g, 4.50 mmol) were combined in dry methylene chloride (30 mL). The homogeneous reaction mixture was maintained at ambient temperature under dry nitrogen for 5 hours, at which time TLC indicated the complete consumption of starting material. The reaction mixture was quenched and subsequently washed with distilled water (2 x 25 mL). The aqueous layers were combined and further extracted with CH₂Cl₂ (1 x 25 mL) and ether (1 x 25 mL). All organic fractions were pooled, dried over sodium sulfate and gravity filtered. The clear colourless filtrate was concentrated *in vacuo* and the crude product purified by flash silica gel chromatography with 25% CH₂Cl₂ in hexanes as the eluent. Single crystals were obtained by slow evaporation of an ethanol solution at -10°C. The product, compound **4.3** (0.191 g, 51%), a white solid showed: mp 136°C (decomp.); TLC: (5%

MeOH in CH₂Cl₂) R_f 0.51; ¹H NMR (200 MHz, CDCl₃): δ 3.90-0.80 (br m, 9H, BH), 3.88 (br s, 2H, CH); ¹³C NMR (150 MHz, CDCl₃): δ 181.83, 59.70; ¹¹B NMR (160 MHz, acetone-*d*₆): δ -3.05, -9.43, -12.60, -13.39, -13.87; IR (CH₂Cl₂, cm⁻¹): 3053, 2622, 2606, 2139; MS (EI): m/z observed boron isotopic distribution at 184 m/z (M+16). X-ray Crystallography: Space group: P2₁/n, a = 6.8607(14) Å, b = 12.298(3) Å, c = 11.582(2) Å, α = γ = 90°, β = 90.40(3)°, V = 977.2(3) Å³, Z = 4, data/parameters: 2234/172, R = 0.0847, R_w = 0.1912, GOF = 0.987.

Method B: The formamide (0.100 g, 0.534 mmol) **4.2** was added to BOP-Cl (0.149 g, 0.587 mmol) and triethylamine (0.163 mL, 0.119 g, 1.17 mmol) in dry methylene chloride (5 mL). The reaction was maintained at ambient temperature at which point additional BOP-Cl (0.149 g, 0.587 mmol) and triethylamine (0.163 mL, 0.119 g, 1.17 mmol) were added. After continuing the reaction for an additional 24 hours, the solvent was removed by rotary evaporation, and the resulting off-white solid was purified by silica gel chromatography with 25% CH₂Cl₂ in hexanes as the eluent giving pure **4.3** (0.044 g, 49%).

Synthesis of propargyl phthalimide (**4.5**)

Potassium phthalimide (7.0 g, 37.79 mmol) and potassium iodide (0.202 g, 1.21 mmol) were combined in dry, degassed DMF (25 mL). Propargyl bromide (6.01 g, 7.51 mL, 50.53 mmol) was added dropwise to the stirring heterogeneous reaction mixture. The reaction was heated to 80°C for 4 h at which time the heat source was removed and the

apparatus allowed to cool to room temperature. Distilled water (25 mL) was added and the aqueous layer extracted with 1:1 EtOAc:Hexanes (3 x 50 mL). The organic fractions were pooled and gravity filtered. The filtrate was treated with anhydrous sodium sulfate. After filtering, the filtrate was concentrated by rotary evaporation giving a yellow oil, which solidified over time. The crude product was purified by silica gel chromatography using 1:1 CH₂Cl₂:Hexanes as the eluent. Subsequent recrystallization was performed using CH₂Cl₂ giving pure alkyne (6.53 g, 93%) which showed: mp 233-234°C; TLC (5% MeOH in CH₂Cl₂): R_f 0.69; ¹H NMR (200 MHz, CDCl₃): δ 7.85 (m, 2H, ArH), 7.77 (m, 2H, ArH), 4.46 (br d, 2H, CH₂), 2.26 (t, ³J = 2.0 Hz, 1H, CH); ¹³C NMR (50MHz, CDCl₃): δ 166.81, 134.11, 131.87, 123.45, 77.00, 71.42, 26.88; IR (CHCl₃, cm⁻¹): 3004, 2945, 2060, 1773; MS (EI): m/z 185 (M⁺), 147 (M⁺-CH₂C≡CH).

Synthesis of 1-(Phthalimidomethyl)-1,2-dicarba-*closo*-dodecaborane (4.6)⁴⁴

A solution of the decaborane adduct (B₁₀H₁₂(CH₃CN)₂) (4.71 g, 23.3 mmol) in dry toluene (100 mL) was added to a stirring solution of propargyl phthalimide **4.5** (3.92 g, 21.2 mmol). The reaction was heated to reflux overnight, at which time the heat source was removed and the reaction mixture allowed to cool to room temperature. The solvent was removed by rotary evaporation leaving a yellow solid. The crude product was recrystallized twice from a minimal amount of toluene. The carborane product **4.6** (3.80 g, 60%) showed: mp >250°C; TLC (1:1 ether:hexanes): R_f 0.46; ¹H NMR (200 MHz, CDCl₃): δ 7.86 (m, 4H, ArH), 4.38 (s, 2H, CH₂), 4.00 (br s, 1H, CH), 3.90-0.70 (br m, 10H, BH); ¹³C NMR (50 MHz, CDCl₃): δ 167.13, 134.88, 131.16, 124.12, 73.15, 59.99,

42.47; ^{11}B NMR (96 MHz, CDCl_3): δ -1.39, -5.19, -10.24, -11.86, -13.16; IR (CHCl_3 , cm^{-1}): 3075, 3021, 2598, 1723; MS (EI): m/z 303 (M^+).

1-(((2-(hydroxymethyl)benzoyl)amino)methyl)-1,2-dicarba-closo-dodecaborane (4.7)

Compound **4.6** (3.70 g, 12.2 mmol) was suspended in isopropanol (111 mL) and to it was added sodium borohydride (0.053 g, 1.49 mmol) with distilled water (18.5 mL). The reaction was maintained at ambient temperature overnight at which time TLC indicated the complete consumption of the starting material. Excess solvent was removed by rotary evaporation giving a white solid. The crude product was suspended in CH_2Cl_2 and extracted with distilled water (2 x 50 mL). The aqueous layers were combined and further extracted with methylene chloride (1 x 50 mL) and ether (1 x 50 mL). All organic fractions were pooled, dried over sodium sulfate and gravity filtered. The clear, colourless filtrate was concentrated *in vacuo* and the resulting white solid was recrystallized once from ethanol/water and isolated by suction filtration. The product (2.70 g, 72%) a white solid, showed: mp 190°C; TLC: (40% hexanes in ether) R_f 0.36; ^1H NMR (200 MHz, $\text{DMSO}-d_6$): δ 9.10 (br t, 1H, NH), 7.48 (m, 4H, ArH), 5.29 (br s, 1H, OH), 4.62 (d, $^2J = 7.0$ Hz, 2H, CH_2), 4.03 (d, 2H CH_2), 3.90-0.90 (br m, 10H, BH), 3.35 (br s, 1H, CH); ^{13}C NMR (50 MHz, $\text{DMSO}-d_6$): δ 168.71, 140.82, 133.43, 130.22, 127.48, 127.31, 126.61, 76.16, 61.82, 60.83; ^{11}B NMR (96 MHz, $\text{DMSO}-d_6$): δ -1.19, -2.72, -4.28, -5.83, -8.58, -10.15, -11.65, -12.99; IR (neat, cm^{-1}): 3247, 3092, 3048, 2578, 1632; MS (CI, NH_3): m/z observed boron isotopic distribution at 308 ($\text{M}+\text{H}$).

Synthesis of 1-(Aminomethyl)-1,2-dicarba-*closo*-dodecaborane hydrochloride (4.8)

Compound 4.7 (2.70 g, 8.78 mmol) was dissolved in a mixture of glacial acetic acid (32.4 mL) and concentrated HCl (8.1 mL). To the resulting heterogeneous solution, distilled water (8.1 mL) was added dropwise over 1 min. The reaction was brought to 100°C for 2.5 h, becoming homogeneous upon heating. The solvent was removed *in vacuo* giving a white solid, which was suspended in CHCl₃, stirred for 3 h, filtered and the residue washed with CHCl₃ (2 x 25 mL). The white solid was taken up in acetone and further filtered through a fine pored fritted funnel. The product (1.60 g, 87%) was isolated by recrystallization from ethanol: mp 210°C; ¹H NMR (200 MHz, DMSO-*d*₆): δ 8.86 (s, 3H, NH₃), 3.80 (s, 2H, CH₂), 3.50-0.50 (br m, 10H, BH), 3.51 (br s, 1H, CH); ¹³C NMR (50 MHz, DMSO-*d*₆): 71.17, 63.30, 42.89; ¹¹B NMR (96 MHz, DMSO-*d*₆): δ -1.20, -2.74, -7.98, -9.60, -11.14; IR (neat, cm⁻¹): 2981, 2949, 2587; MS (ES, positive): *m/z* observed boron isotopic distribution at 174 (M⁺).

Synthesis of 1-(N-Formylmethyl)-1,2-dicarba-*closo*-dodecaborane (4.9)

Compound 4.8 (1.50 g, 7.13 mmol) in dry THF (10 mL) was added to formic acid (16.14 mL, 427.7 mmol) and pyridine (2.08 mL, 25.7 mmol) at 0°C. The reaction was allowed to warm slowly to ambient temperature overnight. The remaining solvent was removed by rotary evaporation giving a thick yellow oil, which was taken up in CH₂Cl₂ (50 mL) and washed with distilled water (2 x 50 mL). All aqueous fractions were pooled and further extracted with CH₂Cl₂ (1 x 50 mL). The organic layers were combined, dried over sodium sulfate, gravity filtered and concentrated *in vacuo*. The product, compound

4.9 (1.50 g, 88%), a colourless solid, was purified by silica gel chromatography (gradient: 100% CH₂Cl₂ to 100% MeOH, 10% intervals). mp 210°C; TLC (25% hexanes in ether): R_f 0.16; ¹H NMR (200 MHz, CDCl₃): δ 8.21 (s, 1H, CHO), 6.39 (br s, 1H, NH), 3.97 (d, ³J = 7.2 Hz, 2H, CH₂), 3.91 (br s, 1H, CH), 3.90-0.80 (br m, 10H, BH); ¹³C NMR (50 MHz, CDCl₃): δ 161.74, 74.05, 60.28, 43.18; ¹¹B NMR (96 MHz, CDCl₃): δ -1.95, -5.28, -9.91, -11.45, -12.99; IR (neat, cm⁻¹): 3042, 3019, 2585, 1672; MS (CI, NH₃): m/z observed boron isotopic distribution at 200 (M⁺), 218 (M+NH₄).

Synthesis of 1-(Isonitrilemethyl)-1,2-dicarba-*closo*-dodecaborane (4.10)

The formamide **4.9** (0.149 g, 0.740 mmol) was combined with the Burgess reagent (0.353 g, 1.48 mmol) and the mixture dissolved in dry CH₂Cl₂ (5 mL) containing 4 Å molecular sieves. The reaction was maintained at an ambient temperature under dry nitrogen for 4 h whereupon it was filtered through a fritted glass funnel. The yellow filtrate was concentrated *in vacuo* and the resulting yellow oil which was purified by silica gel chromatography (gradient: 100% hexanes to 40% ether in hexanes, 5% intervals) giving pure **4.10** (0.030 g, 22%); mp 64-65°C; TLC (25% hexanes in ether): R_f 0.59; ¹H NMR (200 MHz, CDCl₃): δ 4.14 (s, 2H, CH₂), 3.88 (br s, 1H, CH), 3.80-0.70 (br m, 10H, BH); IR (neat, cm⁻¹): 2599, 2151.

Synthesis of pentynyl phthalimide (4.11)

Potassium phthalimide (5.0 g, 26.99 mmol) was combined with 5-chloro-1-pentyne (2.88 g, 2.97 mL, 28.07 mmol) in anhydrous, degassed DMF (~50 mL). A

catalytic amount of potassium iodide (0.112 g, 0.675 mmol) was added and the reaction brought to reflux overnight. Upon cooling to room temperature, the reaction was quenched with distilled, de-ionized water (~25 mL) and transferred to a separatory funnel. The DMF was removed by washing the aqueous phase with 1:1 EtOAc:Hexanes (3 x 50 mL). All organic fractions were pooled, dried over Na₂SO₄ and filtered. The filtrate was concentrated in vacuo giving a yellow semi-solid which was purified by flash silica gel chromatography (gradient: 100% hexanes to 30% hexanes in CH₂Cl₂, 5% intervals) to give compound **4.11** (4.76 g, 80 %). mp 86-87.5°C; TLC: (100% CH₂Cl₂): R_f 0.55; ¹H NMR (300 MHz, CDCl₃): δ 7.81 (m, 2H, Ar-H), 7.70 (m, 2H, Ar-H), 3.77 (t, ³J = 7.0 Hz, 2H, CH₂), 2.25 (t o d, 2H, CH₂), 1.91 (m, 3H, overlap CH, CH₂); ¹³C NMR (75 MHz, CDCl₃): δ 168.28, 133.87, 132.11, 123.18, 82.95, 68.97, 37.12, 27.25, 16.24; IR (CH₂Cl₂, cm⁻¹): 3306, 3057, 2987, 2946, 2363, 1774, 1715.

Synthesis of 1-(1,2-dicarba-closo-dodecaboran-1-yl)-phthalimidopropane (4.12)

Decaborane (1.89 g, 15.48 mmol) was added in one portion to a solution of acetonitrile (~ 50 mL) and stirred at ambient temperature overnight. Compound **4.11** (3.00 g, 14.07 mmol) was added in one portion and the reaction mixture brought to reflux for 48 h. Excess acetonitrile was removed *in vacuo* and the crude product triturated with absolute ethanol until gas evolution ceased (overnight). The solvent was removed by rotary evaporation leaving a yellow oil. The crude product was taken up in methylene chloride (~100 mL) and extracted with 1N NaOH (2 x 50 mL). All aqueous layers were combined and further washed with CH₂Cl₂ (1 x 50 mL). All organic phases were pooled,

dried over Na_2SO_4 and filtered giving a bright yellow crude solid. The product was purified by flash silica gel chromatography (gradient: 50% ether in petroleum ether to 100% ether, 5% intervals) followed by recrystallization from petroleum ether to give pure **4.12** (0.921 g, 20%), mp 176-178°C; TLC: (60% ether in petroleum ether) R_f 0.45; ^1H NMR (300 MHz, CDCl_3): δ 7.83 (m, 2H, Ar-H), 7.74 (m, 2H, Ar-H), 3.65 (t, $^3J = 6.9$ Hz, 3H, overlap CH, CH_2), 3.4-0.8 (br m, 10H, BH), 2.28 (m, 2H, CH_2), 1.87 (m, 2H, CH_2); ^{13}C NMR (75 MHz, CDCl_3): δ 168.31, 134.35, 131.97, 123.55, 74.42, 61.35, 36.97, 35.54, 28.53; ^{11}B NMR (96 MHz, CDCl_3): δ -1.51, -4.87, -8.53, -10.92, -12.22; IR (CH_2Cl_2 , cm^{-1}): 3058, 2968, 2597, 1773, 1716; MS (EI): m/z observed boron isotopic distribution at 331 (M^+).

1-(((2-(hydroxymethyl)benzoyl)amino)propyl)-1,2-dicarba-closo-dodecaborane

(4.13)

The phthalimide **4.12** (0.100 g, 0.302 mmol), was combined with NaBH_4 (0.057 g, 1.51 mmol) in isopropyl alcohol (~ 3 mL) and distilled, de-ionized water (~ 0.5 mL). The reaction was maintained overnight at ambient temperature at which time TLC analysis of the crude reaction mixture indicated the complete consumption of the starting material. The reaction solvent was removed by rotary evaporation leaving a white solid, which was subsequently taken up in CH_2Cl_2 (~25 mL) and washed with distilled, de-ionized water (3 x 25 mL). The aqueous portions were combined and further washed with methylene chloride (2 x 25 mL). All organic fractions were pooled, dried over Na_2SO_4 and filtered. The solvent was removed *in vacuo* and the product (0.060 g, 60%)

recrystallized from ethanol/water. mp 138°C; TLC (100% Ether): R_f 0.47; ^1H NMR (200 MHz, acetone- d_6): δ 7.96 (br s, 1H, NH), 7.58-7.33 (m, 4H, Ar-H), 4.83 (br s, OH), 4.72 (br s, CH), 4.60 (br s, 2H, CH₂), 3.80-0.70 (br m, 10H, BH), 3.41 (m, 2H, CH₂), 2.50 (m, 2H, CH₂), 1.86 (m, 2H, CH₂); ^{13}C NMR (50 MHz, acetone- d_6): δ 170.53, 141.39, 136.76, 131.29, 130.31, 128.69, 128.23, 76.99, 64.17, 63.54, 39.41, 35.89, 31.04; ^{11}B NMR (96 MHz, acetone- d_6): δ -1.73, -4.97, -8.48, -10.39, -11.84.

Synthesis of 1-(1,2-dicarba-closo-dodecaboran-1-yl)-3-aminopropane (4.14)

The azide **4.17** (0.050 g, 0.220 mmol) was combined with 10% Pd/C (10 mg) and ammonium formate (0.069 g, 1.10 mmol) in freshly distilled acetonitrile (5 mL). The reaction was brought to reflux overnight at which point, TLC analysis of the crude reaction mixture indicated the complete consumption of starting material. The heterogeneous reaction mixture was allowed to cool to room temperature and filtered through a plug of Celite™, which was washed with dichloromethane (1 x 5 mL) and ether (2 x 5 mL). The clear, colourless filtrate was concentrated by rotary evaporation and purified by silica gel chromatography (gradient, 100% petroleum ether to 100% ether, 2.5% increments). Three products were isolated in the order of: compound **4.20** (0.002 g, 4%), **4.18** (0.008 g, 16%) and **4.14** (0.036 g, 80%). The amine **4.14** showed: TLC (100% Ether): R_f 0.18; ^1H NMR (200 MHz, CDCl₃): δ 8.15 (s, 1H, CHO), 5.90 (br s, 1H, NH), 4.14 (t o d, 2H, CH₂), 3.80-0.60 (br m, 10H, BH), 3.46 (br s, 1H, CH), 2.23 (m, 2H, CH₂), 1.72 (m, 2H, CH₂); ^{13}C NMR (50 MHz, CDCl₃): δ 161.63, 74.59, 61.56, 37.16, 35.41, 29.67; ^{11}B NMR (96 MHz, CDCl₃): δ -1.99, -5.39, -8.98, -11.47, -12.66; IR (CH₂Cl₂, cm⁻¹

¹): 3454, 3303, 3058, 2929, 2912, 2872, 2587, 1673; MS (ES, positive): m/z observed boron isotopic distribution at 202.1 (M⁺).

Synthesis of 1-(1,2-Dicarboclosododecaboran-1-yl)-3-chloropropane (4.15)

Decaborane (6.55 g, 53.63 mmol) was dispensed into freshly distilled acetonitrile (50 mL) under dry nitrogen at room temperature for 18 hours. To the yellow bis(acetonitrile)decaborane solution was added 5-chloropentyne (5.0 g, 5.11 mL, 48.75 mmol) dropwise. The reaction was brought to reflux until TLC indicated complete consumption of the starting material (3 days). The reaction mixture was cooled to room temperature and the solvent removed by rotary evaporation giving a thick yellow oil. The oil was taken up in diethyl ether (100 mL) and extracted twice with 1N NaOH (2 x 50 mL). The aqueous layer was further extracted with ether (2 x 50 mL). All organic fractions were combined, dried over sodium sulfate and gravity filtered giving a light yellow filtrate. The solvent was removed *in vacuo* and the resulting yellow solid was purified by flash silica gel chromatography with 100% hexanes as the eluent. The product, a white crystalline solid (5.47 g, 51%) showed: mp 53°C; TLC (1:1 Ether:Hexanes): R_f 0.56; ¹H NMR (200 MHz, CDCl₃): δ 3.90-0.80 (br m, 10H, BH), 3.58 (br s, 1H, CH), 3.50 (t, ³J = 5.8 Hz, 2H, CH₂), 2.38 (m, 2H, CH₂), 1.95 (m, 2H, CH₂); ¹³C NMR (50 MHz, CDCl₃): δ 74.21, 61.65, 43.28, 35.48, 31.82; ¹¹B NMR (160 MHz, CDCl₃): δ -2.68, -6.11, -9.69, -12.16, -12.52, -13.49; IR (nujol, cm⁻¹): 3058, 2920, 2595, 723; MS (EI): m/z observed boron isotopic distribution 220 (M⁺).

Synthesis of 1-(1,2-Dicarbacosododecaboran-1-yl)-3-iodopropane (4.16)

Compound 4.15 (0.150 g, 0.670 mmol) was combined with sodium iodide (0.204 g, 1.36 mmol) in dry acetone (15 mL). After 12 hours the white, opaque solution was cooled to room temperature and filtered through a medium pored fritted funnel giving a clear and colourless filtrate. The residue was washed with ether (3 x 25 mL) and all organic fractions pooled and concentrated *in vacuo*, giving a yellow solid. The crude product was taken up in ether (50 mL) and further washed with sodium thiosulfate (2 x 25 mL). The aqueous layer was further extracted with ether (2 x 20 mL) and all organic fractions pooled, dried over sodium sulfate and gravity filtered giving a clear colourless filtrate. The solvent was removed by rotary evaporation giving 4.16 (0.211 g, 99%) in near quantitative yield. mp 56°C; TLC (100% pet ether): R_f 0.18; ¹H NMR (200 MHz, CDCl₃): δ 3.90-0.80 (br m, 10H, BH), 3.59 (br s, 1H, CH), 3.13 (t, ³J = 6.4 Hz, 2H, CH₂), 2.33 (m, 2H, CH₂), 1.99 (m, 2H, CH₂); ¹³C NMR (50 MHz, CDCl₃): δ 73.80, 61.50, 38.75, 32.30, 3.69; ¹¹B NMR (160 MHz, CDCl₃): δ -2.67, -6.08, -9.68, -12.15, -12.57, -13.50; IR (nujol, cm⁻¹): 3059, 2961, 2857, 2598; MS (EI): m/z observed boron isotopic distribution at 312 (M⁺), 183 (M – I).

Synthesis of 1-(1,2-dicarbacosododecaboran-1-yl)-3-azidopropane (4.17)

Method A: The chloride 4.15 (0.500 g, 2.27 mmol), sodium iodide (0.679 g, 4.53 mmol) and sodium azide (0.736 g, 11.33 mmol) were combined in dry acetone (15 mL). The reaction vessel was protected from light and brought to reflux until TLC analysis indicated the consumption of starting material (5 days). The reaction vessel was allowed

to cool to room temperature and filtered through a medium porosity fritted glass funnel and the residue washed with CH_2Cl_2 (3 x 10 mL). The filtrate was concentrated by rotary evaporation and the resulting solid suspended in 20 mL CH_2Cl_2 and re-filtered. The crude azide was purified by flash silica gel chromatography using 3% ether in hexanes as the eluent. The product **4.17** (0.443 g, 86%), a clear colourless oil, showed: TLC (1:1 Ether:Hexanes): R_f 0.53; ^1H NMR (200 MHz, CDCl_3): δ 3.90-0.90 (br m, 10H, BH), 3.58 (br s, 1H, CH), 3.26 (t, $^3J = 5.8$ Hz, 2H, CH_2), 2.27 (m, 2H, CH_2), 1.71 (m, 2H, CH_2); ^{13}C NMR (50 MHz, CDCl_3): δ 74.28, 61.46, 49.99, 35.04, 28.47; ^{11}B NMR (96 MHz, CDCl_3): δ -2.75, -6.16, -9.69, -12.27, -13.44; IR (neat, cm^{-1}): 3067, 2966, 2938, 2871, 2595, 2102; MS (CI, NH_3): m/z observed boron isotopic distribution at 198 (M- N_2), 171 (M- $\text{CH}_2\text{CH}_2\text{N}_3$).

Method B: To a solution of the iodide **4.16** (0.500 g, 2.27 mmol) in dry acetone (15 mL) was added sodium azide (0.736g, 11.33 mmol). The reaction vessel was fitted with a condenser and the solution brought to reflux under dry nitrogen until TLC indicated the consumption of starting material (12 hours). The reaction mixture was concentrated *in vacuo* and the residue taken up in ether (50 mL). The solution was extracted with distilled water (2 x 50 mL) and both aqueous fractions were combined and further washed with ether (2 x 25 mL). All organic fractions were pooled, dried over sodium sulfate and gravity filtered. The clear, colourless filtrate was concentrated *in vacuo* and the crude product purified by flash silica gel chromatography with 3% ether in hexanes as the eluent. The product was obtained as a clear colourless oil (Yield > 99%).

Synthesis of 1-(1,2-dicarboclosododecaboran-1-yl)-3-formylpropane (4.18)

The azide **4.17** (0.143 g, 0.629 mmol), formic acid (0.050 mL, 0.060 g, 0.140 mmol) and catalyst (10% Pd/C, 0.030 g) were dissolved in absolute ethanol (20 mL). The reaction was maintained under 1 atm H₂ in a Parr Hydrogenator at an ambient temperature overnight. The reaction mixture was filtered through a plug of Celite giving a slightly yellow filtrate. The excess solvent was removed by rotary evaporation giving a viscous yellow oil. The oil was taken up in a minimal amount of hexanes and purified by silica gel chromatography with 5% ether in hexanes as the eluent. Three products were isolated, compound **4.18**, **4.19** and **4.20**. The formamide (0.014 g, 10%) showed: TLC (1:1 Ether:Hexanes): R_f 0.23; ¹H NMR (200 MHz, CDCl₃): δ 8.03 (s, 1H, CHO), 4.14 (t, ³J = 6.0 Hz, 2H, CH₂), 3.90-0.70 (br m, 10H, BH), 3.60 (br s, 1H, CH), 2.31 (m, 2H, CH₂), 1.87 (m, 2H, CH₂); ¹³C NMR (50 MHz, CDCl₃): δ 160.59, 74.22, 62.13, 61.47, 34.73, 28.29; ¹¹B NMR (96 MHz, CDCl₃): δ -2.66, -6.16, -9.68, -11.97, -12.33, -13.43; IR (CHCl₃, cm⁻¹): 3068, 3023, 2961, 2932, 2872, 2598, 1726; MS (CI, NH₃): m/z observed boron isotopic distribution at 229 (M⁺).

Attempted synthesis of 1-(1,2-Dicarboclosododecaboran-1-yl)-3-isocyanatopropane, synthesis of 4.19 and 4.20^{71,72}

The iodo-carborane **4.16** (0.100 g, 0.320 mmol) was added as a solid to a stirring solution of ethanol and silver cyanide (0.045, 0.336 mmol). The reaction vessel was protected from light and brought to reflux for 1 day. Additional silver cyanide (0.180 g, 1.344 mmol) was added and the reaction maintained at reflux for an additional 72 hours.

The apparatus was allowed to cool and the solvent removed *in vacuo* giving a brown paste. The reaction mixture was purified by silica gel chromatography using 10% ether in hexanes as the eluent giving two major products. The first product **4.19** was a white amorphous solid while the second **4.20** a clear colourless oil. The first product showed: mp 30°C (subl.); TLC: (1:1 Et₂O: Hexanes) R_f 0.58 ¹H NMR (200 MHz, CDCl₃): δ 3.90-0.80 (br m, 10H, BH), 3.56 (br s, 1H, CH), 2.17 (m, 2H, CH₂), 1.49 (m, 2H, CH₂), 0.91 (t, 3H, CH₃); ¹³C NMR (50 MHz, CDCl₃): δ 75.09, 60.93, 40.10, 22.60, 13.49; ¹¹B NMR (96 MHz, CDCl₃): δ -2.84, -6.33, -9.79, -11.82, -12.59, -13.57; IR (neat, cm⁻¹): 2971, 2938 (s, CH), 2598 (br s, BH). MS (CI, NH₃): m/z observed boron isotopic distribution at 201 (M+NH₄), 185 (M⁺). X-ray Crystallography: Space group: Pna2₁, a = 14.687(3) Å, b = 7.1690(18) Å, c = 22.596(6) Å, α = β = γ = 90°, V = 2379.1(10) Å³, Z = 8, data/parameters: 4187/360, R = 0.0794, R_w, 0.2021, GOF = 0.985.

The second product **4.20**, a colourless oil, showed: TLC (1:1 Et₂O: Hexanes): R_f 0.22; ¹H NMR (200 MHz, CDCl₃), δ 3.90-0.80 (br m, 10H, BH), 3.62 (br s, 1H, CH), 3.40 (overlap, t and q, 4H, CH₂OCH₂), 2.31 (m, 2H, CH₂), 1.72 (m, 2H, CH₂), 1.17 (t, ³J = 7.0 Hz, 3H, CH₃); ¹³C NMR (50 MHz, CDCl₃): δ 75.14, 68.78, 66.29, 61.29, 35.25, 29.46, 15.04; ¹¹B NMR (96 MHz, CDCl₃): δ -2.49, -5.97, -9.59, -12.23, -13.41; IR (neat, cm⁻¹): 3067, 2978, 2935, 2871, 2571, 1116; MS (CI, NH₃): m/z observed boron isotopic distribution at 230 (M⁺), 247 (M+NH₄), 200 (M-CH₂CH₃), 185 (M-OCH₂CH₃), 170 (M-CH₂OCH₂CH₃), 156 (M-CH₂CH₂OCH₂CH₃).

Synthesis of $\text{Re}(\text{CO})_3(\text{L}_2)\text{Br}$ (4.21)

$[\text{NEt}_4]_2[\text{Re}(\text{CO})_3\text{Br}_3]$ (65.5 mg, 85 μmol) and **4.3** (44.6 mg, 264 μmol) were dissolved in anhydrous THF (2.5 mL) and the resulting yellow heterogeneous reaction mixture brought to reflux overnight (18 hours). The solvent was subsequently removed by rotary evaporation leaving a yellow solid, which was purified by either radial chromatography (40% ethyl ether in petroleum ether) or preparative TLC (30:20 DCM/pentane) giving the desired product as a white crystalline solid (11.7 mg, 20%). ^1H NMR (CDCl_3 , 500 MHz): δ 4.03 (s, 2H, CH), 2.68-1.24 (br m, 20H, BH); ^{13}C NMR (CDCl_3 , 125 MHz): δ 183.94, 181.54, 57.47, 57.23; ^{11}B NMR (CD_2Cl_2 , 160 MHz): δ -1.76, -8.53, -12.22, -13.29; IR (KBr, cm^{-1}): 2602, 2183, 2132, 2042, 2004, 1956; MS (ES, negative): m/z observed boron isotopic distribution at 687.5 (M-H). X-ray Crystallography: Space group: $\text{P}2_1/\text{c}$, $a = 15.353(2)$ Å, $b = 10.5819(15)$ Å, $c = 18.485(3)$ Å, $\alpha = \gamma = 90^\circ$, $\beta = 94.771(2)^\circ$, $V = 2992.7(8)$ Å³, $Z = 4$, data/parameters: 6873/402, $R = 0.0374$, $R_w = 0.0737$, GOF = 0.997.

The reaction of **4.3** with $[\text{Re}(\text{CO})_3(\text{solvent})_3]^+$, formation of **4.22** and **4.23**.

$\text{Ag}(\text{PF}_6)$ (114 mg, 0.45 mmol) was added to $[\text{NEt}_4]_2[\text{Re}(\text{CO})_3\text{Br}_3]$ (116 mg, 0.15 mmol) in dry THF (3 mL) under Ar. After 20 minutes the reaction was filtered under Ar, the residue washed with 1 mL of dry THF, and the solution evaporated to dryness. Compound **1** (0.153 g, 0.904 mmol) was added as a solid followed by dry THF (1 mL). After heating to reflux overnight, the solvent was evaporated and the resulting solid dissolved in ether and the mixture purified by radial chromatography (100% petroleum

ether to 100% ether in 5% intervals) giving compound **4.22** (25 mg, 18%) and **4.23** (51 mg, 32%): Compound **4.22** showed: ^1H NMR (CD_2Cl_2 , 200 MHz): δ 4.18 (br s, 3H, overlap CH), 3.47-1.13 (br m, 30H, BH); ^{13}C NMR (CD_2Cl_2 , 50 MHz): δ 184.49, 58.78, 57.85, 57.68; ^{11}B NMR (CDCl_3 , 96 MHz): δ -2.45, -3.69, -7.37, -9.76, -13.56; IR (KBr, cm^{-1}): 2610, 2178, 2122, 2098, 2039, 2007, 1948; MS (ES, positive): m/z observed boron isotopic distribution at 792.3 m/z ($\text{M}+\text{Na}^+$), 778.2 (M^+). X-ray Crystallography: Space group: R3m, $a = b = 21.710(9)$ Å, $c = 6.410(4)$ Å, $\alpha = \beta = 90^\circ$, $\gamma = 120^\circ$, $V = 2616(2)$ Å³, $Z = 3$, data/parameters: 1153/105, $R = 0.0345$, $R_w = 0.0354$, GOF = 1.123.

Compound **4.23** showed: ^1H NMR (CDCl_3 , 300 MHz): 4.49 (br s, 4H, overlap CH), 2.96-0.84 (br m, 40H, BH); ^{13}C NMR (CD_2Cl_2 , 50 MHz): δ 171.65, 64.95, 64.38, 63.97, 62.26; ^{11}B NMR (CDCl_3 , 96 MHz): -2.12, -8.88, -13.27; IR (CH_2Cl_2 , cm^{-1}): 2604, 2210, 2140, 2095, 2025, 2002; MS (ES, positive): m/z observed boron isotopic distribution at 919.7 (M^+).

Synthesis of $[\text{ReL}_6][\text{PF}_6]$ (**4.24**)

$[\text{Re}_2(\text{O}_2\text{CPh})_4\text{Cl}_2]$ (0.152 g, 0.164 mmol) and the isonitrile (0.168 g, 0.994 mmol) were dissolved in freshly distilled diethyl ether (5.0 mL) and low boiling petroleum ether (0.5 mL) giving an orange heterogeneous reaction mixture. The solution was brought to reflux under Ar for 24 hours. The solvents were removed by rotary evaporation and the resulting green solid suspended in a saturated acetone solution of KPF_6 for 1 hour (5 mL). Upon removal of the acetone, the grey/green solid was stirred in ether (25 mL) for 2

hours and filtered, and then stirred in low boiling petroleum ether (25 mL) for 2 additional hours. The resulting solid was collected by filtration, dissolved in THF (1 mL) and the product, a white solid (0.014, 7%), was precipitated from the reaction mixture, upon the addition of an equal portion of distilled, deionized water. The product showed: TLC (25% Pet. Ether in Ether): $R_f = 0.76$; ^1H NMR (acetone- d_6 , 500 MHz): 5.25, 5.10, 4.90 (br s, 6H, CH), 3.01-1.50 (br m, 60H, BH); ^{13}C NMR (acetone- d_6 , 75 MHz): 59.20; ^{11}B NMR (acetone- d_6 , 96 MHz): -1.99, -8.06, -11.66; IR (CH_2Cl_2 , cm^{-1}): 3070, 2602, 2047; MS (ES, positive): m/z observed boron isotopic distribution at 1202.5 m/z (M^+); HRMS (FAB, positive): Calcd for $\text{C}_{18}\text{H}_{66}\text{B}_{60}\text{N}_6\text{Re}$ (M^+) 1202.091. Found 1202.087.

Synthesis of $\text{Re}_2(\text{OAc})_4\text{Cl}_2$ (4.26)

$[\text{NBu}_4]_2[\text{Re}_2\text{Cl}_8]$ (1.088 g, 0.954 mmol) was dissolved in a mixture of freshly distilled acetic acid (40 mL) and acetic anhydride (10 mL). The blue-green heterogeneous reaction mixture was brought to reflux for 1 hour, changing from dark opaque (10 min) to light orange (30 min). The reaction mixture was allowed to cool to room temperature and the orange precipitate isolated by suction filtration. The orange solid was washed with absolute ethanol (4 x 2 mL) and used without further purification. Yield: (0.576 g, 89%).

Synthesis of $\text{Re}_2(\text{O}_2\text{CBn})_4\text{Cl}_2$ (4.27)

Compound **4.26** (0.300 g, 0.294 mmol) was combined with excess benzoic acid (1.0 g, 8.18 mmol). Both solids were dried under high vacuum for one hour prior to heating under nitrogen to reflux (approx. 5 min). The reaction vessel was allowed to cool

to room temperature at which time the resulting dark red solid was suspended in dry, degassed diethyl ether and filtered under a stream of nitrogen. The resulting brick-red solid was further washed with diethyl ether (3 x 10 mL) and used without further purification. Yield: (0.357 g, 87 %).

4.17 References

- ¹ Soloway, A.H.; Tjarks, W.; Barnum, A.-G.; Rong, F.; Barth, R.F.; Codogni, I.M.; Wilson, J.G. *Chem. Rev.* **1998**, 98, 1515.
- ² Valliant, J.F.; Guenther, K.J.; King, A.S.; Morel, P.; Schaffer, P.; Sogbein, O.O.; Stephenson, K. *Coord. Chem. Rev.* **2002**, 232, 173.
- ³ Locher, G.L. *Am. J. Roentgenol. Radium Ther.* **1936**, 36, 1.
- ⁴ Kabalka, G.W.; Smith, G.T.; Dyke, J.P.; Reid, W.S.; Longford, C.P.; Roberts, T.G.; Reddy, N.K.; Buonocore, E.; Hubner, K.F. *J. Nucl. Med.* **1997**, 38, 1762.
- ⁵ Kabalka, G.W.; Tang, C.; Bendel, P. *J. Neuro-Oncol.* **1997**, 33, 153.
- ⁶ Glover, G.H.; Pauly, J.M.; Bradshaw, K.M. *J. Magn. Reson. Imaging* **1992**, 2, 47.
- ⁷ Hawthorne, M.F.; Maderna, A. *Chem. Rev.* **1999**, 99, 3421.
- ⁸ Malatesta, L.; Bonati, F. *Isocyanide Complexes of Metals*, Wiley, London, **1969**.
- ⁹ Coville, N.J. *J. Organomet. Chem.* **1980**, 190, C-84.
- ¹⁰ Bruce, M.I.; Wallis, R.C. *Aust. J. Chem.* **1981**, 34, 209.
- ¹¹ Wizenburg, M.L.; Kargol, J.A.; Angelici, R.J. *J. Organomet. Chem.* **1983**, 294, 415.
- ¹² Treichel, P.M.; Mueh, H.J. *Inorg. Chim. Acta* **1977**, 22, 265.
- ¹³ Abrams, M.J.; Davison, A.; Jones, A.G.; Costello, C.E.; Pang, H. *Inorg. Chem.* **1983**, 22, 2798.
- ¹⁴ Han, H.; Cho, C.-G.; Lansbury Jr., P.T. *J. Am. Chem. Soc.* **1996**, 118, 4500.
- ¹⁵ Valliant, J.F.; Schaffer, P. *J. Inorg. Biochem.* **2001**, 85, 43.
- ¹⁶ Morel, P.; Schaffer, P.; Valliant, J.F. *J. Organomet. Chem.* **2003**, 668, 25.
- ¹⁷ Schaffer, P.; Britten, J.F.; Davison, A.; Jones, A.G.; Valliant, J.F. *J. Organomet. Chem.* **2003**, In Press.
- ¹⁸ Zakharkin, L.I.; Kalinin, V.N.; Gedymin, V.V. *Synth. Inorg. Met.-Org. Chem.* **1971**, 1, 45.
- ¹⁹ Kasar, R.A.; Knudsen, G.M.; Kahl, S.B. *Inorg. Chem.* **1999**, 38, 2936.
- ²⁰ Heřmánek, S. *Chem. Rev.* **1992**, 92, 325.
- ²¹ Atkins, G.M.; Burgess, E.M. *J. Am. Chem. Soc.* **1968**, 90, 4744.
- ²² Burgess, E. M.; Penton Jr., H. R.; Taylor, E. A. *J. Org. Chem.* **1973**, 38, 26.
- ²³ Creedon, S. M.; Crowley, H. K.; McCarthy, D. G. *J. Chem. Soc. Perkin Trans 1*, **1998**, 1015.
- ²⁴ Pavia, D.L.; Lampman, G.M.; Kriz, G.S. *Introduction to Spectroscopy: A Guide for Students of Organic Chemistry*, 2nd ed., Harcourt Brace College, Toronto, **1996**.
- ²⁵ Loewenstein, A.; Margalit, Y. *J. Phys. Chem.* **1965**, 69, 4152.
- ²⁶ Morishima, I.; Mizuno, A.; Yonezawa, T.; Goto, K. *J. Chem. Soc. D.* **1970**, 20, 1321.
- ²⁷ Stephany, R.W.; DeBie, M.J.A.; Drenth, W. *Org. Magn. Resonance* **1974**, 6, 45.
- ²⁸ Walborski, H.M.; Niznik, G.E. *J. Org. Chem.* **1972**, 37, 187.
- ²⁹ Zakharkin, L.I.; Ol'shevskaya, V.A.; Pisarevsky, A.P.; Yanovski, A.I.; Struchkov, Y.T. *Mendeleev Comm.* **1995**, 190.
- ³⁰ Shapiro, R.H.; Heath, M.J. *J. Am. Chem. Soc.* **1967**, 89, 5734.
- ³¹ Gabriel, S. *Ber. dtsh. chem. Ges.* **1887**, 20, 2224.

- ³² Wilson, J. G.; Anisuzzaman, A. K. M.; Alam, A.H.; Soloway, A. H. *Inorg. Chem.* **1992**, 31, 1955.
- ³³ Nakagawa, T.; Watanabe, H.; Yoshizaki, T. *Jap. Pat.* 7031,940. **1970**
- ³⁴ Batsanov, A.S.; Goeta, A.E.; Howard, J.A.K.; Hughes, A.K.; Malget, J.M. *J. Chem. Soc. Dalton Trans.* **2001**, 1820.
- ³⁵ Valliant, J.F.; Schaffer, P. *J. Inorg. Biochem.* **2001**, 85, 43.
- ³⁶ Gibson, M.S.; Bradshaw, R.W. *Angew. Chem. Int. Ed. Engl.* **1968**, 12, 919.
- ³⁷ Alternatively Sjöberg and co-workers also developed a high yielding synthetic procedure for aminoalkyl carboranes using the Gabriel reagent HNBoc₂.
- ³⁸ Finkelstein, H. *Ber.* **1910**, 3, 1528.
- ³⁹ Maderna, A.; Herzog, A.; Knobler, C.B.; Hawthorne, M.F. *J. Am. Chem. Soc.* **2001**, 123, 10423.
- ⁴⁰ Reddy, P.G.; Baskaran, S. *Tetrahedron Lett.* **2002**, 43, 1919.
- ⁴¹ Ram, S.; Ehrenkauser, R.E. *Synthesis* **1988**, 91.
- ⁴² Garteris, T.; Selve, C.; Delpuech, J.-J. *Tetrahedron Lett.* **1983**, 24, 1609.
- ⁴³ Louupy, A.; Monteux, D.; Petit, A.; Aizpurua, J.M.; Dominguez, E.; Palomo, C. *Tetrahedron Lett.* **1996**, 37, 8177.
- ⁴⁴ Sekiya, M. *J. Pharm. Soc. Jpn.* **1950**, 70, 553.
- ⁴⁵ Atanas, P.V.; Ilian, I.I. *Synth. Commun.* **1998**, 28, 1433.
- ⁴⁶ Eckert, H.; Forster, B. *Angew. Chem. Int. Ed. Engl.* **1987**, 26, 894.
- ⁴⁷ Katritzky, A.R.; Xie, L.; Fan, W.Q. *Synthesis* **1993**, 1, 45.
- ⁴⁸ Newman, M.S. *J. Am. Chem. Soc.* **1950**, 72, 4783.
- ⁴⁹ Carretero, J.C.; Ruano, J.L.G. *Tetrahedron Lett.* **1985**, 26, 3381.
- ⁵⁰ Friedrich, K.; Wallenfels, K. In *The Chemistry of the Cyano Group*. Rappoport, Z.; Patai, S., Eds.; Interscience, New York, **1970**, 77.
- ⁵¹ Austad, T.; Songstad, J.; Stangeland, L.J. *Acta Chem. Scand.* **1971**, 25, 2327.
- ⁵² Zakharkin, L.I.; Ol'shevskaya, V.A.; Sulaimankulove, D.D. *Metalloorg. Khim.* **1992**, 5, 925.
- ⁵³ Alberto, R.; Schibli, R.; Egli, A.; Schubiger, P.A.; Herrmann, W.A.; Artus, G.; Abram, Y.; Kaden, T.A. *J. Organomet. Chem.* **1995**, 493, 7987.
- ⁵⁴ Alberto, R.; Schibli, R.; Egli, A.; Abram, U.; Kaden, T.A.; Schubiger, P.A. *J. Am. Chem. Soc.* **1998**, 120, 7987.
- ⁵⁵ Schibli, R.; Bella, R.L.; Alberto, R.; Garcia-Garayoa, E.; Ortner, K.; Abram, U.; Schubiger, P.A. *Bioconj. Chem.* **2000**, 3, 345.
- ⁵⁶ Garcia, R.; Paulo, A.; Domingos, A.; Santos, I.; Ortner, K.; Alberto, R. *J. Am. Chem. Soc.* **2000**, 122, 11240.
- ⁵⁷ Treichel, P.M.; Williams, J.P. *J. Organomet. Chem.* **1977**, 135, 39.
- ⁵⁸ Orpen, A.G.; Brammer, L.; Allen, F. H.; Kennard, O.; Watson, D.G.; Taylor, R. In *International Tables for Crystallography, Volume C; Mathematical, Physical and Chemical Tables*; Wilson, A.J.C.; Prince, E., Eds.; Kluwer Academic: London, 1999; 2nd Ed., p 874.
- ⁵⁹ Alberto, R.; Schibli, R.; Schubiger, P.A.; Abram, U.; Kaden, T.A. *Polyhedron* **1996**, 15, 1079.

- ⁶⁰ Wiesboeck, R.A.; Hawthorne, M.F. *J. Am. Chem. Soc.* **1964**, 86, 1642.
- ⁶¹ Zakharkin, L.I.; Kirillova, V.S. *Izv. Akad. Nauk. SSSR., Ser. Khim.* **1975**, 11, 1642.
- ⁶² Maurer, J.L.; Serino, A.J.; Hawthorne, M.F. *Organometallics*, **1988**, 7, 2519.
- ⁶³ Tomita, H.; Luu, H.; Onak, T. *Inorg. Chem.* **1991**, 30, 812.
- ⁶⁴ Schaekch, J.J.; Kahl, S.B. *Inorg. Chem.* **1999**, 38, 204.
- ⁶⁵ Allison, J.D.; Wood, T.E.; Wild, R.E.; Walton, R.A. *Inorg. Chem.* **1982**, 21, 3540.
- ⁶⁶ Cotton, F.A.; Oldham, C.; Robinson, W.R. *Inorg. Chem.* **1966**, 5, 1798.
- ⁶⁷ Cotton, F.A.; Walton, R.A. *Multiple Bonds Between Metal Atoms*. Wiley-Interscience: New York, **1982**.
- ⁶⁸ Freni, M.; Romiti, P. *J. Organomet. Chem.* **1975**, 87, 241.
- ⁶⁹ Younger, C. G. Ph.D. Thesis, 1992, McMaster University, Hamilton, Canada.
- ⁷⁰ Creedon, S. M.; Crowley, H. K.; McCarthy, D. G. *J. Chem. Soc. Perk Trans. 1.* **1998**, 1015.
- ⁷¹ Gautier, A. *Ann. Chim. Paris*, **1867**, 142, 289.
- ⁷² Hofmann, A.W. *A. Ann.* **1867**, 144, 114.

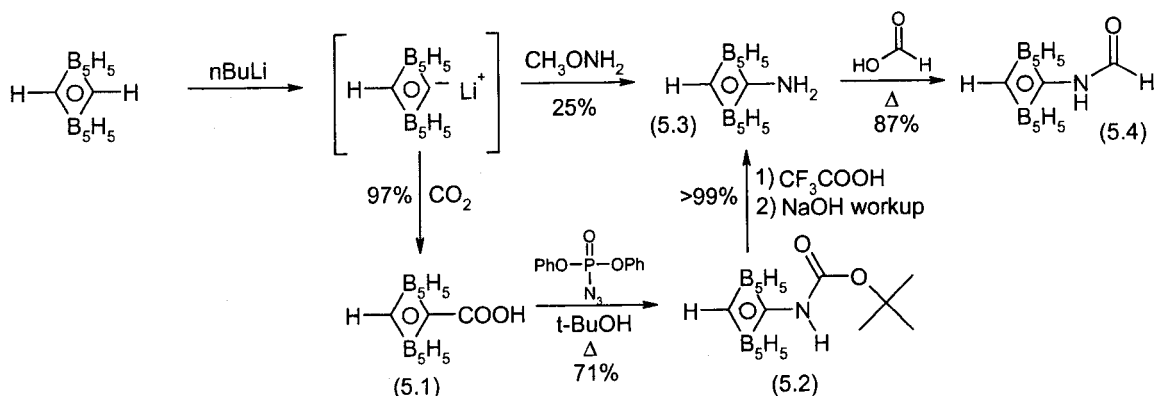
Chapter 5 – The Synthesis and Coordination Chemistry of *para*-Carborane Isonitriles.

5.1 Overview

In the previous chapter, preparation of an *ortho*-carborane isonitrile ligand, in which the isonitrile is located directly off the carbon-vertex, was not attempted. This is a consequence of the base lability of a key intermediate, 1-amino-*ortho*-carborane, which spontaneously degrades to the corresponding *nido*-anion.^{1,2} In order to compensate for the reactivity of *ortho*-carborane, an attempt was made to prepare a carbon-functionalized isonitrile using the more robust *para*-carborane isomer. The work described herein has been recently published.^{3,4}

5.2 Synthetic Strategy

The overall synthetic strategy was modelled after the method used to prepare the *ortho*-carborane isonitriles **4.3** and **4.10**. Initially, 1-amino-1,12-dicarba-*closo*-dodecaborane (**5.3**) was synthesized following the method developed by Kahl and co-workers.⁵ Carboxylation of the C-lithio-salt of 1,12-dicarba-*closo*-dodecaborane with carbon dioxide resulted in the formation of **5.1** (Scheme 5.1). Compound **5.1** was treated with diphenylphosphorylazide in the presence of *tert*-butyl alcohol and heated at reflux, which gave the carbamate **5.2**. Removal of the *t*-butyloxycarbonyl group was carried out in trifluoroacetic acid, which following workup with base, gave the amine **5.3** in excellent yield (> 99%).



Scheme 5.1 – Synthesis of para-carborane formamide (5.4).

5.3 Synthesis and Characterization of 3-Formyl-ortho-carborane

Formylation of 5.3 was performed using the same procedures described for the preparation of the *ortho*-carborane analogue (Scheme 5.1). It was found, however, that longer reaction times were required to maximize the yield of 5.4. Compound 5.4, which was isolated in excellent yield (87%), showed BH and CO stretches in the IR spectrum at 2607 and 1693 cm^{-1} respectively. The mass spectrum exhibited the expected m/z value having a B_{10} isotopic distribution pattern. The ^1H NMR and ^{13}C NMR spectra were in agreement with the proposed structure, with the latter spectrum showing three peaks at 162.93, 87.14 and 55.22 ppm, corresponding to the CO, CH, and substituted carborane carbon atoms, respectively. The proton-decoupled ^{11}B NMR spectrum of 5.4 showed two peaks at -6.0 and -9.0 ppm, consistent with a mono-C-substituted *para*-carborane derivative.

Single crystals of 5.4 were obtained by the slow evaporation of an acetone solution containing the formamide. The X-ray solution (Figure 5.1) showed that the formamide packs in the centrosymmetric $\text{P}2_1/n$ space group with the carborane cage located *trans* to

the formamide oxygen. The structure of the carborane icosahedron is relatively normal, with average B-C bond distances of 1.714(5)Å, ranging from 1.700(3) to 1.730(3)Å, while the average B-B bond length of 1.774(3)Å is also similar to that reported for other *para*-carborane analogues.⁶

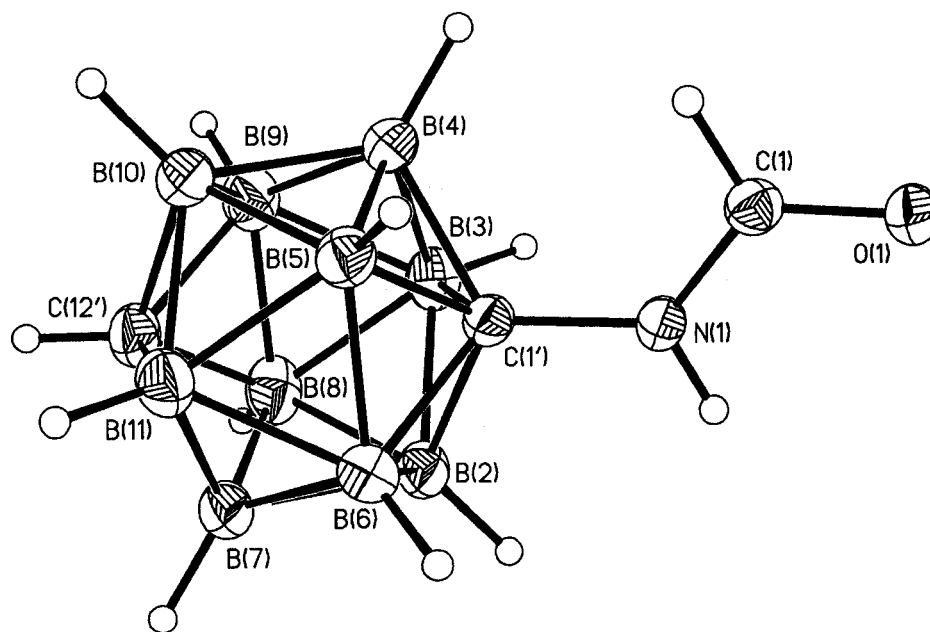


Figure 5.1 - ORTEP representation of 5.4. Thermal ellipsoids shown at the 50% probability level.

The packing mode exhibited by the *para*-isomer 5.4 is much different than that obtained for the *ortho*-carborane analogue 4.2. Hydrogen-bonding plays a major role in the formation of both three-dimensional lattices. However, compound 4.3 exhibits hydrogen-bonding interactions between adjacent formyl groups in a manner that generates columns of interacting molecules. This, in turn, produces a net chiral packing

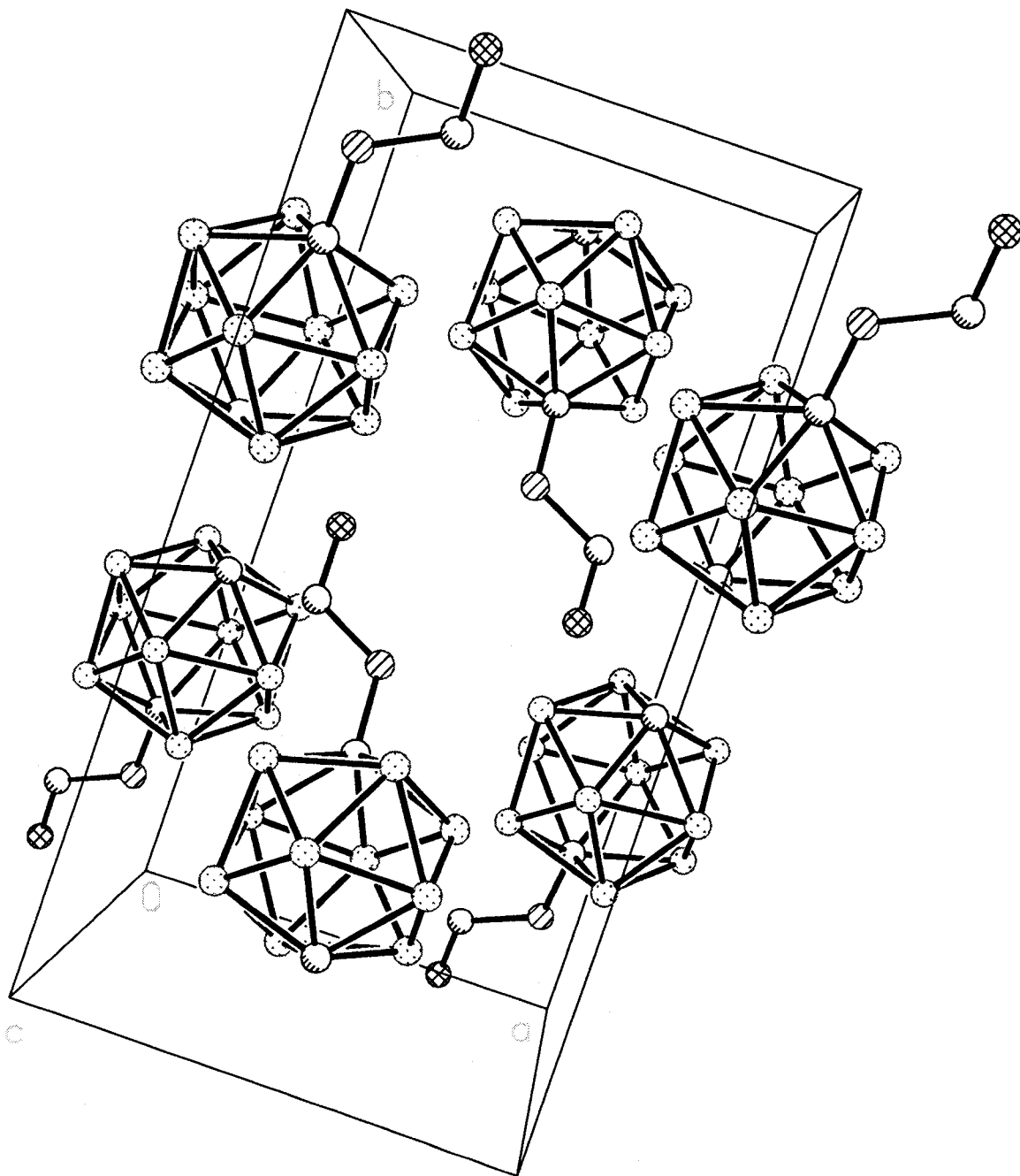


Figure 5.2 - Unit cell representation of 5.4.

mode in which all molecules have a directional preference. Compound **5.4**, on the other hand, has interactions between only two molecules. This serves to generate an inversion center between them, and results in a non-chiral space group designation. Hydrogen-bonding interactions occur down the a-axis, while the spherical carborane cage appeared to govern packing along the b- and c-axes (Figure 5.2).

5.4 Attempted Dehydration of 1-Formyl-1,12-dicarba-closo-dodecaborane

Based on the work described in Chapter 4, dehydration of **5.4** with the Burgess reagent should yield the desired isonitrile.⁷ Surprisingly, the reaction of the formamide with the Burgess reagent led to one major product, which was subsequently identified as methyl carbamate **5.5**.

The IR spectrum of compound **5.5** exhibited strong BH and CO stretching frequencies at 2615 and 1754 cm^{-1} respectively. The carbonyl stretch is shifted significantly from the C=O stretch observed in the formamide precursor (1693 cm^{-1}). The ^1H NMR spectrum showed a broad singlet at 7.42 ppm, due to the exchangeable NH proton, and a singlet at 3.48 ppm arising from the protons on the methyl group. The presence of the carbamate is evident in the ^{13}C NMR spectrum, in which the resonance for the CO groups appears upfield at 152.68 ppm. The proton-decoupled ^{11}B NMR spectrum of **5.5** showed, as would be expected, two resonances located at -12.61 and -15.30 ppm.

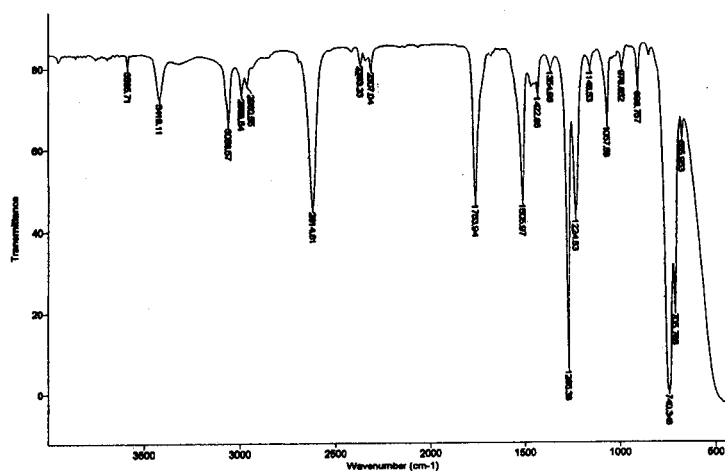
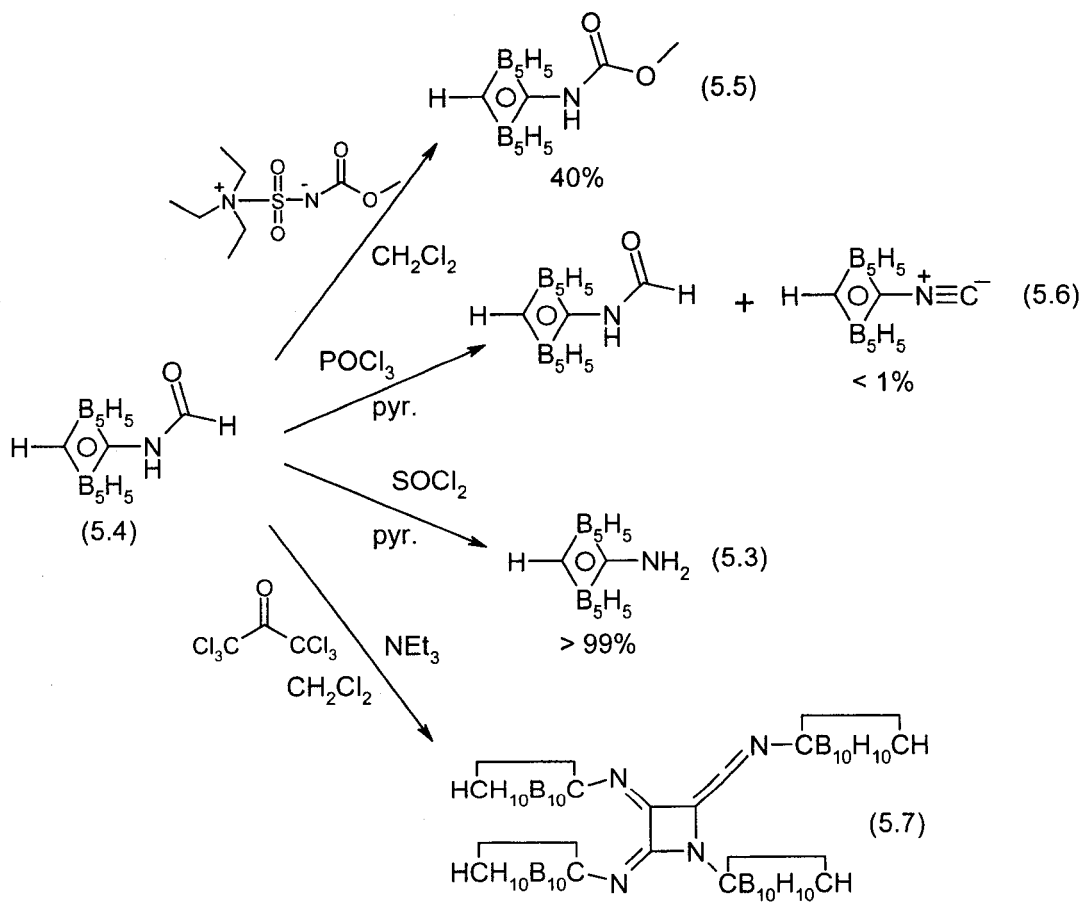


Figure 5.3 - IR spectrum of 5.5.



Scheme 5.2 – Formamide dehydration strategies.

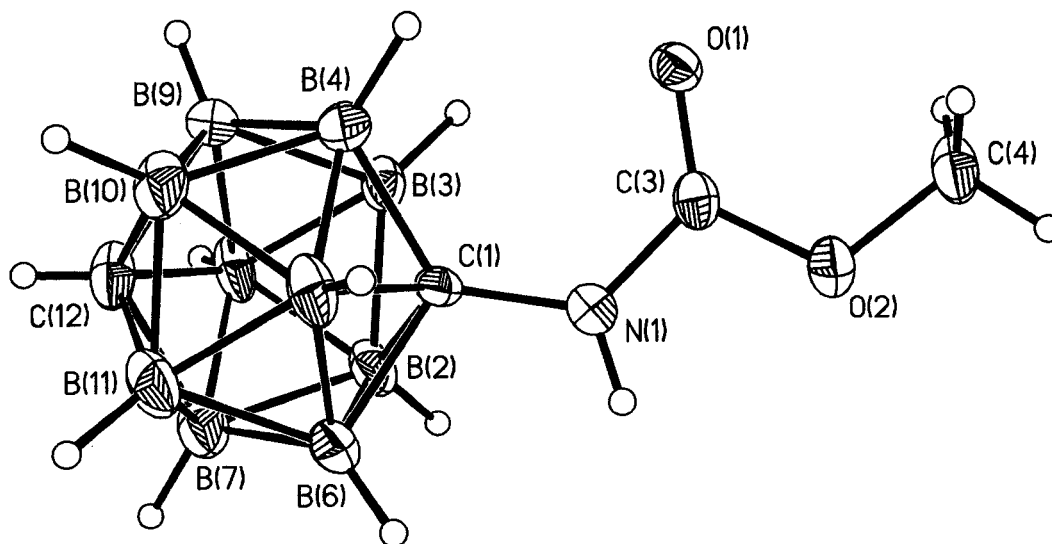


Figure 5.4 – ORTEP representation of 5.5 showing 30% thermal ellipsoids

Single crystals of **5.5** were isolated and analyzed using X-ray crystallography. The resulting structure (Figure 5.4) irrefutably demonstrates that the product is in fact the carbamate. The structure was solved in the $P4_1$ space group with four molecules in the unit cell ($Z = 4$). As mentioned previously (Chapter 4, section 4.4), the non-centrosymmetric space group is a property of the bulk crystal and not of the compound itself. The packing of **5.6** in the tetragonal $P4_1$ space group had, by definition, a four-fold screw axis of symmetry related molecules down the c -axis (Figure 5.5). There was also a series of channels present down the same axis in the lattice, which was modelled as disordered solvent, as there were no chemically identifiable species present. By modelling the presence of partial solvent (oxygen) atoms, the end result was an overall improvement of the residual agreement factor (R_1).

The dimensions of the carborane cage in compound **5.5** are relatively unremarkable with average B-C bond lengths of 1.728(9) Å from C1 and 1.695(9) Å

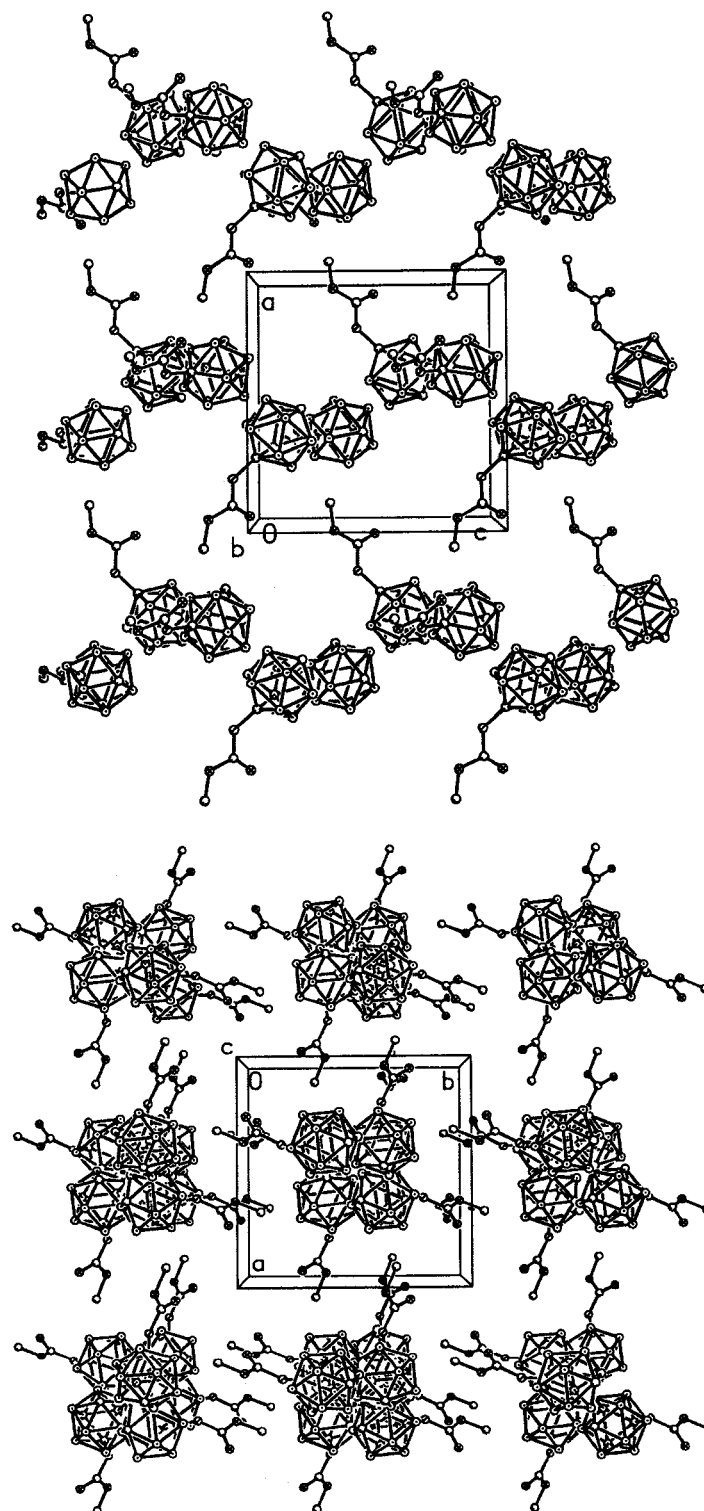
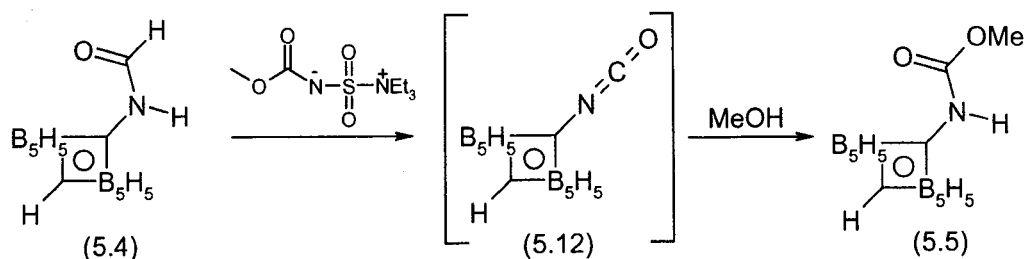


Figure 5.5 - Packing representation of 5.5 down the b (top) and c (bottom) axes. Disordered solvent molecules were omitted for clarity.

from C12, ranging from a maximum of 1.759(8) Å to a minimum of 1.670(11) Å. The average boron-boron bond length was 1.770(11) Å. The C(1)-N(1) bond length at 1.423(7) Å is longer than the nitrogen-carbon bond in the formamide precursor **5.4**. The carbonyl C=O bond distance of 1.209(6) Å is shorter than the observed C=O bond length in **5.4**.

The formation of **5.5** may be the result of the reaction of methanol, produced by the decomposition of the Burgess reagent,⁸ with the intermediate isocyanate (**5.12**) (Scheme 5.3). The isocyanate intermediate, which could not be isolated by standard chromatographic methods, was detected in the crude reaction mixture by infrared spectroscopy ($\nu_{\text{N=C=O}} = 2249 \text{ cm}^{-1}$). Support for the proposed mechanism was obtained by adding methanol to the reaction mixture, which led, according to TLC, to rapid consumption of the isocyanate and formation of compound **5.5** as the major reaction product. Formation of a carbamate by dehydration of the formamide with the Burgess reagent is unique to this example and has not, to the best of our knowledge, been previously reported. Furthermore, the formation of a carbamate was not observed for the dehydration of any *ortho*-carborane formamides under identical reaction conditions (see Chapter 4).



Scheme 5.3 – Proposed mechanistic basis for the formation of 5.5 via the isocyanate 5.12.

5.5 The Unexpected Formation of a Bis(imino)carboranyl Azetidine

After reaction with the Burgess reagent failed to generate the target isonitrile, three other dehydration methodologies (Scheme 5.2) were attempted. The first method involved treatment of compound **5.4** with POCl_3 . This approach was used by Zakharkin *et al.* in the preparation of 3-isocyano-1,2-dicarba-*closo*-dodecaborane (**4.3**, Chapter 4).⁹ Unfortunately, POCl_3 did not react with **5.4** to any appreciable extent, leaving mostly unreacted starting material. Treatment of **5.4** with thionyl chloride (SOCl_2) in the presence of excess NEt_3 , on the other hand, resulted in the loss of the formyl group and formation of the amine **5.3** (Scheme 5.2). Reaction of the formamide with triphosgene, a reagent that has been used previously to prepare isonitriles,¹⁰ formed, according to TLC, a new product that was subsequently isolated.¹¹

The IR spectrum of the main product of the triphosgene-mediated dehydration was surprisingly complicated compared to that of the corresponding *ortho*-carborane isonitriles. There were absorptions centered about 2152 cm^{-1} , which agree with expected values for the target isonitrile, and 2619 cm^{-1} , indicating the presence of BH groups (Figure 5.6). There were, however, additional peaks at 1732 , 1679 , and 1644 cm^{-1} , which at the time of analysis, were thought to have arisen from impurities in the sample. The

results of electrospray mass spectrometry (ESMS) experiments were not consistent with the expected product, and gave no signal indicating the presence of the desired isonitrile. There was, however, a major peak corresponding to exactly four times the mass of the target compound, which had a B₄₀ isotropic distribution pattern. It was not until a trapping experiment was attempted, that the actual structure of **5.7** was revealed (*vide infra*).

Due to the presence of what was thought to be isonitrile stretches in the IR spectrum, and the fact that there was only one major product visible by TLC, an attempt

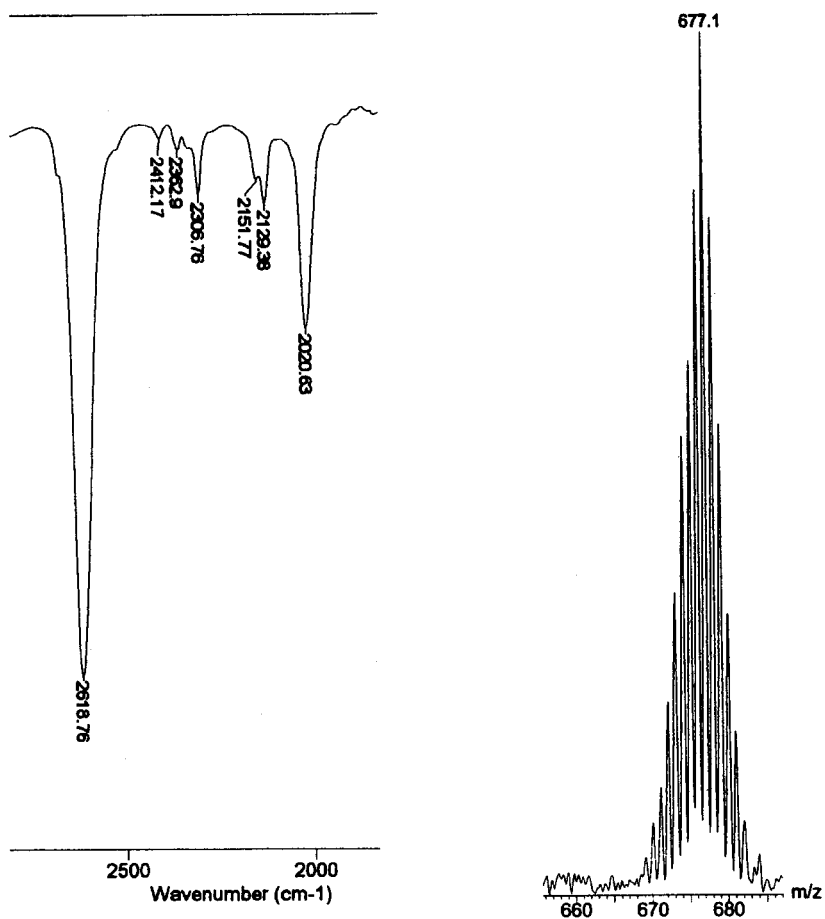
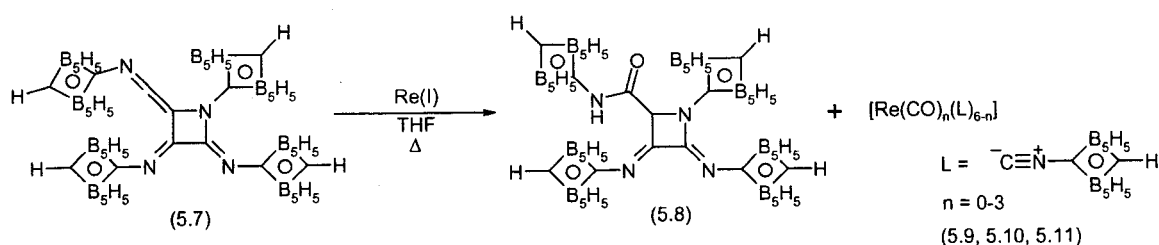


Figure 5.6 - Infrared (left) and ESMS (right) spectra of **5.7**.

was made to trap the target isonitrile as a means of establishing whether or not the ligand was actually being formed. The purified reaction mixture was treated with $[\text{NEt}_4]_2[\text{Re}(\text{CO})_3\text{Br}_3]$, which is known to form the isonitrile complex $[\text{Re}(\text{CO})_3\text{L}_2\text{Br}]$ ($\text{L} = \text{isonitrile}$) (Scheme 5.4).¹² Upon addition of the ligand, TLC analysis showed the formation of a new product, which was isolated by silica gel chromatography.



Scheme 5.4 – Hydrolysis and reaction of 5.7 in the presence of Re(I) .

X-ray quality crystals of the product were grown, and the resulting structure shown in Figure 5.7. Initially, the unit cell was determined to be in the orthorhombic Laue group. However, no adequate solution could be obtained. It was soon realized that the systematic absences of the data set were not consistent with any known orthorhombic system. Thus, changing the Laue symmetry to a monoclinic designation allowed a space group determination of C2/c . With the new space group, it was possible to establish a model, and in turn elucidate the chemical structure of the isolated product. Surprisingly, the X-ray structure revealed that the product was a racemic mixture of the bis(*para*-carboran-1-ylimino)azetidine derivative (5.8).

In addition to the difficulties encountered in the determination of the unit cell, it was also apparent from the electron difference map that a significant amount of disorder was present in the lattice. This feature is likely the source of the aforementioned difficulties in obtaining the correct unit cell. The source of this disorder was the partial occupancy of two different enantiomers in the same crystallographic site (Figure 5.8). A least-squares refinement revealed that one enantiomer is present in a four-fold excess over the other. However, the enantiomeric ratio is in fact 1:1 when the crystallographic inversion center inherent to the space group is taken into account. Inversion of the solution gives a four-fold excess of the other isomer, thereby giving a crystal containing an overall 1:1 ratio of enantiomers.

The four-membered azetidine ring was, as mentioned previously, modeled as the superposition of two enantiomers. In addition, the slightly different spatial requirements of each isomer prompted the modeling of overlapping carborane cages. A superimposed cage of the carborane designated cage A was identified in the difference map and modeled. However, a large number of restraints were required in order to maintain geometry and ideal thermal parameters. There was not enough residual electron density to attempt overlapping models of the other three icosahedral cages. Thus, the ensuing discussion regarding the structure of **5.8** was extrapolated from the major (80%) component of the X-ray solution. With only 20% occupancy, the extraction of structural data from the minor constituent is inappropriate.

The imino groups in **5.8** are located adjacent to one another, while the carboranyl amide is pendent from the 4-position of the ring. The carboranes bound to the imino

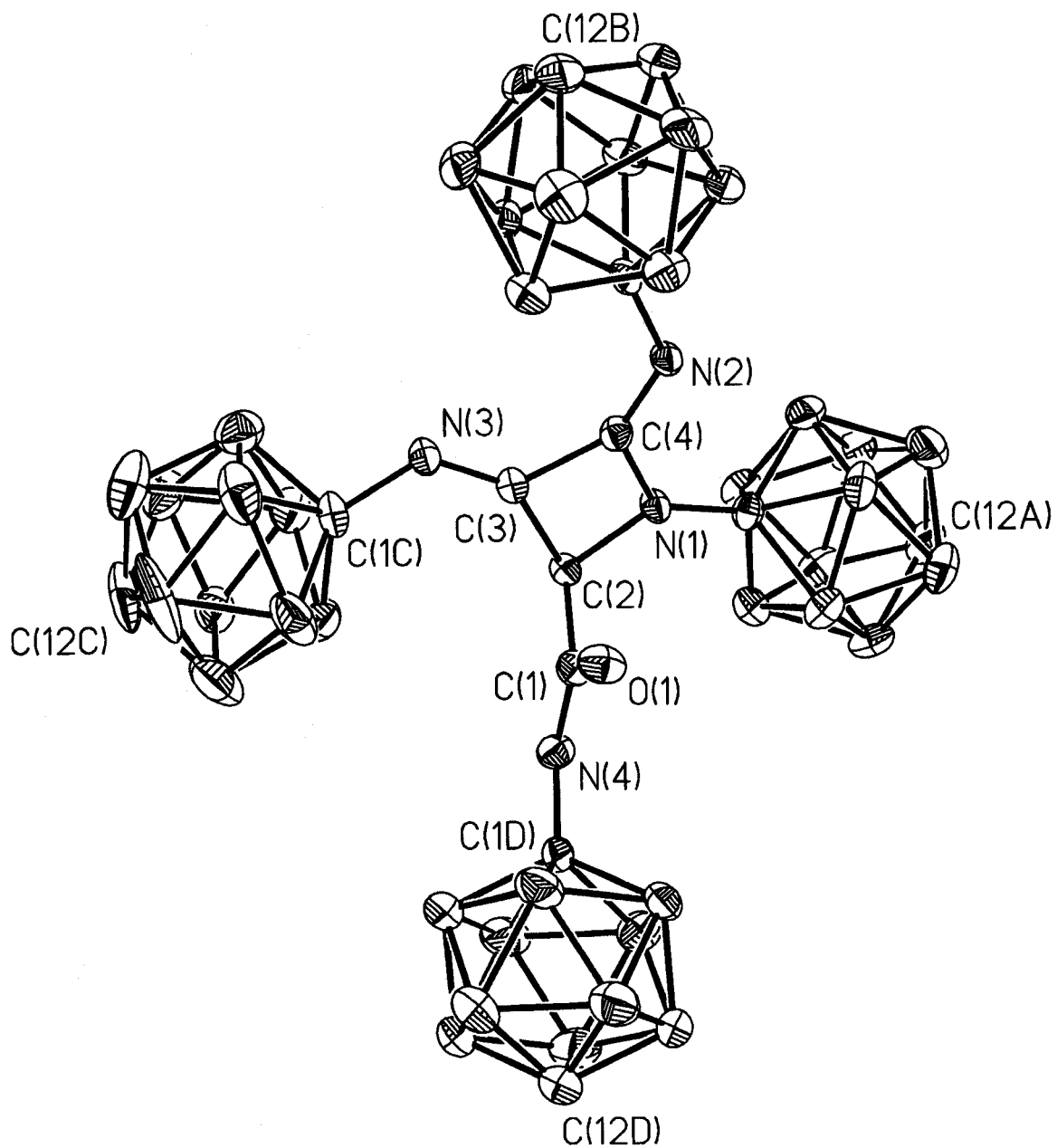


Figure 5.7 – ORTEP representation of 5.8. Thermal ellipsoids are shown at the 30% probability level. H-atoms and a THF of crystallization have been omitted for clarity.

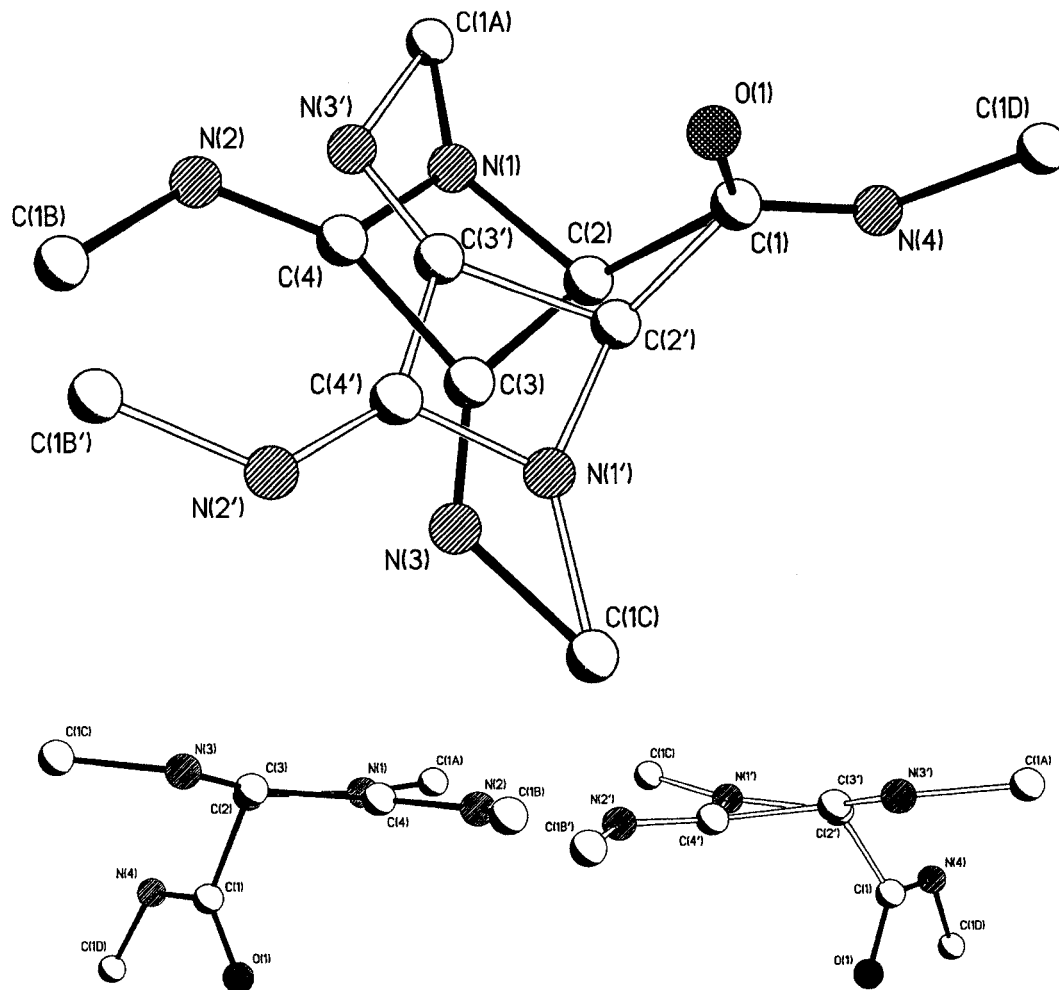


Figure 5.8 - Ball and stick representation of the disordered azetidine core. Both a) overlapping, face on and b) independent, edge-on solutions of 5.8 are shown. Carborane cages, hydrogen atoms, and solvent molecules have been omitted for clarity.

nitrogen atoms are oriented in a propeller-like fashion, while the carborane attached to the amide projects away from the ring in order to minimize steric interactions. A molecule of THF, which interacts with the amide N-H group through H-bonding, co-crystallized with each independent molecule.

The azetidine ring was found to contain a pucker of nearly 9° as found between the planes defined by N(1)-C(2)-C(4) and C(3)-C(2)-C(4). This is similar to the dihedral

angle (11°) found in L-azetidine-2-carboxylic acid.¹³ The dihedral angles in azetidine and azetidinium ions range between 0° and 27° with compounds bearing larger substituents approaching planarity.¹⁴ It has also been reported that in the case where exocyclic imino groups are present, the C=N functionalities introduce a torsional strain great enough to induce planarity in the heterocyclic ring.¹⁵ It is clear that in **5.8**, the azetidine tends toward a planar structure to minimize the interactions between the bulky carborane substituents. The bond distances and angles in **5.8** are in good agreement with other X-ray structures of simpler azetidine and carborane derivatives.¹⁶ Interestingly, the carbon-carbon bond distances in the azetidine ring (C(2)-C(3) 1.566(7)Å vs. C(3)-C(4) 1.524(7)Å) are different, indicating a potentially strong steric interaction between the carborane cages B and C. The slightly shorter N(1)-C(4) (1.401(6)Å) distance, relative to that of N(1)-C(2) (1.487(8)Å), may be due to an overlap between the lone pair on the ring nitrogen and the adjacent imino group. This is not, however, reflected in the imine bond distances, which are nearly identical (1.245(7)Å and 1.262(6)Å). The distances between the nitrogen atoms and the corresponding carborane carbon atoms to which they are attached are nearly identical, and the structures of the carboranes themselves are similar to other *para*-carborane structures reported in the literature.⁶ Compound **5.8** is the first example of a 2,3-bis(imino)azetidine to be characterized by X-ray crystallography.

High resolution Fast Atom Bombardment (FAB) mass spectrometry of the isolated sample confirmed that the major product was the azetidine **5.8**. The IR spectrum shows peaks corresponding to the carborane BH (2617 cm^{-1}) and the imine and amide groups (1602 cm^{-1} and 1716 cm^{-1}). The ^{13}C spectrum is uncomplicated, and shows three

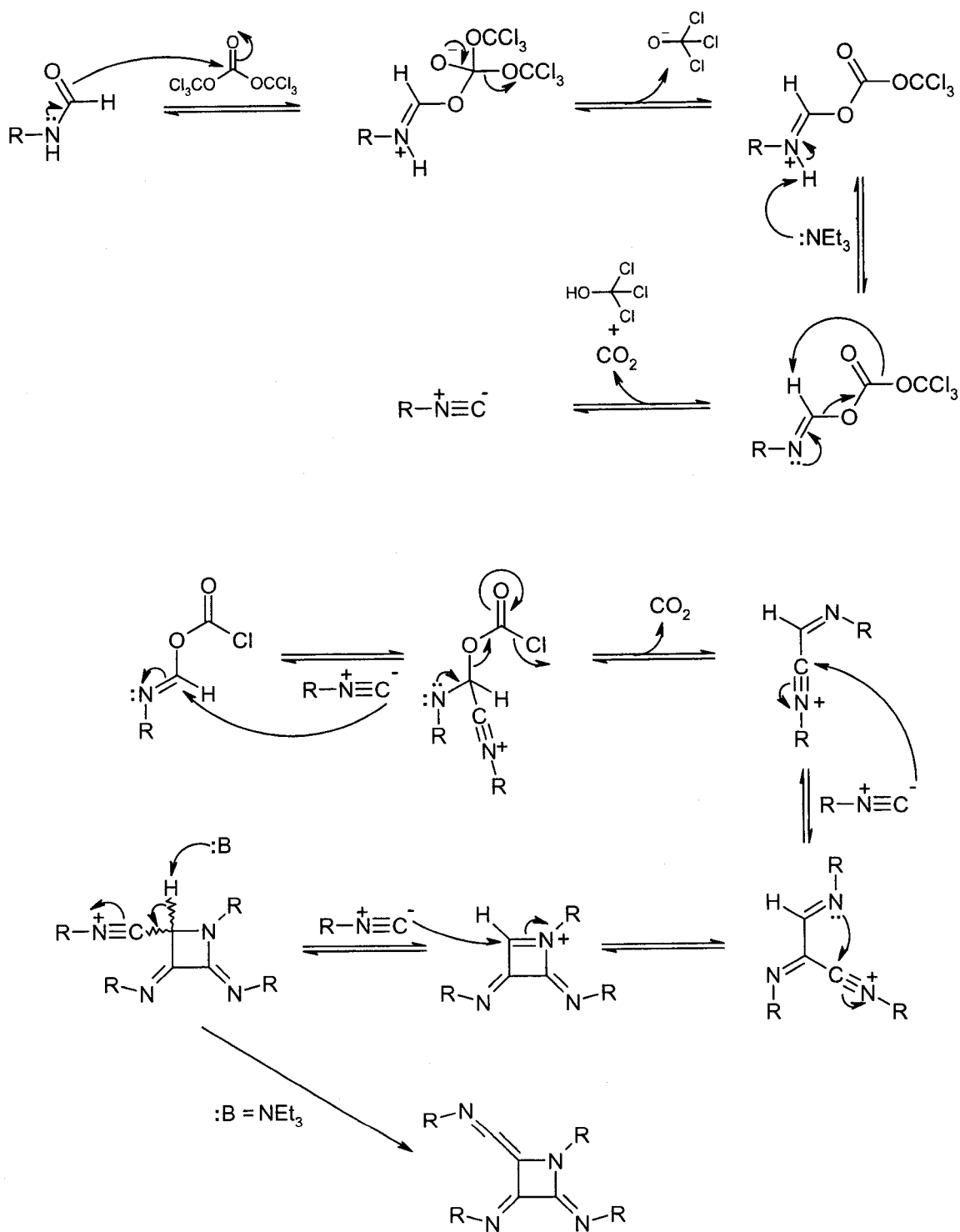
peaks shifted downfield which correspond to the amide carbonyl and two imine carbon atoms (162.73 ppm, 151.96 ppm and 148.66 ppm). Both the substituted and unsubstituted carbon atoms of the four carborane cages are also readily identifiable. The ^1H decoupled ^{11}B NMR spectrum showed four broad overlapping peaks, which provided little additional insight into the structure of **5.8**.

In light of the X-ray structure, the spectral data for compound **5.7** were re-analyzed. Simulation of the main isotopic peak in the high resolution electrospray mass spectrum indicated a B_{40} distribution and an elemental composition corresponding to that of the azetidine **5.7** (Figure 5.6). The previously unexplained peaks in the IR spectrum of **5.7** thus can be associated with the $\text{C}=\text{N}$ and $\text{C}=\text{C}$ groups found in compound **5.7**, which is in good agreement with values reported for related structures.^{17,18}

The ^{13}C NMR spectrum of **5.7** is more complicated than that of **5.8** (Figure 5.9). Given the number of observed peaks, it appeared as though there were two predominant species present in solution, which may be the result of inversion at the ring nitrogen. Although fluxional processes for substituted azetidines are known,¹⁹ they are typically not observed at room temperature. It is apparent, therefore, that the sterically demanding carborane substituents influence the energy barrier of inversion. Detailed variable temperature NMR and theoretical studies are required to comment further on the observed complexities of the NMR spectrum, which are subjects for future research.

5.6 Proposed Mechanism for the Formation of 5.7

The use of isonitriles to form heterocycles, including azetidines, is well established.²⁰ The formation of **5.7** under the mild reaction conditions described here is, however, exceptional. Deyrup and co-workers²¹ showed that N-aryl imines react with *t*-butyl isocyanide to form 2,3-bis(*t*-butylimino)azetidines. Following a similar mechanism, we believe that formation of the target isonitrile is followed by its attack on a reactive chloroformate intermediate (Scheme 5.5). Substitution reactions at vinylic sites are typically slow; however, in this case the electron-withdrawing carborane and chloroformate groups further activate this position to nucleophilic attack. The subsequent loss of CO₂ drives the initial reaction to completion. Successive reactions with two isonitrile ligands, followed by intramolecular ring closure, led to formation of the azetidine **5.7**. We believe that the reaction of **5.7** with [NEt₄]₂[Re(CO)₃Br₃], under the specified conditions, simply results in metal-mediated hydrolysis to yield amide **5.8** (Scheme 5.4). It should also be noted that altering the number of triphosgene equivalents in the reaction did not give the same result. Introducing the *para*-carborane formamide to 1/3 equivalents of triphosgene yielded primarily unreacted starting material, but also a small amount of the amine **4.1**.



Scheme 5.5 – Proposed mechanism for the formation of 5.7.

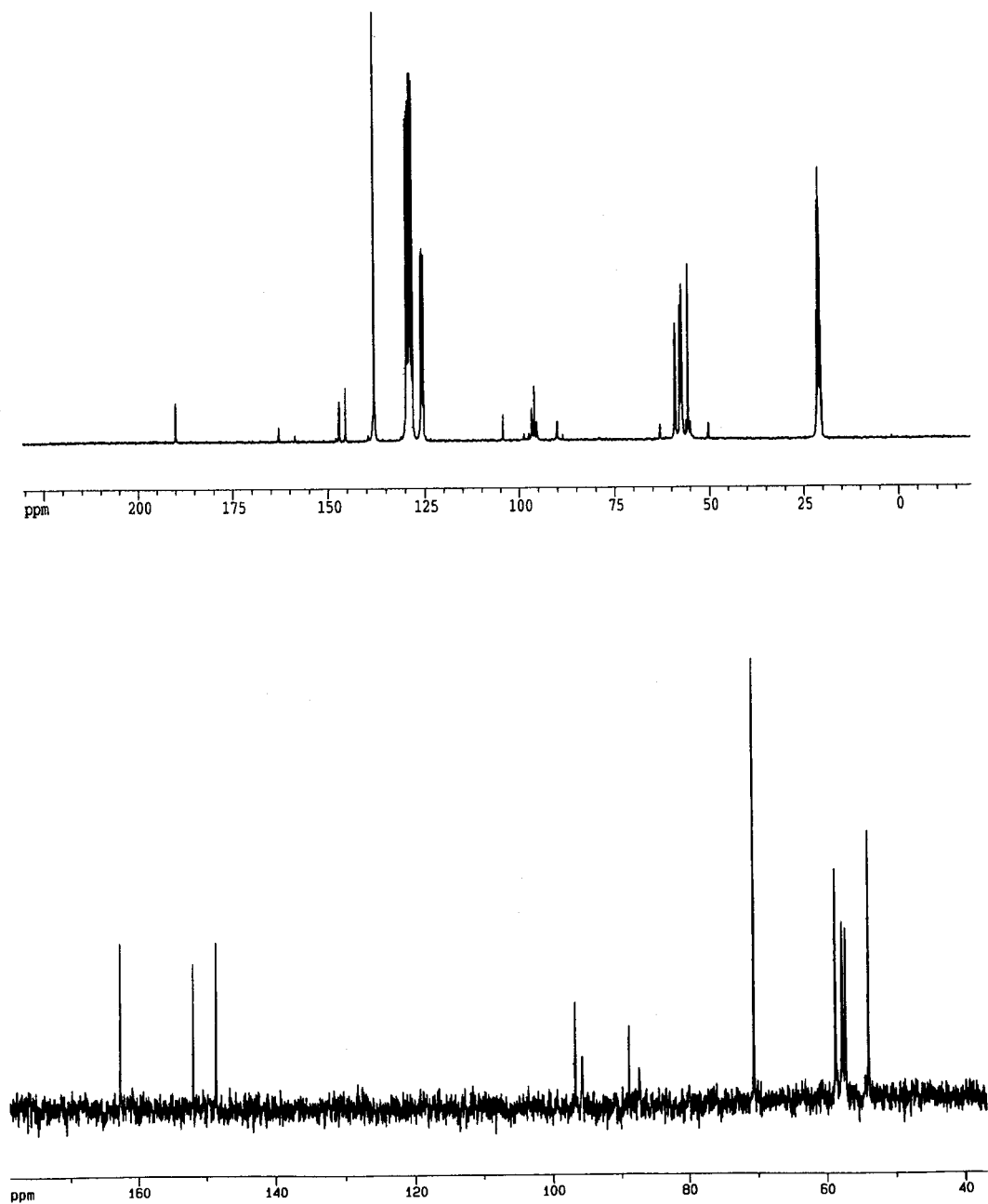


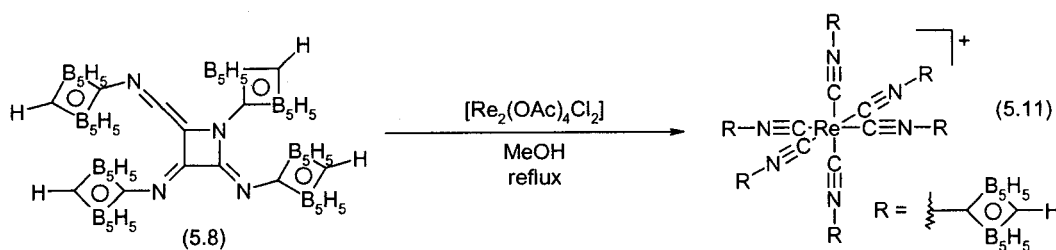
Figure 5.9 – ^{13}C NMR of 5.7 (top) and 5.8 (bottom)

5.7 Homoleptic *para*-Carborane Isonitrile Complex of Rhenium(I)

The yield of the azetidine **5.8** from the reaction of **5.7** with $[\text{Re}(\text{CO})_3(\text{solvent})_3]^+$ was low (27%). In an attempt to determine the composition of the reaction mixture, an ESMS analysis was performed. The crude reaction mixture from which **5.8** was isolated contained a number of other products, of which MS revealed a series of peaks corresponding to $[\text{Re}(\text{CO})_x(\text{CNR})_{6-x}]^+$ ($x = 0 - 3$, $L = \textit{para}$ -carboran(1)-yl) complexes. This suggests that the azetidine could potentially serve as a source of *p*-carborane isonitrile.²² In response to this, the synthesis of the hexacoordinate Re(I) isonitrile complex **5.11** was attempted, using the strategy described for the synthesis of compound **4.24** (Chapter 4). Reaction of the dirhenium tetracarboxylate **4.22** with 1.5 equivalents of the azetidine **5.7** heated to reflux in ether or THF did not yield the desired product, but led to the re-isolation of the starting materials. A new product was observed when the azetidine **5.7** was added to $\text{Re}_2(\text{OAc})_4\text{Cl}_2$ and the reaction mixture heated to reflux in methanol (Scheme 5.6). A TLC analysis of the reaction indicated the presence of unreacted starting materials and a new compound, which was isolated in low yield (10%) by precipitation following ion exchange with KPF_6 . In an effort to improve the yield, the reaction was carried out in diglyme heated to reflux ($T = 162^\circ\text{C}$), which, unfortunately, had no benefit.

The electrospray mass spectrum of the new product exhibited only one major peak at an m/z value of 1201.6, which had an isotopic peak distribution consistent with that expected for complex **5.11**. This data was further supported by high resolution Fast Atom Bombardment (FAB) mass spectrometry, which exhibited the precise mass and

isotope distribution expected for the proposed target, $C_{18}H_{66}B_{60}N_6Re$ or $[Re-(CNR)_6]^+$ ($R = C_2B_{10}H_{11}$). The IR spectrum of **5.11** exhibited peaks corresponding to the CH (3046 cm^{-1}) and BH (2621 cm^{-1}) stretches, as well as a broad CN stretch at 2091 cm^{-1} . The latter value is in close agreement with the CN stretching frequency reported for hexakis(phenyl isocyanide)technetium(I).²³



Scheme 5.6 – Synthesis of the hexacoordinate *Re(I)* *para*-carborane isonitrile complex (**5.11**).

The 1H NMR of **5.11** showed a singlet appearing at 3.31 ppm (CH) and a broad multiplet between 3.7 – 1.5 ppm, which is representative of the signals typically observed for hydrogen atoms bound to the boron atoms of the cage (Figure 5.10). The proton-decoupled ^{11}B spectrum contains two resonances at -11.71 and -15.13 ppm, which is consistent for a mono-substituted *para*-carborane derivative, as the ligand is in a homoleptic octahedral complex (Figure 5.11).

Air stable, single crystals of compound **5.11**, were grown from an acetone solution at room temperature. X-ray crystallography, using synchrotron radiation, confirmed that the structure of the isolated product was in fact the desired homoleptic *Re(I)* complex (Figure 5.13). The compound crystallized in the monoclinic $C2/c$ space group, with one molecule in the asymmetric unit ($Z=8$). The *Re(I)* center is surrounded by a nearly octahedral arrangement of six *para*-carborane isonitrile ligands. The average

Re-C distance, 2.030(6) Å, ranging from 2.015(6) Å (Re-C5) to 2.052(7) Å (Re-C6), is similar to the metal-carbon atom distances reported for the only other published structure of a homoleptic isonitrile-Re(I) complex.²⁴ The average isonitrile bond distances, 1.166(8) Å, ranges from 1.139(8) Å to 1.197(8) Å, is also comparable to the distances reported for other isonitrile complexes.²⁵

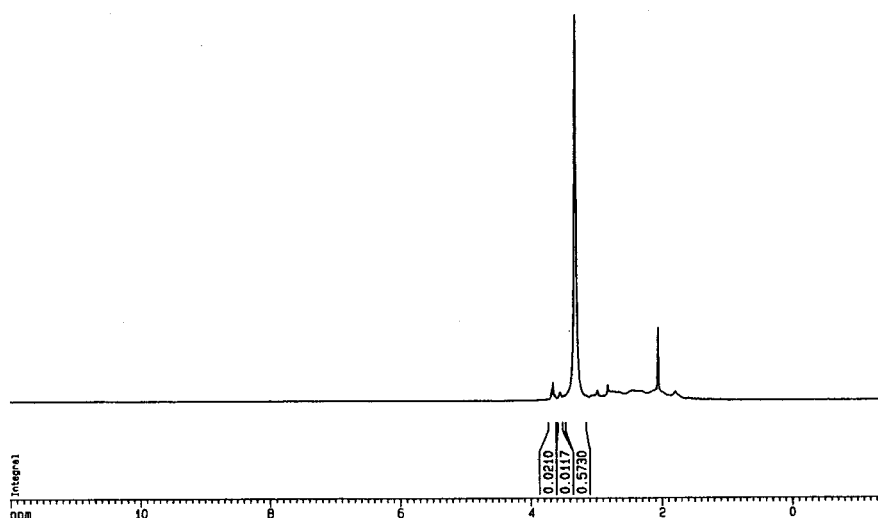


Figure 5.10 - ^1H NMR spectrum of 5.11 in acetone- d_6

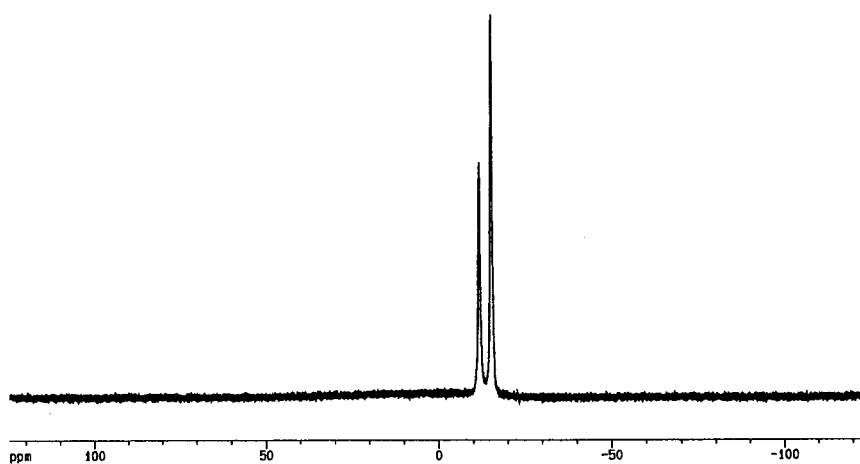


Figure 5.11 - $^{11}\text{B}\{^1\text{H}\}$ NMR spectrum of 5.11.

The Re-C-N bond angles in **5.11** are essentially linear, with the average angle being $176.7(5)^\circ$, ranging from $173.7(5)^\circ$ to $179.3(5)^\circ$. The orientation of the carborane substituents, on the other hand, shows remarkable variation, reflecting the steric crowding of the bulky carborane ligands. The average C-N-C bond angle is $163.3(7)^\circ$, ranging from $147.2(6)^\circ$ to $174.4(7)^\circ$. The angles at N2 ($156.1(6)^\circ$) and N5 ($147.2(6)^\circ$) are similar to the smallest bend angles in a recently reported homoleptic Cr(0) complex of isocyanoferrocene.²⁶

Substantial bending at the nitrogen in isonitrile complexes is not unusual and has been previously observed.^{18,27} In $[\text{Tc}(\text{CNtBu})_4(\text{bpy})]\text{PF}_6$, for example, one of the isonitrile ligands trans to a bipyridine ligand shows a bend of $148(2)^\circ$.²⁸ This type of bending is commonly attributed to donation of electron density from the metal to the ligand according to valence bond theory (Figure 5.12). For $[\text{M}(\text{CN-tC}_4\text{H}_9)_6]$ (M = Mo, Cr), a plot of decreasing C-N-C bending angle shows an approximately linear correlation with increasing metal-carbon bond length.²⁹ The analogous plot for **5.11**, however, does not show the same relationship, suggesting that the pronounced bending at N2 and N5 is most likely the result of packing effects associated with the bulky carborane ligand.

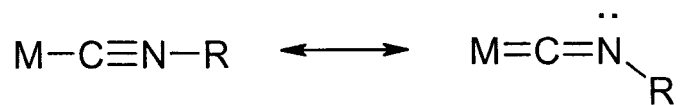


Figure 5.12 - Valence bond theory representation of metal back-donation.

In compound **5.11**, there is no notable elongation of the C5-N5 or C2-N2 bonds compared to the other C-N bonds in the complex. In $[\text{Tc}(\text{CNtBu})_4(\text{bpy})]\text{PF}_6$, the C-N

bond distance for the isonitrile having a significant bending angle at the nitrogen atom is 1.25(2) Å as compared to 1.15(2) Å for the other “unbent” ligands. The Re-C5 bond distance in **5.11** is identical to that of Re-C1, where the bend at nitrogen is significantly less (179.3(7)°). Furthermore, the Re-C5 distance in **5.11** is only marginally shorter than for the metal-carbon distances reported in the Re and Tc hexa(*t*-butyl) isocyanide complexes, which did not report significant bending at any isonitrile nitrogen atom.

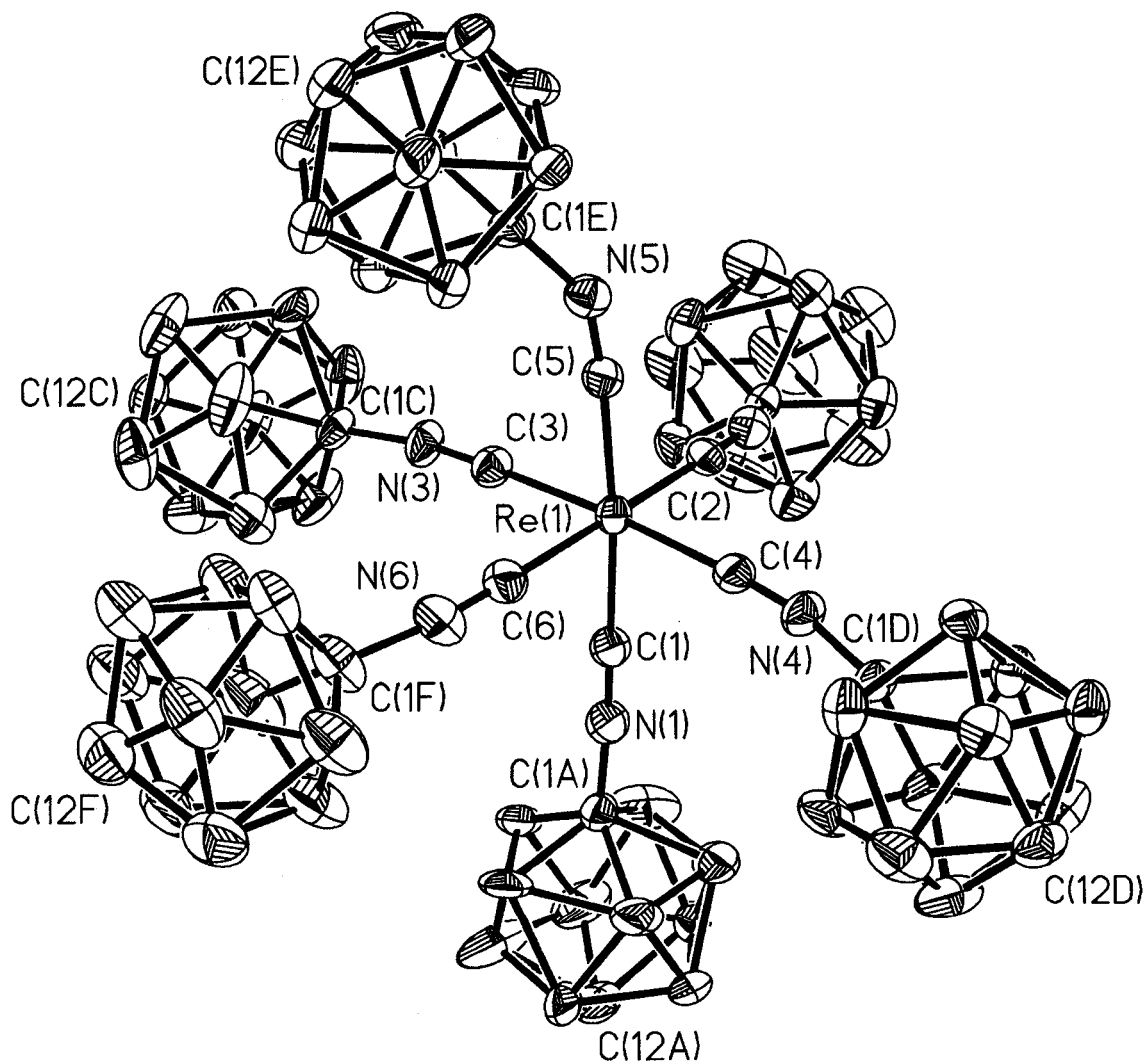


Figure 5.13 - ORTEP representation of **5.11** with 30% thermal ellipsoids. Hydrogen atoms and counter ions removed for clarity.

Bond	Distance (Å)	Bond	Angle (°)
Re(1)-C(1)	2.025(6)	Re(1)-C(1)-N(1)	179.0(5)
Re(1)-C(2)	2.026(6)	Re(1)-C(2)-N(2)	173.8(5)
Re(1)-C(3)	2.038(5)	Re(1)-C(3)-N(3)	177.8(5)
Re(1)-C(4)	2.029(5)	Re(1)-C(4)-N(4)	176.4(5)
Re(1)-C(5)	2.016(5)	Re(1)-C(5)-N(5)	174.5(5)
Re(1)-C(6)	2.048(7)	Re(1)-C(6)-N(6)	177.7(6)
C(1)-N(1)	1.193(8)	C(1)-N(1)-C(1A)	175.2(9)
C(2)-N(2)	1.150(7)	C(2)-N(2)-C(1B)	155.9(6)
C(3)-N(3)	1.168(7)	C(3)-N(3)-C(1C)	169.4(6)
C(4)-N(4)	1.170(7)	C(4)-N(4)-C(1D)	169.2(6)
C(5)-N(5)	1.172(7)	C(5)-N(5)-C(1E)	147.3(6)
C(6)-N(6)	1.145(8)	C(6)-N(6)-C(1F)	164.1(7)

Table 5.2 – Selected bond lengths (Å) and angles (°) of **5.11**.

The six carborane cages were essentially symmetrical icosahedra with an average B-B bond distance of 1.775(15) Å, ranging from 1.712(15) Å to 1.841(18) Å, while the average boron-carbon bond distance was 1.701(13) Å.³⁰ The solid-state structure of **5.11** contained three different counter ions: acetate, ReO_4^- , and PF_2O_2^- , the latter of which is an oxidative product of PF_6^- . The PF_2O_2^- and ReO_4^- occupied the same crystallographic site in a 77:23 ratio as determined by least-squares analysis. The presence of the various counter ions was verified by negative ion ESMS (Figure 5.14). Subsequent anion exchange experiments enabled a complete conversion to the chloride salt, which was again confirmed by ESMS.

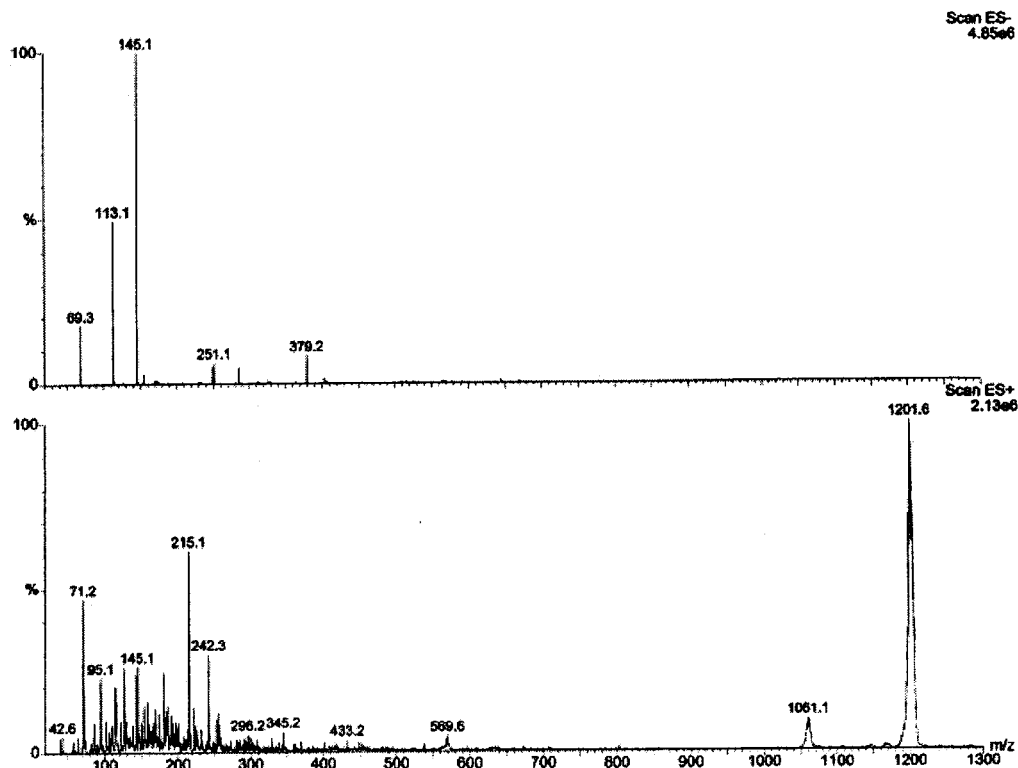


Figure 5.14 – ESMS spectrum of 5.11 prior to ion exchange.

Compound **5.7** was not reactive to heating in a variety of solvents, whether in the presence or absence of strong Lewis acids (HCl, ZnCl₂, CuCl), even when reactions were allowed to proceed for extended periods of time. We conclude then, that interaction of the azetidine with rhenium was thus required in order to initiate complex formation.

The first step in the formation of **5.11** is likely the coordination of the azetidine to the Re complex. Coordination of the azetidine to Re₂(OAc)₄Cl₂ likely occurs at one of the nitrogen atoms through the displacement of one of the axial carboxylate ligands, according to the work of Walton and Andersen.^{31,32} Re₂(OAc)₄Cl₂ is known to form two types of coordination complexes when placed in the presence of Lewis bases

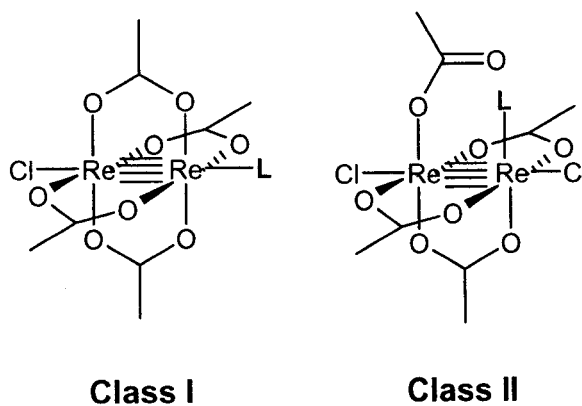


Figure 5.15 – Class I and II complexes of $Re_2(OAc)_4Cl_2L$.

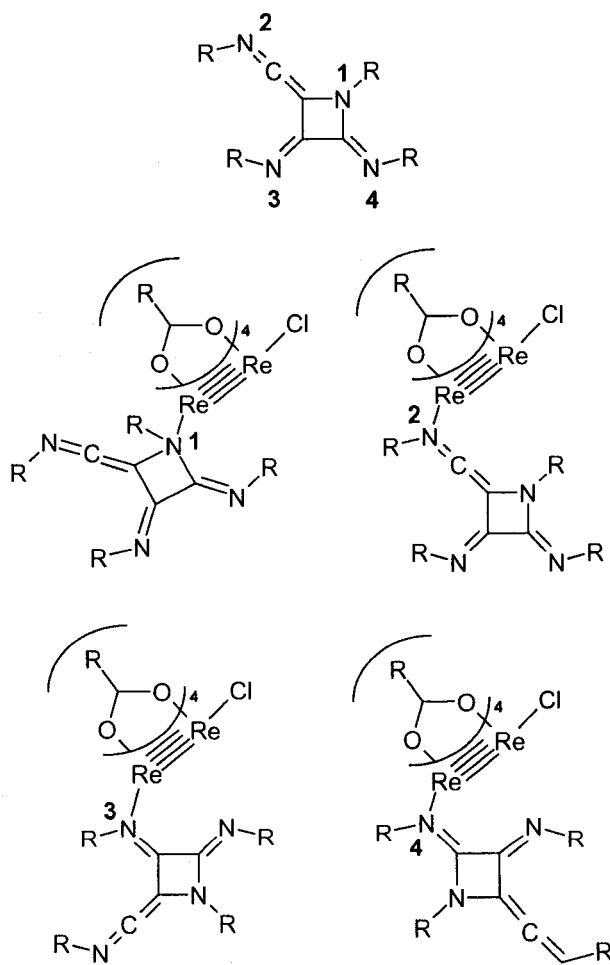


Figure 5.16 – Possible coordination modes between 5.7 and $Re_2(OAc)_4Cl_2$

(Figure 5.15).³³ Class I complexes form with strong, bulky σ -electron donors,³⁴ where coordination to the metal occurs in the axial position. Smaller Lewis bases that possess some π -accepting capacity, form class II complexes, in which the ligand binds in an equatorial fashion. The steric bulk associated with **5.7** suggests that it will form a class I complex. Examination of compound **5.7** revealed four possible sites at which rhenium could bind (Figure 5.16). In light of the hydrolysis of **5.7** in the presence of $[\text{Re}(\text{CO})_3(\text{solvent})_3]^+$ to give **5.8**, however, it is likely that coordination occurs at the N4 position (site 2, Figure 5.15). The path by which the azetidine-Re complex subsequently converts to compound **5.11**, is at present, unknown.

5.8 *ortho*- versus *para*-Carborane Formamides

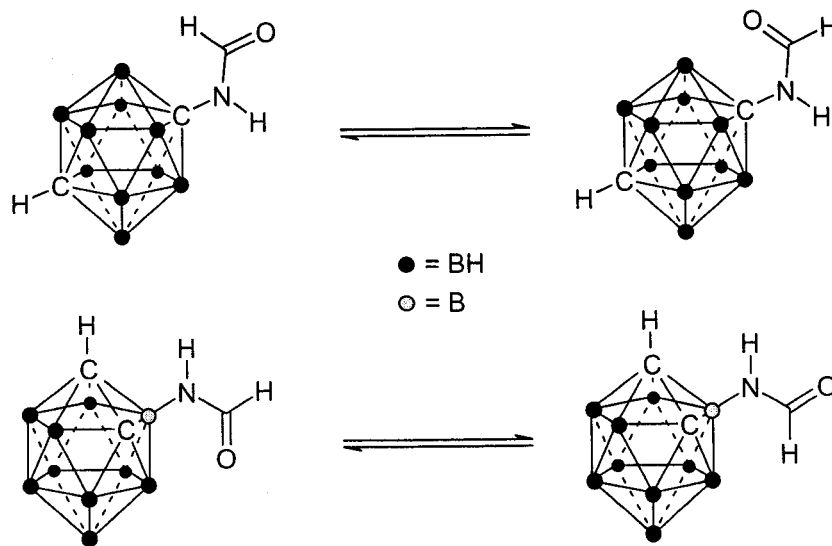
One unexpected observation from the aforementioned research is that compound **4.2**, reacts very differently than compound **5.4**. In order to gain a better understanding of the difference in reactivity between the formamides **4.2** and **5.4**, the solid and solution-state structures were analyzed in detail.

While the *ortho*-carborane formamide **4.2** and the *para*-isomer **5.4** appear to be structural isomers, there are some fundamental differences between the two compounds. The solid-state packing of the **4.2** prefers the *cis* (*Z*) orientation, while the *para*-carborane formamide prefers the *trans* (*E*) orientation. Furthermore, there are slight differences in the atomic distances of the two compounds (Scheme 5.7). The distance between the formyl nitrogen and the carborane cage in **4.2** is 1.469(3)Å, which is longer than that found in **5.4** (1.4336(18)Å). This suggests a stronger electronic interaction between the

carbon-vertex of *para*-carborane and the formyl nitrogen than the corresponding boron-vertex of the *ortho* isomer. The N-C(formyl) distance is slightly longer for the *ortho*-isomer, suggesting a greater overlap of the nitrogen lone-pair in **5.4** with the π -system of the adjacent carbonyl group. This is also supported by the longer H-bond contacts for **4.2** (2.909Å for **4.2** and 2.839Å for **5.4**) between adjacent molecules.

	B-N (Å)	C-N (Å)	N-CHO(Å)	N-C-O (°)	C-N-C (°)	B-N-C(°)
4.2	1.469(3)	-	1.350(3)	125.2(2)	-	125.6(2)
5.4	-	1.4336(18)	1.3376(18)	123.27(13)	125.67(12)	-

Table 5.1 – Comparison of selected bond lengths and angles for compounds **4.2** and **5.4**.



Scheme 5.7 – Rotational isomers of **4.2** and **5.4**.

5.9 VTNMR Analysis of the Formyl-Carborane Isomers

Formamides containing bulky substituents can exist in two discreet (*E* vs. *Z*) conformations (Scheme 5.7). If the barrier to rotation about the N-CHO bond is large,

two major conformations can often be observed on the NMR time scale. Variable temperature NMR of both formamide isomers should help to determine the degree that the nitrogen lone pair participates in the adjacent carbonyl π -system. Spectra were obtained at five-degree intervals as a means of identifying the coalescence temperature (rotational barrier) about the nitrogen-carbonyl bond. Spectra were then re-acquired at one-degree intervals in the necessary temperature range. Due to complications brought about by the presence of the cage B-H atoms and the quadrupolar relaxation caused by other neighbouring nuclei, an exact coalescence temperature could not be determined. Instead, the coalescence temperature was narrowed to a small (five degree) interval.

The barrier of rotation experienced by the formyl group about the C-N bond would be a direct measure of the π -delocalization, hence the degree of influence the electron-deficient carborane cage has on the adjacent formyl group. The ^1H NMR spectra of **4.2** and **5.4** clearly show at least two distinct conformations. Figures 5.18 and 5.19 show a series of spectra obtained at five-degree intervals as an overview of the solution-state behaviour of both formamides. It is important to note that while these methods give some insight toward the reactivity of the formyl group, they do not explain the observed preference of one conformer (*Z* vs. *E*) over the other.

^1H NMR spectra of compound **5.4** were collected over a temperature range of 218 K to 333 K in toluene- d_8 (Figure 5.17). The doublet at 7.63 ppm (2290 Hz, $^3J_{\text{trans}} = 10.5$ Hz) is associated with the *trans* isomer, while the less intense, higher frequency doublet at 7.74 ppm (2320 Hz, $^3J_{\text{cis}} = 8.4$ Hz, not visible in Figure 5.17) indicates the presence of

a minor *cis*-oriented population. Upon warming, the peaks coalesce between 303 and 308 K.

For compound **4.2**, the minor component is the *trans* isomer, which is in agreement with the solid-state structure (Figure 5.18). The low intensity doublet present at 8.09 ppm (2430 Hz, $^3J_{\text{trans}} = 11.8$ Hz), visible as a small shoulder of at 273 K, represents the *trans* population; while the downfield broad singlet at 7.45 ppm arises from the *cis* population. Coalescence for this derivative appears to occur between 323 and 328 K.

The higher barrier of interconversion exhibited by the *ortho*-carborane formamide must be a result of the increased double bond character of the formyl C-N bond. These results correlate with the observed lower reactivity of **5.4** compared to **4.2** toward various electrophilic reagents.

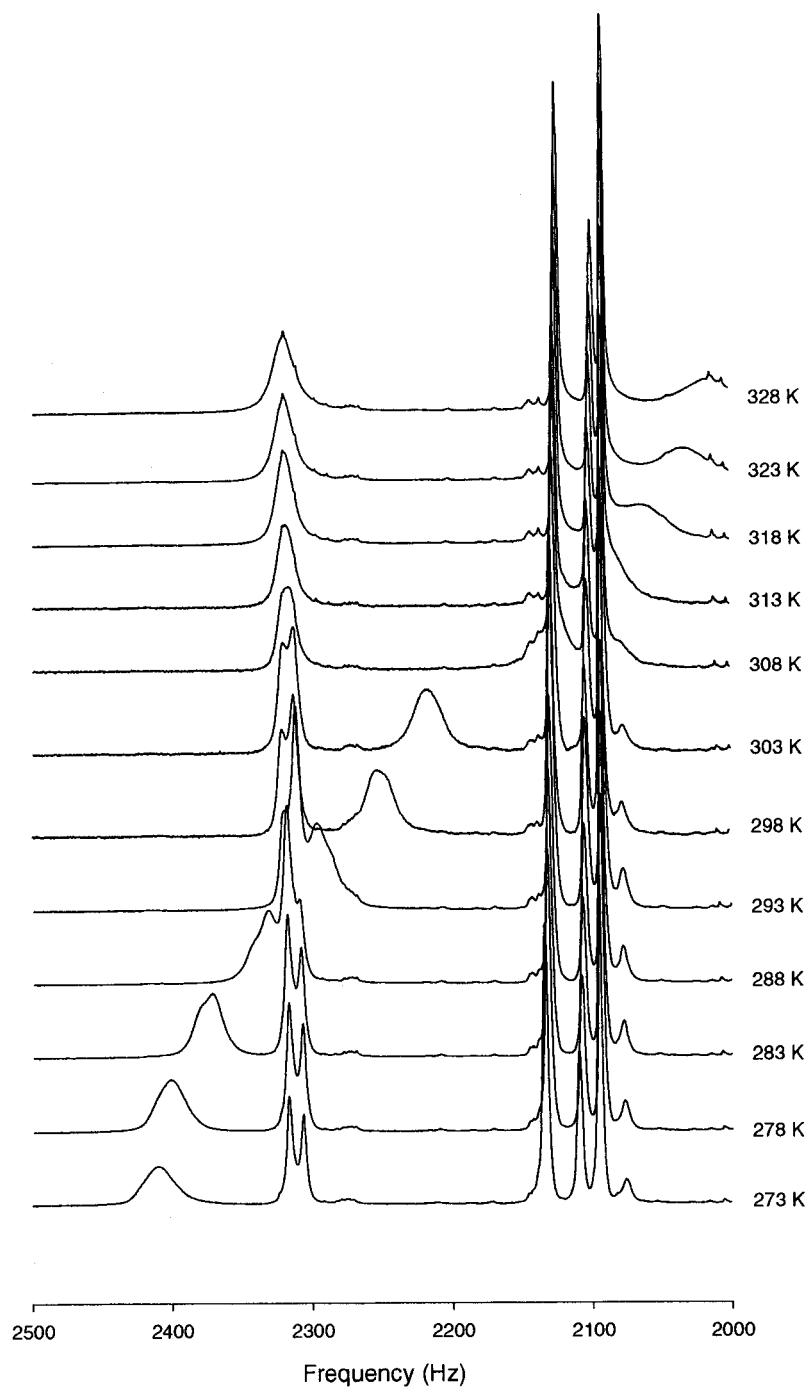


Figure 5.17 – Stacked VTNMR plot of 5.4.

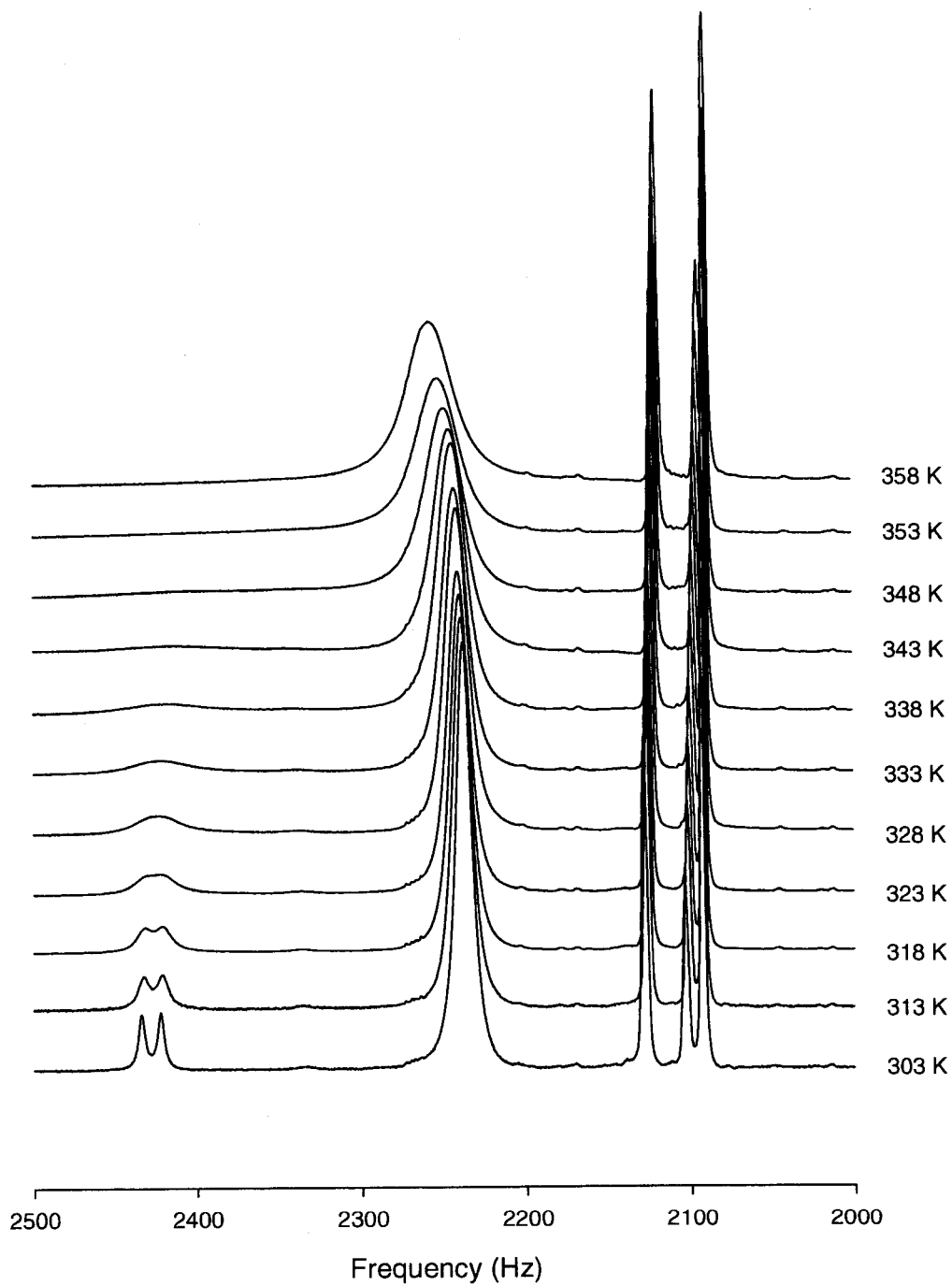


Figure 5.18 – Stacked VTNMR plot of 4.2.

5.10 Summary and Future Work

The *para*-carboranyl formamide **5.4** was synthesized in an effort to generate the C-linked isonitrile analogue of compound **4.3**. The reaction of **5.4** with the Burgess reagent led to the surprising formation of the methyl carbamate **5.5** which was characterized by X-ray crystallography. Additional attempts to dehydrate compound **5.4** using the procedure reported by Zakharkin and co-workers was not successful, affording only unreacted starting material. Other attempts, including the use of thionyl chloride were attempted and found to cause rapid deformylation, giving 1-amino-*para*-carborane (**5.3**). Upon treatment with triphosgene, a new product was isolated and later shown to be the novel bis(imino)azetidine **5.7**.

Compound **5.7** was subsequently used to synthesize the desired homoleptic rhenium complex **5.11**. The X-ray structure of hexakis(*para*-carboran-1-yl-isonitrile)Re(I) was obtained, conclusively demonstrating that the azetidine **5.7** can, under the specified reaction conditions, act as a source of *para*-carborane isonitrile. The bis(imino)azetidine **5.7** is also an ideal synthon from which to prepare bifunctional metal-isonitrile derivatives through derivatization of the remaining carborane CH vertices. Substitution of the second carbon vertex can be performed either prior to or after complexation.

Future work should entail investigating the mechanisms for the formation of **5.7** and the homoleptic metal complex **5.11**. In addition, the feasibility of using **5.11** as a metal-based BNCT agent should also be explored through the preparation of the technetium analogue.

5.11 Experimental

Synthesis of 1-carboxy-1,12-dicarba-*closo*-dodecaborane (5.1)

para-Carborane (5.0 g, 34.67 mmol) was dissolved in dry ether (100 mL) and cooled to -78°C . *n*-BuLi (1.6 M in hexanes, 21.67 mL, 34.67 mmol) was added dropwise and after 2 hours the reaction was allowed to slowly warm to room temperature. The reaction vessel was subsequently cooled to -78°C and solid CO_2 (~10g) added in small portions. Upon complete addition of the CO_2 , the cold bath was removed and the reaction stirred for 1 hour while warming to room temperature. The reaction mixture, a heterogeneous, colourless solution, was quenched with distilled, deionized water (100 mL). The layers were separated and the aqueous phase acidified to $\text{pH} < 2$. The aqueous layer was extracted with ether (3 x 50 mL) and all organic fractions pooled, dried over Na_2SO_4 , and gravity filtered; giving a colourless, transparent filtrate. The solvent was removed by rotary evaporation giving the product (6.31 g, 97%) as a white amorphous solid: mp $161\text{--}162^{\circ}\text{C}$; T.L.C. (30% ether in pet. ether): $R_f = 0.41$; ^1H NMR (200 MHz, CDCl_3): δ 10.79 (br s, 1H, COOH), 3.9 – 0.9 (m, 10H, BH), 2.83 (br s, 1H, CH); ^{13}C NMR (50 MHz, CDCl_3): δ 168.33, 78.47, 62.83; ^{11}B NMR (96 MHz, CDCl_3): δ -12.94, -14.58; IR (CH_2Cl_2 , cm^{-1}): 3065, 2621, 1720; MS (CI, NH_3): m/z observed boron isotopic distribution at 205 ($\text{M}+\text{NH}_4$), 159 ($\text{M}+\text{H}-\text{CO}_2$).

Synthesis of 1-*tert*-butylcarbonyl-1,12-dicarba-*closo*-dodecaborane (5.2)

To a round bottom flask containing freshly distilled *tert*-butanol (150 mL) was added the carboxylic acid (3.0 g, 15.94 mmol). Stirring was initiated under dry nitrogen

when dimethylaminopyridine (DMAP) (catalytic amount) and freshly distilled triethylamine (TEA) (4.59 g, 6.32 mL, 45.37 mmol) were added. The solution was stirred for 5 minutes and diphenylphosphoryl azide (DPPA) (4.82 g, 3.78 mL, 17.53 mmol) was added. The reaction was heated to reflux for 20 hours. Upon cooling to room temperature, excess tert-butanol was removed by rotary evaporation giving a viscous yellow oil. The crude product was purified by flash silica gel chromatography (gradient elution, 100% hexanes to 50% ether in hexanes, 2% intervals) giving pure carbamate (2.94 g, 71 %) which showed: mp 168-173°C; T.L.C. (1:1 Ether in Hexanes): $R_f = 0.68$; ^1H NMR (200 MHz, CDCl_3): δ 5.00 (br s, 1H, NH), 4.10 – 0.9 (br m, 10H, BH), 2.63 (br s, 1H, CH), 1.36 (s, 9H, CH_3); ^{13}C NMR (50 MHz, CDCl_3): δ 151.48, 88.97, 81.43, 55.22, 28.23; ^{11}B NMR (96 MHz, CDCl_3): δ -12.01, -15.98; IR (CH_2Cl_2 , cm^{-1}): 3433, 3282, 3070, 3068, 3046, 3007, 2983, 2614, 1742, 1721, 1700; MS (CI, NH_3): m/z observed boron isotopic distributions at 277 (M+ NH_4), 260 (M+H), 204 (M+H-C(CH_3) $_3$).

Synthesis of 1-amino-1,12-dicarba-closo-dodecaborane (5.3)

Method A: The carbamate **5.2** (2.84 g, 10.95 mmol) was dissolved in dry methylene chloride (100 mL) and to it was added trifluoroacetic acid (TFA) (30 mL). The reaction was maintained at ambient temperature for 8 h. Excess TFA and solvent were removed *in vacuo* giving an off-white semi-solid which was subsequently taken up in ether (100 mL) and washed with 1N NaOH (3 x 100 mL) then distilled water (3 x 100 mL). All aqueous layers were pooled and further washed with ether (1 x 100 mL). Both organic fractions were pooled, dried over Na_2SO_4 and gravity filtered. The remaining solvent was removed

by rotary evaporation giving a crude white solid, which was purified by flash silica gel chromatography (gradient elution, 100% hexanes to 20% ether in hexanes, 1% intervals). The product (1.74 g, >99%) an amorphous white solid showed: mp 158°C; T.L.C. (1:1 Ether in hexanes): $R_f = 0.52$; $^1\text{H NMR}$ (200 MHz, CDCl_3): δ 3.90-0.6 (br m, 12H, BH, NH_2), 2.75 (br s, 1H, CH); $^{13}\text{C NMR}$ (50 MHz, CDCl_3): δ 63.68, 50.41; $^{11}\text{B NMR}$ (96 MHz, CDCl_3): δ -11.36, -15.78; IR (cm^{-1} , CH_2Cl_2): 3084, 3027, 2597; MS (CI, NH_3): m/z observed boron isotopic distribution at 160 (M+H).

Method B: *para*-Carborane (0.327 g, 2.27 mmol) was dissolved in freshly distilled ether (20 mL) under dry N_2 . The reaction vessel was cooled to -78°C whereupon n-BuLi (1.6M in hexanes, 1.40 mL, 2.24 mmol) was added dropwise. The cold bath was removed and the reaction mixture allowed to warm to room temperature (2 hrs). To a separate flask was added methoxyamine·HCl (0.379 g, 4.54 mmol). The solid was cooled to -78°C and to it was added MeLi (1.4 M in diethyl ether, 6.42 mL, 9.0 mmol) dropwise. Stirring was maintained at -78°C for 2 hours at which time the *para*-carborane anion was transferred via glass syringe into the methoxyamine solution followed by an ether wash (5 mL). The reaction mixture was allowed to warm to -15°C stirring over 2 hours. Distilled, de-ionized water (10 mL) was added to quench the reaction after which the vessel was allowed to warm to room temperature. The resulting bi-phasic solution was transferred to a separatory funnel with distilled, de-ionized water (1 x 15 mL) and ether (1 x 15 mL). The aqueous phase was washed with ether (3 x 25 mL). All organic fractions were combined, dried over Na_2SO_4 and gravity filtered, giving a clear, colourless filtrate.

Excess solvent was removed by rotary evaporation. The crude product was purified by flash silica chromatography (gradient elution, 100% hexanes to 20% ether in hexanes, 1% intervals) giving the purified amine (0.090 g, 25%).

Synthesis of 1-formyl-1,12-dicarba-*closo*-dodecaborane (5.4)

The amine **5.3** (1.18 g, 7.41 mmol) was dissolved in formic acid (~50 mL) and the reaction brought to reflux for 36 hours. Upon cooling to room temperature the excess acid was removed by rotary evaporation giving an off-white solid. The crude product was taken up in CH₂Cl₂ (50 mL) and washed with a saturated solution of NaHCO₃ (2 x 50 mL) and 1N HCl (2 x 50 mL). The sodium bicarbonate and HCl solutions were separately pooled and individually washed with CH₂Cl₂ (1 x 50 mL). All organic fractions were pooled, dried over Na₂SO₄ and gravity filtered giving a transparent colourless filtrate. Remaining solvent was removed by rotary evaporation and the crude product was purified by flash silica gel chromatography (gradient elution, 100% hexanes to 50% ether in hexanes, 2.5% intervals) giving pure formamide (1.207 g, 87%) as a semi-solid, which showed: T.L.C. (5% MeOH in CH₂Cl₂): R_f = 0.70; ¹H NMR (200 MHz, CDCl₃): δ 7.91 (d, 1H, ³J = 10.9 Hz, CHO), 7.38 (br d, 1H, NH), 3.90-0.50 (br m, 10H, BH), 2.66 (br s, 1H, CH); ¹³C NMR (50 MHz, CDCl₃): δ 162.93, 87.14, 55.22; ¹¹B NMR (96 MHz, CDCl₃): δ -6.0, -9.0; IR (CH₂Cl₂, cm⁻¹): 3178, 3061, 2607, 1693; MS (CI, NH₃): m/z observed boron isotopic distribution at 186 (M+H), 205 (M+NH₄). HRMS (FAB, +): Calcd for C₃H₁₃B₁₀NO (M⁺) 190.2008. Found 190.2015. X-ray Crystallography: Space group: P2₁/n, a = 6.685(2) Å, b = 12.887(4) Å, c = 12.547(4) Å, α = γ = 90°, β =

90.724(11)°, $V = 1080.8(6) \text{ \AA}^3$, $Z = 4$, data/parameters: 2460/189, $R = 0.0469$, $R_w = 0.0816$, GOF = 1.036.

Attempted synthesis of 1-isonitrile-1,12-dicarba-*closo*-dodecaborane, synthesis of 1-methylcarbanyl-1,12-dicarba-*closo*-dodecaborane (5.5)

The formamide **5.4** (0.100 g, 0.534 mmol) was dissolved in freshly distilled CH_2Cl_2 (20 mL) and to this solution was added fresh Burgess reagent (0.255 g, 1.07 mmol) in one portion. The reaction vessel was brought to reflux for 40 h. The heat source was removed and the remaining methylene chloride was removed by rotary evaporation, giving an orange solid. The crude product was taken up in a minimal amount of petroleum ether and purified by flash silica gel chromatography (gradient elution: 100% hexanes to 50% ether in hexanes, 2.5% intervals) giving the pure carbamate (0.065 g, 72%). X-ray quality crystals were obtained by slow evaporation of the carbamate in ethanol. mp 101-102.5°C; T.L.C.(30% ether in hexanes): R_f 0.65; ^1H NMR (200 MHz, acetone- d_6): δ 7.42 (br s, 1H, NH), 3.90-0.50 (br m, 10H, BH), 3.48 (s, 3H, CH_3), 3.32 (br s, 1H, CH); ^{13}C NMR (50 MHz, acetone- d_6): δ 152.68, 89.99, 56.48, 28.29; ^{11}B NMR (96 MHz, acetone- d_6): δ -12.61, -15.30; IR (CH_2Cl_2 , cm^{-1}): 3418, 3057, 2615, 1754; MS (CI, NH_3): m/z observed boron isotropic distribution at 159 (M- CO_2CH_3). HRMS (EI): Calcd for $\text{C}_4\text{H}_{15}\text{B}_{10}\text{NO}$ (M^+) 219.2033. Found, 219.2048. X-ray Crystallography: Space group: P4_1 , $a = b = 11.529(8) \text{ \AA}$, $c = 11.402(12) \text{ \AA}$, $\alpha = \beta = 90^\circ$, $\gamma = 120^\circ$, $V = 1516(2) \text{ \AA}^3$, $Z = 4$, data/parameters: 2177/209, $R = 0.0755$, $R_w = 0.1333$, GOF = 0.982.

Attempted synthesis of 1-isonitrile-1,12-dicarba-*closo*-dodecaborane. Synthesis of 1-(N-1,12-dicarba-*closo*-dodecaboran-1-yl)-2,3-bis(imino(1,12-dicarba-*closo*-dodecaboran-1-yl))-4-(N-1,12-dicarba-*closo*-dodecaboran-1-yl)enimino)azetidine (5.7)

The formamide **5.4** (1.156 g, 6.17 mmol) was dissolved in dry methylene chloride (20 mL) with freshly distilled triethylamine (TEA) (2.50 g, 3.44 mL, 24.69 mmol). The solution was cooled to -78°C and triphosgene (1.76 g, 9.26 mmol) in 15 mL of CH_2Cl_2 added dropwise. Upon addition, the formation of a precipitate and gas evolution were apparent. The reaction was allowed to warm to 0°C over 0.5 hours and then to room temperature over an additional 3 hours, and maintained overnight at ambient temperature. The reaction was quenched using distilled, deionized water (25 mL) followed by additional washings of water (3 x 50 mL) in a separatory funnel. All aqueous fractions were pooled and further washed with CH_2Cl_2 (2 x 50 mL). The organic fractions were pooled, dried over Na_2SO_4 and gravity filtered giving a bright yellow filtrate, which was concentrated *in vacuo*. The crude product was purified by flash silica gel chromatography (100% hexanes) giving the azetidine (0.648 g, 62 %) as a bright yellow solid. (0.648 g, 62 %) which showed: mp $313.5\text{-}314.5^{\circ}\text{C}$; T.L.C. (100% Pet. ether): R_f 0.41; ^1H NMR (500MHz, C_6D_6): δ 3.60-1.10 (br m, BH), 1.91 (br s, CH), 1.84 (br s, CH), 1.58 (br s, CH); ^{13}C NMR (75 MHz, toluene- d_8): δ 189.91, 162.83, 158.63, 147.04, 145.47, 104.24, 98.66, 97.42, 96.63, 96.38, 95.94, 95.24, 90.01, 88.49, 58.92, 57.58, 57.16, 55.47, 51.00; ^{11}B NMR (160 MHz, acetone- d_6): δ -12.70, -13.26, -16.58; IR (CH_2Cl_2 , cm^{-1}): 3058,

2619, 2152, 2129, 2021; MS (ES, negative): m/z observed boron isotopic distribution at 677.1 (M-H); HRMS (FAB, +): Calcd for $C_{12}H_{44}B_{40}N_4$ (M+) 678.7586. Found 678.7621.

Synthesis of 1-(1,12-dicarba-closo-dodecaboran-1-yl)-2,3-bis(1,12-dicarba-closo-dodecaboran-1-ylimino)-4-(N-1,12-dicarba-closo-dodecaboran-1-ylcarboxamido)azetidine (5.8)

To a suspension of $[NEt_4]_2[ReBr_3(CO)_3]$ (50 mg, 0.065 mmol) in THF (1.3 mL) was added dropwise to a solution of $AgPF_6$ (49 mg, 0.195 mmol) in THF (1 mL). The white suspension was exposed to light for 20 minutes to facilitate the precipitation of $AgBr$ whereupon it was filtered under a stream of argon. The residue was rinsed with THF (1 mL) and compound **5.8** (70 mg, 0.098 mmol) added to the supernatant. The reaction mixture was heated to reflux overnight affording a clear yellow-green solution. After cooling to room temperature, the solvent was removed under reduced pressure. The crude product was purified by preparative thin-layer chromatography eluting with a petroleum ether/diethyl ether (90:10) mixture. The oily product was triturated with ice-cold hexanes affording a white precipitate, which was collected by decanting the liquid. The solid was further purified by flash chromatography (gradient from pure petroleum ether/diethyl ether to 90:10 petroleum ether/diethyl ether). After crystallization in CH_2Cl_2 , the product was obtained as X-ray quality crystals (19 mg, 27 %). mp: 328-330°C; TLC (70:30 petroleum ether/diethyl ether): R_f 0.50; 1H NMR (acetone- d_6 , 500 MHz): δ 4.58 (s, NH), 3.60-1.10 (br m, BH), 3.45 (br s, CH), 3.40 (br s, CH), 3.29 (s, CH (ring)), 2.93 (br s, CH); ^{13}C NMR (acetone- d_6 , 125 MHz): δ 162.73, 151.96, 148.66,

96.76, 95.79, 88.88, 87.38, 58.72, 57.76, 57.27, 53.92; ^{11}B NMR (acetone- d_6 , 160 MHz): δ -11.35, -11.78, -14.54, -14.97; IR (CH_2Cl_2 , cm^{-1}): 3687, 3603, 3405, 2617, 1717, 1607, 1502.; HRMS (FAB, +): Calcd for $\text{C}_{12}\text{H}_{45}\text{ON}_4\text{B}_{40}$ (M^+) 696.7726. Found 696.7747. X-ray Crystallography: Space group: $\text{C2}/c$, $a = 38.496(13)$ Å, $b = 11.9820(4)$ Å, $c = 27.523(10)$ Å, $\alpha = \gamma = 90^\circ$, $\beta = 127.050(5)^\circ$, $V = 10079(6)$ Å 3 , $Z = 8$, data/parameters: 8586/857, $R = 0.0862$, $R_w = 0.1835$, $\text{GOF} = 1.025$.

Synthesis of $[\text{ReL}_6][\text{Cl}]$ ($\text{L} = 1\text{-isonitrile-1,12-dicarboclosododecaborane}$)(5.11)

$[\text{Re}_2(\text{OAc})_4\text{Cl}_2]$ (0.100 g, 0.148 mmol) and the azetidine (0.212 g, 0.314 mmol) were dissolved in freshly distilled methanol (5.0 mL) giving an orange heterogeneous reaction mixture. The solution was brought to reflux for 72 hours under an inert Ar atmosphere. The solvent was removed by rotary evaporation and the resulting green solid suspended in a saturated acetone solution of KPF_6 for 1 hour (5 mL). Upon removal of the acetone, the grey/green solid was stirred in ether (25 mL) for 2 hours and filtered, and the filtrate concentrated *in vacuo*. The resulting solid from this fraction was stirred in low boiling petroleum ether (25 mL) for 2 additional hours. The resulting suspension was filtered and the solid purified by first subjecting to an anion exchange resin (AMBERJETTM, 4200(Cl) ion-exchange resin) in 2:3 water:THF, then dissolving in THF and the pure product isolated upon precipitation by the addition of an equal portion of distilled, deionized water. Yield 10%. ^1H NMR (acetone- d_6 , 500 MHz): δ 3.31 (s, CH), 3.7 – 1.5 (br m, BH); ^{11}B NMR (acetone- d_6 , 160.46 MHz): δ -11.71, -15.13. IR (CH_2Cl_2 , cm^{-1}): 3076, 2619, 2085; MS (ES, positive): m/z observed boron isotopic distribution at

1202.5 (ReL_6^+). HRMS (FAB, +): Calculated for $\text{C}_{18}\text{H}_{66}\text{B}_{60}\text{N}_6\text{Re}$ (M+) 1202.091. Found 1202.087. X-ray Crystallography: Space group: C2/c, $a = 24.1564(19)$ Å, $b = 31.177(3)$ Å, $c = 21.1752(12)$ Å, $\alpha = \gamma = 90^\circ$, $\beta = 94.706(4)^\circ$, $V = 15894(2)$ Å³, $Z = 8$, data/parameters: 15290/848, $R = 0.0662$, $R_w = 0.0805$, GOF = 1.555.

5.12 References

- ¹ Totani, T.; Aono, K.; Nakai, H.; Shiro, M. *Chem. Commun.* **1979**, 23, 1051.
- ² Todd, L.J.; Siedle, A.R.; Bodner, G.M.; Kahl, S.B.; Hickey, J.P. *J. Magn. Res.* **1976**, 23, 301.
- ³ Schaffer, P.; Morel, P.; Britten, J.F.; Valliant, J.F. *Inorg. Chem.* **2002**, 41, 6493.
- ⁴ Schaffer, P.; Britten, J.F.; Davison, A.; Jones, A.G.; Valliant, J.F. *J. Organomet. Chem.* **2003**, In Press.
- ⁵ Kahl, S. B. *Tetrahedron Lett.* **1990**, 11, 1517.
- ⁶ Yang, X.; Jiang, W.; Knobler, C.B.; Hawthorne, M.F. *J. Am. Chem. Soc.* **1992**, 114, 9719.
- ⁷ Valliant, J.F.; Schaffer, P. *J. Inorg. Biochem.* **2001**, 85, 43.
- ⁸ Burgess, E.M.; Penton Jr., H.R.; Taylor, E.A. *J. Org. Chem.* **1973**, 38, 26.
- ⁹ Zakharkin, L.I.; Kalinin, V.N.; Gedymin, V.V.; *Synth. Inorg. Met.-Org. Chem.* **1971**, 1, 45.
- ¹⁰ Eckert, H.; Forster, B. *Angew. Chem. Int. Ed. Engl.* **1987**, 26, 894.
- ¹¹ Mayr, A.; Yu, M.P.Y. *J. Organomet. Chem.* **1999**, 577(2), 223.
- ¹² Alberto, R.; Schibli, R.; Shubiger, P.A.; Abram, U.; Kaden, T.A. *Polyhedron* **1996**, 15, 1079.
- ¹³ Berman, H.M.; McGandy, E.L.; Burgner II, J.W.; VanEtten, R.L. *J. Am. Chem. Soc.* **1969**, 91, 6177.
- ¹⁴ Towns, R.L.; Trefonas, L.M. *J. Am. Chem. Soc.* **1971**, 93, 1761.
- ¹⁵ Meervelt, L.V.; L'abbé, G.; King, G.S.D. *Bull. Soc. Chim. Belg.* **1986**, 95, 97.
- ¹⁶ Fuks, R.; Baudoux, D.; Piccinni-Leopardi, C.; Declerq, J.-P.; VanMeerssche, M. *J. Org. Chem.* **1988**, 53, 18.
- ¹⁷ Aumann, R.; Heinen, H. *Chem. Ber.* **1986**, 119, 2289.
- ¹⁸ Marchand, E.; Morel, G.; Sinbandhit, S. *Eur. J. Org. Chem.* **1999**, 1729.
- ¹⁹ Katrizky, A.R.; Rees, C.W.; *Comprehensive Heterocyclic Chemistry I*; Lwowski, W. (Ed.); Pergamon Press: New York, NY, 1984.
- ²⁰ Moderhack, D. *Synthesis* **1985**, 1083.
- ²¹ Deyrup, J.A.; Vestling, M.M.; Hagan, W.V.; Yun, H.Y. *Tetrahedron* **1969**, 25, 1467.
- ²² Morel, P.; Schaffer, P.; Valliant, J.F. *J. Organomet. Chem.* **2002**, 668, 25.
- ²³ Abrams, M.J.; Davison, A.; Jones, A.G.; Costello, C.E.; Pang, H. *Inorg. Chem.* **1983**, 22, 2798.
- ²⁴ Tulip, T.H.; Calabrese, J.; Kronauge, J.F.; Davison, A.; Jones, A.G. In *Technetium in Chemistry and Nuclear Medicine*, Nicolini, M., Bandoli, G., Mazzi, U., Eds.; Raven Press: New York, 1986, p 119.
- ²⁵ Ericsson, M.-S.; Jagner, S.; Ljungström, E. *Acta Chem. Scand. A* **1979**, 33, 371.
- ²⁶ Barybin, M.V.; Holovics, T.C.; Deplazes, S.F.; Lushington, G.H.; Powell, D.R.; Toriyama, M. *J. Am. Chem. Soc.* **2002**, 124, 13668.
- ²⁷ Chiu, K.W.; Howard, C.G.; Wilkinson, G.; Galas, A.M.R.; Hursthouse, M.B. *Polyhedron* **1982**, 1, 801.

- ²⁸ O'Connell, L.A.; Dewan, J.; Jones, A.G.; Davison, A.; *Inorg. Chem.* **1990**, *29*, 3539.
- ²⁹ Acho, J.A.; Lippard, S.J. *Organometallics* **1994**, *13*, 1294.
- ³⁰ Cage A was omitted from these calculations due to the disorder associated with its participation in multiple packing modes.
- ³¹ Allison, J.D.; Wood, T.E.; Wild, R.E.; Walton, R.A. *Inorg. Chem.* **1982**, *21*, 3540.
- ³² Girolami, G.S.; Andersen, R.A. *Inorg. Chem.* **1981**, *20*, 2040.
- ³³ Girolami, G.S.; Mainz, V.V.; Andersen, R.A. *Inorg. Chem.* **1980**, *19*, 805.
- ³⁴ Bigorne, M.; Bouquet, A. *J. Organomet. Chem.* **1963**, *1*, 101.

Chapter 6 – Conclusions

Two unique strategies were developed for the synthesis of BNCT agents. Two novel classes of compounds were prepared, including a tamoxifen-carborane derivative and a series of rhenium(I) isonitrile complexes.

The total, stereoselective synthesis of an analogue of tamoxifen, in which ring A was replaced with a *nido*-carborane cage, was reported. This tamoxifen-carborane has the added advantage of becoming a novel imaging agent for breast cancer through the incorporation of a radionuclide onto the open face of the *nido*-carborane cage. In this approach, the carborane cage acts as a bifunctional system, covalently binding both the radioactive isotope and the targeting entity.

In parallel to the synthesis of the novel tamoxifen-carborane analogue, homoleptic rhenium(I) complexes of both *ortho*- and *para*-carborane isonitriles were synthesized as model systems for metal-based BNCT agents. In addition to the possibility of incorporating a radionuclide at the center of the complex, these compounds can be derivatized with any number of targeting agents to allow for selective uptake in the desired tissue. With a total of sixty boron atoms, these complexes will also aid in achieving the required therapeutic concentration of boron for BNCT. In the process of this research the unique behavior of a *para*-carborane formamide in the presence of different electrophiles was reported. Future research will entail the evaluation of these compounds for their biodistribution profiles, in addition to the synthesis and *in vivo* behavior of a number of analogues.

Overall, in the process of establishing novel synthetic methodologies for the derivatization of these polyhedra, the use of carboranes for the development of inorganic pharmaceuticals was examined.